# Unlocking Offshore Hybrid Projects

## Modelling Price and Volume Risks and their Mitigation Measures for Offshore Hybrid Projects in Offshore Bidding Zones under Flow-Based Market Coupling


By

**Daan Verkooijen**


| | | |
|---|---|---|
| Student Number: | 5702283 | |
| Project duration: | February 4, 2024 – August 7, 2024 | |
| Graduation Committee: | Prof. Dr. Ir. L.J. de Vries | TU Delft, Chairman |
| | Dr. Ir. K. Bruninx | TU Delft, First Supervisor |
| | Dr. Ir. Ö. Okur | TU Delft, Second Supervisor |
| | Dr. M. Bahlo | RWE, External Supervisor |

Submitted in fulfilment of the requirements for the Master of Science degree of
[Complex Systems Engineering and Management]


Faculty of Technology, Policy and Management
Delft University of Technology

August 7, 2024


TU Delft Delft University of Technology

# Executive Summary

### *Introduction*

The European Commission (EC) has set ambitious targets of achieving 60 GW and 300 GW of offshore wind capacity by 2030 and 2050, respectively, to meet its energy and climate objectives. This push towards renewable energy necessitates the integration of hybrid offshore wind farms (OWFs) connected to multiple countries and markets, facilitating cross-border electricity connections, security of supply, and increased renewable energy integration. Hybrid projects, combining OWFs and interconnector transmission cables, play a crucial role in this transition, aiming to create a meshed offshore energy network in the North Sea.

The development of the European Target Model, incorporating Flow-Based Market Coupling (FBMC), Advanced Hybrid Coupling (AHC), and the Offshore Bidding Zone (OBZ), aims to address challenges in hybrid projects but introduces new price and volume risks. These risks, stemming from the unique market mechanisms of the OBZ and the increased dependency on interconnectors, lead to revenue uncertainties and potential curtailment for offshore wind farms (OWFs), complicating investment climates and hindering the achievement of renewable energy targets.

### *Research Goal and Questions*

The main objective of this thesis is to identify the key factors leading to price and volume risks for hybrid projects and assess the effectiveness of mitigation measures. This is achieved by answering the main research question in this thesis:

*How do the offshore grid topology, onshore grid attenuations and the integration of renewable energy sources influence price and volume risk and to what extend do regulatory and technological measures mitigate these risks?*

Aiding in answering this question, four subquestions have been introduced, aimed at identifying specific price and volume risks, exploring regulatory and technological mitigation measures, determining the most impactful risk factors on OWFs' economic viability, and evaluating the potential mitigation measures' effectiveness.

### *Research approach and methods*

The research approach consists of two phases: qualitative desk research and quantitative modelling. The first phase involves a literature review to identify and categorize price and volume risks and mitigation measures, forming a risk framework. The second phase addresses the Risk Framework from phase 1 and uses it to extend the model from Kenis et al. (2023) to quantify the frequency and severity of the risks and ultimately determine the key factors leading to these risks.

The primary research method applied in this thesis is a linear optimisation model mimicking the FBMC process of TSOs deployed in Julia. The methodology encompasses a four-key steps process. In the first step, the Case Determination, indicators are established to define case groups and systematically vary variables and isolate the primary considered variables, i.e. offshore grid topology, onshore grid attenuations, and renewable energy integration. In the second step, the Case Simulation, the base case (D-2), day-ahead market clearing (D-1) and redispatch (D-0) modelling steps of the FBMC process are simulated, followed by the added modelling step to distinguish between the capacity calculation and allocation volume risk and the calculation of the risk indicators. In the third step, the Case Group Analysis, case-specific results are collected and analysed per case group and an ex-post analysis of the FTR and TAG compensations is conducted. Th final step, the Cross-Case Group Analysis, involves aggregating and analysing all results with the aid of standardisation methods to create Risk Matrices.

## *Key findings & Conclusions*

The study identifies two key factors leading to price and volume risks: the transmission *grid's physical characteristic*, i.e. the OBZ's export capacity or FB domain as influenced by the offshore grid topology and onshore outages, and the *market characterises* of the bidding zones connected via the hybrid interconnector, i.e. the level of competition between the OBZ and onshore (renewable) generators for the allocation of scarce transmission capacity.

Changes in offshore grid topology primarily impact price and volume risks by altering the OBZ's export capacity, with increased transmission capacity generally reducing curtailment by capacity calculation but potentially affecting price collapses and curtailment by capacity allocation depending on onshore grid restrictions and market dynamics. Onshore grid attenuations similarly influence these risks, with high-priced zone outages typically increasing curtailment by capacity allocation and price collapses, while low-priced zone outages increase curtailment by capacity calculation and positive non-intuitive price formation. The integration of renewable energy sources in onshore markets exacerbates competition for transmission capacity, leading to more frequent curtailment by capacity allocation and price collapses during high-wind hours.

Technological mitigation measures, i.e. flexible demand agents (e.g. offshore and onshore electrolysers), mitigate price and volume risks by increasing local demand in the OBZ, setting a floor price and raising electricity prices, and decreasing the need for wind exports, which reduces curtailment by the capacity allocation and calculation risks. FTRs effectively cover price spreads, prevent price collapses and non-intuitive price formation. The TAG moderately compensates for curtailment by the capacity calculation volume risk.

## *Recommendations*

Policy makers should actively promote the deployment of flexible demand technologies to balance supply-demand mismatches and support renewable energy generation. They should also decide on a support strategy for hybrid projects, either a merchant-based approach focusing on flexible demand deployment or a regulatory approach implementing FTRs and TAG, potentially including 2-sided capability-based CfDs for initial projects to address supply/demand mismatches. TSOs should strategically select inland landing points and prioritize grid enhancements to mitigate structural congestion and reduce hybrid projects' exposure to price and volume risks, while timely communicating potential delays in intra-zonal and cross-border transmission developments to developers. Developers should pro-actively invest in flexible demand assets to mitigate price and volume risk and increase OWF revenues, optionally focussing on strategic locations of onshore assets near landing points. Finally, uniform decision-making and alignment in hybrid project design and support instrument deployment across North Sea countries are crucial, potentially facilitated by establishing an independent Offshore Transmission System Operator and an Offshore Investment Bank to manage transmission assets and reallocate costs and benefits among stakeholders.

# Table of Contents

# List of Tables

# List of Figures

# List of Abbreviations

| | |
|---|---|
| **AC** | Altering Current |
| **AHC** | Advanced Hybrid Coupling |
| **ATC** | Available Transmission Capacity |
| **BESS** | Battery Electric Storage System |
| **CAES** | Compressed Air Energy Storage |
| **CCR** | Capacity Calculation Region |
| **CfD** | Contracts for Differences |
| **CNE** | Critical Network Element |
| **CNEC** | Critical Network Element Contingency |
| **DA** | Day Ahead |
| **DC** | Direct Current |
| **EEZ** | Exclusive Economic Zone |
| **EI** | Export Indicator |
| **EST** | Energy Storage Technology |
| **FB** | Flow-Based |
| **FBMC** | Flow-Based Market Coupling |
| **FAMC** | Fleet Average Marginal Costs |
| **FTR** | Financial Transmission Right |
| **GSK** | Generation Shift Key |
| **HM** | Home Market |
| **HVDC** | High Voltage Direct Current |
| **ID** | Intermediate Deliverable |
| **II** | Interconnectivity Indicator |
| **LTTR** | Long-Term Transmission Rights |
| **MPI** | Multi-Purpose Interconnectors |
| **NTC** | Net Transfer Capacity |
| **OBZ** | Offshore Bidding Zone |
| **OIB** | Offshore Investment Bank |
| **ONP** | Offshore Nodal Pricing |
| **OTSO** | Offshore Transmission System Operation |
| **OWF** | Offshore Wind Farm |

| | |
|---|---|
| **PHS** | Pumped Hydro Storage |
| **PPA** | Power Purchase Agreement |
| **PTDF** | Power Transfer Distribution Factor |
| **PtG** | Power-to-Gas |
| **PtP** | Point-to-Point (interconnector) |
| **RAM** | Remaining Available Margin |
| **RES** | Renewable Energy Sources |
| **SQ** | Sub Question |
| **TAG** | Transmission Access Guarantee |
| **TSO** | Transmission System Operator |
| **ZPTDF** | Zonal Power Transfer Distribution Factor |

# Acknowledgements

This thesis marks the conclusion of my master's degree in Complex Systems Engineering and Management, a journey I have thoroughly enjoyed. I would like to extend my heartfelt thanks to all the professors who have imparted their knowledge on subjects ranging from energy markets, socio-technical developments, multi-actor and geopolitical influences on energy systems, energy systems engineering, and all the other interesting topics that have been covered throughout this program. While my interest in the renewable energy transition was sparked during my bachelor's degree, particularly in socio-technical changes and the broader landscape in which these transitions and technologies form, this master's program provided me with valuable technical skills. During my professional career, I hope to continue working in some capacity in the energy transition, wherever my skills and energy are most valued. I truly believe that with the competencies and skillset gained during my studies, I can contribute to tackling global climate change by accelerating the energy transition. This thesis has further fuelled my interest in contributing to the most complex and advanced projects that can boost this transition. My interest, however, is not limited to this alone. This graduation project, undertaken combined with an internship at RWE, has provided me with invaluable practical experiences.

I would like to express my gratitude to my first supervisor, Kenneth Bruninx, for his profound feedback. The weekly meetings with him always gave rise to interesting new insights and discussions on the profound intricacies and complexities of flow-based market coupling, which aided me in demarcating and profoundly understanding the thesis' topic better. His prompt communication and responses have been immensely helpful. Similarly, I extend my thanks to my graduation chairman, Laurens de Vries, for his feedback and valuable insights. I am also grateful to my second supervisor, Özge Okur, for taking the time to read and evaluate what has become quite an extensive thesis.

A special thanks to my supervisor at RWE, Marc Bahlo, for always providing me with insights and swift communication on a daily basis. His holistic points of view and advice on a structured approach to tackling problems were invaluable. He mentored me in many ways, and I am extremely grateful for his support. Lastly, thanks to those colleagues at RWE who provided me with profound expert knowledge from within the industry.

Furthermore, I want to express my thanks to my friends and family, mostly for having the patience and still supporting me, despite my frequent absence at social occasions during the past couple of months.

On a final note for all actors potentially involved in the future development of hybrid projects who have found their way to this master thesis: knowledge sharing and collaboration are key! If any uncertainties or lack of understanding remain, please feel free to reach out. Additionally, for those daredevils who will read the entire thesis, please let me know if you do so I can thank you in person.

*Daan Verkooijen*

*August 7, 2024*

# Chapter 1. Introduction

## 1.1 Context

To achieve the EU's 2030 and 2050 energy and climate objectives, the European Commission (EC) has set targets of 60 GW and 300 GW of offshore wind capacity by 2030 and 2050, (European Commission, 2020a). Additionally, the EC aims to enhance energy market interconnectivity among Member States for improved cross-border electricity connections, increased security of supply, and greater integration of renewable energy sources (European Commission, 2015). The future European offshore transmission system will become more meshed or integrated to support these goals, where offshore wind farms (OWFs) are connected to multiple countries and markets (Dedecca et al., 2017; Dedecca et al., 2018). In addition to the classical radial connections of the OWFs to shore and point-to-point interconnections between countries, the European representative organisation for Transmission System Operators (TSOs), ENTSO-E, foresees at least 14% of offshore renewable energy sources (RES) – corresponding to roughly 80 GWs - to be connected via hybrid interconnectors (ENTSO-E, 2024). Within these 'hybrid projects' both the EC's offshore wind development and interconnectivity targets come together, as hybrids serve the dual purpose of connecting OWFs to the onshore grid of two or more countries, while simultaneously interconnecting the countries' power markets for cross-border trade (Nieuwenhout, 2022). The system design of hybrid projects explicitly integrates two technical artefacts, offshore wind farms and interconnector transmission cables (typically HVDC), to fulfil two power system functions: renewable energy production and cross-border power trade.

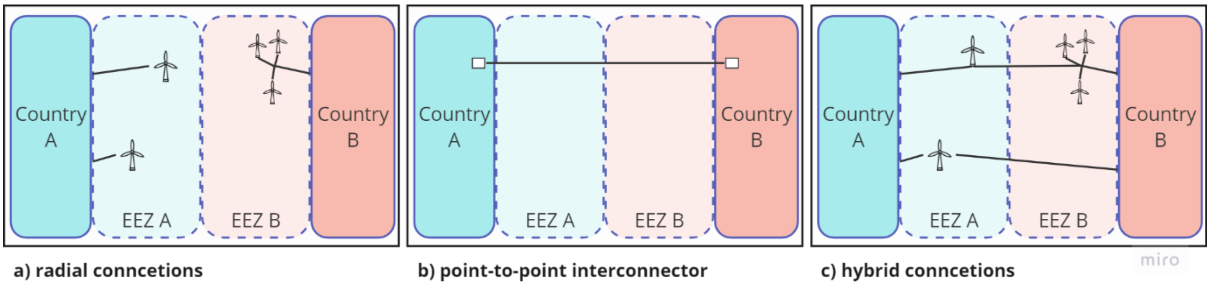


*Figure 1: Visualisation of the different connection types of the future offshore transmission grid. a) radially connected OWFs (left) and radially connected hub (right); b) point-to-point interconnector; c) hybrid interconnector between countries A and B*

The deployment of hybrid projects in the North Sea is seen as the first step towards an integrated offshore energy network where several offshore energy hubs will collect generated offshore wind power, connect the OWFs to the European markets and (potentially) convert wind energy to other energy carriers such as hydrogen (NSWPH, 2022). The members of the North Seas Energy Cooperation[1] encourage in a joint statement the development of hybrid projects and a meshed offshore grid and stressed the importance of increased strengthening of the EU electricity market arrangements to support these efforts (NSEC, 2022). The ENTSO-E's ten-year network development plan (TYNDP) identified the hybrid interconnectors that will be developed in the coming years (Figure 2). Additionally, the second joint publication by the North Seas TSO outlined a list of nine prospective energy hubs or hybrid interconnectors, including Dutch, Belgian, German, and Danish power hubs, each projected to have an installed offshore wind capacity of at least 2 GW (OTC, 2024). The first project to be realised among these is the Belgian Princess Elisabeth Island, of which the first tender for plot 1 is scheduled for Q4 2024 (Elia Group, 2024). This timeline and the EC's ambitious targets underscores the urgency for

[1] North Seas Energy Cooperation is a regional partnership between Belgium, the Netherlands, Luxembourg, Germany, France, Ireland, Denmark, Sweden and Norway

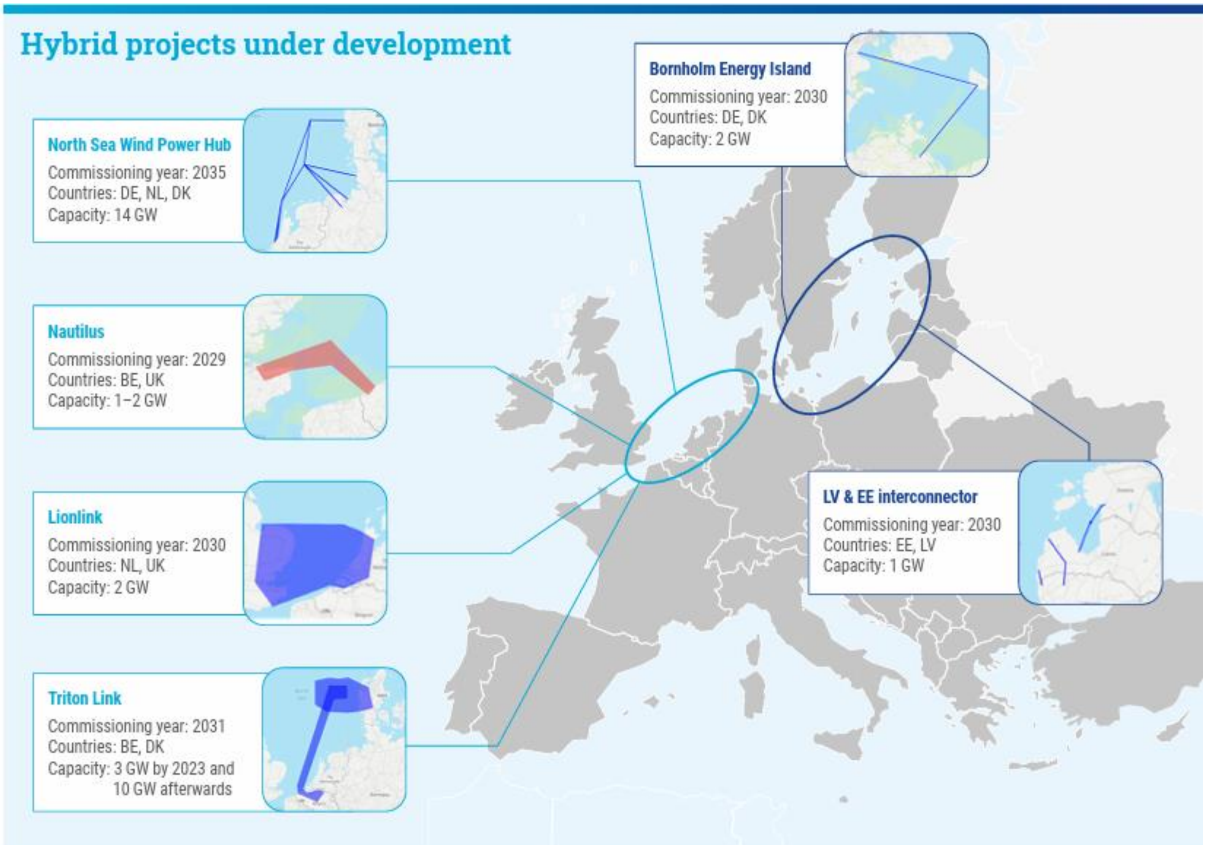


*Figure 2: The Hybrid Projects under development around the North Sea region (Source: ENTSO-E, 2024a).*

establishing a clear market and policy framework to reap the many benefits that these hybrid projects offer to society and the power system at large.

Hybrid projects enhance socio-economic welfare (Tosatto et al., 2022; Traber et al., 2017), foster CO2 emission reduction in the countries adjacent to the hybrid (Kristiansen et al., 2018) and even beyond directly connected countries by displacing carbon-intensive coal and lignite power plants (Jansen et al., 2022). Furthermore, hybrid projects enable more cost-effective system deployment by reducing the need for physical infrastructure by minimising offshore cabling length and the necessity for converter stations (THMA Consulting Group, 2020). They also facilitate more efficient utilisation of maritime space, thereby aiding in the reduction of environmental impacts associated with offshore development (ENTSOE-E, 2024). Additionally, hybrid projects can be combined with offshore hydrogen production, thereby becoming *multi-purpose interconnectors* (MPI), to enable additional integration of offshore RESs and system flexibility (ENTSOE-E, 2024). Crucially, hybrid projects facilitate the efficient integration of offshore wind power into Europe's electricity systems and markets by enabling the transmission of power to where it is most needed. Additionally, should wind conditions be unfavourable in one country, the infrastructure can be utilized to import clean energy from other regions.

However, the development of hybrid projects faces significant challenges and uncertainties that need to be addressed. These include limited coordination in planning and funding (Sunila et al., 2019), divergent incentives for stakeholding investors (Tosatto et al., 2022), unresolved trade-offs and uncertainties (Härtel et al., 2018), and unequal cost and benefit distribution among stakeholders and countries (Dedecca et al., 2018). Such factors highlight the complexity of aligning multiple actors and making collaborative decisions across involved countries. Additionally, the inherent cross-border nature of hybrid project system design introduces further challenges, such as jurisdictional responsibilities and ownership definitions. Moreover, the technical design of hybrid projects often leads to structural congestion, where it is not feasible to manage full cross-border exchanges and full wind power injections simultaneously (Elia Group, 2024). There is also uncertainty concerning the specific deployment of the future meshed onshore grid. While the Ten-Year Network Development Plan (TYNDP) outlined by the Offshore Transmission Consortium (OTC) provides a vision for the future offshore transmission system, many details remain undetermined. These include the distribution of interconnection capacity to adjacent countries, the availability of offshore HVDC conversion stations, the precise timings for connecting wind farms to power markets, and potential increases in interconnectivity. Furthermore, existing onshore congestion in many North Sea countries poses additional challenges for hybrid projects as it could potentially compromise the export capabilities from the OBZ to the onshore markets (Netbeheer Nederland, 2024; Rajgor, 2024). In addition, the *cannibalization effect*, referring to the phenomenon where the increasing penetration of zero marginal cost renewable capacity in the generation mixes leads to lower electricity prices, is observed to be more severe for offshore wind power hubs, i.e. hybrid projects (Jansen et al., 2022). To address these challenges and to make optimal use of the offshore infrastructure in the interest of society, a well-structured market design is crucial to the successful development of hybrid projects.

## 1.2 The European Target Model for Electricity Markets

As the European energy landscape evolves, two pivotal mechanisms facilitate this transformation: Flow-Based Market Coupling (FBMC) and Advanced Hybrid Coupling (AHC). FBMC is since 2015 the methodology implemented in the Core[2] Capacity Calculation Region[3] (CCR) to allocate cross-border transmission capacity for the trading of electricity between the coupled bidding zones. FBMC dynamically assesses the available cross-border transmission capacity based on real-time network conditions and optimises the allocation of that transmission capacity (Schönheit et al., 2021). Because the FBMC-methodology comes with a better grid representation, it allows for more commercial transmission capacity being available for trade in the day-ahead, which aids in reducing price differences between interconnected markets (Ovaere et al., 2023). Where FBMC is already active in a large area in Europe, Advanced Hybrid Coupling is aimed to be integrated into this framework (Core TSOs, 2023).

AHC is a mechanism to integrate the impact of cross-border HVDC power flows within the Core region (as well as between the Core CCR and adjacent CCRs) on the AC network into the market coupling algorithm (Schönheit & Marjanovic, 2024). AHC is an improvement on the currently implemented Simple Hybrid Coupling and employs a method that allows for the creation of virtual bidding zones (Müller et al., 2017). This advanced coupling mechanism eliminates the need for forecasts in managing cross-border exchanges, thereby fostering non-discriminatory competition and ensuring equitable access to transmission capacity. Specifically for offshore hybrid projects, AHC enables more accurate calculation of the available commercial transmission capacity for the interconnectors connecting the OBZ based on the physical capabilities of the surrounding onshore transmission grids.

FBMC is an integral component of the European electricity target model (Van den Bergh, 2016), and with all Transmission System Operators (TSOs) proposing its adoption (ENTSO-E, 2023a), AHC is poised to become a fundamental part of the electricity market model. Specifically, in the context of hybrid projects, it is anticipated that both FBMC and AHC will be jointly implemented (Elia Group, 2024).

---

[2] The Core CCR consists of the bidding zone borders between the following EU Member States' bidding zones: Austria, Belgium, Croatia, the Czech Republic, France, Germany, Hungary, Luxemburg, the Netherlands, Poland, Romania, Slovakia and Slovenia (JAO, 2022).

[3] Capacity Calculation Regions (CCRs) are specific areas within Europe designated for coordinated management of cross-border electricity flows.

## 1.3 The European Target Model for Offshore Hybrid Projects

Currently, the implemented offshore electricity market design in Europe is the Home Market (HM) setup, where wind farms are integrated into the administrative bidding zone to which they are connected and thereby receive an electricity wholesale price equivalent to that of the mainland (Kenis et al., 2022). The administrative bidding zones in the HM setup generally correspond to the borders of the Exclusive Economic Zones (EEZ). Under the HM model, a hybrid-connected OWF is restricted to bid and dispatch its generated wind power in the country it is located in, receiving the market price of its respective HM while the power can flow over the interconnector across the border. This complicates the marketing of the produced electricity when the interconnector is used for cross-border trade (Nieuwenhout, 2022) and would require counteractive actions from the TSO (TenneT, 2024). Additionally, the HM setup conflicts with Article 16(8a) of Regulation (EU) 2019/943, commonly known as the '70%-rule', due to the interconnection functionality in the hybrid project. This regulation depicts that a minimum of 70% of transmission capacity of the interconnector shall be available for cross-zonal power exchanges (Council of the European Union and European Parliament, 2019). This implies that only 30% of the transmission capacity on the interconnector remain available for wind power exports with 70% of the capacity put available to the market. This restriction often results in the curtailment of wind generation, as any production exceeding this fraction cannot be marketed domestically, leading to underutilization, inefficiencies, and economic losses for operators (Nieuwenhout, 2022).

Besides this inefficiency due to the legal setup of the current market design for hybrid projects exists the issue of structural congestion embedded in a hybrid grid design. As mentioned in Section 1.1, the coexistence of offshore wind generation and interconnector flows on the same transmission corridors can create competition for limited transmission capacity leading to structural congestion (Elia Group, 2024). There exist two alternative market designs that organize this competition for the scarce offshore transmission capacity differently. The first alternative is the implementation of one dedicated market zone for all hybrid projects, the Offshore Bidding Zone (OBZ) market design. The second alternative is the implementation of small price zones per hybrid project or offshore wind cluster, the Offshore Nodal Pricing. Figure 3 visualises these different market designs.

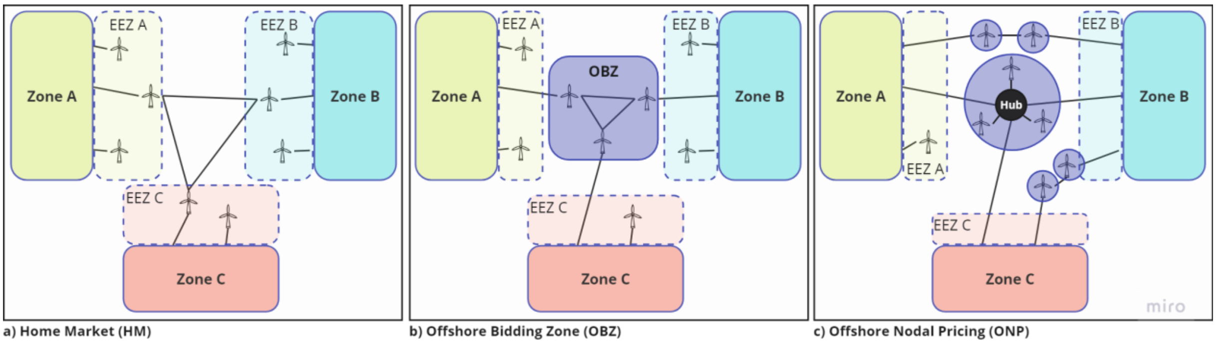


*Figure 3: Visual Representation of the different electricity market designs for hybrid projects. Figure a) represents the HM setup, where the bidding zones are defined by the country's respective Exclusive Economic Zone (EEZ). Figure b) represents the OBZ setup, with a separate market zone for all hybrid projects. Figure c) represents the ONP setup, where each hybrid project has its own bidding zone.*

In the OBZ model a separate market zone is established for offshore generating capacity, optimising the integration of OWFs into the power system (Kenis et al., 2022). Prices, revenues, generation, and congestion costs are determined within this specific OBZ, providing a more tailored approach to OWF operation and interaction with the broader market. Furthermore, the OBZ configuration adheres to the 70% rule by classifying cables as cross-zonal interconnection links (TenneT, 2024). This classification means that the market coupling algorithm manages the capacity allocation on the interconnectors. Consequently, the full cable capacity is dedicated to cross-zonal trading, ensuring optimal utilisation of the interconnectors. Furthermore, the OBZ setup is designed to mitigate the structural congestion observed in the HM by implementing a market-based mechanism that optimizes the utilisation of transmission capacity and manages electricity over the interconnectors (Elia Group, 2024). It achieves this primarily through efficient market arbitrage, wherein offshore wind generation competes with import/export activities over interconnectors. This competition effectively balances regional electricity supply and demand, thereby enhancing the utilisation of transmission capacity and reducing congestion risks. Moreover, compared to the HM setup, the OBZ setup leads to higher socio-economic welfare (NSWPH, 2021) and achieves a higher degree of overall efficiency since energy is allowed to flow where it is most needed (European Commission, 2020b).

In the Offshore Nodal Pricing (ONP) model, each node in the offshore electricity grid acts as an independent bidding zone, with the market clearing algorithm incorporating all relevant transmission constraints, thereby reflecting the locational value of energy, including the cost of energy and the associated delivery costs (Antonopoulos et al., 2020). ONP is considered as the most promising market design for a meshed offshore grid where the price zones would be determined by the presence of grid congestion, similar to the Nordpool system (PROMOTioN, 2020). This model essentially represents the offshore implementation of the Location Marginal Pricing model used in several U.S. power markets. It can also be viewed as a derivative of the Offshore Bidding Zone design, where each wind farm or wind cluster would have a small OBZ. An additional advantage of ONP compared to the OBZ setup is that the HVDC transmission cables between the OWFs in the hybrid project are incorporates in the market clearing algorithm, thereby also signalling congestion between the OWFs.

The European Commission is in favour of the implementation of OBZs, as they argue that "*... establishing an offshore bidding zone for a hybrid project can be done in a way that is compatible with the electricity market rules and can be a well-suited option for a large scale-up of offshore renewables…*" – European Commission (2020). ACER (Agency for the Cooperation of Energy Regulators) and CEER (Council of European Energy Regulators) express broad support for the EC's position on OBZs. However, they highlight that current real-time trading rules favour the home market approach, stressing the need for non-discriminatory solutions for internal and cross-zonal trade and recommending further analysis of creating OBZs and the potential mitigation measures to address possible concerns (ACER & CEER, 2022). The North Sea Wind Power Hub (NSWPH) - a consortium of the Dutch-German TSO TenneT the Danish TSO Energinet, and GasUnie – also support the OBZ market setup, as it "*…improve[s] market and system operation efficiency, allows market representation of the physical limitations of the grid, and provides appropriate price signals to market parties including PtG developers.*" – NSWPH (2023). ENTSOE-E states that the OBZ concept is a "*…prominent solution when considering the efficiency of markets and system operations…"* but warn for the fact that the OBZ concept provides less market revenue to OWFs compared to the HM setup (ENTSOE-E, 2020). This potential adverse side effect of the OBZ configuration, in comparison to the HM setup, is the lower revenues from day-ahead markets for OWF owners.

In conclusion, both the OBZ and ONP models present clear benefits over the existing HM setup, with the OBZ model emerging as the preferred target model over ONP for effectively integrating hybrid interconnectors into Europe's power markets. However, the adoption of this new market model may introduce additional uncertainties and challenges. The next section dives deeper into the specific problems that arise with the envisioned European electricity target model, tailored to hybrid projects.

## 1.4 Problem Definition

Reflecting on the discussions from previous sections, it is evident that the development of the European Target Model, which incorporates elements of Flow-Based Market Coupling (FBMC) and Advanced Hybrid Coupling (AHC), along with the introduction of the Offshore Bidding Zone (OBZ), addresses several challenges associated with the development of hybrid projects. In particular, the introduction of the OBZ addresses the structural congestion embedded in a hybrid gird design and adheres to the European Regulations on the internal market for electricity. Furthermore, with the OBZ being part of the FBMC capacity allocation methodology, efficient cross-border electricity trading and alignment with the physical state of the electricity network is ensured such that the offshore infrastructure for the hybrid project is utilized optimally. Lastly, by implementing the AHC methodology for hybrid projects that connect different CCRs, it ensures the maximization of socio-economic welfare and guarantees non-discriminatory competition for limited transmission line capacity in these power flow exchanges.

While several crucial challenges are addressed, the combination of these new market models for hybrid projects introduces also new challenges and uncertainties that complicate the forming of a business case for developers. OWF developers require a predictable business case early on for wind site tendering (TenneT, 2024). Additionally, it is crucial to secure investment in wind farms linked to offshore hybrid projects through support schemes that are non-distortive (OTC, 2024). The combination of an OBZ under FBMC, and specifically subject to AHC, give rise to price and volume risks, explained hereafter. These price and volume risks lead to curtailment and revenue losses for OWFs connected with a hybrid interconnector, deteriorating the investment climate for developers and, consequently, hindering the achievement of offshore renewable energy targets. Since in the upcoming offshore wind tenders, such as the Princess Elizabeth Island in Q4 of 2024, the OBZ will be included, as well as the AHC method implemented (Elia Group, 2024), more clarity is required regarding these challenges and uncertainties that developers face.

The first issue relates to the unique price formation mechanism to witch the OBZ is subject to – a mechanism not seen in onshore bidding zones. Given the relatively small size of the OBZ, compared to the larger onshore zones often represented by entire country boarders, and the minimal or absent demand within the OBZ, prices in the OBZ are solely determined by market coupling processes (TenneT, 2024). As mentioned in Section 1.2, the AHC enables the OWF within an OBZ to compete non-discriminatorily for the limited capacity between the OBZ and adjacent onshore bidding zones, as well as for the use of the onshore grid. Consequently, the price in the OBZ reflects the competition for scarce transmission capacity across the entire grid of the involved CCRs. Therefore, the determining factor for price formation in the OBZ is the allocated cross-border exchange capacity to the adjacent bidding zones. This unique setup of a small bidding zone devoid of demand exacerbate the *price risk* compared to the large onshore bidding zones of entire countries, where the price risk is defined as the uncertainty or potential for fluctuations in electricity prices that can impact the revenue streams and profitability of offshore hybrid projects (THEMA Consulting Group, 2020).

Specifically, as Kenis et al. (2023) have shown, OWF owners with an hybrid interconnector are significantly worse off when located in an OBZ than compared to the HM setup since average prices in the OBZ are significantly lower and more frequently at 0 €/MWh, leading to a significant decrease in obtained revenues. The zero-priced hours emerge when commercial transmission capacities with the mainland are fully utilised, since the transmission constraints is the limiting factor for the flow of electricity and thus the marginal value of energy in the OBZ. This zero-priced hour is often referred to a *price collapse* hour. It is a broadly expressed concern of OWF developers, but TSOs state that it is not so likely to occur (TenneT, 2024), indicating the unclarity regarding the exact impact of these price collapse hours between stakeholders. Kenis et al. (2023) conclude that the OBZ configuration demonstrates advantages in capturing and signalling generation and transmission scarcity, leading to decreased congestion management costs compared to the HM configuration. However, the OBZ configuration leads to a transfer of welfare, with lower revenues for offshore wind farm owners and increased congestion rents for TSOs, indicating the need for a potential redistribution mechanism for costs and benefits among the stakeholders in this new system design.

The second issue arising from this new market setup is the risk that OWFs may not be able to sell all generated wind energy when production surpasses interconnector capacity (Laur et al., 2022). Coupled with the small bidding zone that lacks demand and the reliance on interconnectors to export electricity to shore, the volume that the OWF can offer to the market is further constrained by the market coupling processes of the OBZ. Consequently, there is a risk that the OWF may need to curtail part of its generated wind capacity due to the limited availability of allocated transmission capacity. This increased reliance on limited transmission capacity and its allocation through market clearing to export all generated wind power from the OBZ heightens *volume risk* for hybrid projects. Volume risk is defined as the uncertainty or potential variability in the quantity of electricity generated or traded compared to the expected quantity, independent of price changes (THEMA Consulting Group, 2020).

In conclusion, despite the advancements made with the European Target Model, significant challenges and uncertainties remain, complicating the development of a robust business case for hybrid projects and potentially impeding the attainment of the EC's offshore wind energy targets. These challenges, particularly the unique price and volume risks arising from the OBZ setup, highlight critical gaps in our understanding of the new market dynamics.

## 1.5 Knowledge Gaps and Research Questions

Moving from the identified problem to formulating a research question, it is crucial to consider existing literature and recent studies on this topic. Therefore, the following sections outline literature that has addressed price and volume risks, then review specific papers that have modelled the OBZ market design under FBMC. Additionally, several studies that discuss mitigation measures to address the price and volume risk are considered. Finally, the discussion will cover recent studies that specifically consider point of view of OWF developers in an OBZ. This section concludes with the research question central to this thesis that will address the identified knowledge gaps, substantiated with the thesis' objectives.

### 1.5.1 Literature on Price and Volume risk

The price and volume risks, as discussed in the previous section, along with additional challenges unique to the OBZ setup subject to AHC with FBMC, have been identified and described in recent papers. The consultation report for the Princess Elisabeth Zone (PEZ) from the Belgium TSO Elia Group (2024) discuss price and volume risk in the context of the OBZ, and more specifically when introducing AHC in under FBMC. The paper provides substantiated qualitative insights into price and volume risk and explains with clear examples how concepts such as flow-factor competition and the implications of forecast errors affect price formations in the OBZ, however, this paper does not provide quantitative substantiation of the described price and volume risks. Furthermore, the paper identifies several driving factors that might lead to price and volume risk, including transmission constraints, renewable energy integrations and regulatory frameworks, but detailed empirical analysis or numerical data to quantify the impact of price and volume risks on electricity market outcome is lacking.

The Blueprint for OBZs by Dutch/German TSO TenneT (2024) also clearly addresses the price risk emerging in an OBZ and makes an important categorisation within the volume risk, which differentiates between the aspects and conditions for the volume risk to occur. Furthermore, several mitigation strategies to address the price and volume risk are discussed, such as Power Purchase Agreements, Contracts for Difference and the Transmission Access Guarantee. The blueprint identifies key challenges, highlighting the complex interplay between market design, technical infrastructure, and regulatory frameworks necessary to support the development and operation of OWFs within an OBZ. This paper implies a knowledge gap regarding the effects of Advanced Hybrid Coupling (AHC) on market prices and volumes in Offshore Bidding Zones (OBZs), emphasizing the complexity and interdependencies within the AHC system. Specifically, as TenneT (2024) indicates, this complexity hinders market participants' ability to make accurate forecasts, impacting the predictability and stability of business cases for offshore wind farms due to the sensitive nature of price and volume responses to network changes and other factors.

The lack of quantitative evidence on the price and volume risk (Elia Group, 2024) and the knowledge gap regarding the effects of AHC on prices and volumes in OBZs (TenneT, 2024) are addressed by modelling efforts by Kenis et al. (2023) and Kenis et al. (2024), discussed hereafter.

### 1.5.2 Literature on OBZ Modelling

Kenis et al. (2023) have modelled the price formation of an OBZ and compared it to the conventional HM configuration, considering various representations of the transmission grid in the market clearing algorithm, amongst which the Advanced Hybrid Coupling methodology. They showed that for OWFs in an OBZ with AHC electricity prices on average decrease (and congestion rents for TSOs increase), curtailment emerges only in this specific market design and the share of offshore wind power sold at 0 €/MWh to the total available wind power increases from 0% to 79% moving from the HM to the OBZ configuration (Kenis et al., 2023). The decrease in prices, increase in congestion rents, curtailment, and higher occurrence of zero-priced GWh are primarily attributed to the improved detection of congestion and utilization of transmission capacities by AHC, leading to a more restrictive market clearing process and impacting the economic outcomes for off-shore wind farms in the European electricity market. The potential adverse implications of the lowered Day-Ahead revenues on the investment attractiveness and, consequently, the renewable energy targets is stressed. They indicate that future studies should examine the effect of different power network topology as this impacts the magnitude of the observed effects and stress the importance to reconsider support instruments for OWFs in an OBZ.

Kenis et al. (2024) take a broader perspective compared to Kenis et al. (2023) thereby addressing the knowledge gap of power network topology changes on the observed effects, where investments in offshore energy infrastructure are considered in their model to assess effects of HVDC and electrolyser investment decisions on the implications on welfare, wind farm profitability and offshore electricity price formations for different offshore market designs, ranging from full zonal to full nodal pricing. Specifically, for the HVDC transmission investment decisions Kenis et al. (2024) find that lower transmission capacities connecting the OBZ to the mainland are associated with lower electricity prices, more frequent zero-priced hours and increased curtailment. For the electrolysers, Kenis et al. (2024) find that their presence in the OBZ limits the need for curtailment (as electricity is consumed at the same node where the power is generated), drives up offshore electricity prices as the willingness-to-pay of electrolysers set the price more often, ultimately leading to increased profitability for the OWFs. Additionally, they observe (again) lower profitability for OWFs under the OBZ (or ONP) configurations compared to the HM.

While Kenis et al. (2024) demonstrated the impact of lower transmission capacities on prices and exported volumes in the OBZ, their analysis determined optimal HVDC capacities under varying unit electrolyser investment cost levels, which were then used as inputs for further study. Consequently, their analysis did not explicitly consider variations in HVDC transmission capacities ceteris paribus. This unexplored analysis allows for deeper exploration of offshore transmission variations, particularly given the dual functionality of hybrid assets. Investment decisions in HVDC transmission capacity for hybrid projects might not align with the theoretical optimal system configuration from a social welfare perspective (following Kenis et al. (2024)) but may instead be driven by the strategic choices of individual TSOs and governments involved in the project.

### 1.5.3 Literature on Mitigation Measures

The offshore electrolyser can thus be considered as a technological measure that could alleviate some of the price and volume risk. There are also several support mechanisms that could be implemented to address the risk coming from the institutional landscape. Laur et al. (2022) covered a number of regulatory instruments that could help safeguard a positive business case for developers. They specifically justify the implementation of mitigation measures for price and volume risks asses the effectiveness of the Financial Transmission Rights (FTR) and Contracts for Differences (CfD), and introduce the Transmission Access Guarantee (TAG) which is specifically aimed at mitigating the volume risk. Laur et al. (2022) argue that the TAG instrument is the preferred regulatory mitigation measure for volume risks since it concentrates on addresses the volume risk issue, avoids creating overcompensations and related problems, and is realistic and scalable operationally. PROMOTiON (2020) points out the FTR as effective hedging instrument to stabilize revenue streams and mitigate financial uncertainty, thereby addressing the price risk.

In response to this conclusion of Laur et al. (2022), Magid & Winge (2024) have analysed the impact of several different designs of the TAG instrument on mitigating price and volume risks for OWFs in an OBZ. Doing so, they first examined the reasons behind the reduction of Day-Ahead (DA) market access and the extent to which it generates price and volume risks for hybrids. On this they concluded that curtailment in the OBZ, and associated zero-priced hours, are caused by reductions in line capacity of transmission lines directly connected to the OBZ, as well as further away in the grid. While this study represents a commendable initial effort to model the effects that lead to price and volume risks using FBMC, it exhibits several limitations. These include the use of a limited grid topology, employing the SHC method instead of AHC, and relying on hourly snapshot analysis rather than simulating effects over extended periods, all of which suggest opportunities for enhancement. Recommendations for future research are to analyse the effectiveness of the TAG using more sophisticated energy system models that incorporate simulations over longer periods of time on an hourly resolution.

## 1.6 Research Questions and Thesis' Objectives

Combining the insights and recommendations from the discussed literature with the problem definition, this thesis aims to achieve several objectives. First, it seeks to decompose and operationalize the price and volume risks described in the literature to better understand the conditions under which they occur within the intricate dynamics of FBMC. Second, building on the quantitative analysis by Kenis et al. (2023, 2024), this thesis aims to extend the model to quantify and analyse the impact of various variables on the frequency and magnitude of these decomposed price and volume risks. The third objective of this thesis is to integrate technological mitigation measures into the model of Kenis et al. (2023) and apply regulatory mitigation measures to the model's outcomes to provide quantitative evidence of their effectiveness. Based on the recommendations for future research and untapped modelling exercises discussed in the previous section, primary variables considered in this thesis are the offshore grid topology of the hybrid project and onshore grid attenuations, since they potentially lead to price and volume risks. Additionally, the integration of renewable energy sources in the onshore markets is examined, as it likely increases the cannibalization effect in the OBZ, further exacerbating price and volume risks. Ultimately, the main objective is *to identify the key factors leading to price and volume risks for hybrid projects and to assess the effectiveness of their mitigation measures.* Therefore, the central research question of this thesis is:

***How do the offshore grid topology, onshore grid attenuations and the integration of renewable energy sources influence price and volume risk and to what extend do regulatory and technological measures mitigate these risks?***

The price and volume risks central to this research question are studied in the context of Hybrid Projects in an Offshore Bidding Zone, considering the intricacies and complexities associated with Flow-Based Market Coupling for cross-border capacity calculation and Advanced Hybrid Coupling for representing HVDC interconnectors in the market clearing process. By answering this research question, this thesis aims to develop a profound understanding of the price and volume risks associated with hybrid OWFs, identify the risk-driving factors, and quantify the severity and frequency of these risks, as well as the effectiveness of various mitigation measures. In doing so, it helps policymakers, industry actors, and TSOs better understand the underlying factors leading to price and volume risks and pinpoint the most severe risks, enabling them to proactively address these risk-driving factors during the design and implementation process of the first hybrid projects. This contributes to ensuring the timely and cost-effective development of hybrid projects, ultimately aiding in fulfilling the European Commission's

2050 offshore wind targets and realizing the North Sea's potential as the envisioned renewable powerhouse for European society.

The following four subquestions (SQs) have been formulated to aid in answering the main research question:

> **SQ.1**: *What are the specific Price and Volume risks emerging for hybrid OWFs in an OBZ under flow-based market coupling?*
>
> **SQ.2**: *What are Regulatory and Technological Mitigation Measures for Price and Volume risks and how could they alleviate the risks?*
>
> **SQ.3**: *What are the factors leading to the most frequent and severe price and volume risks and how do they impact the economic viability of OWFs?*
>
> **SQ.4**: *To what extent can Regulatory and Technological measures potentially mitigate price and volume risk?*

Answering these subquestions ultimately aids in answering the central research question of this thesis. Additionally, two deliverables are introduced in this thesis:

> **ID.1**: *Compel a comprehensive risk framework to navigate and categorise different price and volume risk types systematically, their conditions of occurrence, and their potential mitigation measures.*
>
> **ID.2**: *Create a replicable and structured modelling methodology that includes developing universal risk indicators to simulate specific grid topologies and dimensions of hybrid projects within the FBMC process.*

These intermediate deliverables (IDs) have been implemented for the following purposes. The first intermediate deliverable has been implemented to address the novelty and complexity of the new market design for hybrid offshore wind farms. Given that existing literature addresses and labels specific price and volume risks differently, a systematic approach is essential for navigating between risk categories and mitigation measures. This will aid stakeholders—including OWF developers, TSOs, and regulators—in gaining a clearer understanding of the complex concepts and mechanisms influencing these risks.

The second intermediate deliverable ensures that the modelling methodology applied in this research is both structured and replicable. This is crucial as the thesis employs a hypothetical grid topology (See Chapter 5) to illustrate and quantify the risks and their driving factors across multiple cases, thereby avoiding the complexities and intensive computational efforts associated with realistic European power system grid topologies. However, for future research it is desirable for risk analyses to be conducted using more realistic models that incorporate the entire CORE region and potentially other CCRs. This would allow developers to apply this methodology on a case-specific basis during the tendering process for hybrid projects. By achieving this intermediate deliverable, a scientific and structured approach is thus designed for future simulations, which developers can later use for their internal risk mitigation analyses.

## 1.7 Research Approach

This section details the research approach and the role of subquestions in answering the research question and achieving the research objectives. The research is divided into two phases, which are explained hereafter.

### 1.7.1 The Qualitative Desk Research Phase

The first phase serves to identify and categorise price and volume risks and mitigation measures through a literature review. It begins with establishing a theoretical foundation on FBMC, crucial for understanding the complex context in which the OBZ operates and distinguishing specific price and volume risks and their causes, detailed in Chapter 2.

Chapter 3 develops a risk framework to categorise risk types and potential mitigation measures, addressing ID.1. This involves analysing literature on price and volume risks to understand price formation mechanisms in the OBZ (Section 3.1), explaining and categorising these effects to determine risk (Section 3.2), thereby answering SQ1. Regulatory and technological mitigation measures are then identified, explained, and assessed for effectiveness (Sections 3.3), leading to a selection suitable for further analysis in the modelling phase, answering SQ2. The culmination of these steps is the Risk Framework (Section 3.4), providing a comprehensive overview of risk categories and mitigation measures for the modelling phase.

### 1.7.2 The Quantitative Modelling Research Phase

The second phase addresses the Risk Framework from phase 1 and uses it to extend the model from Kenis et al. (2023) to quantify the frequency and severity of the risks and ultimately determine the key factors leading to these risks.

The first step in this phase is model development, based on the open-access FBMC model by Schönheit et al. (2021) and the model by Kenis et al. (2023), retrofitted for OBZ analysis and written in Julia. The developed Methodology ensures a structured and replicable approach, addressing ID.2. This four-step methodology, detailed in Chapter 4, includes formulating, simulating, and analysing all cases, followed by an inter-case analysis to assess risk-driving factors. An ex-post analysis is conducted for regulatory mitigation measures to evaluate their effectiveness, while a specific case group is simulated for technological mitigation measures due to its impact on the DA market coupling outcomes.

## 1.8 Scientific Contribution

The scientific contribution of this thesis is multifaceted. Firstly, the model used to quantify price and volume risks, based on the work by Kenis et al. (2023), has been extended by integrating a flexible demand agent. Specifically, two new parameters—reflecting the willingness-to-pay for electricity and the installed capacity of demand—along with three new variables—reflecting the relative production of the demand agents and the upward and downward redispatch—have been added to the mathematical model. Additionally, several constraints have been extended and included, as detailed in section 4.2.2.

Secondly, this thesis introduces a detailed decomposition of price and volume risks, particularly distinguishing between the capacity calculation risk and capacity allocation risk within the volume risk. These decomposed risks have been operationalized by integrating metrics to measure their frequency and severity into the model's simulation process. A novel optimization problem, derived from the mathematical model by Kenis et al. (2023), has been introduced to operationalize the distinction between capacity calculation and allocation volume risks. Lastly, the risk mitigation instruments have been connected to the model.

Thus, the primary scientific contribution of this thesis is enabling the differentiation of curtailment by the capacity calculation and allocation steps in the FBMC process within the model from Kenis et al. (2023), a novel approach that has not been previously explored.

## 1.9 CoSEM Affiliation

This thesis is written in fulfilment of the requirements for the degree in Complex Systems Engineering and Management (CoSEM). It explores the challenges of integrating hybrid offshore wind farms into the European energy market, focusing on technical, regulatory, and socio-economic dimensions.

Technologically, the core focus is on hybrid offshore wind farms, integrating offshore wind farms and HVDC interconnector transmission cables to produce renewable energy and facilitate cross-border power trade. The study highlights engineering optimisation in FBMC, demonstrating advanced algorithms and grid management techniques for new market design implementations and addressing the economic and societal impacts of hybrid projects.

Regulatory analysis centres on the OBZ market design, examining how OBZs manage the integration of hybrid OWFs into the European electricity market, ensuring optimal cross-border electricity trading in compliance with European regulations. Additionally, regulatory instruments such as FTRs and TAG are assessed as risk mitigation measures to ensure the economic viability of hybrid OWFs.

Economically, the thesis evaluates the implications of price and volume risks on the profitability of hybrid projects from the perspective of offshore wind developers. It considers the interaction between supply and demand under scarce transmission capacity and bidding strategies in day-ahead markets based on marginal costs for generators and willingness to pay for consumers, which are all key economic principles implicit under FBMC.

The research addresses the complexities of socio-technological systems as hybrid offshore wind projects combine technical innovation with regulatory and market reforms. This thesis examines the socio-technical interface, focusing on the impact on societal goals like reducing carbon emissions and enhancing energy security. The multi-layered nature of these projects, from technological components to regulatory frameworks, exemplifies the CoSEM approach to managing complex systems.

Hybrid projects are inherently international and multi-actor endeavours, requiring collaboration among TSOs, governmental entities, wind developers, and industrial partners. The thesis emphasises coordinated efforts that transcend national borders, highlighting the role of multi-level governance and stakeholder engagement in the successful implementation of hybrid offshore wind projects.

By integrating CoSEM methods, tools, and techniques, this thesis advances technical knowledge and contributes to strategic decision-making processes. It provides insights into the interplay between technological advancements, market mechanisms, and policy imperatives, offering comprehensive solutions to contemporary socio-technical challenges in the energy sector.

## 1.10 Thesis Outline

Chapter 2 provides the theoretical background of the European electricity system and Flow-Based Market Coupling. Chapter 3 develops the Risk Framework, identifying price and volume risks and mitigation measures. Chapter 4 outlines the four-step methodology applied in this thesis. Chapter 5 describes the case definitions. Chapter 6 presents the results. Chapter 7 discusses the implications of the results and research limitations. Chapter 8 provides the conclusions and recommendations for policy makers, stakeholders and future modelling and research directions. Finally, chapter 9 entails a personal reflection on this graduation project.

# Chapter 2. Theoretical Background

Understanding the theoretical background is essential to comprehend the context in which hybrid offshore wind farms operate within the OBZ. This foundation is crucial for analysing the complexities of Flow-Based Market Coupling (FBMC) and Advanced Hybrid Coupling (AHC) that influence price and volume risks.

**Box 1: The Working Example Definition**

Throughout this thesis the following simple 5 nodal system will be used for explanatory purposes. There are three zones, 2 onshore zones and 1 offshore zone with only wind generation, depicting the OBZ.

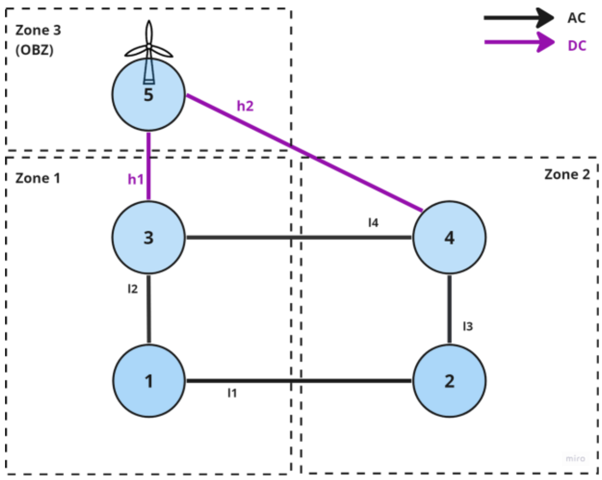


This chapter outlines the fundamental aspects of the European electricity system and market coupling principles (Section 2.1), necessary for understanding the system's multi-layered structure and market dynamics. It then details the FBMC methodological process (Section 2.2), explaining the sequence of steps for efficient cross-border electricity trading. Discussing Flow-Based parameters (Section 2.3) provides insights into key elements used in modelling approach applied in this thesis. Additionally, the concept of the flow-based domain is elaborated (Section 2.4) which stands at the basis in . Finally, the chapter explains the concepts of unscheduled flows and outages (Section 2.5), highlighting their impact on grid stability and market operations. These theoretical insights set the stage for the subsequent risk framework provided in Chapter 3.A simplified working example is occasionally used throughout this chapter for illustrative purposes (Box 1).

## 2.1 The European Electricity System and Market Coupling

To understand Flow-Based Market Coupling (FBMC), it is essential to grasp the fundamentals of the European electricity system. This system operates within a multi-layered system, including the physical electricity flow directed by economic interactions involving various actors ranging from electricity producers, consumers, and independent TSOs (See Figure 4).

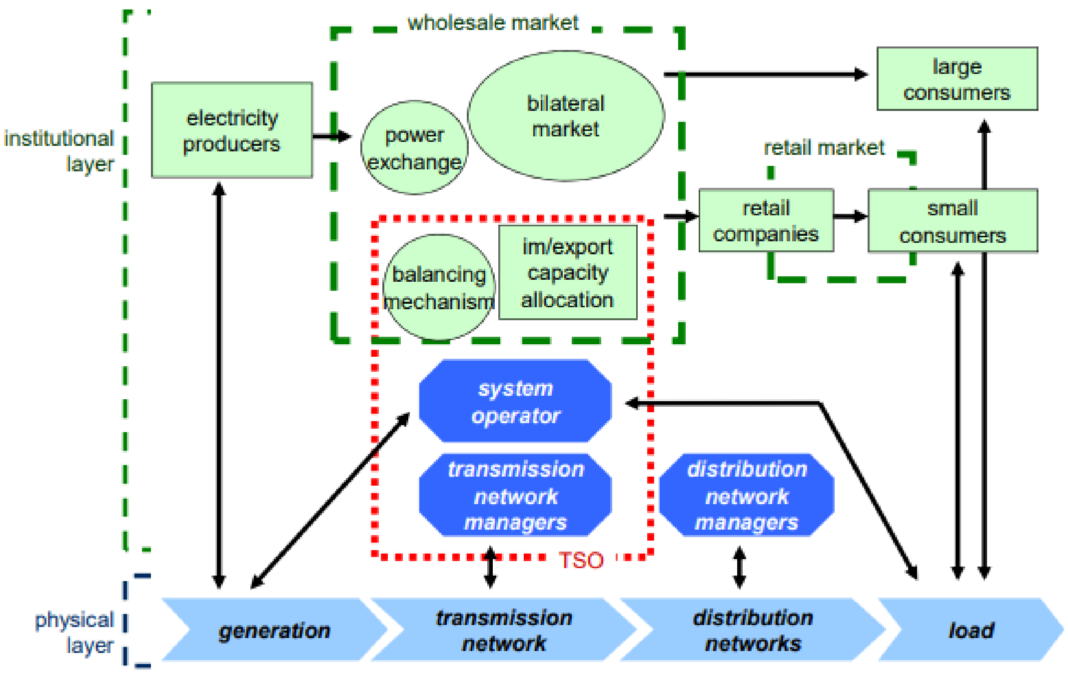


*Figure 4: Diagram of the electricity system's layers and actors (Source: De Vries et al., 2020)*

The system relies on short-term power markets, including the Day-Ahead (DA) market, Intraday market, and Balancing market, to ensure production and consumption are balanced at all times. The DA market, where electricity trading for the next day occurs by matching supply and demand bids, plays a crucial role in determining the market clearing price (See Figure 5). Following the DA market, the Intraday market allows for adjustments based on more accurate forecasts, and the Balancing market addresses real-time discrepancies between generation and consumption to maintain grid stability (De Vries et al., 2020). Within the scope of this thesis only the DA market is considered.


*Figure 5: Market results of the Day Ahead market in the Netherlands for 08:00-09:00 on June 5th, 2024. The aggregated demand and supply curves intersect at the market clearing price, being 99.22 €/MWh in this particular hour (Source: Epexspot, 2024)*

The market clearing process determines the optimal allocation of resources to meet demand at the least cost, whereby social welfare is maximised within the cleared market. In light of the European Union's aim for a fully liberalised, well-functioning, internal market for electricity trade (Directive 2019/944), the concept of market coupling is introduced, which is defined as "*the process of consolidating individual national markets to enable electricity trading over a broad geographical area*" – Schönheit et al. (2021).

Market coupling builds upon the principles of *capacity allocation* and *congestion management*. Capacity allocation involves assigning available transmission capacity on electricity networks to market participants, facilitating cross-border electricity trading (European Commission, 2015). This process determines the volume of electricity that can be transmitted between various areas or bidding zones, considering technical limitations and promoting efficient and secure electricity exchanges. The revenue generated by the TSO from capacity allocation is known as congestion income (European Commission, 2015, Art. 2). Congestion management involves strategies and procedures to manage and mitigate congestion on electricity networks (European Commission, 2015). Congestion arises when the demand for transmission capacity exceeds what is available, potentially causing bottlenecks and restricting electricity trade. Effective congestion management is aimed at optimising the use of existing infrastructure, preventing grid overloads, and ensuring the reliable and secure functioning of the electricity system.

Market coupling (MC) integrates multiple energy markets (or bidding zones) into one coupled market, making the trade of electricity across a large geographical area possible. This mechanism enhances the overall welfare of the day-ahead market by optimising the allocation of cross-border exchange capacity among various coupled bidding zones while adhering to the physical constraints of the electrical grid (Müller et al., 2017). By extending demand and supply orders beyond local market boundaries, MC enables transactions between sellers and buyers from different areas, constrained only by the capacity of the electricity network (NEMO Committee, 2019). The market coupling mechanism also establishes the electricity market prices and the net positions[4] of the coupled bidding zones. If the capacity of the cross-border transmission lines is unlimited, similar market prices could exist across all bidding zones (Müller et al., 2017). The primary advantage of MC lies in enhancing market liquidity, resulting in less volatile electricity prices. This benefits market players as they no longer need to obtain transmission capacity rights for cross-border exchanges; instead, these exchanges are facilitated by the MC mechanism. Participants submit a single order that matches the competitive orders within their market or with other markets (NEMO Committee, 2019).

Initially, the day-ahead market coupling methodology used was the *Available Transfer Capacity* (ATC) method to determine the available cross-border exchange capacity for the day-ahead market in the Central Western European (CWE) region. The ATC method requires TSOs to designate fixed capacities on their inter-zonal network connections for commercial trading. However, this method does not sufficiently consider transmission constraints within market zones, often resulting in conservative capacity allocations to limit internal congestion (Weinhold, 2021). Since 2015, the *Flow-Based Market Coupling* (FBMC) approach has been adopted in the CORE Capacity Calculation Region (CCR) (See Figure 6). Flow-Based Market Coupling refers to a sophisticated method of allocating cross-border transmission capacities by accounting for actual physical power flows and grid constraints, aimed at enhancing the efficiency of electricity trading across borders and ensuring better alignment with the physical state of the electricity network (Schönheit et al., 2021). The primary advantages of the FBMC method include increased transparency due to a clearly defined methodology for capacity allocation and the allocation of transmission capacity according to the net positions of each bidding zone based on

[4] Net positions refer to the net import/export of power from/to a bidding zone. A negative net position implies that the bidding zone is importing power, whereas a positive net position implies the export of power.

specific network elements, rather than bilateral agreements (Weinhold, 2021). Furthermore, FBMC leads to increased cross-border exchange volumes and price convergence among the coupled market, Furthermore, FBMC leads to increased cross-border exchange volumes and price convergence among the coupled market, especially beneficial in systems with high renewable integration and thus large price spreads and variability, although these effects tent to diminish in the long term (Ovaere et al., 2023). The improved cross-border trade and price convergence across coupled bidding zones are especially advantageous in systems with high renewable integration, which often exhibit significant price spreads and variability across zones. Consequently, FBMC supports the EC's goals of enhancing cross-border electricity connections and power exchange, thereby increasing security of supply and enhancing the integration of renewable energy sources in Europe’s power markets.

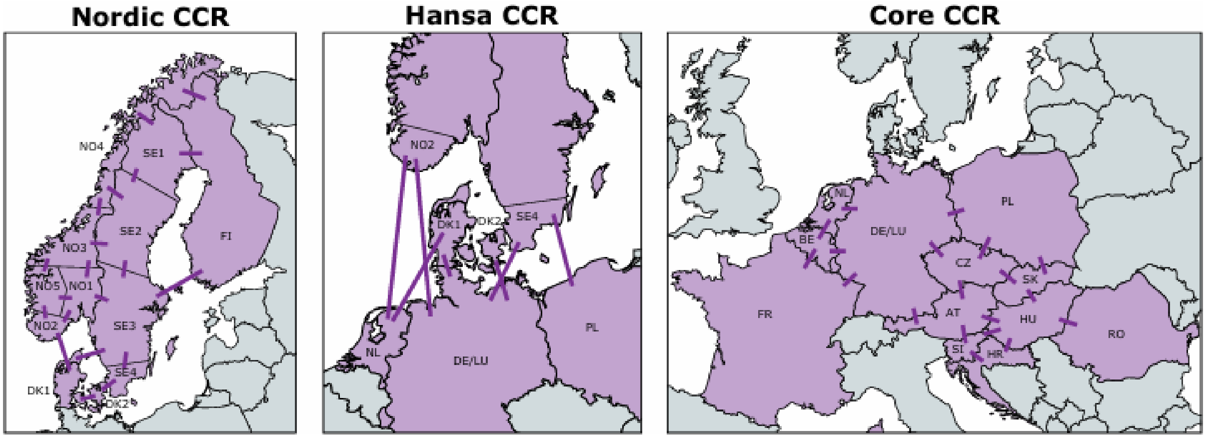


*Figure 6: Capacity Calculation Regions Nordic, Hansa and CORE. (Source: Schönheit & Marjanovic, 2024)*

The CORE CCR is currently the only region where the FBMC method is active in the Day Ahead markets, while the Nordic CCR is expected to go-live with FBMC in October 2024 (Nordic CCM Project, 2023). Other CCRs, such as the Baltic CCR (ENTSO-E, 2024c) and Italy North CCR (ENTSO-E, 2020c) continue to use the ATC (or NTC) method. It is, therefore, essential to adequately manage the impact of cross-zonal exchanges between CCRs. Each Capacity Calculation Region (CCR) calculates the cross-zonal capacity for its assigned bidding zone borders. However, cross-zonal exchanges at bidding zone borders outside a particular CCR also affect flows within that CCR's onshore grid. For instance, while the Norway-Netherlands border is managed by CCR Hansa, exchanges through the NorNed HVDC interconnector impact the onshore grids in both CCR Nordic and CCR Core, as the electricity travels through the meshed AC grid beyond the HVDC interconnector's landing points (Elia Group, 2024). To address these differing methodologies for handling cross-border power exchanges, namely the FBMC and ATC methods, the concept of *hybrid coupling* was introduced.

*“Hybrid coupling refers to the combined use of Flow-Based (FB) and Available Transmission Capacity (ATC) constraints in a single capacity allocation mechanism.”* – Core TSOs (2023). There are two types of hybrid coupling: *Standard Hybrid Coupling* (SHC) and *Advanced Hybrid Coupling* (AHC) (Müller et al., 2017). Standard Hybrid Coupling (SHC) involves TSOs granting access to scarce capacity on critical transmission lines based on forecasted power flows on the interconnectors. The unavoidable inaccuracies in these forecasts can lead to inefficiencies or increased redispatch costs. Advanced Hybrid Coupling (AHC) is a mechanism where HVDC power flows on the interconnectors within the Core FB area, and between the Core CCR and adjacent CCRs, are integrated into the market coupling algorithm. Essentially, the method of hybrid coupling describes how the HVDC transmission lines are incorporated in the FB capacity calculation and allocation process (explained in section 2.2). The key difference between the SHC and AHC methods is that the SHC method does not explicitly model and consider the impact of transactions over the HVDC interconnectors on the physical margins of the critical network elements in the FB region, whereas the AHC method does account for this impact (Schönheit & Marjanovic, 2024). To facilitate cross-border transactions while maintaining operational security, the

SHC method assumes the most constraining scenario of allocated transmission capacity to be reserved in the physical margins in the FB zones. In contrast, the AHC method allows the usage of physical margins to be determined by market decisions without prior reservation for operational security (Schönheit & Marjanovic, 2024). Specifically, conserving the impact of cross-border power flows on HVDC transmission lines on the AC grid is realised in AHC by introducing "virtual bidding zones" (VBZ) on the nodes of corresponding interconnectors (Schönheit & Marjanovic, 2024). By directly inputting this information into the market coupling algorithm, AHC enables non-discriminatory competition for the allocation of cross-zonal transmission capacity among all power flows within the Core FB region and across the CCRs where AHC is applied, aiming to maximise socio-economic welfare while ensuring fair access to scarce network capacity (Müller et al., 2017; Core TSOs, 2023). The introduction of AHC in the day-ahead market is planned in both Nordic CCR and Core CCR before the end of 2025 (Core TSOs, 2023; Nordic CCM Project, 2023).

In conclusion, understanding the European electricity system's unbundling sets the stage for exploring the complexities of Flow-Based Market Coupling. This necessity for independence among network operators, producers, and suppliers underpins the need for sophisticated market coupling strategies like FBMC and AHC, which balances supply and demand in real-time markets across geographical regions. The next subchapter will delve into the detailed steps involved in FBMC, examining its role in managing congestion, optimising capacity allocation, and enhancing grid efficiency.

## 2.2 The Flow-Based Market Coupling Process

As established in the previous section, FBMC involves complex management of cross-border electricity trading while considering physical grid constraints. A well-structured and sophisticated approach is thus essential to ensure that the electricity trading capacities calculated are accurate and reflect the actual capabilities of the grid. This way, the efficiency of electricity trading across borders is enhanced and closely aligned with the physical state of the electricity network. Since the cross-border exchange capacities and the price formation in the OBZ are the direct result of the outcome of the FBMC computation steps, it is important to understand the key elements within this methodological tool chain. Therefore, an explanation of the steps within the FBMC process is provided hereafter. The next section further explains the flow-based parameters that are used within the different steps of the FBMC process.

In reality, the FBMC processes in the Core CCR region exist of a set of subsequential and interlinked steps and sub-steps and involves multiple actors such as the Core TSOs, regional Coordination Centres and the Auction Office JAO (ENTSO-E, 2024b). For the scope of this thesis, it is sufficient to follow the guide to the theory of modelling FBMC from Schönheit et al. (2021). Modelling the flow-based market coupling (FBMC) process can be structured into three critical stages: the base case (D-2), day-ahead market clearing (D-1), and redispatch or congestion management (D-0). Figure 7 visualises these FBMC modelling steps, along with the information flow between these steps. Noteworthy is that in reality the FBMC entails much more (intermediary) steps and additional information flows than is represented in Figure 7 (See ENTSO-E, n.d.).

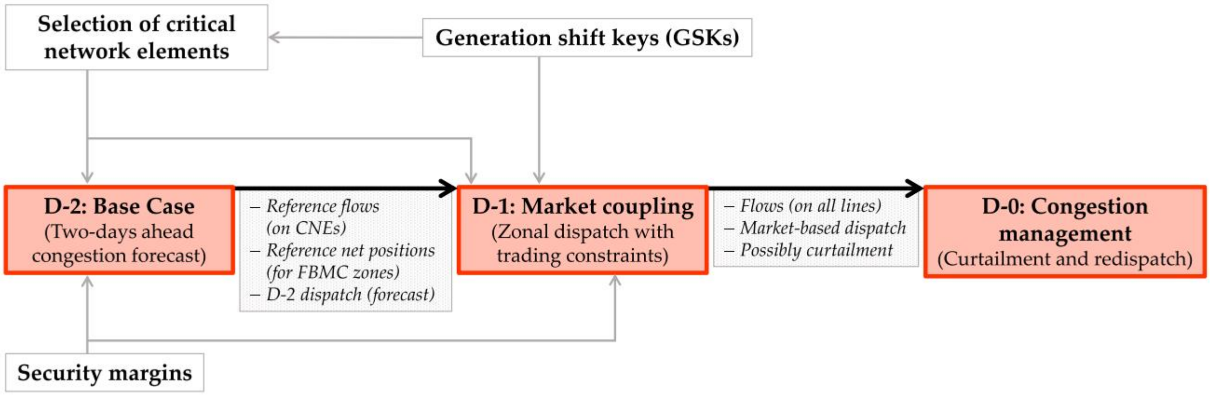


*Figure 7: The process steps and the flows of information within the modelling of flow-based market coupling (Source: Schönheit et al., 2021).*

The *base case*, also known as *D-2*, entails a forecast of the electricity system two days ahead of actual delivery. Essentially, this step in the FBMC process calculates the maximum available cross-zonal transmission capacities that can be made available for commercial exchanges between bidding zone (ENTSO-E, 2024b). Therefore, this step is commonly known as the *capacity calculation* step. The base case establishes reference values for expected flows on transmission lines and determines the expected dispatch of generators, based on load forecasts, renewable generation forecasts and historical data, while considering the effect of power flows in the physical network as represented with the help of Power Transfer Distribution Factors (PTDFs) and Generation Shift Keys (GSKs) (see Section 2.3). These reference flows on cross-zonal transmission lines and Critical Network Elements and Contingencies (CNECs) are then used to calculate the remaining available margin (RAM), i.e. the capacity available to the market for cross-border trade (Schönheit, et al., 2021). The outputs of the base case include the reference flows, reference net positions, forecasted dispatch, and calculated RAM values, which serve as primary inputs for the next step, the day-ahead market clearing. Additionally, the RAM values, along with the zonal PTDFs, form the flow-based domain (see Section 2.4), representing the operational space within which the market-clearing process is permitted to allocate cross-border transmission capacity.

The *day-ahead market clearing*, or *D-1,* is where actual market transactions take place based on bids and offers submitted by market participants. It aims to efficiently match electricity supply and demand across bidding zones while considering transmission constraints. The inputs for this step include bids and offers from market participants, the flow-based domain (transmission constraints) from the base case, and reference net positions from the base case (Schönheit et al., 2021). The outputs of the day-ahead market clearing step are the cleared market results, including cross-zonal trade volumes, electricity prices per bidding zone, and generation schedules for market participants. In modelling practices, the electricity price per bidding zone is determined by the shadow prices of the zonal power balance constraint within the day-ahead market clearing algorithm. The objective of the DA market clearing is to minimize generation costs (or maximise socio-economic welfare) and the power balance constraint stipulates that within each zone, the supply and demand bids and the net positions are balanced (Schönheit et al., 2021). Following the duality principles (Hillier & Liberman, 2015), a marginal increase in the power balance reflects the change in generation costs within the objective function. Since the zonal power balances are always active constraints (being equality constraints), the shadow prices of these active constraints thus reflect the electricity prices of the respective bidding zones.

The DA market clearing step essentially allocates the available cross-zonal transmission capacity, as determined in the base case, in such a way that the highest socio-economic welfare generating set of commercial exchanges is achieved across all the FB zones. This step is therefore commonly known as the *capacity allocation* step. Since 2014, this capacity allocation computation for all Capacity Calculation Regions (CCRs) is performed by a single price coupling algorithm, known as EUPHEMIA (acronym for Pan-European Hybrid Electricity Market Integration Algorithm). EUPHEMIA maximises overall social welfare across all coupled regions, taking into account the cross-border transmission constraints across the CCRs (NEMO Committee, 2019).

The *congestion management* step, also known as (real-time) *redispatch* or *D-0*, involves corrective actions taken by Transmission System Operators (TSOs) to manage congestion and ensure grid stability in real-time. While the day-ahead market clearing (D-1) aims to efficiently match supply and demand across bidding zones considering transmission constraints, congestion issues still occur due to differences between forecasted generation and power flows (D-2) and actual operational conditions (D-0), such as unplanned line outages, changes in (renewable) generation patterns and load/generation imbalances (Schönheit et al., 2021). Moreover, the zonal representation of the European electricity markets naturally comes with intra-zonal congestion patterns, necessitating the need for remedial actions after closure of the day-ahead market (Poplavskaya et al., 2020). Redispatch is one of the remedial actions that allow TSOs to manage these real-time congestion issues to ensure operational security of the transmission grid. In reality, the inputs for the redispatch process typically include dispatch schedules provided by Balancing Responsible Parties (BRPs), detailing the dispatch plans on an asset-by-asset basis (Poplavskaya, 2021), where in modelling practices the inputs are typically limited to the market-clearing results from the D-1 step (Schönheit et al., 2021). The outputs are instructions for market participants issued by TSOs to adjust generation schedules, activate demand response, or take other remedial actions to alleviate the real-time congestion. Thus, redispatch complements the flow-based market coupling process by providing a means for TSOs to manage real-time congestion issues after the day-ahead market clearing, ensuring grid security is maintained despite forecast errors and changing conditions.

To summarize, the base case (D-2) sets the stage by forecasting electricity system conditions, establishing reference flows and net positions, and calculates the available cross-zonal commercial exchange capacity, which is used in the day-ahead market clearing (D-1) where the commercial exchange capacities are allocated, based on market participant bids and system constraints to efficiently match supply and demand. The outcomes of D-1 then guide the congestion management step (D-0), where TSOs take corrective actions to address any identified congestion or grid constraints, ensuring overall grid stability.

## 2.3 The Flow-Based Parameters

There are several key Flow-Based (FB) parameters that er used in the computational steps. Before describing these parameters and their roles within the FBMC process, it is important to note that DC load flow approximation is used in FBMC, which is the linearization of AC power flows (Van den Bergh et al., 2014). Linearization of AC power flows simplify the complex nonlinear equations of electrical grids into linear models, focusing primarily on active power and generally omitting reactive power, which is often managed separately. This process assumes flat voltage profiles and minimal voltage deviations to enhance computational efficiency and facilitate quicker analyses. While this approach allows for straightforward modelling and is relatively insensitive to varying grid operating conditions, it also comes with notable limitations. The accuracy of linearized models may suffer in scenarios where reactive power or significant voltage deviations are crucial, potentially leading to discrepancies in system behaviour predictions. Consequently, linearized models are less suitable for in-depth studies that demand high precision in voltage control and reactive power management, where full nonlinear AC power flow analysis would be more appropriate. For the purpose of this thesis, the assumption of linearizing AC power flows is perfectly suitable since energy trading and pricing is primarily driven by active power flows, it allows for less computationally intensive modelling efforts and even though there are some accuracy limitations, the level of precision retained is generally sufficient for high-level analyses.

Coming back to the FB parameter, the first two parameters that are required for the FBMC process are the Power Transfer Distribution Factors (PTDF) matrix and the Generation Shift Keys (GSKs). The

PTDF matrix quantifies how a unit change in power injection at one node affects the power flow on each transmission line in the network (Schönheit et al., 2021). It provides a mapping between injections at network nodes and resulting power flows on transmission lines. There are two different types of PTDF matrixes, being the node-to-line PTDF (or nodal $nPTDF_l^n$) and the zone-to-line PTDF (or $zPTDF_l^z$). Both PTDF types are important input parameters used in the analysis of FBMC, but they serve a different purpose and describe different aspects of the power system. Nodal PTDFs provide a granular analysis of how changes in power injections at individual nodes affect transmission line flows, offering detailed insights into the local impacts on congestion and grid stability (Schönheit et al., 2021). In contrast, Zonal PTDFs aggregate this sensitivity across broader zones or areas, focusing on how shifts in zonal generation or demand influence the flows across interconnecting transmission lines (Schönheit et al., 2021). In order to calculate the zonal PTDF matrix, so-called Generation Shift Keys (GSK) are required. GSKs are estimations made by each TSO for the relationship between changes in generation at specific nodes and the overall net position of a zone within the power system, giving the nodal contribution to a change in zonal balance (Van den Bergh, 2016). The GSKs define how a change in import or export in a given bidding zone should be distributed to each production and load unit in that bidding zone. Appendix A provides the equations and further explanation of how the $PTDF_l^n$ and GSKs are computed, to ultimately derive the $zPTDF_l^z$ matrix, which is a required input parameter for the next FB parameter, the Remaining Available Margin (RAM) explained hereafter. One final consideration regarding the PTDF computation is the application of a threshold α to streamline the computational process. Given that the Core CCR contains thousands of transmission lines, it is common practice in FBMC modelling to select only those transmission lines for the zonal PTDF that are most likely to impact cross-zonal flows and manage congestion effectively. This approach focuses on crucial network elements (CNEs), enhancing system efficiency and manageability (Schönheit et al. 2021). However, the specific methods TSOs use to select CNECs and whether they apply a similar threshold approach remain unclear in practice.

The Remaining Available Margin (RAM) is another important FB parameter. The RAM parameter is introduced to account for the mismatch between commercial flows as determined by FBMC process during the DA market clearing step and the actual physical power flows occurring during the moment of operation caused by loop flows and transit flows (see Section 2.5). Additionally, not all energy is traded in the DA market clearing leaving room for intra-day trading. This difference between the commercial flows and the physical flows have to stay within the physical limits of the power grid, whereby TSOs compute the Remaining Available Margins (RAMs) of all the CNEs. The RAM for a transmission line indicates the additional power that can flow through that line without violating its thermal limit. RAM calculations use zPTDF values to estimate how changes in power generation or consumption in various zones affect the power flow on specific lines and the reference flows ($F_l^{ref}$) and reference net positions ($p_z^{ref}$) computed during the D-2 base case, ensuring that these flows remain within safe operational limits. The RAM values giving the commercial exchange capacity given to the market will never be equal to the thermal capacity of the transmission lines. This is due to the existence of loop and transit flows (see Section 2.5) and the reservation of a security margin on the transmission lines to account for uncertainties in the FB calculation, depicted by the Flow Reliability Margin (FRM) parameter (Finck, 2021). Another parameter is the Final Adjustment Value (FAV) for critical branch $l$, measured in megawatts (MW), which enables TSOs to incorporate expert knowledge and experience not accounted for in the formal FBMC methodology, such as adding a margin for intricate remedial actions (Van den Bergh et al., 2016). Lastly, the Adjustment for minRAM (AMR) is a parameter used to add a virtual RAM value if the minRAM target is not achieved. The minRAM criterium, commonly known as the '70%-rule', imposes a minimal fraction of commercial exchange capacity, specifically 70% (starting 2025) of the physical transmission capacity, should be made available to the market to stimulate cross-border trade (Council of the European Union and European Parliament, 2029). Where in reality this criterion specifically applies to cross-zonal transmission lines only, in FBMC modelling it is common practise to impose this criterion on all CNEs (Schönheit et al., 2021). According to JAO (2020), the RAM values can then be computed following:

$$RAM_l = \bar{F}_l - F_l^{ref} - FRM_l - FAV_l - AMR_l \quad (2.1)$$

Where the reference flow ($F_l^{ref}$) is determined by the product of the zonal PTDF value and the reference zonal net position ($zPTDF_l^z \cdot p_z^{ref}$) for all bidding zones, as this describes the expected power flow on the considered transmission line $l$ resulting from all expected commercial transactions between the bidding zones determined during the D-2 base case step. The obtained RAM values for all CNEs $l$ are key input parameters for the D-1 market clearing step.

A last parameter used in FBMC, specifically linked to the coupling of different CCRs via AHC as referred to in the previous section, is the Net Transfer Capacity (NTC) parameter for the DC lines. The NTC parameter is used to limit the bilateral export values from the flow-based area tot non-FBMC zones (Schönheit et al., 2021). The NTC limits the flow on cross-zonal HVDC interconnectors and is used via the AHC approach to explicitly model the impact of transaction over this interconnector on the CNEs in a given FB region (Schönheit & Marjanovic. 2024). Kenis et al. (2023) use the NTC parameter to limit the flows for all cross-border DC lines between zones, regardless of it being part of the FBMC area or not. Since the mathematical model from Kenis et al. (2023) will stand basis to the formulation of the FBMC model (Section 4.2.2), this approach of the NTC parameter is further assumed.

## 2.4 The Flow Based Domain

As mentioned in Section 2.2, a key output of the FBMC process, computed during the capacity calculation step (D-2) and based on the FB parameters, is the Flow Based (FB) domain. Essentially, the FB domain represents the set of feasible net positions (imports/exports) between bidding zones that can be accommodated by the transmission grid without violating any security constraints (Amprion, 2018). In other words, it defines the solution space in which the day-ahead market clearing (D-1) optimization operates for a given hour, ensuring compliance with physical grid limitations. From the perspective of an OWF located in an OBZ, the FB domain boundaries delineate the maximum possible exports during the D-1 market clearing (for a specific hour) from the OBZ to its adjacent bidding zones. These boundaries, graphically represented by the innermost linear lines enclosing the grey area in Figure 8, are determined by the active constraints (or CNEs) in the D-2 base case computation.

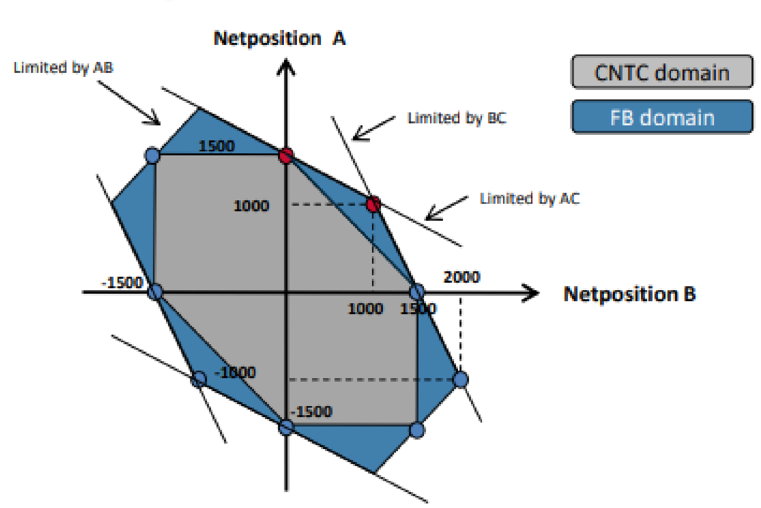


*Figure 8: Graphical representation of the Flow Based domain (Source: Statnett, n.d.). CNTC stands for the Coordinated Net Transfer Capacity market coupling, which is similar the ATC coupling as referred to in Section 2.1.*

The FB domain is geometrically defined for each critical branch $l$ by equations (2.2) and (2.3) (Li & Seguinot, 2017):

$$\Delta F_l = \sum_{l \in \mathcal{L}} zPTDF_l^z \cdot p_z \quad (2.2)$$

$$\Delta F_l \leq RAM_l \quad (2.3)$$

These formulas can then be combined to obtain a singular formulation of a linear equations for all AC lines $l$:

$$RAM_l^- \leq \sum_{l \in \mathcal{L}} zPTDF_l^z \cdot p_z \leq RAM_l^+ \quad (2.4)$$

The RAMs establish upper and lower bounds for each AC line $l$, represented by two linear equations: one for the upper limit ($RAM_l^+$) and one for the lower limit ($RAM_l^-$). These equations take the form $ax + by = c$ where $a$ and $b$ are the zonal PTDF values multiplied by the respective net positions $x$ and $y$ for the zones on the x-axis and y-axis, and c is the numerical RAM value. Using this approach, the FB domain for two zones can be plotted. In reality, however, this is more complex, as it represents a multidimensional space. The number of bidding zones in the FB area (e.g., 12 zones for the CORE region) corresponds to the number of dimensions in this solution space.

Furthermore, the net positions of a specific zone are constrained by the total export and import capacity across all cross-border lines. These lines can be both AC and DC lines, whereby both the NTC and the RAM values must be incorporated in the restriction on the zonal position. The limits of the net position for a zone can then graphically be represented by equation:

$$\sum_{h \in \mathcal{H}} NTC_{h,cb}^- + \sum_{l \in \mathcal{L}} RAM_{l,cb}^- \leq p_z \leq \sum_{h \in \mathcal{H}} NTC_{h,cb}^+ + \sum_{l \in \mathcal{L}} RAM_{l,cb}^+ \quad (2.5)$$

Equation (2.5) produces two sets of linear equations for the upper and lower limits, which are plotted on the Flow-Based (FB) domain graph. Equations (2.3) and (2.4) facilitate the construction of a two-dimensional graph that visualizes the FB domain, where each axis represents the net positions of two different zones. The number of zones involved in the system corresponds to the dimensions in the multidimensional space of the FB domain. For illustrative purposes, the FB domain is illustrated for the 3-zonal working example (See Box 1). Since the working example has 3 zones, there exist 2 ‘slices’ within the 3-dimensional solution space that together show the 3-dimensional solution space being the FB domain (Figure 9).

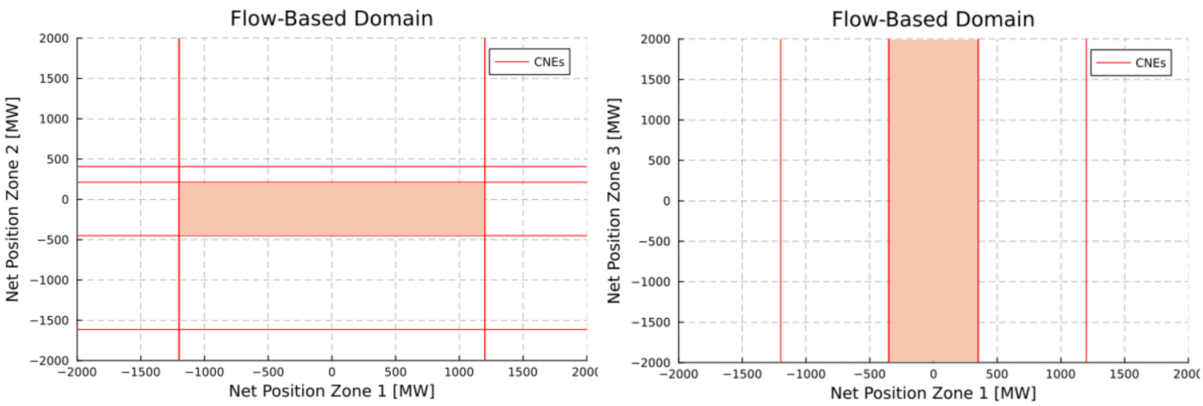


*Figure 9: The Flow Based domain of the working example (See Box 1) The left figure visualises the FB net positions of zone 1 and 2, the right figure of zone 1 and 3, together they make up the 3-D solution space.*

The innermost red surface area, enclosed by the CNEs, represents the Flow-Based domain for each of the two slices. Together, these two graphs depict a three-dimensional solution space. Since the zonal PTDF values of the OBZ are zero (Box 2), due to the absence of AC lines for distributing cross-border power flows and reliance solely on DC lines, the linear equations used in the graph visualization, based on formula (2.5), all reduce to zero. This is due to dividing by zero-valued PTDF values. However, this does not imply that the net position of the OBZ is unrestricted and can assume an infinitely large value; it is simply a consequence of using simplified formulas to visualize the Flow-Based domain.

## 2.5 Unscheduled Flows and Outages

There are two concepts in FBMC unaddressed so far that could influence the mechanisms at play within an OBZ under FBMC, being the concepts of unscheduled flows and line outages, explained hereafter.

For the first concept, unscheduled flows, it is important to acknowledge that transactions occur both within a bidding zone (*internal flows*) and between different bidding zones (*import/export flows*). Moreover, it is important to note that the commercial transactions taking place in the transmission grid between supply and demand nodes do not necessarily match the physical flows of electricity. This is because electricity flows through the grid according to Kirchhoff's first and second laws (Weibelzahl, 2017). Following Kirchhoff's laws, electricity injections are spread out across all parallel paths between the supply and demand agents within the transmission grid. Following these physical laws, it occurs that an internal commercial energy transaction within one bidding zone causes physical power flows in another bidding zone, which is referred to as *loop flows* (ENTSO-E, 2020b). These loop flows are inherent to any zonal market design (Amprion, 2018). Additionally, commercial exchanges between bidding zones (imports/exports) might lead to physical flows in other bidding zones, referred to as *transit flows* (ENTSO-E, 2020b). The difference between loop flows and transit flows is that transit flows are captured by the market clearing, whereas loop flows are not, making loop flows unscheduled flows and transit flows scheduled flows. The FBMC method is in particular more accurate in representing these loop flows in the market clearing algorithm (Ovaere et al., 2023).

Figure 10 below visualises the different power physical flows and commercial transactions happening in a typical power system.

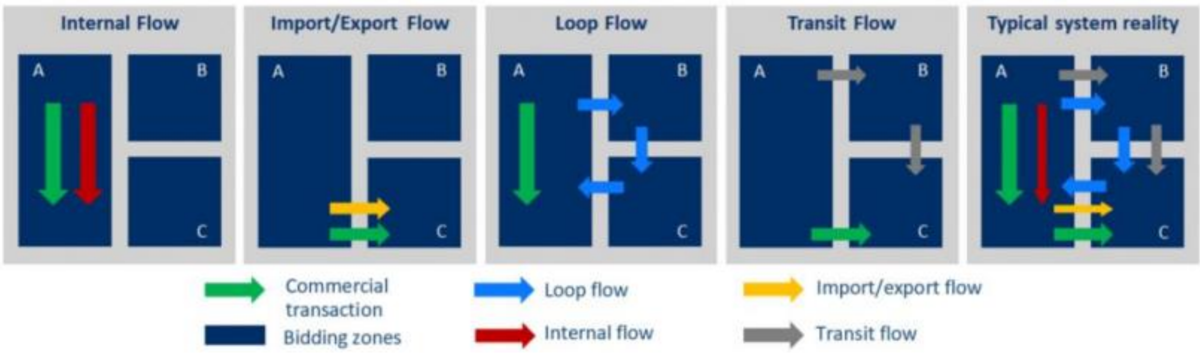


*Figure 10: Physical power flow categories resulting from different commercial energy transactions (Source: ENTSO-E, 2020b)*

To further illustrate these unscheduled flows, Box 2 represents an hour in which loop flows are occurring within the working example.

Considering that these unscheduled flows always take place, one can note that in the event of a single transmission line outage, there are implications for all power flows occurring in the transmission grid. Therefore, TSOs must always take into account that unplanned outages of elements in the system might occur. For this purpose, the N-1 security criterion is defined by CEER which essentially stipulates that the electric power network should remain operational and maintain system integrity despite the unplanned outage of "1 element out of n" (CEER, 2004). Adhering to the n-1 criterion within the context of FBMC implies that load outage distribution factors (LODFs) are used to adjust the regular PTDF matrices. LODFs account for the probability of line outages and indicate the additional flow on transmission lines caused by an outage (Schönheit et al., 2021). Incorporating these LODFs to account for possible outages thus restricts the flow-based domain due to an increased flow on specific lines due to possible outages. The CNEs are then updated with the adjusted PTDFs whereby they are referred to as critical network elements and contingencies (CNECs).

**Box 2: Illustration of Loop Flows**

Consider the working example having on node 1 a nuclear generator of 1000 MW (MC = 15 €/MWh), on node 3 a demand of 1000 MWh and on node 5 the OWF of 1000 MW (Mc = 0 €/MWh).
The AC transmission lines between nodes 1-2 and 3-4 have a Thermal Capacity (TC) of 200 MW, for lines between node 2-4 and 1-3 the TC is 1000MW, and both DC lines have a TC of 500 MW. The RAM and NTC values for the AC and DC lines respectively are set equal to the thermal capacities. For simplicity reasons an hour without wind is assumed.

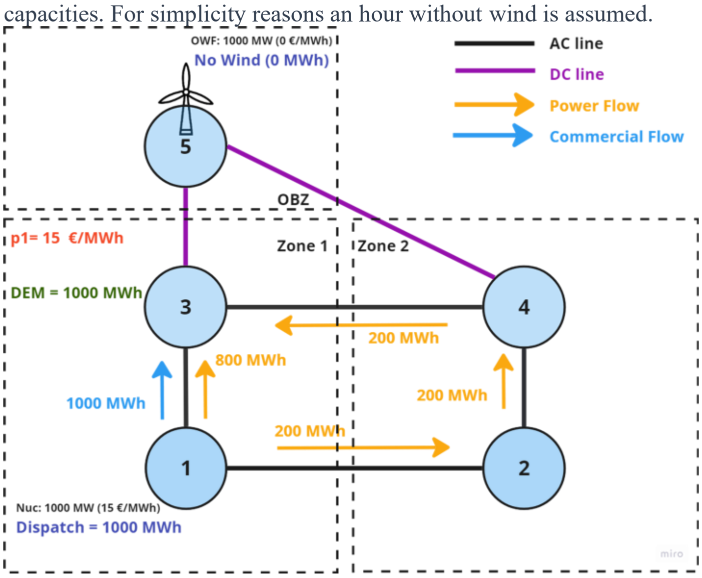


When the market is cleared for this hour, the nuclear generator dispatches its full installed capacity such to supply the 1000 MWh for demand at node 3, setting the price at its marginal costs of 15 €/MWh within zone 1. Even though the commercial transactions taking place here is between nodes 1 and 3 within zone 1, the power partially flows through the parallel path over nodes 2 and 4 through zone 2, representing the loop flow.

# Chapter 3: The Risk Framework

In this chapter, the risk framework around the price and volume risks is laid down. The chapter begins in Section 3.1 with the theoretical price formation in the OBZ according to the 'rule of thumb' as described in the literature, which stands as the basis for the understanding of price and volume risk. In Section 3.2, the price and volume risks as described in the literature are collected, explained and categorised such that a clear distinguishment can be made between the specific price and volume effects, effectively formulating an answer to SQ1. Section 3.3 dives into the regulatory and technological risk mitigation measures as described in literature, and explains how these risk address which risk category from Section 3.2, effectively providing an answer to SQ2. Finally, Section 3.4 integrates the insights gained from Sections 3.2 and 3.3 into a theoretical framework which is the end product of this chapter and which serves as a foundational guide for the methodology Chapter 4.

## 3.1 Theoretical Price Formation in the OBZ: The Rule of Thumb

To understand how the price formation in an OBZ under FBMC and AHC in theory occurs, it is important to reflect back on the definition of the hybrid project. As defined in Section 1.1, hybrid OWFs have the dual functionality of transporting the generated wind energy to shore and enabling cross-border electricity trade between the countries connected to the hybrid (Nieuwenhout, 2022). Having established in Section 2.2 how the FBMC process determines the dispatch of generators and cross-border trade capacity between bidding zones, it can be noted that these two functionalities in place in the OBZ compete with each other in the EUPHEMIA market dispatch and social welfare optimization algorithm. Where OWF developers naturally want to use the transmission capacity of the interconnectors to export their generated wind power in order to maximise revenues, TSOs want to use this same interconnector for cross-border trade to maximise congestion rents. The results is thus a 'battle' between the export of wind power and cross-border trade existing in the OBZ for the physical transmission capacity of the transmission lines connecting the OBZ to the shores. The limiting factor in this competition is thus the physical transmission capacity constraining both functions.

For the situation of the OBZ, where there is no or limited local demand, the price formation is thus purely the result of market coupling (TenneT, 2024). The day ahead market clearing determines the optimal combination all generation and demand bids to maximise commercial exchange while adhering to the grid's limitations as depicted in the Flow Based domain from the D-2 step. Therefore, the prioritization of OWF production versus cross-border trade within the OBZ depends on all factors influencing the DA optimization problem, including supply and demand bids, physical grid constraints both adjacent to the OBZ and onshore, price spreads between zones, weather conditions and unexpected outages. Despite these complexities, there exists a 'rule of thumb', describing the price formation in an OBZ.

In short, this rule of thumb by TenneT (2024) states that the price in the OBZ reflects the marginal cost of producing one additional unit of electricity and tends to converge towards the highest price of bidding zones to which an uncongested path exists. This rule of thumb definition line with the theoretical explanation of the price formation in an OBZ by Nieuwenhout (2022), stating that with the absence of demand in the OBZ, the price is determined by the marginal value of electricity, which is the determined by the highest value of electricity in a neighbouring bidding zone to which transmission capacity is still available. If capacity to the highest-priced zone is unavailable, the marginal value shifts to the next-highest priced zone.

To better understand this rule of thumb and to illustrate how this would translate to the formation of the price in the OBZ, Figure 11 represents several snapshots of the market clearing of an imaginary simple hybrid system, which is explained hereafter.

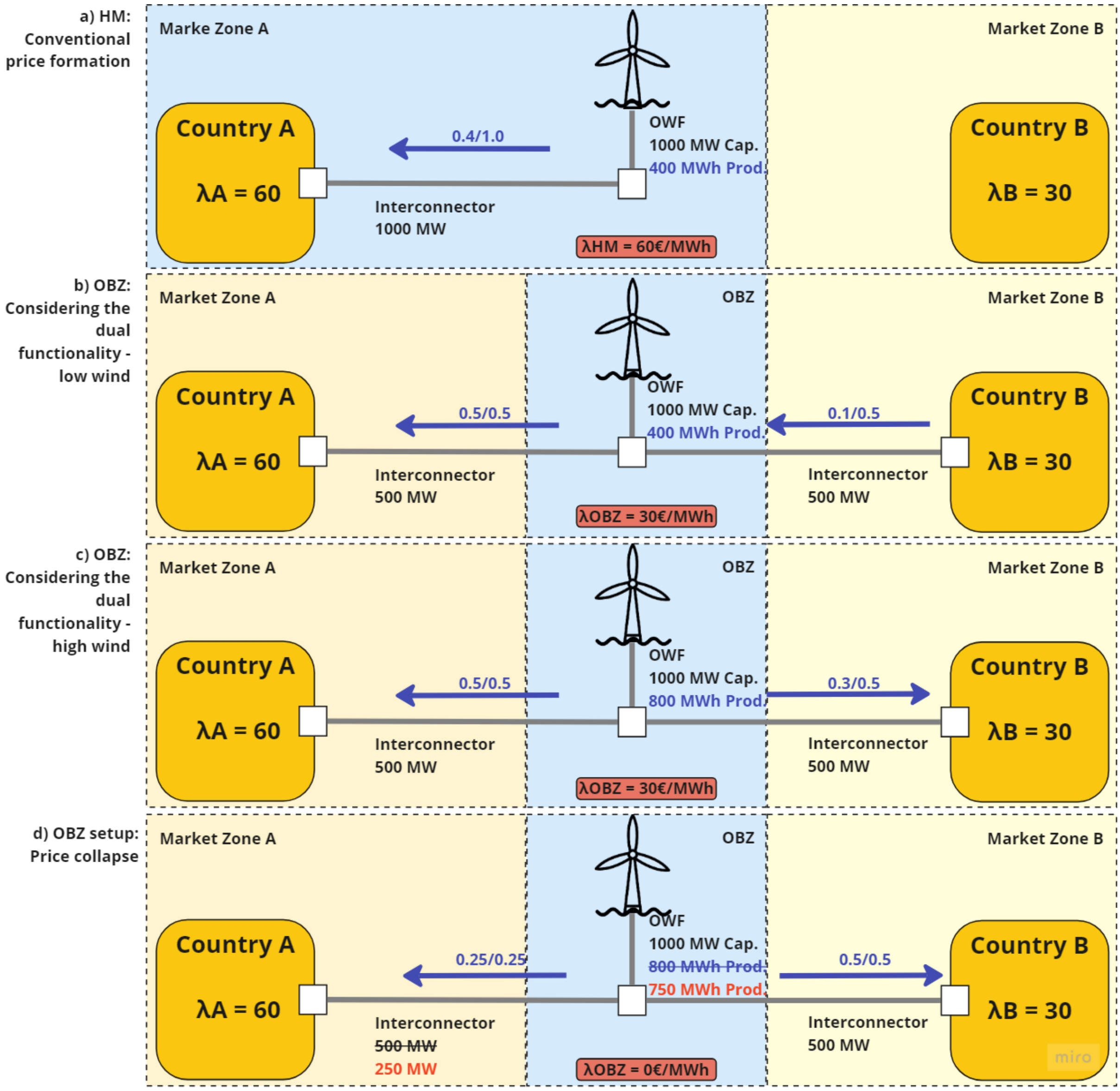


*Figure 11: Visualisation of the price formation mechanisms within an OBZ, coupled to two adjacent markets. Situation a) represents the conventional HM setup of a radial connected OWF. Situation b) represents a simple hybrid OWF located in an OBZ, where only the wind export is considered. Situation c) and d) illustrate the price convergence to the lower priced market for the OBZ with low and high wind production.*

In the example shown in Figure 11, market zone A has a higher electricity price of 60 €/MWh ($\lambda_A$), while market zone B has a lower electricity price of €30/MWh ($\lambda_B$**).** It is assumed that the OWF bids in the market clearing at marginal costs of 0 €/MWh.

For a radially connected OWF in the conventional HM setup, the OWF always receives the market price of the bidding zone it is located in, which would correspond to the $\lambda_A$ in Figure 11. However, when the OWF is connected to both adjacent markets, with its total transmission capacity equally split over both interconnectors, a different price formation mechanism occurs. If only the export of wind power to shore is considered out of the two functionalities of the hybrid, and the wind production in the OBZ is lower than the transmission capacity to the highest priced market, producing an additional unit of power in the OBZ would still be valued by the higher priced market, making the OBZ price $\lambda_A$. However, this is an unrealistic scenario because it ignores the second functionality of the hybrid: trade between bidding zones. Since the OWF bids with zero marginal costs, the market clearing is likely to first allocate transmission capacity for the generated wind power. Any remaining capacity can be used for cross-border trade, with exports from lower-priced country B to higher-priced country A (Figure 11b). This results in congestion on the transmission line between the OBZ and country A. Following the rule of thumb, the marginal value of electricity in the OBZ converges to the lower priced market B, as the additional unit of power is now valued by market B due to the available transmission capacity. Consequently, the OBZ price always converges to the lowest priced market.

During periods of high wind production (Figure 11d), when generating capacity exceeds transmission capacity to the highest priced market, the OBZ price also converges to the lower priced market, leaving no available transmission capacity for cross-border trade by the TSO**.**

In the last snapshot Figure 11d, a situation is considered in which the available transmission capacity on the DC line to market A is reduced. The reason for this reduction in available transmission capacity can have several reasons, which will be further elaborated on in Section 3.2.3. However, since the resulting price formation remains the same regardless of the reason of the reduction in the available transmission capacity, whereby the cause is neglected for now. In this particular hour, both transmission lines from the OBZ to the adjacent markets are congested and the OWF cannot produce its full potential capacity whereby it is curtailed for 50 MWh. This curtailed power of 50 MWh by the OWF reflects the volume risk, which will be elaborated further in Section 3.2.3. Following the rule of thumb, producing one additional unit of energy in the OBZ is in this situation not possible due to both lines being congested, whereby the marginal value of power in the OBZ converges to the marginal costs of the OWF. Under the assumption that the OWF bids in at marginal costs of 0 €/MWh, the price in the OBZ thus also becomes 0 €/MWh. This convergence of the electricity price in the OBZ to the marginal costs of the OWF is also known as the price collapse risk, which will be further defined in Section 3.2.2.

Additionally, the electricity price of the OBZ can be 'out of bounds' compared to the prices in the adjacent bidding zones, referred to as a non-intuitive price. Section 3.2.2 further elaborates on this price peculiar price formation.

In conclusion, following the Rule of Thumb as the theoretical price formation mechanism in the OBZ results in a price convergence for the electricity price in the OBZ to the lowest priced adjacent market in most situations. For situations with reductions in transmission capacity where the OWF cannot export its full potential wind power, a price converges to the marginal costs of the OWF occurs, which is assumed to be at zero. Following this rule of thumb mechanism would hold in theory for most situations, however, considering the principles of FBMC and AHC the practical outcome can deviate. As mentioned in Section 2.2, the electricity prices in the bidding zones are in modelling practices determined by the shadow prices of the zonal power balance constraints within the DA market clearing optimization problem. For the DA market clearing optimization that takes into account the FBMC and AHC principles, a set of equations directly or indirectly constrain the zonal net positions (See Section 4.2.2), and thus co-influencing the zonal power balance. This make that the actual price formation in the OBZ is more complex in reality than this rule of thumb constipates.

The next section further differentiates between price and volume risks, while keeping in mind the underlying principles of FBMC and AHC.

## 3.2 Defining the Price and Volume Risk

As mentioned in the Problem Statement (Section 1.4), the introduction of the European Target Model tailored to hybrid OWFs brings about several unique adverse effects, which could become risks for the developers under specific circumstances. Based on a literature review, this section identifies and explains how the intended system design and market setup potentially lead to adverse effects for developers and how these effects become risks, to ultimately distinguish and categorize specific risks types. Doing so, SQ1 will be effectively answered.

**SQ.1**: *What are the specific Price and Volume effects for hybrid OWFs in an OBZ under flow-based market coupling and how do these effects become risks?*

### 3.2.1 Introduction to Risks

Considering the entire system scope of hybrid OWFs, there are several risk categories developers might face, such as Technical and Operational risk, Financial risks, Environmental risk, Strategic and Business risk, Regulatory risk and Market risk (NSWPH, 2023). Of these risk categories, the market risk is to be considered in this thesis, referring to risks inherent to the overall market in which an investment is made and the specific risks related to the market design in place in which the investment will operate. In this context, all risk that emerge from the specific market design of the hybrid OWF located in an OBZ under FBMC with AHC are within the scope of this thesis.

The notions of *price* and *volume* risks are widely referred to as the two main market risks for developers within the literature and debate on hybrid OWFs located in OBZs. Generally speaking, *price risk* is defined as the uncertainty or potential for fluctuations in electricity prices that can impact the revenue streams and profitability of offshore hybrid projects (THEMA Consulting Group, 2020). *Volume risk* is be defined as the uncertainty or potential variability in the quantity of electricity generated or traded compared to the expected quantity, independent of price changes (THEMA Consulting Group, 2020). As these definitions for price and volume risks are rather broad, and different type of price and volume risks exists that emerge under different circumstances, the following three sections will discuss the specific price risks (3.2.2), volume risks (3.2.3) and the interacting price and volume risk (3.2.4).

### 3.2.2 Defining the Price Risks

The North Sea Wind Power Hub Consortium (2023) differentiates within price risk between the flat price risk and the locational basis price risk. The first of these two price risks, the *flat price risk*, is somewhat like the general definition of price risk as it refers to the uncertainty of the future absolute price level or capture price (NSWP, 2023). The uncertainty about the future prices and its fluctuation is not necessarily a risk only observed in an OBZ; all energy markets and commodities face this risk. However, due to the unique system design of the OBZ (small bidding zone with little or no local demand), there is an additional uncertainty with respect to onshore bidding zones (or the HM setup) on how the formation of the price levels and their fluctuations. This price risk will be referred to as the flat price risk.

The second of these two price risks, the *locational basis price risk*, refers to *"the risk that the price of a specific electricity contract will differ from the price of a benchmark or reference contract*" – NSWPH (2023). Elia Group and Orsted (2024) refer to this as the price spread risk and specifically express that the price difference between the generator located in the OBZ and the consumer located in the onshore zone complicates establishing power purchase agreements (PPAs) for offshore wind investments (Elia Group & Orsted, 2024). In short, this is the risk that the electricity price for the hybrid OWF in the OBZ could differ from the electricity price of the onshore bidding zones. While in practice the prices in the core region regularly converge due to the efficient FBMC in place, the risk mentioned here mostly originates from the different setup of the OBZ compared to the HM. The fact that the price in the OBZ could differ from the onshore bidding zones difficults the process of establishing electricity contracts or risk mitigation instruments, which did not previously exist in the HM setup. The price risk referred to as the locational basis price risk is thus not so much a risk of the fact that the price differs, but it is more about how to deal (contractually) with these price differences. Financial Transmission Rights could potentially hedge against this risk (Section 3.3.1.3). The location basis price risk is thus a risk that market actors have to take into account, but it is a not a market risk, whereby it will be further referred to as the *location basis price effect.*

Elia Group and Orsted (2024) introduced another risk, being the lower price level risk. The price risk referred to here is a consequence of the 'rule of thumb' price formation mechanism, as explained in Section 3.1, in which the electricity price in the OBZ converges to the bidding zone where the interconnector is uncongested, which results in the price of the OBZ structurally converging to the lowest-priced bidding zone (as naturally the interconnector to the higher priced bidding zone is the first to become congested due to the higher valued electricity). However, with the introduction of an OBZ under FBMC with AHC it is somewhat certain that the price in the OBZ converges to the lower priced zone in most hours since this reflects the efficient allocation of capacity in the market clearing algorithm. The lower structural price level is thus rather an adverse effect for developers than a risk, whereby this effect will be referred to as the *structural price convergence effect*. Moreover, the risk lies rather in the uncertainty that this rule of thumb price formation will not occur, which is described in the next two price risks.

Elia Group (2024) describe this unusual price formation as non-intuitive price formation. A non-intuitive price occurs when the capture price of the OBZ is 'out of bounds' compared to the prices in the adjacent bidding zones. Generally, market exchanges from the OBZ, whether due to wind or import/export activities, can lead to non-intuitive prices in different ways. If these exchanges place greater stress on the critical network elements of the involved CCR(s) compared to transactions between onshore bidding zones, the price within the OBZ must be reduced to ensure these transactions contribute to an optimal welfare solution. Conversely, if the impact of the OBZ on the critical network elements is lower or even alleviates stress, a higher price within the OBZ could still align with market exchanges that foster the optimal welfare solution. This price effect is unpredictable by simple economic reasoning and is the result of the introduction of AHC. Therefore, this (adverse) effect is considered the be a risk and will hereafter be referred to as the *non-intuitive price risk*.

The final price risk category is the price collapse risk. Price collapses refer to the situation when export capacity from the OBZ to the adjacent bidding zones is limited, whereby the price in the OBZ converges to the marginal value of electricity in the OBZ, which is (under perfect competition assumption) zero. As shown in Section 3.1, Figure 11d, this can happen due to direct congestion between the OBZ and adjacent markets, often from reduced transmission capacity of HVDC interconnectors. However, from a flow-based perspective (Chapter 2), price collapses occur whenever a restricted FB domain limits additional power exports from the OBZ. Both DC interconnectors and AC onshore transmission lines can limit the FB domain (Section 2.4), meaning that onshore CNEs, not just HVDC interconnectors, can also restrict OBZ export capacity, leading to price collapses. Developers have expressed concern about this risk since, during that hour, no revenues are earned (without any support mechanism in place). Conversely, TSOs state that '*price collapses…. will not be so likely to occur."*- TenneT (2024). Since both stakeholders have somewhat opposing positions on this risk, it is important to objectively assess this risk on its severity and frequency. This risk will be referred to as the *price collapse risk.*

### 3.2.3 Defining the Volume Risks

As mentioned, volume risk is the risk that the actual volume of electricity traded deviates from the anticipated volume, regardless of changes in price. Various type of volume risks exists, each influenced by distinct factors. Distinguishing these differences is crucial as they each require unique risk mitigation approaches. TenneT (2024) clearly identified 4 different volume risk categories, which will be used as the main input to the identification and categorization of volume risks.

The first volume risk arises from the technical unavailability or commissioning delays of HVDC interconnectors linking the Offshore Bidding Zones (OBZ) to onshore bidding zones. Such unavailability could be due to maintenance, forced outages, or delays in commissioning. This risk will thus be referred to as the *technical unavailability volume risk*.

The second volume risk indicated by TenneT (2024) occurs when total connection capacity of generators exceeds the maximum export transmission capacity of the (DC) interconnectors. This situation leads to a supply-demand dependency in the OBZ, where the demand can influence pricing if generation capacity exceeds interconnector capacity. A prerequisite for this volume risk to occur is thus the presence of a local demand agent in the OBZ, e.g. an offshore electrolyser for hydrogen production. In this setup, the price in the OBZ will be set by the willingness-to-pay of the demand agent if the generating capacity of the OWF exceeds the interconnector capacity to the adjacent bidding zones. This dynamic could potentially encourage strategic withholding of supply by offshore wind farms (OWFs) and demand by consumers to manipulate market prices, also known as gaming. Additionally, this setup places OWFs at risk related to fluctuations in the gas market, which impacts electrolysers dependent on gas transport and pricing. Since the emergence of this risk is only possible under the prerequisite of local demand existing in the OBZ, this risk will be referred to as the *local demand volume risk.*

The third volume risk is associated with the connection capacity of generators exceeding the export transmission capacity to the surrounding AC onshore grid, as seen under flow-based market coupling. Put differently, it is the risk that the total generated capacity by the OWF cannot fully be absorbed by the onshore AC grid which is subject to the grid constraints in the entire grid. In FBMC terminology: it is the risk when the maximum net position of the OBZ, determined during the capacity calculation or D-2 step, limits the available cross-zonal capacity against which the market coupling, e.g. the capacity allocation or D-1 step, will be performed. The maximum net position of the OBZ corresponds to the maximum allowed wind export that exists in the FB domain of the OBZ, where the boundaries of the FB domain are determined during the base case computation. If the D-2 optimization results in a calculated FB domain in which the total expected wind generation is not allowed to be fully exported, the D-1 optimization will reduce the cross-zonal capacity put available for the OBZ to ensure that the exported power from the OBZ stays within the FB domain. In this case, the maximum net position of the OBZ is thus limited by the available cross-zonal capacity, potentially leading to curtailed wind volumes. Since both the cross-zonal transmission lines and the onshore transmission lines restrict the FB domain, constraints in the onshore grid can thus also limit export capacity below the total connection capacity of OWFs. This form of congestion is generally expected to be temporary and resolvable through grid reinforcement or reconfiguration of the onshore bidding zone (TenneT, 2024). It is mentioned by TenneT (2024) and Elia Group (2023) that this risk is primarily pertinent when utilizing AHC, however it should be noted that under SHC this risk also arises and potentially be more severe, as the SHC method might lead to conservative capacity calculations whereby the FB domain is reduced with increased chance to curtailed volumes. This risk can also occur for other cross-border trades between larger (onshore) bidding zones. However, the impact of this risk may be more pronounced in OBZs than in onshore zones, due to the direct dependency of the OBZ on the ability of the onshore AC grid to absorb the exported power. Since the capacity calculation step of the FBMC procedure calculates the FB domain which primarily determines the volume that is allowed to be exported from the OBZ, this risk will be referred to as the *capacity calculation volume risk*.

The fourth volume risk involves reduced allocated interconnector capacity due to the FBMC processes. Even if the total transmission capacity is adequate to support all available offshore generation (so volume risk 3 is not active), the actual allocated capacity at the OBZ borders may be insufficient. Within the flow-based capacity allocation procedure, the OBZ competes with all other bidding zones (both onshore and offshore) for limited transmission capacity. Allocation decisions are driven by the optimization algorithm designed to maximize the economic surplus (or minimize costs) of all participating markets. If transactions in other zones or cross-border exchanges, including transits through the OBZ, generate more economic benefit, the OBZ might receive a smaller portion of the transmission capacity, potentially leading to unfulfilled sell orders. This risk for the developers is thus a result of the existence of more efficient market transactions by other bidding zones, determined during the capacity allocation step of the FBMC procedure, whereby this risk will be referred to as *the capacity allocation volume risk*.

### 3.2.4 Interacting price and volume risk

Price and volume risks are interlinked, often referred to as interacting price and volume risks (TenneT, 2024). This is particularly expected to be true for the price collapse risk and volume risk. As defined in sections 3.2.2 and 3.2.3, price collapses and curtailment by the capacity calculation both arise when the export capacity of the OBZ is limited. Therefore, if the export capacity of the OBZ restricts the OWFs to export all available wind power, the price in the OBZ collapses and curtailment by the capacity calculation occurs. These two risk are thus expected to coexist.

## 3.3 Identification and Selection of the Mitigation Measures

This subchapter dives into the mitigation measure as observed in literature. First the mitigation measures will be identified and explained, whereafter a selection will follow for those mitigation measures that will be considered within further analysis. Generally, there are two approaches to mitigate the risks for OWFs in an OBZ, regulatory mitigation measures, coming from the institutional framework, and technological mitigation measures, implementable by market actors. The regulatory mitigation measures are discussed in Section 3.3.1 and the technological in Section 3.3.2. Section 3.3.3 then explains the reasoning on the selection of the mitigation measures for further analysis. After completion of this subchapter, SQ2 will be answered effectively.

> **SQ.2**: *What are Regulatory and Technological Mitigation Measures for Price and Volume risks and how could they alleviate the risks?*

### 3.3.1 Regulatory Mitigation Measures

This section discusses the regulatory mitigation measures for price and/or volume risks as identified in the literature. For all measures discussed, it will be mentioned how the instruments work, how they would be applicable to the unique case of the hybrid OWF in the OBZ, and which risks, as defined in the previous section, they mitigate.

#### 3.3.1.1 Power Purchase Agreements

A widely used financial hedging instrument in power markets are (corporate) Power Purchase Agreements (PPAs) which contractually binds a consumer to buy the generated output of the producer. While officially this is not a regulatory mitigation measure as it is implementable by market actors without the intervention of a governmental entity, this hedging instrument is worth mentioning and explaining since mitigating risk directly by market actors themselves avoids potential timely and costly procedures to award or setup governmental support schemes.

PPAs are bilateral, long-term contracts between a power producer and an off-taker that specify the amount of electricity to be supplied at a predetermined price over a defined period (TenneT, 2024). There are two main types of PPAs: physical PPAs, where electricity is delivered directly (on-site PPA) or through the public grid (off-site PPA), and financial or virtual PPAs, where no physical delivery occurs. Instead, financial PPAs involve differential payments based on a market reference price and a contractually defined strike price. This allows PPAs to be designed across borders as purely financial products, enabling cross-border electricity trading (TenneT, 2024).

In the context of hybrid OWFs in an OBZ, PPAs can be adapted to address specific risks. In theory, the regular PPA structure could potentially addresses the flat price risk, the price collapse risk and the non-intuitive price risk by stabilising the revenue streams and thus hedging against price volatility. Furthermore, innovative PPA designs, such as the proxy generation PPA design, could address the capacity calculation and allocation volume risk because these PPAs "… *are settled based on the expected* *amount of energy a project should have produced based on the measured weather conditions, rather than the actual production*" – TenneT (2024). However, as mentioned earlier, the locational basis price effect inherent in the OBZ setup complicates the establishment PPAs between offshore generators and onshore demand agents (Elia Group & Ørsted, 2024), because one of the parties could still be exposed to the flat price risk when the wholesale prices of these markets do not move in tandem (TenneT, 20204). Additionally, without practical experience to assess the severity of risks for the first hybrid projects, PPA off-takers are likely to allocate an excessive share of risks to the hybrid OWFs, resulting in OWF operators struggling to establish PPAs with off-takers (Elia Group & Ørsted, 2024). Lastly, since PPAs are contracts between two market parties with no guarantee of implementation from the government, there is always uncertainty as to whether these contracts will successfully come into effect. Thus, while potentially address both price and volume risks, relying solely on market-based risk mitigation instruments like PPAs is uncertain for the initial hybrid projects.

In conclusion, depending on the specific design of the PPA contract, this mitigation measure could address the flat price risk and the volume risk by creating revenue stability, but there are still barriers to PPA adoption and design improvements to make to effectively and with certainty mitigate the risks for hybrid OWFs in an OBZ.

#### 3.3.1.2 Contracts for Differences

A second instrument are the Contracts for Differences (CfDs), which are financial agreements where payments are made between a seller and a buyer based on the difference between an agreed-upon strike price and a market reference price. In the electricity markets, CfDs typically involve long-term contracts between electricity generators and governments, providing a stable revenue stream for generators. When the market price is below the strike price, the generator is compensated for the difference, and when the market price is above the strike price, the generator pays back the difference (TenneT, 2024).

There are various CfD designs applicable to OWFs in an OBZ, each having their own specific advantages and disadvantages (For full analysis see van Delzen, 2023). The CfD design that is envisioned for the Belgian Princess Elisabeth Island hybrid project is the two-sided capability-based CfD (Elia Group, 2024), further considered here. This specific type of CfD guarantees a fixed price based on the potential, rather than actual, injection of electricity (Elia Group, 2024). The capability-based component is thus the power that the wind farm could have produced, even if the actual injection is reduced. The two-sided component implies that this financial arrangement functions in both directions: the regulatory body compensates the generator when the market price is lower, and conversely, the generator reimburses the regulatory body when the market price is higher.

The two-sided capability-based CfD effectively covers both price and volume risks. It stabilizes revenue by ensuring payments based on potential production capacity, thus protecting against revenue losses from not being dispatched due to market constraints or negative prices (Elia Group & Orsted, 2024). Specifically, the two-sided capability-based CfDs potentially address the flat price risk, the price collapse risk and the non-intuitive price risk, since the strike price is always received by the OWF owner. Moreover, due to the capability-based specification, all volume risk categories (except for technical unavailability volume risk) would be addressed.

Advantages of this approach include the predictability of revenue streams and reducing financing costs for OWFs, thereby encouraging investment in hybrid OWFs. However, potential disadvantages include possible market distortions, as widespread adoption of CfDs might impact the liquidity of other hedging options like Power Purchase Agreements (PPAs) and futures markets (Elia Group & Orsted, 2024). Especially this possible market distortion makes Dutch policy makers reluctant to implement this measure (Jetten, 2024). Additionally, the fixed strike price might reduce the incentive for wind farms to innovate or optimize operations based on market needs, as their revenue is secured regardless of market prices. Furthermore, there is a risk that the strike price set in a CfD may be higher than necessary to incentivize investment, especially as technology costs decrease over time. This overcompensation can result in excessive profits for developers at the expense of consumers, reducing the net social welfare.

#### 3.3.1.3 Financial Transmission Rights

A third regulatory instrument are Financial Transmission Rights (FTRs). As established in the Section 2.5, physical power flows and commercial power flows do often not match, whereby products in forward markets such as futures do not implicitly represent the transmission system, as they are financial instruments not binding for physical delivery. However, TSOs explicitly sell transmission products in the form of Long-Term Transmission Rights (LTTRs) interconnectors (Laur et al., 2022). LTTRs can be either physical or financial transmission rights, with Financial Transmission Rights (FTRs) being a potentially applicable regulatory risk mitigation instrument for hybrid OWFs in an OBZ. FTRs are financial instruments designed to hedge against locational price risks in electricity markets. Essentially, FTRs allow participants to secure the price difference between two neighbouring bidding zones in a specific direction. Typically, TSOs auction these contracts forward, and holders of FTRs are remunerated when the price spread between the zones is unfavourable (Laur et al., 2022). FTRs can shift the congestion income from TSOs to offshore generators, thereby addressing the transfer of socio-economic welfare observed in the OBZ (Kenis et al., 2023).

In practice, FTRs allow OWF operators to sell a contracted volume of electricity at market prices are compensated for when market prices differ from the contracted price in the FTR. Specifically, the FTR payment is determined by the contracted volume of the FTR times the difference between the contract price and the local market price. The OWF must purchase these rights, which can cover multiple assets, meaning the OWF could buy FTRs for all interconnections of the hybrid asset. The TSO then pays the OWF the price difference between the electricity markets on both sides of the interconnection, multiplied by the volume of transported electricity, up to a contracted maximum. The payout is capped by the total congestion rents received by the TSO (PROMOTioN, 2020). Applying FTRs to hybrid OWFs in an OBZ could involve a pre-allocation round where some FTRs are allocated for free to hybrid OWF owners in the OBZ before the remaining FTRs are auctioned to other market participants. This ex-ante distribution can be integrated into the competitive tendering process for connection contracts at the investment decision level (Laure et al., 2022).

Specifically, because the market price received by the OWFs in the OBZ is determined by the electricity price in the bidding zone where the contract is in force rather than the price in the OBZ, the FTR covers the price convergence effect, the price collapse risk, and the non-intuitive price risk for the portion of wind power produced contracted under the FTR. The FTR would not cover the volume risk as it only ensures that for the non-curtailed volume a fair market price is received (PROMOTioN, 2020). This is immediately a disadvantage of this instrument as the compensation is only provided for the electricity actually sold. If there are operational deratings (albeit during the capacity calculation or allocation step) or failures of the interconnection, the OWF will not be compensated for the curtailed volume under an FTR (PROMOTioN, 2020). Another disadvantage of FTRs is that they are currently only auctioned with delivery periods up to a year, whereby this measure would require either re-allocation rounds or regulatory changes if it is to be implemented as a long-term risk-hedging instrument for the OBZ (Laure et al., 2022).

Lastly, Laur et al. (2022) indicate that FTRs could lead to overcompensation for offshore generators. This is because they argue that the primary goal of suitable mitigation measures for hybrid assets in the OBZ is to compensate for the operational deratings, referring to the reduction in transmission capacity to shore from the OBZ, whereby curtailment takes place and potentially the price collapses to zero. Having an FTR in place would mean that the OWF owner would receive compensation whenever the price in the reference zone exceeds the price in the OBZ and not solely when reductions in transmission capacity take place. Noteworthy is that this notion assumes that the FTRs are (partly) handed out for free, as highlighted by Laur et al. (2022). However, if the FTRs are extended in their current form, overcompensation would not occur, since a fair price for the transmission rights would be paid through auctions.

#### 3.3.1.4 Transmission Access Guarantee

The last regulatory option is the Transmission Access Guarantee (TAG), which is an instrument proposed by Laur et al. (2022) that is specifically designed for hybrid OWFs. The TAG aims to mitigate the volume risk by guaranteeing that the total export capacity of the offshore bidding zone (OBZ) is always at least equal to the total net installed offshore renewable generation capacity. If this capacity cannot be met due to operational reasons, a compensation mechanism is put in place. The compensation paid to the offshore generator is calculated based on the price difference between the reference bidding zone and the OBZ, multiplied by the total available offshore generation. This ensures that generators are compensated for any loss in revenue due to reduced transmission capacity. The idea is that this compensation is paid by the TSOs responsible for restricting network elements, encouraging them to limit transmission capacity only when the benefits to the system outweigh the opportunity costs for offshore generators. The payments from the TSO to the OWF operators would have to come from the congestion income, thereby the TAG aims to tackle the social welfare transfer inherent to the OBZ's setup by reallocating the congestion income to the OWF operators.

Within the definition of the TAG of Laur et al. (2022), the TAG would be activated when the Flow-Based domain of the OBZ does not contain a clearing point through which the full wind capacity can be exported. In other words, if the transmission grid is physically unable to absorb all generating capacity of the OWF, the OWF will receive compensation for all its potential export capacity. This would thus effectively cover the capacity calculation risk. As explained in Section 2.4, the FB domain is determined by the most restricting CNEs, which can both be the RAMs of AC lines in the adjacent onshore bidding zones, as the available transfer capacity on the DC lines connecting the hybrid OWF to shore. Therefore, in case of activation of the TAG the compensation should be paid by the TSO responsible for the CNEs restricting the FB domain which lead to the inability of the OWF to export all of its generated capacity (Laur et al., 2022). In theory this could involve a TSO in a bidding zone not directly adjacent to the OBZ, but in practice it is expected that the most restricting CNEs are those connecting the OBZ and those located in its vicinity, whereby the local TSOs are most of the time the responsible party for the TAG compensation.

Advantages of the TAG include the stabilization of revenues for offshore generators and the avoidance of endangering system reliability since curative measures can still be employed. According to Laur et al. (2022) it as a simple, transparent measure directly targeting the issue of transmission capacity reductions. Thus far, it is also the only instrument proposed that specifically aims at tackling the volume risk. However, there are several concerns raised by other stakeholders regarding the TAG.

TenneT (2024) raise the issue that compensation through congestion income is likely to be ineffective. Congestion income is inherently unstable and allocated to various priority objectives set by NRAs, such as reducing consumer tariffs, investing in new transmission capacity, or addressing existing congestions. Consequently, the amount available for offshore generators would be highly variable and unreliable for providing consistent revenue. Therefore, TenneT (2024) states that this form of compensation would not adequately hedge offshore generators' volume risk, necessitating additional public support mechanisms.

Additionally, ENTSO-E (2023b) raise the concern that offering a guaranteed and regulated income via TAG to selected commercial market participants shields developers' risk premiums for volume risk from competitive market forces, hindering optimisation through competitive tendering. As a result, TAG fails to provide transparent investment signals for offshore hybrid projects and does not support the goal of cost-efficient deployment of offshore renewable generation.

Another issue that could arise is that with the implementation of the TAG, TSOs could have a new incentive to be less restrictive in the FBMC domain calculation. After all, enlarging the FB domain of the OBZ could potentially create a clearing point in which all produced wind volume could be exported, whereby no curtailment occurs and thus the TSO would not have to compensate the OWF operator via the TAG from congestion income. The consequence is that with this enlarged FB domain likely additional redispatch operations are needed, whereby the costs would shift to the consumer.

## 3.3.2 Technological Mitigation Measures

In Section 3.2.3 the local demand volume risk was defined. However, in Section 1.5.2 it was noted that local demand agents could potentially play a role in reducing curtailment and increasing prices in the OBZ. Therefore, first is explored how this local demand volume risk could become an opportunity. Thereafter, several technological options for local demand agents are discussed. Lastly, it is discussed which risks the local demand agent could potentially address.

### 3.3.2.1 Transforming the Local Demand Volume Risk into an Opportunity

As noted earlier in Section 1.5.2, Kenis et al. (2024) indicated that offshore demand agents, e.g. offshore electrolysers, could act as a price and volume risk-mitigating entity as they could reduce curtailment and increase the price in the OBZ, leading to an improved business case for OWF developers. Electrolysers' presence in the OBZ reduces curtailment and the necessity for congestion management actions by acting as electricity consumers at the same node where wind power is generated, leading to less frequent zero price hours (Kenis et al., 2024). Where TenneT (2024) flagged the presence of local demand in the OBZ as a risk, defined in Section 3.2.3 as the local demand volume risk, Kenis et al (2024) foresee an opportunity for offshore electrolysers to act as mitigation measure. Since subquestion 2 aims at identifying mitigation measures for price and volume risks, it is worthwhile to address the specific issues within the local demand volume risk indicated by TenneT (2024), to effectively transform this risk into an opportunity and later explore its effectiveness.

The specific risks indicated by TenneT (2024) within the local demand volume risk are in the nature of potential gaming and the additional level of uncertainty due to the dependence of a fluctuating gas market. However, for the latter this risk is present in any onshore market zone, whereby it is not so much of an additional risk for an offshore demand agent in the OBZ. The indicated risk of gaming in this specific setup would an exploitation of market power by the supply and or demand agents participating in this strategic withholding. While officially strategic withholding in electricity markets is prohibited by the Regulation on Wholesale Energy Market Integrity and Transparency (European Commission, 2020c), due to the limited market participants in the OBZ this could still form a problem. Nevertheless, it is reasonable to assume in the scope of this thesis that there will be no gaming within the OBZ. Under this assumption, the electrolyser operator would bid into the market with its Willingness-to-Pay and the OWF operator with its marginal cost. Within this context, the electrolyser could still act as an risk mitigating entity without raising gaming concerns. Regarding the second aspect of local demand volume risk—the influence of the gas market and the dependency of the electrolyser on the infrastructure and pricing of transportation—this thesis will not address these factors. Optimizing the interplay between the electricity and gas systems would require extensive research which is beyond the scope of this study.

In conclusion, the local demand volume risk could be transformed to a opportunity, assuming that the is no gaming nor direct influence from the gas market at play.

### 3.3.2.2 Options for Local Demand Agents

In theory, any type of demand agent could serve as a potential technological mitigation measure for the price and volume risks in the OBZ. Instead of relying solely on an electrolysis device for hydrogen production and its associated dependencies on the hydrogen market and supporting transportation infrastructure, hydrogen production offshore could be combined with nitrogen extraction from the air to produce ammonia, which is from a thermodynamic point of view a much better energy carrier whereby it is easier and less costly transportable and storable (Arellano-Prieto et al., 2022). In the future, hybrid offshore wind farms might be located on offshore hubs or energy islands (NSWPH, 2022), whereby the possibility arises for local demand for ammonia at those energy islands since ammonia is seen as an attractive and low risk choice for a sustainable marine fuel for the shipping industry (Alfa Laval et al., 2020).

Additionally, energy storage technologies deployable offshore could act as temporary demand agents. Suitable technologies include Battery Energy Storage Systems (BESS), such as Lithium-ion or Lead-Acid batteries (Arellano-Prieto et al., 2022), Pumped-Hydro Storage (PHS) or compressed air energy storage (CAES) systems. Additionally, underground hydrogen storage in depleted gas reservoirs is possible solution (Muhammed et al., 2023). Especially the Liquid Piston technology for CAES is promising in the context of offshore wind farms as these isothermal storage systems are placed sub-sea thereby enhancing the heat exchange due to the cold-water environment with high heat capacity (Gouda et al., 2021). Moreover, innovative concepts of PHS specifically designed for submerged applications, such as the Ocean Grazer (Ocean Grazer, n.d.), are potential candidates for utility scale energy storage at offshore wind farms. However, due to the limited energy consumption potential of storage devices, their role as a demand agent to avoid structural congestion might be restricted. Moreover, since storage devices use the same transmission capacity to export their stored energy, the interplay between OWFs and these storage devices must be closely aligned to act as demand agents during times that can influence price formation the most. This area complicates the deployment of storage devices to act purely as a mitigation measure against the price and volume risks in an OBZ.

To conclude, energy conversion technologies (or Power-to-Gas; PtG), such as electrolysers to produce hydrogen (or ammonia), could act as a structural demand sink within the OBZ, thereby potentially mitigating price fluctuations, non-intuitive price forming, price collapses and curtailment due to both the capacity calculation and allocation risks. Arguably, they could mitigate the technical unavailability risk if the unavailable transmission capacity does not exceed the power consumption at maximum production. Energy Storage Technologies (EST) could potentially mitigate the same risks (except for technical unavailability risks), but to a limited extent as they primarily shift the exported power instead of consuming it.

### 3.3.3 Selection of the Mitigation Measures

Table 1 provides an overview of all risk mitigation measures discussed and indicates the specific risks that they (partially) mitigate.

*Table 1: Overview of the Mitigation Measures and the risks they address. Green checkmarks indicate potential complete mitigation of the risk, black checkmarks partial mitigation, red crosses no mitigation.*
**Provided the design is a is 2-sided capability-based CfD*
***Provided the design is a proxy generation PPA design*
****Depending on the (yet t.b.d.) TAG design.*

| | **Risk Category** | **PPA** | **CfD*** | **FTR** | **TAG** | **PtG** | **EST** |
|---|---|---|---|---|---|---|---|
| **Price Risk** | Flat Price Risk | ✓ | ✓ | ✓ | ✗ | ✓ | ✔ |
| | Non-intuitive Price risk | ✓ | ✓ | ✓ | ✗ | ✓ | ✔ |
| | Price collapse risk | ✓ | ✓ | ✓ | ✗ | ✓ | ✔ |
| **Volume risk** | Technical unavailability | ✗ | ✗ | ✗ | ✗ | ✓ | ✗ |
| | Capacity Calculation Volume Risk | ✓** | ✓ | ✗ | ✓ | ✓ | ✔ |
| | Capacity Allocation Volume Risk | ✓** | ✓ | ✗ | ✓*** | ✓ | ✔ |

After having identified the regulatory and technological mitigation measures and determined how each measure potentially mitigates which specific risk, a selection can be made for the mitigation measures that are best fit for the unique situation of the hybrid OWF in the OBZ to be considered in further analysis. The effectiveness of the selected mitigation measures will then be determined during the modelling phase of this research, where their quantitative effect on the price and volume risks can be observed.

Regarding the regulatory mitigation instruments, the FTR comes out as the preferred mitigation measure for the price risks and the TAG is potentially best suited to specifically mitigate the volume risks. PPAs could potentially address the price risks and the capacity allocation and calculation volume risks (Section 3.3.1.1). However, this instrument is not guaranteed to be established for the first hybrids due to the lack of governmental guarantees and market parties potentially incorporating high risk premiums. CfDs could potentially cover (almost) all risks, and the Belgian hybrid project Princess Elisabeth Island is likely to implement the 2-sided capability-based CfD (Elia Group, 2024). However, since Van Delzen (2024) extensively assessed various CfD designs applicable to OWFs in an OBZ, further analysis of this measure is less interesting from a scientific contribution perspective. This leaves the FTRs and the TAG, which together, could be a very suitable combination of regulatory instruments that each cover part of the price and volume risk. Additionally, as mentioned the OBZ shifts social welfare form the OWF operators to the TSOs and in the end, the FTR and the TAG both reallocate congestion rents.

Taking the FTR and the TAG as the regulatory mitigation measures to analyse, further specification on their design must be made. For the design specifications of the FTR, the FTR design as explained in PROMOTioN (2020) will be taken, as further specified in the methodology (Section 4.2.3). For the TAG further specification on its design can be made based on the most recent amendments of the European Commission's Electricity Market Design (EMD) Regulation (European Parliament & European Council, 2024). As stated in this amendment, TSOs should compensate for reduced transmission capacity for the hybrid project in case where "*they either have not made available the capacity agreed in the connection agreements on the interconnector or have not made available the capacity on the critical network elements pursuant to the capacity calculation rules laid down in Article 16(8) of Regulation (EU) 2019/943, or both.*" If this capacity on the interconnector or the CNEs has been made available, the TSO does not have to pay compensation. This definition indicates the possibility that transmission capacity for the hybrid can also be reduced due to the capacity allocation risk, in which situation the TSO does not have to compensate the hybrid asset. Additionally, "*Compensation should be payable either if the available transmission capacities are reduced to the extent that the full amount of electricity generation that the offshore renewable electricity generation plant would have otherwise been able to export cannot be delivered to the surrounding markets, or where, despite being able to export, there is a corresponding price decrease in the offshore bidding zone due to capacity reductions as compared to without-capacity reductions, or both.*" This means that it is a capability-based instrument, similar to the capability-based CfD, ensuring that any price depressions or potential price collapses in the OBZ resulting from capacity calculation volume risks will be compensated. Additionally, the "polluter pays" principle will be used as the cost-sharing rule, meaning that the TSO responsible for the volume risk will be responsible for paying the compensation. It is also emphasized that double compensation for the same risk, such as through CfDs, should be avoided. Additionally, it is indicated that the compensation measure may have conditions under which it may expire, such as the existence of sufficient demand in the OBZ (e.g., a large electrolyser) or a sufficient number of markets for the risk to disappear. The exact details of the TAG are to be published through the amendments to Commission Regulation (EU) 2015/1222.

For the technological mitigation measures, hydrogen and ammonia production technologies come out as the preferred options as they potentially mitigate all risks. Moreover, the energy storage solutions could be more complicated to model due to their limited energy capacity and the usage of the same transmission capacities as the OBZ, whereby this measure is not further regarded. As for the other two options, the production of hydrogen or ammonia offshore, the latter requires the production of hydrogen for its chemical process, whereby looking solely at hydrogen would be the best option for simplicity purposes. Electrolysis as a demand agent is thus chosen as the technological mitigation measure.

## 3.4 The Risk Framework

Having established the specific price and volume risk categories in Section 3.2, followed by the identification, explanation and selection of the risk mitigation measures in Section 3.3, the insights gathered in these sections can now be combined into a Risk Framework. Doing so, intermediate objective 1 is achieved.

> **IO.1**: *Develop a comprehensive risk framework to systematically navigate and categorize different risk types and their potential mitigation measures.*

Table 2 contains the Risk Framework, specifying between the specific price and volume risks categories. For every risk category, a short definition of the risk is provided and the specific condition for the risk to occur. "Conditions for occurrence" refers to the system design specifications that are necessary for a risk to manifest. For instance, the structural price convergence effect inherently occurs with the implementation of an OBZ configuration, regardless of whether FBMC or ATC is used for the capacity calculation of cross-border transmission capacity. Conversely, capacity calculation and allocation risks only arise when the OBZ is integrated into the FBMC system. The last column indicates which mitigation measure could potentially address each risk. An asterisk (*) signifies that only part of the risk is covered. For example, FTRs hedge against the structural price convergence effect only for the portion of the FTR contracted in the higher-priced zone to which the OBZ, according to the rule-of-thumb, does not typically converge. The mitigation measures in bold (PtG, FTR and TAG) are those that will be considered in further analysis in this thesis.

*Table 2: The Risk Framework.*

| Risk/ Effect | Name | Explanation | Condition for occurrence | Mitigation Measure |
|---|---|---|---|---|
| ***Price Effect*** | **Locational basis price effect** | The price in the OBZ differs from the price of the onshore bidding zones. | Inherent to OBZ configuration | - |
| | **Structural price convergence effect** | The 'rule of thumb' price formation leads to prices structurally converging to the lower-priced adjacent market. | Inherent to OBZ configuration | CfD |
| ***Price Risk*** | **Flat price risk** | The risk that the absolute price level (the flat price) of electricity in the OBZ is uncertain and will fluctuate | Always exists, OBZ configuration potentially enlarges severity. | PPA*, **FTR***, CfD, **PtG**, EST* |
| | **Non-intuitive price risk** | The risk that the capture price of the OBZ could be 'out of bounds' compared to prices in the adjacent bidding zones. This effect is negative when market exchanges originating from the OBZ are loading the CNEs from the involved CCR(s) more compared to other onshore market exchanges, and positive when the OBZ has a lower impact on the CNEs | OBZ part of FBMC with AHC | PPA*, FTR, CfD, **PtG**, EST* |
| | **Price collapse risk** | The risk that restricted export capacity from the OBZ to the adjacent onshore bidding zones lead to the price in the OBZ converging to the marginal bid inside the OBZ, which is, under perfect competition assumption, zero | OBZ part of FBMC (SHC/AHC) | PPA*, **FTR***, CfD, **PtG**, EST* |

| | | | | |
|---|---|---|---|---|
| ***Volume Risk*** | **Technical unavailability volume risk** | The risk that technical unavailability of the interconnector(s) connecting the OBZ leads to inability to export the total available generating capacity of the OWF(s) | Outage | **PtG** (if large inst. Cap.) |
| | **Local demand volume risk** | The risk that the interconnection capacity - set to the net of connection capacity of generation and load - exceeds the maximum export capacity of the interconnectors, leading to the price of the OBZ being set by demand if generation exceeds interconnector capacity, and potential gaming to steer price formation. | OBZ + local demand | **-** |
| | **Capacity Calculation volume risk** | The risk that the total available wind generation of the OWF(s) exceeds the maximum export capacity to the surrounding AC onshore grid, limiting the total export capacity. | OBZ part of FBMC (SHC/ AHC) | PPA*, CfD, **TAG, PtG**, EST* |
| | **Capacity Allocation volume risk** | The risk that FBMC algorithm determines higher welfare-generating cross-border exchanges for other participating bidding zones, whereby the allocated transmission capacity to the OBZ is insufficient to export the total available wind generation of the OWF(s) | OBZ part of FBMC (SHC/ AHC) | PPA*, CfD, **PtG**, EST* |
| ***Price + Volume risk*** | **Interacting Price/Volume Risk** | The coexistence of the price collapse risk and the capacity calculation volume risk. | OBZ part of FBMC (SHC/ AHC) | PPA*, CfD, **TAG, PtG**, EST* |

The risk that will be considered for further analysis in this thesis are the flat price risk, the non-intuitive price risk, the price collapse risk, the capacity calculation volume risk, the capacity allocation volume risk and the interacting price/volume risk. Additionally, the structural price convergence effect is considered. The locational basis risk is not considered as it has more contractual implications than market implications. The technical unavailability volume risk is also not explicitly further considered. Note that the technological mitigation measure, indicated as PtG (Power-to-Gas) in the risk framework, is further considered as hydrogen production. The next chapter, and specifically Section 4.2.3, elucidates on how the frequency and severity of these specific risk categories is determined.

# Chapter 4: Methodology

This chapter outlines the modelling methodology employed in this thesis. The methodology consists of four steps, visualised in Figure 12 and substantiated hereafter.

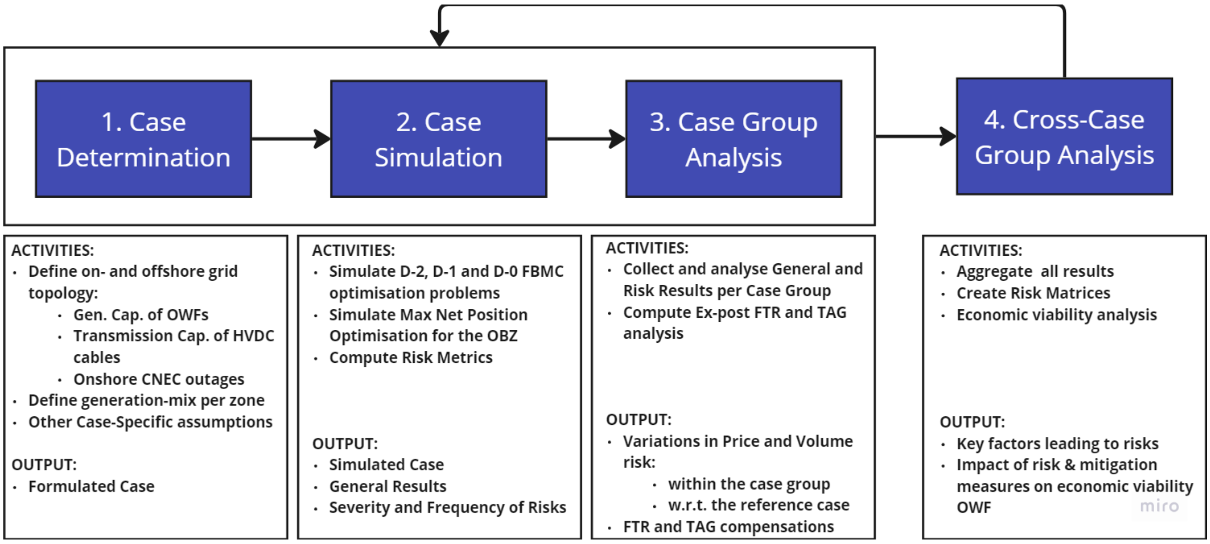


*Figure 12: The Four Steps of the Methodology.*

The first step of the methodology establishes indicators to systematically define case groups. Within each group, a specific variable is varied across cases, ceteris paribus. This is a key consideration within this thesis' methodology as it isolates the effects on price and volume risk per considered variable. The variables considered include offshore grid topology, onshore grid attenuations, and the integration of renewable energy sources (See Section 1.6). Additionally, a case group for technological mitigation measures is included. The case groups and the formulated cases are described in Chapter 5.

In the second step, the market coupling process is simulated for every hour in the considered timespan to replicate the FBMC process chain, as described in Section 2.2. The maximum net position of the OBZ is determined to distinguish between capacity allocation and calculation volume risk. Additionally, for all identified price and volume risk categories (summarized in Table 2, Section 3.4), risk indicators are formulated and simulated per case to determine their frequency and magnitude.

In the third step, case-specific results are collected and analysed per case group, focusing on relative variations within the group and with respect to the reference case in perceived price and volume risks. This provides an initial indication of the most frequent and severe risks and their impact on the economic viability of the OWFs (SQ3). Additionally, an ex-post analysis of FTR and TAG compensations is also conducted.

The fourth step involves aggregating and analysing results across all cases to identify relationships between simulated cases and their impact on risk categories, revealing overarching patterns. The main output is identifying key factors leading to price and volume risks, their economic impact, and the effectiveness of mitigation measures, addressing SQ3 and SQ4.

**SQ.3**: *What are the factors leading to the most frequent and severe price and volume risks and how do they impact the economic viability of the hybrid OWF?*

**SQ.4**: *To what extent can Regulatory and Technological measures potentially mitigate price and volume risk?*

The first three steps are case-specific and are completed per case group before moving to the fourth step. Following this methodology aims to achieve intermediate deliverable 2 and provides an effective approach to answering research questions of this thesis.

**ID.2**: *Create a replicable and structured modelling methodology that includes developing universal risk indicators to simulate specific grid topologies and dimensions of hybrid projects within the FBMC process.*

Sections 4.1 to 4.4 explain each step of the four-step methodology. This chapter concludes by elaborating on the steps that have been undertaken to validate the model in Section 4.5.

# 4.1 Step 1: Case Determination

The first step in the four-step modelling approach is determining the case to be simulated. Since offshore grid topology is a primary variable of interest (see Section 1.6), three indicators are designed to structure the variations in offshore grid topology, as explained hereafter. The consideration of the other two main variables—onshore grid attenuations and the integration of renewable energy sources—as well as the full description of the case groups and their cases, is provided in Chapter 5.

## 4.1.1 Establishing Indicators for Offshore Grid Topology Changes

To analysis to a deeper extend how variations in offshore grid topology affect price and volume risks, it is essential to establish specific indicators to structurally vary in offshore grid setups within the OBZ. Considering the dual functionality of hybrid OWFs—exporting produced renewable energy to shore and interconnecting adjacent power markets—indicators that reflect these functions systematically are necessary for robust variation analysis. The first indicator is the Export Indicator of the OBZ ($EI_{obz}$), represented by equation (4.1):

$$EI_{obz} = \frac{\sum \bar{F}^{DC}_{obz \to z}}{\sum Q^{OWF}_{obz}} \quad (4.1)$$

Where the Export Indicator of the OBZ ($EI_{obz}$) is the ratio between the sum of the transmission capacities on DC lines from the OBZ to onshore zones $z$ ($\sum \bar{F}^{DC}_{obz \to z}$), and the sum of the installed capacities of the OWFs in the OBZ ($\sum Q^{OWF}_{obz}$). This indicator thus reflects the direct export capacity from the OBZ to shore with respect to the installed wind capacities inside the OBZ. An EI of 1.0 indicates that the full wind capacity can be exported to shore. In theory the export capacity of the OBZ could also be restricted by limited transmission capacity internal in the OBZ. However, even if internal transmission capacity within the OBZ is limited, the OWFs could still export up to the maximum transmission capacity to their respective Home Markets, in case the transmission capacity is fully allocated to the OBZ. Therefore, the export indicator disregards the transmission capacity inside the OBZ.

Furthermore, since the specific ration between OWF and transmission capacities for the envisioned hybrid projects are as of today not set and stone, an indicator describing the export capacity of an OWF from its Home Market to other bidding zones is also necessary. The maximum exporting capacity of a single OWF in the OBZ is restricted by either the total transmission capacity from the OBZ to all connected onshore markets or by the total internal transmission capacity in the OBZ. The Export indicator for market $z$ then becomes:

$$EI_z = \frac{\min\left(\sum \bar{F}^{DC}_{obz\to z}, \sum \bar{F}^{DC}_{obz}\right)}{Q^{OWF}_z} \quad (4.2)$$

Where the Export Indicator for market $z$ ($EI_z$) is computed by taking the minimum value of total transmission capacities from the OBZ to the onshore markets $z$ ($\sum \bar{F}^{DC}_{obz\to z}$) and total internal transmission capacity in the OBZ ($\sum \bar{F}^{DC}_{obz}$), and dividing this value by the installed capacity of the OWF directly connected to the considered market z ($Q^{OWF}_z$). An $EI_z$ of 1.0 indicates that all the total installed wind capacity of the respective zone can potentially be exported to the other zones.

Regarding the interconnectivity function of hybrid projects, it is important to consider the perspective of the TSOs. For instance, a TSO might find it desirable to oversize the hybrid to enable more cross-border electricity trade. Therefore, the ratio between the transmission capacity connecting the OBZ to the considered market $z$ ( $\bar{F}^{DC}_{obz\to z}$) and the installed capacity of the OWF directly connected to the considered market $z$ ($Q^{OWF}_z$) forms the first component of the Interconnectivity Indicator. Additionally, interconnectivity is restricted by the maximum export capacity from the zone, which is equal to Equation (4.2). Therefore, the Interconnectivity Indicator for zone $z$ becomes:

$$II_z = \frac{\bar{F}^{DC}_{obz\to z}}{Q^{OWF}_z} \cdot \frac{\min\left(\sum \bar{F}^{DC}_{obz\to z}, \sum \bar{F}^{DC}_{obz}\right)}{Q^{OWF}_z} \quad (4.3)$$

Box 3 explains how the Interconnectivity Indicator should be interpreted. These three indicators will be used to determine Reference Case and the variations for the cases in Case Groups 2 and 3, where the offshore grid topology is the changing factor subject to study.

**Box 3: Explaining the Interconnectivity Indicator.**

Consider a simple hybrid setup as visualised in the picture below:

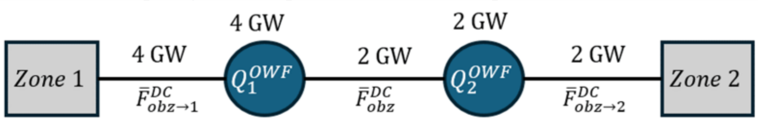


Computing the II for zone 1 would give: $II_1 = \frac{4}{4} \cdot \frac{\min([4+2],2)}{4} = 0.5$. The restricting factor in the interconnectivity indicator for zone 1 in this case is the internal transmission line in the OBZ, having a capacity of 2GW, since the sum of the transmission lines to shore (4GW to zone 1 and 2GW to zone 2) is larger.

If the internal OBZ line is decreased from 2GW to 1GW, the interconnectivity indicator becomes: $II_1 = \frac{4}{4} \cdot \frac{\min([4+2],1)}{4} = 0.25$, indicating that only half of the power can be traded from zone 1 to zone 2, compared to the initial setup with an II of 0.5.

If the TSO from zone 1 decides to install a larger transmission cable compared to the installed wind capacity, let's say 5GW instead of 4GW, the II for zone would become: $II_1 = \frac{5}{4} \cdot \frac{\min([4+2],2)}{4} = 0.625$, indicating that interconnectivity increase with 25% compared to the initial setup.

## 4.2. Step 2: Case Simulation

After having formulated the cases following the methods explained in the previous section, each case can be simulated. This subchapter initiates by delving into the simulation process of the model in Section 4.2.1. Thereafter, the mathematical model standing basis to the simulation process is described in Section 4.2.2. Lastly, Section 4.2.3 outlines the methodological steps undertaken to trace the risks and structure the results of the simulation, to ensure that the risks can be analysed in the next step of the four-step methodology.

### 4.2.1 Simulation process

Figure 13 visualises the simulation process applied in this thesis for each case, detailing the main input and output parameters, as well as the key steps within the simulation. The process begins with simulating the three steps within the FBMC process (explained in Section 2.2 visualised in Figure 7). Following this, three additional modelling steps are undertaken (blue boxes in Figure 13). First, the Max Net Position of the OBZ is determined for each case, a critical optimization problem distinguishing curtailed volumes by capacity calculation and capacity allocation, explained in Section 4.2.3. The second step is the Risk Metric Simulation, where risk indicators for all price and volume risk categories, defined in Section 4.2.4, are simulated. The final step is an ex-post simulation determining the FTR and TAG compensations, defined in Section 4.3.3.

The optimisation model, based on the model of Kenis et al (2023)[5] and written in Julia, is publicly available on GitHub[6]. The optimiser used is the Gurobi optimiser (Gurobi, n.d.), known for its speed and efficiency in solving large-scale linear programming problems. Moreover, Gurobi's advanced algorithms and parallel processing capabilities provide fast solutions and include useful features for model validation purposes (See Section 4.6.1). For the Risk Metric Simulation, Python is used. The simulations of the three consecutive FBMC optimization problems are executed on an hourly resolution. To represent seasonal patterns while limiting computational intensity, the first month of each quarter is simulated (totalling 2952 hours per case) instead of an 8760-hour year. To further speed up the process and limit required RAM, each month is simulated separately.

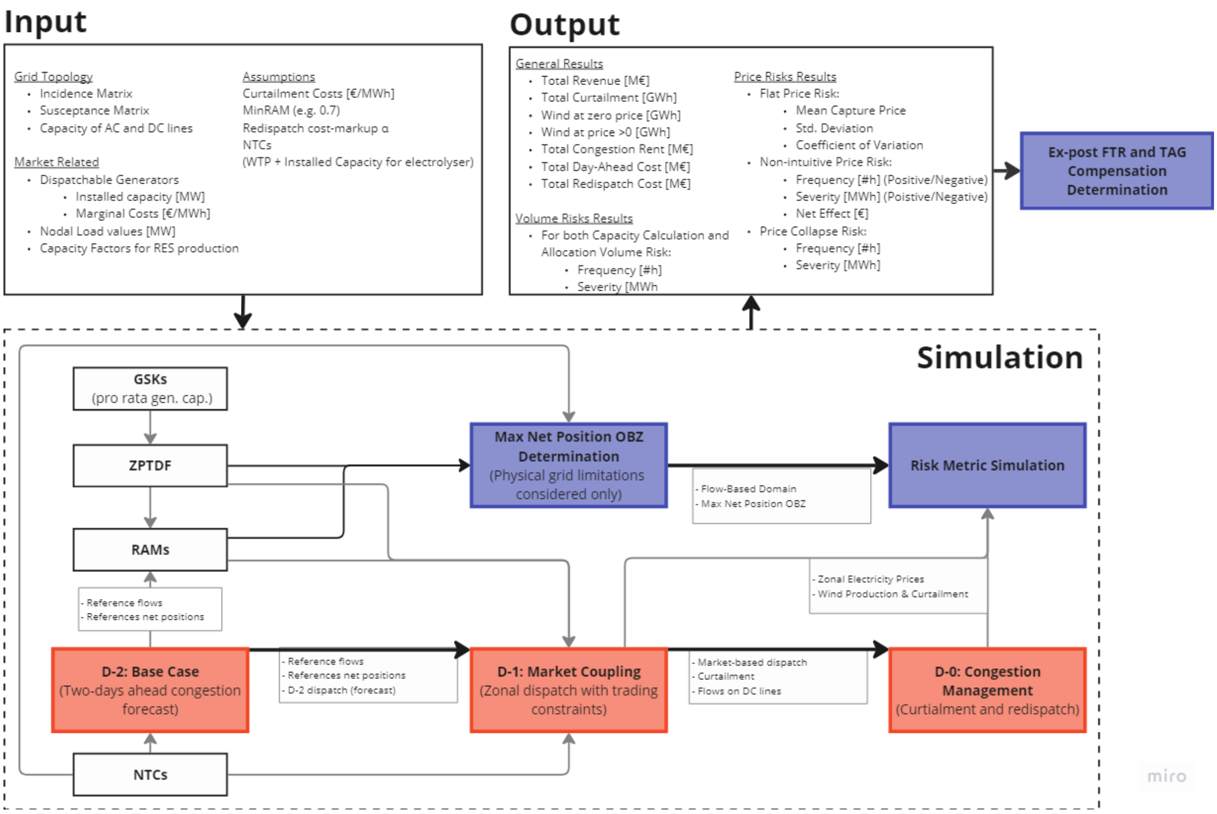


*Figure 13: Visualisation of the Simulation Process of the Model. The red boxes represent the three main modelling steps within flow-based market coupling (Based on Schönheit et al., 2021). The blue boxes represent the additional modelling steps*

[5] https://github.com/kbruninx/OBZvsHM.git
[6] https://github.com/DVerkooijen/Verkooijen-MSc-Thesis-OBZ-Risks.git

*introduced in this thesis. The white boxes represent the flow of information between the various modelling steps within the simulation.*

### 4.2.2 Mathematical Representation of the Model

This section describes the mathematical model that is used for the simulation of the three FBMC steps (red boxes Figure 13). The mathematical model used in this thesis is taken from Kenis et al. (2023) and extended to implement flexible offshore demand agents, such as offshore electrolyser. As explained in Section 2.2, there are three main steps to the flow-based market coupling simulation: the D-2 base case computation, the D-1 day-ahead market clearing and the D-0 redispatch computation. Table 3 below provides an overview of the nomenclature used in the Base Case (D-2), Market Coupling (D-1) and Congestion Management (D-0), and distinguishes for all sets, parameters and decision variables in which of these three flow-based simulations steps they are used.

*Table 3: Nomenclature for the mathematical model. For all Sets, Parameters and Decision Variables it is indicated in which of the three FBMC steps they are used.*

| **Sets** | | **D-2/D-1/D-0** |
|---|---|---|
| $\boldsymbol{\mathcal{N}}$ | Nodes in zone $z$ | *All* |
| $\boldsymbol{\mathcal{G}}$ | Dispatchable Generators $g$ | *All* |
| $\boldsymbol{\mathcal{Z}}$ | Zones | *All* |
| $\boldsymbol{\mathcal{L}}$ | AC Lines | *All* |
| $\boldsymbol{\mathcal{H}}$ | DC Lines | *All* |
| $\boldsymbol{\mathcal{R}}$ | Renewable, intermittent generators | *All* |
| $\boldsymbol{\mathcal{T}}$ | Timesteps | *All* |
| $\boldsymbol{\mathcal{H}2}$ | Dispatchable electrolysers $h2$ | *All* |
| **Parameters** | | |
| $\boldsymbol{MC_g}$ | Marginal Costs of generator $g$ [€/MWh] | *All* |
| $\boldsymbol{CC}$ | Curtailment Cost of Offshore Wind Farm [€/MWh] | *D-2/D-0* |
| $\boldsymbol{Q_g^s}$ | Generating capacity of dispatchable generator $g$ [MW] | *All* |
| $\boldsymbol{Q_n^d}$ | Demand for electricity at node $n$ [MW] | *All* |
| $\boldsymbol{zPTDF_l^z}$ | Zonal PTDF for AC-line $l$ and zone $z$ | *D-1* |
| $\boldsymbol{nPTDF_l^{n(h)}}$ | Nodal PTDF for AC-line $l$ and node $n$ (with $h$ indicating starting end $(h-)$ or ending end $(-h)$ of a DC flow) | *All* |
| $\boldsymbol{R_n}$ | Renewable injection for each node [MW] | *All* |
| $\boldsymbol{I_{l,z}^{AC}}$ | Flow direction on cross-border AC-line $l$ from/to zone $z$, $\in -1,0,1$ | *D-2/D-1* |
| $\boldsymbol{I_{h,z}^{DC}}$ | Flow direction on cross-border DC-line $h$ from/to zone $z$, $\in -1,0,1$ | *All* |
| $\boldsymbol{I_{h,z,z'}^{DC}}$ | Flow direction on cross-border DC-line $h$ between zone $z$ and $z'$, $\in -1,0,1$ | *D-1* |
| $\boldsymbol{I_{n(h-),h}^{ACDC}}$ | Flow direction on cross-border DC-line $h$ into/away from node $n(h-)$, $\in -1,0,1$ | *D-1* |
| $\boldsymbol{I_{n(-h),h}^{ACDC}}$ | Flow direction on cross-border DC-line $h$ into/away from node $n(-h)$, $\in -1,0,1$ | *D-1* |
| $\boldsymbol{RAM_l^+}$ | Maximum RAM of AC line $l$ [MW] | *D-1* |
| $\boldsymbol{RAM_l^-}$ | Minimum RAM of AC line $l$ [MW] | *D-1* |
| $\boldsymbol{NTC_{z,z'}^+}$ | Maximum NTC of DC line connecting zone $z$ and $z'$ [MW] | *D-1* |
| $\boldsymbol{NTC_{z,z'}^-}$ | Minimum NTC of DC line connecting zone $z$ and $z'$ [MW] | *D-1* |
| $\boldsymbol{\bar{F}_l}$ | Upper transmission capacity limit AC line $l$ | *D-2/D-0* |
| $\boldsymbol{\bar{F}_h^{DC}}$ | Upper transmission capacity limit DC line $h$ | *D-2/D-0* |
| $\boldsymbol{\alpha}$ | Redispatch cost mark-up | *D-0* |
| $\boldsymbol{WTP_{h2}}$ | Willingness-to-Pay of electrolyser $h2$ [€/MWh] | *All* |
| $\boldsymbol{Q_{h2}^d}$ | Installed capacity (demand) for electricity at electrolyser $h2$ [MW] | *All* |
| **Decision Variables** | | |
| $\boldsymbol{v_g}$ | Relative production of dispatchable generator $g$ | *D-2/D-1* |
| $\boldsymbol{c_n}$ | Curtailment at node $n$ | *D-2/D-1* |
| $\boldsymbol{f_l^{AC}}$ | Flow on AC line $l$ | *D-2/D-1* |
| $\boldsymbol{f_h^{DC}}$ | Flow on DC line $h$ | *D-2/D-1* |
| $\boldsymbol{p_z}$ | Net position at zone $z$ | *D-2/D-1* |

| | | |
|---|---|---|
| $\boldsymbol{p_z^{FB}}$ | Net position at zone $z$ impacting the flow-based domain | *D-1* |
| $\boldsymbol{u_g}$ | Upward adjustment of scheduled output generator $g$ | *D-0* |
| $\boldsymbol{d_g}$ | Downward adjustment of scheduled output generator $g$ | *D-0* |
| $\Delta \boldsymbol{c_n}$ | Curtailment adjustment of scheduled output OWF at node n | *D-0* |
| $\Delta \boldsymbol{f_h^{DC}}$ | DC flow adjustment line $h$ | *D-0* |
| $\boldsymbol{e_{h2}}$ | Relative production of dispatchable electrolyser $h2$ | *D-2/D-1* |
| $\boldsymbol{u_{h2}}$ | Upward adjustment of scheduled input electrolyser $h2$ | *D-0* |
| $\boldsymbol{d_{h2}}$ | Downard adjustment of scheduled input electrolyser $h2$ | *D-0* |

To implement an offshore demand agent, such as an offshore electrolyser, the mathematical from Kenis et al. (2023) has been extended to account for local electricity consumption and the reduced total generation costs. This extension was partially inspired by the mathematical model provided in Kenis et al. (2024), where electrolysers have been introduced in the optimization problem. However, their mathematical model optimises the utility of newly added electrolysers while deciding on the electrolyser's capacities and optimal investments, whereby the use of electrolysers is represented in the optimization model differently[7]. Therefore, the mathematical model from Kenis et al. (2023), has been extended to include flexible electrolysers operating solely based on its Willingness-to-Pay for electricity in a merchant-based manner.

In essence this extension incorporates the following. The offshore hydrogen production is represented by an electrolyser that has an installed capacity ($Q_{h2}^{d}$ in MW), representing the maximum electricity demand of the electrolyser, and a Willingness-to-Pay ($WTP_{h2}$ in €/MWh), representing the maximum value the demand agent is willing to pay per MWh of electricity. New decision variables for an electrolyser $h2$ are the relative production ($e_{h2}$) for the D-2 and D-1 problems, and the upward ($u_{h2}$) and downward ($d_{h2}$) adjustment of the scheduled dispatch for the D-0 problem.

Specifically, the mathematical model of Kenis et al. (2023) is extended as follows. From the objective functions in all three optimization problems (explained hereafter) is subtracted the $WTP_{h2}$ times the scheduled consumption ($Q_{h2}^{d} \cdot e_{h2}$) of the electrolysers $h_2$. This is to factor in the additional income generated for the TSO from the power consumption of the electrolyser. From the power balance constraints is also subtracted the scheduled consumption ($Q_{h2}^{d} \cdot e_{h2}$), to account for the additional electricity load of the electrolysers. Additionally, in the nodal power balances of the offshore nodes the consumption of electricity by the demand agent is also incorporated, ensuring adherence to Kirchoff's laws. The following three sections explain the complete mathematical model applied in this thesis.

#### 4.2.2.1 Base Case (D-2)

The base case describes the linear optimization problem that determines the expected power flows and net positions two days ahead of real-time delivery. Here, a nodal market clearing is assumed as the base case. The goal of the Base Case is to determine the FB parameters (See Figure 7, Section 2.2), being the reference flows ($F_l^{ref}$) and the reference net positions ($p_z^{ref}$). These FB parameters, together with the pre-determined GSKs, are used to compute the zonal PTDFs and RAMs (See equations A.2 to A.4 in Appendix A). These parameters will then serve as input parameters in the D-1 flow-based market clearing. The mathematical representation of the D-2 Base Case optimization is described as follows:

---

[7] Kenis et al. (2024) maximise the surplus from the wholesale market (same as minimising generation costs) while considering electrolysers' investment costs. In their model, electrolysers' operational behaviour is influenced by investment conditions. This thesis, however, focuses on investigating the operational behaviour of an electrolyser present in the OBZ without considering investment costs, similar to the treatment of OWFs.

$$\min_{v_n, e_{h2}, p_z, c_n, f_h^{DC}, f_l^{AC}} \quad GC = \sum_{g \in \mathcal{G}} MC_g \cdot Q_g^s \cdot v_g + c_n \cdot CC \; - \sum_{h2 \in \mathcal{H}2} WTP_{h2} \cdot Q_{h2}^d \cdot e_{h2} \quad (4.1a)$$

*Subject to*

$$\sum_{g \in \mathcal{G}} Q_g^s \cdot v_g + \sum_{n \in \mathcal{N}} R_n - c_n - Q_n^d - \sum_{h2 \in \mathcal{H}2} Q_{h2}^d \cdot e_{h2} \; = p_z, \quad \forall n \in \mathcal{N} \quad (4.1b)$$

$$\sum_{l \in \mathcal{L}} f_l^{AC} \cdot I_{l,z}^{AC} + \sum_{h \in \mathcal{H}} f_h^{DC} \cdot I_{h,z}^{DC} = p_z, \quad \forall n \in \mathcal{N} \quad (4.1c)$$

$$f_l^{AC} = \sum_{n \in \mathcal{N}} nPTDF_l^n \cdot \left[ \sum_{g \in \mathcal{G}(\mathcal{N})} Q_g^s + R_n - c_n - Q_n^d - \sum_{h2 \in \mathcal{H}2} Q_{h2}^d \cdot e_{h2} - \sum_{h \in \mathcal{H}} f_h^{DC} \cdot I_h^{DC} \right], \quad \forall l \in \mathcal{L} \quad (4.1d)$$

$$-\bar{F}_l \leq f_l^{AC} \leq \bar{F}_l, \quad \forall n \in \mathcal{N} \quad 4.1e)$$

$$-\bar{F}_h^{DC} \leq f_h^{DC} \leq \bar{F}_h^{DC}, \quad \forall h \in \mathcal{H} \quad (4.1f)$$

$$0 \leq v_g \leq 1, \quad \forall g \in \mathcal{G} \quad (4.1g)$$

$$0 \leq c_n \leq R_n, \quad \forall n \in \mathcal{N} \quad (4.1h)$$

$$0 \leq e_{h2} \leq 1, \quad h2 \in \mathcal{H}2 \quad (4.1\mathrm{i})$$

$$\sum_{h \in \mathcal{H}} f_h^{DC} \cdot I_{h,n}^{DC} = R_n - c_n - \sum_{h2 \in \mathcal{H}2} Q_{h2}^d \cdot e_{h2}, \quad \forall n \in \mathcal{N}' \quad (4.1j)$$

The objective function (4.1a) minimizes the day-ahead generation costs (DAC), which is calculated as the sum of the product of the marginal cost ($MC_g$) and the scheduled production ($Q_g^s \cdot v_g$) for each non-intermittent generator $g$, and the congestion costs which is the sum of the curtailment times curtailment costs ($c_n \cdot CC$) for all renewable generators, while assuming the cost of renewable energy sources (RES) production is zero. The congestion costs can be interpreted as the compensation payments of the TSO to the OWF operator in case there is curtailment. The income generated by the scheduled consumption of all electrolysers $h_2$ is added ($WTP_{h2} \cdot Q_{h2}^d \cdot e_{h2}$). Constraint (4.1b) is the nodal power balance constraint, as it ensures that the sum of the dispatchable generators ($Q_g^s \cdot v_g$) and renewable energy production ($R_n$) , minus the curtailed power ($c_n$), inelastic demand and sum of all flexible demand agents ($Q_{h2}^d \cdot e_{h2}$) at all nodes within one zone, equals the net position ($p_z$) of that zone. Constraint (4.1c) ensures that the net position ($p_z$) matches the flows $f_l^{AC}$ and $f_h^{DC}$ on each cross-border AC line $l$ and DC line $h$ respectively, with $I_{l,z}^{AC}$ and $I_{h,z}^{DC}$ equalling 1 (or -1) for flows flowing outward (or inward) with respect to zone $z$, or otherwise 0 for non-cross-border flows. Constraint (4.1d) determines the expected power flow $f_l^{AC}$ on each AC line $l$, by summing the total power injection at node $n$. This total is derived by summing the contributions of all generators $g$ at the node ($Q_g^s \cdot v_g$), the net renewable energy production after accounting for curtailment ($R_n - c_n$), subtracting inelastic ($Q_n^d$) and elastic demand ($Q_{h2}^d \cdot e_{h2}$), and considering the power injections from connected DC lines ($f_h^{DC} \cdot I_h^{DC}$). The resultant power at each node is then multiplied by the nodes' PTDF values for all lines $l$, reflecting how sensitive the flow on each line is to injections at node $n$, thereby capturing the impact of these injections across the entire transmission network. The nodal PTDF is determined following equation (A.2) (Appendix A). Constraints (4.1e) and (4.1f) ensure that the flows $f_l^{AC}$ and $f_h^{DC}$ on each AC line $l$ and DC line $h$ stay within the limits of the thermal capacities $\bar{F}_l$ and $\bar{F}_h^{DC}$ respectively. Constraint (4.1g) and (4.1i) ensure the relative production ($v_g$) for each non-intermittent generator $g$ and relative hydrogen production ($e_{h2}$)

for each electrolyser $h2$, is between 0 and 1. Constraint (4.1h) restricts the curtailment ($c_n$) to be non-zero and to be maximum equal to the injection from the renewable generator ($R_n$) at each node $n$. Finally, constraint (4.1j) describes the nodal power balance at the offshore nodes $n \in \mathcal{N}' \subset \mathcal{N}$, specifically for the nodes that are not connected to an AC line, to ensure that the offshore power flows adhere to the Laws of Kirchoff.

#### 4.2.2.2 Day-ahead market clearing (D-1)

After having simulated the D-2 base case optimization, the D-1 problem will be optimized. This optimization problem 'clears' the market by determining the dispatch of each generator, the curtailment necessary for intermittent renewable generators, all while adhering to the physical limitations of the transmission grid. The electricity prices for each zone are also determined, as they are represented by the shadow prices of the power balance (constraint (4.2b)). See below the mathematical representation of the D-1 Day-Ahead market clearing problem.

$$\min_{v_{n,e_{h2}},p_z p_z^{FB},c_n,f_h^{DC},f_l^{AC}} \quad GC = \sum_{g \in \mathcal{G}} MC_g \cdot Q_g^s \cdot v_{g,t} + c_n \cdot CC - \sum_{h2 \in \mathcal{H}2} WTP_{h2} \cdot Q_{h2}^d \cdot e_{h2} \tag{4.2a}$$

*Subject to*

$$\sum_{g \in \mathcal{G}} Q_g^s \cdot v_g + \sum_{n \in \mathcal{N}} R_n - c_n - Q_n^d - \sum_{h2 \in \mathcal{H}2} Q_{h2}^d \cdot e_{h2} = p_z, \quad \forall z \in \mathcal{Z} \tag{4.2b}$$

$$\sum_{l \in \mathcal{L}} f_l^{AC} \cdot I_{l,z}^{AC} + \sum_{h \in \mathcal{H}} f_h^{DC} \cdot I_{h,z}^{DC} = p_z, \qquad \forall z \in \mathcal{Z} \tag{4.2c}$$

$$p_z^{FB} = p_z - \sum_{h \in \mathcal{H}} f_h^{DC} \cdot I_{h,z}^{DC}, \qquad \forall z \in \mathcal{Z} \tag{4.2d}$$

$$-RAM_l^- \leq \sum_{z \in \mathcal{Z}} zPTDF_l^z \cdot p_z^{FB} + \sum_{h \in \mathcal{H}'} f_h^{DC} \cdot \left[ nPTDF_l^{n(h-)} \cdot I_{n(h-),h}^{ACDC} + nPTDF_l^{n(-h)} \cdot I_{n(-h),h}^{ACDC} \right] \leq RAM_l^+, \qquad \forall l \in \mathcal{L} \tag{4.2e}$$

$$-NTC_{z,z'}^- \leq \sum_{h \in \mathcal{H}} f_h^{DC} \cdot I_{h,z,z'}^{DC} \leq NTC_{z,z'}^+, \qquad \forall z, z' \in \mathcal{Z} \tag{4.2f}$$

$$0 \leq v_g \leq 1, \qquad \forall g \in \mathcal{G} \tag{4.2g}$$

$$0 \leq c_n \leq R_n, \qquad \forall n \in \mathcal{N} \tag{4.2h}$$

$$0 \leq e_{h2} \leq 1, \qquad h2 \in \mathcal{H}2 \tag{4.2i}$$

$$\sum_{h \in \mathcal{H}} f_h^{DC} \cdot I_{h,n}^{DC} = R_n - c_n - \sum_{h2 \in \mathcal{H}2} Q_{h2}^d \cdot e_{h2}, \qquad \forall n \in \mathcal{N}' \tag{4.2$j$}$$

For the Day-Ahead market clearing optimization, the objective function (4.2a) and constraints (4.2c), (4.2g), (4.2h), (4.2i) and (4.2j) are equal to objective function (4.1a) and constraints (4.1c), (4.1g), (4.1h), (4.1i) and (4.1j) of the base case respectively. Where constraint (4.1b) was the nodal power balance in the base case optimization, the DA market clearing optimization considers a zonal power balance, described in constraint (4.2b). Constraints (4.2d), (4.2e) and (4.2f) are additional constraints that consider the limitations of the AC lines using the flow-based methodology, and considering the impact of DC-flows on AC-flows as is the practice with the Advanced Hybrid coupling methodology. Constraint (4.2d) defines the Flow-Based net positions ($p_z^{FB}$) of each zone $z$ that impact the flow-based domain. Constraint (4.2e) explicitly consider the effect of DC line $h$ on AC line $l$, distinguishing the AHC approach from its predecessor, the SHC approach. Alternatively, this could also be explained using a virtual bidding zone that explicitly serves as the interface between the DC and AC grids. In this approach, the net position of the virtual hub reflects the exchange over the DC line to which it is connected (Müller et al., 2017). In mathematical formulation, the impact of a DC line $h$ on AC line $l$ is considered using the nodal PTDFs, specifically $nPTDF_l^{n(h-)}$ and $nPTDF_l^{n(-h)}$, where $n(h-)$ and $n(-h)$ denote the starting and ending nodes of DC line $h$ respectively. $I_{n(h-),h}^{ACDC}$ and $I_{n(-h),h}^{ACDC}$ equal 1(or -1) if the flow on DC line $h$ is directed into (or away from) node $n(h-)$ (or $n(-h)$), and zero otherwise. The zonal PTDF is determined following equation (A.2) (and (A.3) for the GSKs used in equation (A.2)) and the RAM values are determined following equation (A.4) (Appendix A). Lastly, constraint (4.2f) restricts the transmission across the cross-border DC-lines between zone $z$ and $z'$, utilizing $NTC_{z,z'}^{-}$ and $NTC_{z,z'}^{+}$ for both flow directions. Also here, the $I_{h,z,z'}^{DC}$ equals 1 (or -1) if the DC line $h$ is a cross-border line running from zone $z$ to $z'$ (or reverse) and is set to 0 otherwise. Within this method, only cross-border DC-lines are monitored and thus the impact of non-cross-border DC-lines on AC lines is not captured.

#### 4.2.2.3 Redispatch (D-0)

After having cleared the DA market 1 day before actual operations, congestion management is needed during the operation day itself since the market clears based on several assumptions and parameters which might lead to violation of the physical grid limitations. Therefore, the redispatch is often necessary. In this thesis the redispatch optimization is assumed to be a cost-based redispatch as the tool for congestion management. The decision variables used in the D-1 day-ahead market clearing become input parameters in the D-0 redispatch optimization. New decision variables for this optimization are the upward ($u_g$) and downward ($d_g$) adjustments of the scheduled output of each non-intermittent generator $g$. Decision variable $\Delta c_n$ represents the modifications to the curtailment of the renewable energy sources at each node $n$. The alterations into the DC flows on each DC line $h$ are represented by $\Delta f_h^{DC}$. The mathematical representation of the redispatch problem is described below.

$$\min_{u_g, d_g, u_{h2}, d_{h2}, \Delta c_n, \Delta f_h^{DC}} \quad RDC = \sum_{g \in \mathcal{G}} \Big[ [1+\alpha] \cdot Q_g^s \cdot MC_g \cdot u_g - [1-\alpha] \cdot Q_g^s \cdot MC_g \cdot d_g \Big]$$
$$- \sum_{h2 \in \mathcal{H}2} \Big[ [1+\alpha] \cdot Q_{h2}^d \cdot WTP_{h2} \cdot u_{h2} - [1-\alpha] \cdot Q_{h2}^d \cdot WTP_{h2} \cdot d_{h2} \Big] \quad (4.3a)$$

*Subject to*

$$\sum_{g \in \mathcal{G}} u_g \cdot Q_g^s - \sum_{h2 \in \mathcal{H}2} d_{h2} \cdot Q_{h2}^d = \sum_{g \in \mathcal{G}} d_g \cdot Q_g^s - \sum_{h2 \in \mathcal{H}2} u_{h2} \cdot Q_{h2}^d \quad (4.3b)$$

$$-\bar{F}_l \le \sum_{n \in \mathcal{N}} nPTDF_l^n$$
$$\cdot \Bigg[ \sum_{g \in \mathcal{G}(\mathcal{N})} Q_g^s \cdot [v_g + u_g - d_g] - \sum_{h2 \in \mathcal{H}2} Q_{h2}^d \cdot [e_{h2} + u_{h2} - d_{h2}] + R_n - c_n - \Delta c_n$$
$$- Q_n^d - \sum_{h \in \mathcal{H}} [f_h^{DC} + \Delta f_h^{DC}] \cdot I_{h,n}^{AC} \Bigg] \le \bar{F}_l, \qquad \forall l \in \mathcal{L} \quad (4.3c)$$

$$-\bar{F}_h^{DC} \le f_h^{DC} + \Delta f_h^{DC} \le \bar{F}_h^{DC}, \qquad \forall h \in \mathcal{H} \quad (4.3d)$$

$$0 \le u_g \le 1 - v_g, \qquad \forall g \in \mathcal{G} \quad (4.3e)$$

$$0 \le d_g \le v_g, \qquad \forall g \in \mathcal{G} \quad (4.3f)$$

$$-c_n \leq \Delta c_n \leq R_n - c_n, \qquad \forall n \in \mathcal{N} \quad (4.3g)$$

$$-f_h^{DC} \leq \Delta f_h^{DC} \leq \bar{F}_h^{DC} - f_h^{DC}, \qquad \forall h \in \mathcal{H} \quad (4.3h)$$

$$\sum_{h \in \mathcal{H}} f_h^{DC} \cdot I_{h,n}^{DC} + \sum_{h \in \mathcal{H}} \Delta f_h^{DC} \cdot I_{h,n}^{DC}$$
$$= R_n - c_n - \Delta c_n - \sum_{h2 \in \mathcal{H}2} Q_{h2}^{d} \cdot [e_{h2} + u_{h2} - d_{h2}], \qquad \forall n \in \mathcal{N}' \quad (4.3i)$$

$$0 \leq u_{h2} \leq 1 - e_{h2}, \quad \forall h2 \in \mathcal{H}2 \quad (4.3j)$$

$$0 \leq d_{h2} \leq e_{h2}, \qquad \forall h2 \in \mathcal{H}2 \quad (4.3k)$$

The objective function of this cost-based redispatch optimization is to minimise the redispatch costs RDC (4.3a), by considering a redispatch cost mark-up as identical to Kenis et al. (2024). The cost mark-up $\alpha$ ensures that redispatch actions are only taken to address line overloading, not to correct any inefficient market dispatch. This approach aligns with real-world practices in zonal wholesale markets, focusing on managing congestion rather than optimizing market dispatch (Weibelzahl, 2017). If the cost markup is zero, the outcome of objective function (4.3a) would reflect the costs of the remedial actions to return the zonal market clearing of objective function (4.2a) back to the nodal state of objective function (4.1a). Constraint (4.3b) ensures that sum of all upward and downward redispatch actions are equal. Constraint (4.3c) is somewhat similar to constraint (4.1d) from the D-2 optimization, where the combined effects of power injections and withdrawals at each node and their impact on the transmission network is accounted for. Here, constraint (4.3c) also accounts for the change in net power injection, induced by the redispatch efforts, and ensures that the flows on each AC lines stays within its limits ($\bar{F}_l$). Constraint (4.3d) ensures that the change in flow on the DC lines $h$ stays within its limits $\bar{F}_h^{DC}$. The constraints (4.3e) to (4.3h) ensure that the decision variable stay within their technical limits. Constraint (4.3i) is similar to constraints (4.1i) and (4.2i) from the D-2 and D-1 optimization problems. Constraints (4.3j) and (4.3k) are added to ensure that the decision variables of the electrolysers stay within their technical limits.

## 4.2.3 Defining the Risk Metrics

This section describes the methodological steps undertaken to trace the risks and structure the results of the simulation, to ensure that the risks can be analysed in the next step of the four-step methodology. The next section will first explain this optimisation problem and elaborates how it is used to assess the volume risk. Section 4.2.3.2 defines risk metrics for all price risks and explains how these metrics assist in analysing the results.

### 4.2.3.1 Defining the Volume Risk Metrics: The Net Position Maximalisation

It is important to consider the determining factor that distinguishes curtailment by the capacity calculation and the capacity allocation (see Section 3.2.3 for the explanation on these two different volume risk categories). The core difference between these two risks lies within the fact that curtailed volumes by the capacity calculation risk are a result of available wind generation exceeding the maximum allowed commercial exports, whereas curtailed volumes by the capacity allocation risk are a results of socio-economic welfare maximising market clearing outcome. During an hour when curtailment exists, it is thus important separate the amount of MWh being curtailed due to the grid limitations and the amount of MWh being curtailed due to the efficient market coupling. Moreover, making this distinguishment is crucial to determine the effectuation of the TAG since only the capacity calculation risk is covered by the TAG (see Section 3.3.1.4).

In order to make this distinguishment, first the maximum possible exporting capacity of the OBZ is determined. This is done by calculating the maximum possible commercial flows allowed during the DA market clearing step. In other words, it must be known how much wind power can theoretically be exported from the OBZ to the adjacent zones without violating the transmission grid's limitations. This is the maximum net position that exists for the offshore bidding zone, within the multidimensional solution space of all other bidding zones when each bidding zone's zonal position represents one dimension in this solution space. As an example, consider the working example of the 5-node, 3-zonal grid (See Box 4). Within this 3-zonal grid, each zone's net position represents one dimension, whereby the solution space of this problem can be represented in a 3-dimensional polygon with an x, y and z axis. If one of the net positions is then maximized, let's say the OBZ's net position represented in the z-axis, it means that there exists a 'slice' within this 3-dimensional solution space in which the net positions of the other two bidding zones, represented in the x- and y-axis, are not zero. It thus represents the maximum possible wind injection from the OBZ to the other bidding zone, while adhering to the physical grid constraints. It could also be the case that the maximization of the OBZ's net position leads to a solution with a single point in the 3-dimensional solution space. When this happens rather unique situation occurs, it means that all dimensions are fully constrained by the constraints of the problem. Translating this to our problem, this would mean that the maximum possible injection of offshore wind power from the OBZ to the other zones would completely congest the transmission system. This is thus a highly unlikely scenario and implicates inherent curtailment for the OWF to adhere to the grid's safety limits.

The optimization problem that describes the maximization of the zonal position of the OBZ, while adhering to the physical limitations of the transmission grid, is described in optimization problem (4.4) below. The objective is to maximise the net position of the OBZ. Constraints (4.4c) to (4.4f) are identical to constraints (4.2c) to (4.2f) from the D-1 market clearing optimization problem, as they represent the physical constraints of the transmission grid. Constraint (4.4b) is added to explicitly ensure that while the net position of the OBZ is maximized, the total of zonal positions is balanced, as the export of one zone must equal the import of another. This is a slight adjustment to the original problem, where the zonal net position balance is indirectly guaranteed by equalling the net positions to the difference in supply and demand (constraint 4.2b) and to the sum of all AC and DC flows, which collectively implies a zonal net position balance.

$$\mathrm{NP}^{\mathrm{OBZ}} = \max_{p_z, p_z^{FB}, f_l^{AC}, f_h^{DC}} \boldsymbol{p_{OBZ}} \quad (4.4a)$$

*Subject to*

$$\sum_{z \in Z} p_z = 0 \quad (4.4b)$$

$$\sum_{l \in \mathcal{L}} f_l^{AC} \cdot I_{l,z}^{AC} + \sum_{h \in \mathcal{H}} f_h^{DC} \cdot I_{h,z}^{DC} = p_z, \forall z \in \mathcal{Z} \quad (4.4c)$$

$$p_z^{FB} = p_z - \sum_{h \in \mathcal{H}} f_h^{DC} \cdot I_{h,z}^{DC} \quad (4.4d)$$

**Box 4: The Working Example Definition**

With three bidding zones in this example, the market clearing optimization can find solutions along the directions of each of these zones, whereby there exists a 3-dimansional solution space for this optimization problem.

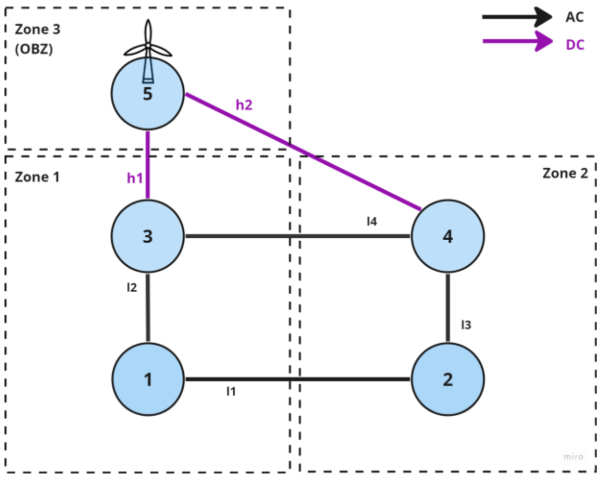

$$-RAM_l^- \leq \sum_{z \in Z} zPTDF_l^z \cdot p_z^{FB} + \sum_{h \in \mathcal{H}'} f_h^{DC} \cdot \left[ nPTDF_l^{n(h-)} \cdot I_{n(h-),h}^{ACDC} + nPTDF_l^{n(-h)} \cdot I_{n(-h),h}^{ACDC} \right] \leq RAM_l^+, \forall l \in \mathcal{L} \quad (4.4e)$$

$$-NTC_{z,z'}^- \leq \sum_{h \in \mathcal{H}} f_h^{DC} \cdot I_{h,z,z'}^{DC} \leq NTC_{z,z'}^+, \forall z, z' \in \mathcal{Z} \quad (4.4f)$$

The outcome of this optimization problem can then be used to determine whether the OWFs in the OBZ are being curtailed due to the capacity calculation step or the capacity allocation step. Optimization problem (4.4), like optimization problem (4.2), takes the calculated RAM values based on the D-2 base case optimization as input and optimizes the net position of the OBZ while adhering to the physical limits of the system based on the expected commercial flows. The outcome of this optimization problem thus reflects the maximum calculated capacity that can be exported from the OBZ to the adjacent markets. By comparing the optimal solution of objective function (4.4a) to the expected offshore wind production in the OBZ gives insight into whether full wind injection is possible or not. In other words, whether the OWF is being curtailed due to the capacity calculation volume risk. The way this is done is explained hereafter.

If the maximum net position of the OBZ is lower than the expected production of the OWF, it means that the D-2 calculation step limits all available wind power to be exported whereby the wind farm is (partially) curtailed during the D-1 step. The difference between the maximum net position of the OBZ and the expected volume of wind production represents the capacity calculation volume risk. Furthermore, it could be the case that the market does not clear at the maximum net position of the OBZ and that the volume of the theoretical possible generation of the OWF will even be further reduced. This additional reduction in volume from the maximum net position of the OBZ, as determined by the D-1 market clearing, then represents the capacity allocation volume risk. Box 5 summarizes the 'rules' for the distinguishment between the capacity calculation and allocation risk.

**Box 5: Capacity Calculation and Allocation Volume Risk rules**

To determine the distribution between the capacity calculation and allocation risk in during hours when curtailment ($c$) is occurring for the OWF in the OBZ ($c_{OBZ} \neq 0$), the following steps are undertaken:

1. Simulate the Case following the regular optimization chain (Problems (4.1), (4.2) and (4.3))
2. Optimize the net position of the OBZ (Problem (4.2))
3. Compare theoretical maximum net position of the OBZ ($p_z^{maxOBZ}$) to the potential ($R_{OBZ}^{D-1}$) and actual ( $R_{OBZ}^{D-1} - c_{OBZ}$) OWF production in the OBZ to determine the volume risk distribution following this algorithm:

- If $p_z^{maxOBZ} < R_{OBZ}^{D-1}$ and $p_z^{maxOBZ} \geq (R_{OBZ}^{D-1} - c_{OBZ})$:
  - Capacity Calculation Volume (CCV) = $R_{OBZ}^{D-1} - p_z^{maxOBZ}$
  - Capacity Allocation Volume (CAV) = $c_{OBZ} - CCV$
    - If $CCV > 0$ and $CAV = 0$ → Only capacity calculation volume risk occurs
    - If $CCV = 0$ and $CAV > 0$ → Only capacity allocation volume risk occurs
    - If $CCV > 0$ and $CAV > 0$ → Both volume risks occur
- If $p_z^{maxOBZ} \geq R_{OBZ}^{D-1}$ and $p_z^{maxOBZ} \geq ( R_{OBZ}^{D-1} - c_{OBZ})$:
  - Only capacity allocation volume risk occurs and $CAV = c_{OBZ}$

To get a better understanding of the visual context of this optimization, to the Flow-Based domain of zone 1 and 2 from the working example (see Section 2.4, Figure 9), is now added the new CNEs' linear equations. These CNEs' are obtained by running optimization problem (4.4) and using the $p_z$ values from this problem (4.4) to recalculate the RAM values using formula (A.4). The $p_z^{ref}$ is thus replaced by $p_z^{maxOBZ}$, whereby new, more restricted RAM values ($RAM_l^{maxOBZ}$) are obtained, which are then used to recompute the geographical equations described in formulas (2.4) and (2.5) to visualise the FB domain. Figure 14 below shows this additional set of CNEs' in the graph and shows the surface area enclosed by these constraints that represents the represents the solution space in which the net positions of zones 1 and 2 can move, if the OBZ's net position is maximized. Where previously 2 graphs described the 3-dimensional solution space of the three zones in the working example (Figure 9), there is now left only 1 graph. This is because one of the axes of the 3D space (e.g. the z-axis) has been fixed to a single point in which it is at its maximum (the max position of the OBZ). Essentially, the FB domain in Figure 14 is a 2-dimensioanl slice in the 3-dimensional solution space of this particular problem at the maximum value of the third dimension.

To graphically determine whether a volume risk is occurring, and if so, whether the curtailed volume is due to the capacity calculation and/or capacity allocation volume risk, one can introduce the market clearing point of the D-1 simulation.  The market clearing point can be understand in this context as the coordinates describing the zonal net positions, as determined by the DA market clearing algorithm. The blue diamond in Figure 14 shows this clearing point. Within the example of Figure 14, the market clearing point in this hour just falls outside the FB domain of the $p_{OBZ}^{max}$, as it is outside the pink box. This indicates that the market clearing outcome does not allow for full wind injection from the OBZ to the rest of the grid. To determine whether this hour has a volume at risk and which risk this volume would be attributed to, the reasoning from before and described in Box 5 must be followed once more.

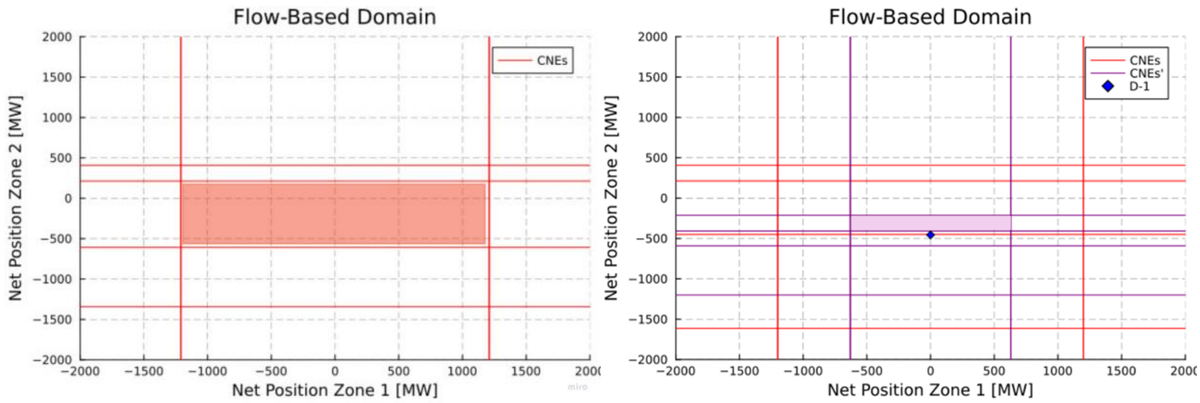


*Figure 14: Visualisation of the Flow Based domain before (left) and after (right) optimizing the net position of the OBZ.  The CNEs (red lines) encapsulate the original FB domain (from the D-2), where the red box is the solution space for zones 1 and 2 while the allowed net positions for the OBZ exist in a third dimension. The right picture includes the FB domain after maximizing the net position of the OBZ. The pink box, encapsulated by the more restricted CNEs', describes the allowed net positions for zones 1 and 2, while the net position of the OBZ is at its maximum.*

Considering the 4-zonal grid topology that is used in this thesis (Section 5.1), this representation becomes slightly more complicated. A 4-dimensional representation is inherently impossible for the human brain, but by maximizing 1 dimension, being the net position of the OBZ, the 4-dimensional solution space can reduce to a 3-demensional space in which the x, y and z axis are represented by the net positions of zone 1, 2 and 3. For the sake of simplicity in graphical representation, it is possible to take two slices of this 3-D solution space in which in the first slice the solution space for the x and y (e.g. zone 1 and 2) axis are represented and in the second slice the solution space for the x and z axis (e.g. zone 1 and 3). This is visualised in Figure 15. In this particular hour, the market clearing point falls inside the 3-dimensional solutions space, indicating that the potential wind generation is not being restricted by limited export transmission capacity to the surrounding onshore grid. Thus, in this example there will be no curtailment caused by the capacity calculation risk. In case the D-1 market clearing does not accept the full generation bid of the OWFs, the curtailed volume is thus caused by the capacity allocation risk.

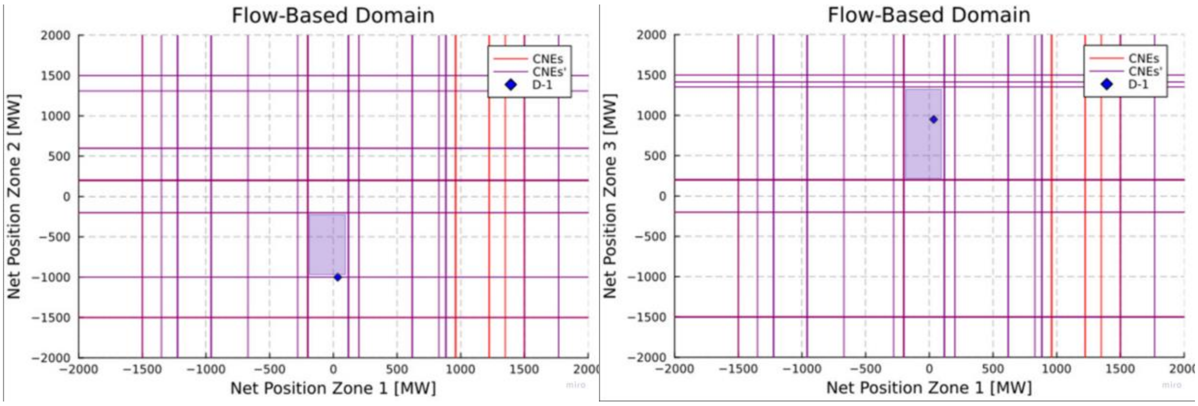


*Figure 15: The Flow-Based domain of the representative grid after the $p_{OBZ}^{max}$ optimization. The purple boxes represent the net positions zone 1 and 2 (left figure) and zone 1 and 3 (right figure) can have when the net position of the OBZ is at its maximum.*

### 4.2.3.2 Defining the Price Risk Metrics

To determine the frequency and severity of the different price risk categories, several metrics have been defined. By implementing these metrics, the different types of price risks are systematically quantified, providing a comprehensive methodology to assess their occurrence and severity across multiple simulated cases. This structured approach aids in identifying the key factors driving these risks, ultimately contributing to a answering the main research question.

The first price effect category indicated in the Risk Framework, the locational basis price effect, will not be traced in this thesis. The second price effect, the price convergence effect, it will be traced how often the price of the OBZ converges to lowest priced zone to trace the frequency of hours in which the rule of thumb price formation applies. Furthermore, it is traced how much wind power is exported during these hours to trace the magnitude. Additionally, the same is done for the price in the OBZ converging to the higher priced level than the lowest adjacent market. Specifically, the frequency of hours is traced in which the price of the OBZ converges to the price of the adjacent bidding zones with the highest price, labelled 'High-priced' hours. The hours in which the price of the OBZ is identical not to the lower priced market, nor the higher priced market, but to the other market, is labelled the 'middle-priced' hours. Both the frequency and magnitude of exported wind power during these hours is traced.

For the flat price risk, several statistical metrics are computed to indicate the uncertainty and fluctuations in price levels intra- and inter-zonally. First of all, the mean price level provides an idea of the price level within a simulated case and helps observe shifts across cases, reflecting the influence of changes in drivers. Secondly, standard deviation is used to measures the amount of variation or dispersion of a set of values (Bonamente, 2022). A high standard deviation indicates higher price volatility and variations in standard deviation across cases can indicate changes in price volatility with different parameter inputs. Lastly, the Coefficient of Variation (CoV) is used which is a standardized measure of dispersion around the mean, expressed as a percentage (Bonamente, 20220). The CoV puts the standard deviation in relation to the mean, providing a dimensionless quantity ideal for comparing the degree of variability between datasets with different units or means, thus indicating price volatility across cases.

For the non-intuitive price risk, the metric implemented to trace this involves comparing the OBZ price to prices in other zones. If the OBZ price differs from all the other zones' prices and is not equal to zero (f the price would be zero, this would indicate the price collapse risk), it can be assumed that a non-intuitive price risk hour occurs. However, as mentioned in Section 3.2.2, the non-intuitive price risk can be either negative or positive, depending on if it is loading or relieving the CNEs restricting the FB domain. To determine whether it is a positive or negative non-intuitive price risk hour, it is checked if the price in the OBZ is higher or lower than the lowest price of all of the other zones. If it the OBZ price would be higher than the lowest priced onshore zone, it means that the non-intuitive price has a positive outcome since it exceeds the lowest priced adjacent zone and no longer converges to that zone. Reversely, if lower, a negative non-intuitive price hour occurs. All non-intuitive hours (both positive and negative) are counted and the corresponding wind production during that hour is stored in MWh. Moreover, the effect is calculated by multiplying the produced wind power in a non-intuitive priced hour with the electricity price. Doing so, the total net effect of the simulated time can be calculated by subtracting the negative effect from the positive effect.

For the price collapse risk, it is traced how many hours over the simulated timespan experience zero prices. Moreover, it is traced how much MWh of OWF production takes place in these hours, as well as the curtailment during these hours. Important in this metric is that the prices of the other bidding zones are first assessed to ensure that the price collapse risk occurs and not just an hour in which renewable generation could completely supply demand in a specific zone. After all, if one of the other bidding zones also has a zero priced hour, it indicates that the demand is fully met by renewable supply. These renewables supplied zero priced hours are also traced in frequency and magnitude, to distinguish from the price collapse risk.

For the interacting price and volume risk there is no specific indicator included. This risk will be assessed based on the results of both price and volume risk metrics. Specifically, it will be analyses during what type of price hours the volume risk categories occurred.

## 4.3 Step 3: Case Group Analysis

After completion of the simulation step, the next step is to analyse the results per case group. First Section 4.3.1 describes how the results have been extracted from the model and are analysed per case group. Second, the methodology applied to determine the compensation payments via the FTR and TAG is explained in Section 4.3.2.

### 4.3.1 Results Extraction and Analysis per Case Group

To extract results from the Julia model, all parameters, variables, objective function outcomes, and shadow prices of constraints were exported to CSV files. Specifically, the JuMP programming language was utilized for extracting the dual variables of the constraints (JuMP, 2024). During this results processing, the congestion rents for the TSOs were also calculated and stored in CSV format. As the simulations were conducted on a monthly basis, the monthly results from the CSV files were aggregated using a Python script, specifically employing the pandas package. After aggregating the results, the risk metrics defined in Section 4.2.4 were computed using another Python script and subsequently exported to CSV files. Price duration curves and load duration curves were then created in a separate Python script. All results were stored in an Excel file to facilitate the analysis of the cases per case group, as explained in the next section.

To analyse the case results per case group, the frequency and magnitude for all price and volume risks are analysed for all cases. Additionally, the results are compared to the reference case to assess the impacts of changed input parameters per case. The analysis follows a structured approach. Initially, general results are presented, encompassing total figures such as total wind exports, curtailments, and revenues for the OWFs. This is followed by a detailed examination of price risk results and volume risk results, where the frequency and magnitude of the respective risk categories are discussed. Each case is compared with the reference case using percentage changes to highlight the effects of the modified input parameters. Additionally, cases within a case group are compared to see the marginal changes between the cases within a group. For the visual representation of the data, different chart types are employed. Price risk frequency is illustrated using pie charts, while price risk severity is shown through bar charts. Volume risk frequency is depicted using stacked bar charts, and volume risk severity is also represented by bar charts. Additionally, price and volume risk duration curves are utilised to provide further insights into the risks. This systematic approach ensures a thorough analysis of the cases within each case group, setting the stage for the subsequent cross-case group analysis.

### 4.3.2 FTR and TAG Compensation Methodology

This section describes how the compensation for two regulatory mitigation instruments is determined. As said, for the FTR the description from PROMOTioN (2020) is followed. Following their explanation, and adjusted to align better with the TAG design explained hereafter, equation 4.5 describes the Revenues obtained via the FTR ($R^{FTR}$) to the OWF operators:

$$R^{FTR} = \sum_{z \in Z} \min\left(Q_{FTR}^{generated,z}, Q_{FTR}^{contract,z}\right) \cdot max\left(P_{FTR}^{contract,z} - P_{market}^{OBZ}, 0\right) \quad (4.5)$$

FTRs are bilaterally contracted between an OWF and a specific market to effectively cover the price differences between the OBZ and that bidding zone. For practical purposes, it is assumed that the FTR contract is with the bidding zone to which the OWF is directly connected. Thus, compensation payments are calculated for each OWF in the OBZ relative to their closest adjacent bidding zone, and these individual payments are summed to obtain the total compensation payment for all OWFs in the OBZ ($R^{FTR}$ ).

For simplicity, it is assumed that the contracted volume of the FTR ($Q_{FTR}^{contract,z}$) to each bidding zone z follows an equal distribution with a 1:4 ratio to installed OWF capacity. For instance, with 4 GW of installed OWF capacity, 1 GW is covered by the FTR, equally distributed over the connected bidding zones[8]. The contracted volume represents the maximum export volume to be compensated. However, if the generated wind power of the OWF ($Q_{FTR}^{generated,z}$) is lower than the contracted volume, the actual generated volume will be used for FTR compensation to avoid overcompensation during low wind hours. The contracted price of the FTR ($P_{FTR}^{contract,z}$), is taken as the market price of the respective bidding zone where the FTR contract is in force. The total revenue of the OWF via the FTR is then calculated according:

$$R_{total}^{FTR} = R^{OBZ} + R^{FTR} \quad (4.6)$$

The total revenue for an OWF in an OBZ with an FTR is thus the sum of the revenue obtained from wind exports at market prices for all generated power ($R^{OBZ}$) and the compensation payment covered by the FTR contract ($R^{FTR}$), as determined by equation 4.6.

As described in Section 3.3.3, the exact definition of the TAG compensation measures is yet to be published in the amendments to Commission Regulation (EU) 2015/1222, but the proposal for the amendment of the European Commission's EMD Regulation (European Parliament & European Council, 2024) implied that the TSOs should compensate OWF operators via the TAG for the curtailment induced only by the capacity calculation volume risk, not the capacity allocation volume risk. Equation 4.7 determining the TAG compensation is based on Laur et al. (2022), but adjusted to follow more closely the definitions provided in the EMD Regulation:

$$TAG = max\left(p_{TAG}^{ref} - P_{market}^{OBZ}, 0\right) \cdot c^{CC} \quad (4.7)$$

[8] This is in case the installed capacities of the OWFs are equal within the OBZ. In case of an asymmetric setup, the ratio of installed capacity to the corresponding zone is used. E.g. with a dual hybrid with one OWF of 1.5GW and one of 3GW, the contracted volume of the FTR also follows a 1:2 ratio.

Where ($P_{TAG}^{ref}$) is the price of the reference bidding zone for the TAG and $c^{CC}$ is the curtailment by the capacity calculation risk. Regarding the choice of the reference price ($P_{TAG}^{ref}$), Laur et al. (2022) do not further specify how the reference is determined and on what bidding zone it is based, nor does the Market Reform amendment (European Commission 2020b) elaborate on the specifications for choosing a reference market for the reference price. One could argue that the reference price for the TAG compensation should be the price of the onshore market that would otherwise be its Home Market if not connected interconnected to other markets via the hybrid setup. However, following the rule of thumb, the OBZ generally converges to the lowest priced adjacent bidding zone, whereby having a reference zone that is structurally not the lowest price bidding zone (but its own HM price) would overcompensate the OWF operators. Therefore, it is chosen to always take the price of lowest priced adjacent bidding zone as the reference price for the TAG compensation to the hybrid asset, to ensure that the OWF operator is compensated up until the point that he would otherwise would have received.

Combining these two instruments would in the end lead to the new revenue obtained by the OWFs in the OBZ ($R_{new}^{OBZ}$) following:

$$R_{new}^{OBZ} = R_{total}^{FTR} + TAG \quad (4.8)$$

For all the cases that will be simulated, the FTR and the TAG compensations will be calculated to assess the effectiveness of these regulatory mitigation measures. Section 6.7 presents the results on this analysis.

## 4.4. Step 4: Cross-Case Group Analysis

The last step within this four-step modelling approach is the Cross-Case Group Analysis. In this section, the methods applied to standardize the results of all cases to enable cross-case comparison of the cases is discussed. The standardisation of the results aids in preparing the results for the construction of Risk Matrix, explained in Section 4.4.2.

### 4.4.1. Risk Metrics Standardization

For all risk indicators, the results are standardized using the standardization method described in equation (4.14a) for results that are considered **benefits**:

$$Standardized\ metric = \frac{value_{case} - value_{Ref\ Case}}{\max\,(value_{all\ cases}) - \min\,(value_{all\ cases})} \quad (4.9a)$$

And for results that are considered **costs** equation (4.14b) is used:

$$Standardized\ metric = \frac{value_{Ref\ Case} - value_{case}}{\max\,(value_{all\ cases}) - \min\,(value_{all\ cases})} \quad (4.9b)$$

With results being considered benefits is meant that an increase of the value with respect to the reference case is considered a positive result for OWF developers, and for results being considered costs an increase with respect to the reference case is considered a negative result. Table 4 indicates the metrics considered in the cross-case analysis and indicates whether their results are considered costs or benefits.

This method scales differences relative to the total range of values observed, ensuring that the standardized values are comparable across different units or magnitudes of measurement. In the numerator, the difference between the case and the reference case directly shows how much the case value deviates from the reference case. The denominator represents the range of all values, providing a normalization factor that keeps the score within a relative scale based on the most extreme values observed across all cases. Using this standardization method ensures a reliable comparison of the cases with respect to the reference case. A standardized value of 0 corresponds to the reference case. A standardized value above 0 indicates a ‘less risky’ perception, whereas a value below 0 indicates a ‘more risky’ perception compared to the reference case.

*Table 4: Overview of the metrics that serve as input for the Risk Matrix. It is indicated if the metrics are Costs (C) or Benefit (B), i.e. if standardization equation (4.9a) or (4.9b) is used.*

| **General Result Metric** [Magnitude] | **C/B** | **Price Risk Metric** [Frequency/Magnitude] | **C/B** | **Volume Risk Metric** [Frequency/Magnitude] | **C/B** |
|---|---|---|---|---|---|
| Total Revenue OWFs [M€] | B | Mean Price | B | No Volume Risk [hours/-] | B |
| Total Wind Export [GWh] | B | CoV OBZ | C | Capacity Calculation [-/MWh] | C |
| Total Curtailment [GWh] | C | Rule of Thumb [hours/GWh] | B | Capacity Calculation & Allocation [hours/-] | C |
| Export at Zero-Price [GWh] | C | Price conv. To Middle [hours/GWh] | B | Capacity Allocation [hours/MWh] | C |
| Export at Positive Price [GWh] | B | Price conv. to High Zone [hours/GWh] | B | Total Wind Export [-/GWh] | B |
| Total Congestion Rent [M€] | B | Non-Int. Positive [hours/MWh] | C | Total Volume Risk [-/ MWh] | C |
| Total Day-Ahead Cost [M€] | C | Non-Int. Negative [hours/MWh] | C | | |
| | | Price Collapse [hours/MWh] | C | | |
| | | Zero-Price due to RES [hours/MWh] | C | | |

### 4.4.2 The Risk Matrices

The last step of the fourth step is the creation of the Risk Matrices. A risk matrix, often referred to as heat map, is an effective methodology to simultaneously aggregates the results of all cases while exposing the changes in the frequency and magnitude across the cases. The matrix visually represents the frequency and severity of different risks, making it easier to identify and compare the impact of various factors. Colour schemes are used to expose the marginal changes between frequency and severity of all risks per, compared to the reference case. By consolidating data from multiple simulated cases with different input parameters, the matrix highlights patterns and trends not immediately apparent from numerical data alone. It pinpoints key drivers of price and volume risks, showing which factors significantly influence these risks. It also prioritizes risks by visually differentiating between high and low-risk areas. Furthermore, the matrix serves as an effective communication tool by translating complex data into an accessible format. This is thus an important last step of the methodology.

## 4.6 Model validation

This section discusses the steps that have been undertaken to validate the model. First, the steps undertaken during the model creation phase are explained in Section 4.6.1. Then, section 4.6.2 discusses the steps undertaken for the validation of model’s operation.

### 4.6.1 Validation of Model Creation

Throughout the model creation process, several model validation steps have been implemented. Throughout the entire model creation process, antibugging served as an important check to assess if the behaviour of the model was as intended and to find errors within the code. Between important steps in the model, such as after transforming data and creating the FB parameters, several manual output prints were implemented to ensure that the optimizer uses the correct data entries and input parameters in the optimization calculations. Furthermore, the validation functions provided in the Gurobi software were used. Specifically, after optimizing each of the three linear optimization problems, the complete model with all constraints was written to an LP file which could be used to compare the model’s formulation of the objective function and constraints with the mathematical equations provided in section 4.2.2.

The 5-node grid topology model, referred to as the Working Example (Box 1), served as a useful demo model to enable fast testing and debugging of the model. Extensive test runs have been performed win this demo model with various combinations of generators, load values and bidding zone configurations, before moving to the large grid topology used in this thesis. This allowed for testing of the code and validation of the intended model's functionalities. Moreover, it enabled comprehension of the model whereby it served as a valuable learning vehicle to both learn the Julia programming language and get acquainted with complex optimization algorithms.

Another important validation step during the model creation process, was the formulation of the Karush-Kuhn-Tucker (KKT) conditions to validate if the formulated optimization model in Julia followed the mathematical model. The KKT conditions of the mathematical model have been formulated following the instruction document provided during the course Engineering Optimization (Bruninx, 2022), and can be found in Appendix B. To validate the correctness of the formulated optimization problem in Julia, for several demo simulations the solutions of the optimisation problem were checked against the KKT conditions. Specifically, the solutions of the solver were filled in the optimality conditions to validate if the objective function was optimized, and double checked against the primal and dual feasibility constraints, to see if the solution meets these conditions and does not violate any constraints. This step specifically validated the mathematical formulation of the model.

## 4.6.2 Validation of the Model Operation

After the model creation step, with the demo model and the mathematical model validated, the full grid topology and the larger data sets were implemented. To validate that the transition from a small model to the larger model di d not inherent unexpected errors, a functionality validation and an extreme values validation been undertaken.

### 4.6.2.1 Model Functionality Validation

First a functionality validation was performed. Here it was checked if all desired functionalities of the model were correct. A first important functional validation step was to check the zonal power balance constraint's outputs. Here, it was checked whether the combination of dispatched generators and produced renewable power equalled the total load value of that hour, to ensure satisfaction of the constraint. Moreover, the shadow prices of the zonal power balance were compared to the marginal costs of the dispatchable generators. Except for some hours where non-intuitive price formation could occur, the shadow prices of the zonal power balance should equal the marginal costs of a generator, reflecting the marginal increase of the objective function if one additional unit needs to be generated.

Furthermore, the line loadings of both the AC and DC lines were checked after redispatch operations, to validate that these loadings stayed within the physical limits of the grid. To validate of the AC line loadings within the grid stay within the intended physical limits as depicted in constraints (4.2e) and (4.3c), the following validation step has been undertaken. First, it was checked how many hours the loading of all AC lines exceeded the transmission capacity of that line for the line loadings after the redispatch optimization. One line seemed to violate this constraint for 183 hours out of the 2952 hours simulated. However, when adding the total MWh of exceedance of the transmission capacity, the total violation was $1.124 \cdot 10^{-10}$, whereby this is completely neglectable. The AC line loadings thus seemed to be in order. For the DC line loadings, a similar validation was done only now by comparing the loading of the DC lines with their NTC values, conform constraint (4.2f). Here it was found that the internal DC lines in the OBZ exceeded maximum transmission capacities of these lines in the D-1 optimisation. The original source code for the mathematical model of Kenis et al (2023) did not constrain the internal DC lines in the OBZ with respect to its maximum transmission capacity in the D-1 market clearing optimisation. To account for this error, additional constraints were added specifically restricting the flow on these lines to stay within their physical limits. After these validation steps, the model's functionalities all seemed to be in order.

#### 4.6.2.2 Extreme Values Validation

In a last validation step an extreme values validation has been performed. This validation was particularly useful in testing the limits of the model under extreme conditions, and specifically, the physical limits of the transmission grid with extreme values for wind injections by the OBZ. For the extreme values validation the installed offshore wind capacities and the DC transmission lines to the onshore zones and internal in the OBZ were set to 100 GW. A simulation was done for the same weather, demand and generation mix input data.

The results of this simulation showed that the price formation seems to be in order, since all prices dropped significantly and converging to zero most of the simulated time, which is expected with a tremendously high injection of cheap renewable power. Regarding the physical limitations of the grid, a total wind export of 10657.53 GWh was observed, which is recalculated a value of 1203.36 MWh of exported wind power per hour per wind farm. This means that whenever offshore wind capacity factors exceed 0.802, it is likely that there will be curtailment caused by the inability of the onshore grids to import the wind power, hinting at the capacity calculation volume risk.

Furthermore, from running the $p_{OBZ}^{max}$ optimization (Section 4.2.4.1) for the extreme values simulation, the maximum possible imports from the OBZ to each respective zone could be derived, indicated in Table 5. Since the interconnection capacity to shore did not restrict the maximum export capacity, the values in Table 5 represent the theoretical maximum import capacity by the onshore grid. An important observation here is that the maximum imports to zone 1 are below the transmission capacity from the OBZ to this zone.

*Table 5:Maximum Imports per Zone. Values present the minimum observed net positions form optimization problem (4.7)*

| | Maximum Import/ Minimum Net Position |
|---|---|
| **Zone 1** | -774.502 MWh |
| **Zone 2** | -2888.68 MWh |
| **Zone 3** | -5696.29 MWh |

Another relevant outcome of this extreme values validation is that throughout the 2952 simulated hours, the maximum observed flow on all three DC lines internal in the OBZ was 491.56 MWh. This 491.56MWh is the same value as the thermal capacity of many onshore AC lines (of the 248 onshore AC lines, 186 have a thermal capacity of 491.56 MW). This indicated that one (or more) of the zones' CNEs is the limiting factor for the FB domain of the OBZ. To further assess this, the shadow prices of constraint (4.2e), which explicitly consider the effect of flows from DC lines on the AC lines, were investigated and compared to the DC flows. Specifically, whenever one of the three DC lines internal in the OBZ showed a (absolute) value of 491.56 MWh, it was checked for which of the AC lines a non-zero shadow price from constraint (4.2e) existed. Here it was found that every time on one of the DC lines internal in the OBZ a flow of 491.56 MWh occurred, the shadow price of constraint (4.2e) for the line connecting nodes 37 and 43 showed a non-zero value, indicating that this line specifically restricts the FB domain of the OBZ. This AC line connects the landing point from the OBZ to zone 1 (at node 43) with the node where the point-to-point interconnected from zone 1 to zone 2 is connected (at node 37), indicating its crucial role in this grid.

The implications of this specific identified CNE in the onshore area of zone 1 is primarily that this CNE could frequently limit the FB domain of the OBZ. This is also indicated with the maximum import capability from Table 5. Specifically, since the theoretical maximum export capability of the OBZ is reduced from 4.5 GWh (three 1.5 GW interconnectors) to 3.78 GWh (resulting from a maximum of 774 MWh to zone 1), whenever wind generation in the OBZ exceeds a capacity factor of 0.839, curtailment by the capacity calculation is expected to occur. Additionally, since zone 1 is the higher priced zone with more dispatchable fossil generators and zone 2 and 3 the lower-priced zones with more renewable capacity (see Section 5.1), it could be more frequently the case that generation capacity in the OBZ and renewable-rich zones 2 and 3, which cannot be fully transmitted to Zone 1, lead to higher prices in zone 1 and curtailment of the OWFs, especially during periods of high renewable output.

In conclusion, the extreme values analysis revealed critical limitations in the transmission grid. Despite these, the decision to maintain 1.5 GW installed wind capacity per OWF stands, as the grid topology operating near its limits helps identify key price and volume risk drivers. This approach also mirrors the real-world scenario where onshore congestion frequently leads to offshore wind curtailment, as will be explained in Section 5.1.2.

# Chapter 5. Case Definitions

This chapter defines the cases that will be simulated in this thesis. First, the reference case is explained in Section 5.1. It should be noted that the purpose of having a reference case in this thesis is primarily to serve as a benchmark to which the results of the other cases can be compared to. Specifically considering SQ3, aimed at finding the factors leading to the most frequent and severe price and volume risks, it proves useful be able to compare the increases and decreases of the risks induced by different case setups relative to the reference case, such that the marginal effects can be assessed.

After having established the reference case, the specific Case Groups will be discussed in Section 5.2, where first is explained why these Case Groups are of interested to be simulated, followed by a hypothesis per case group on the expected results. Additionally, the specific variation in the input data and parameters and how these variations have been structurally selected is explained.

## 5.1 Reference Case

To establish the Reference Case, first the general parameter inputs and data assumptions that are not varied across the cases is explained (Section 5.1.1), followed by the formulation of the Reference Case (Section 5.1.2).

### 5.1.1 General Parameter Inputs and Data Assumptions

The grid topology used in this thesis is taken from Kenis et al. (2023), which is based on the representative grid from Schönheit et al. (2021). This grid comprises 103 nodes, 237 AC lines, and 12 DC lines. To this grid, three offshore nodes have been added, each connected to shore with a single DC line and interconnected in a triangular setup. The grid includes three onshore zones plus an offshore bidding zone (OBZ). Figure 16 visualizes the grid topology.

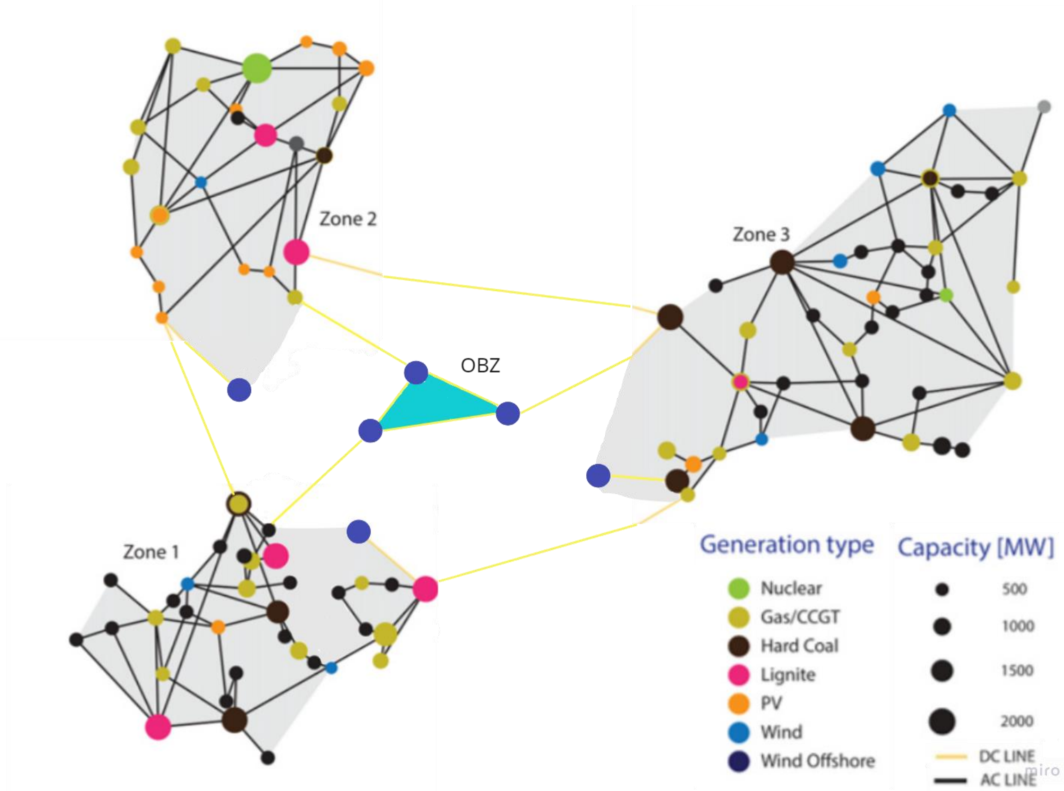


*Figure 16: The representative Grid Topology. The generator types are indicated with colours and their capacity sizes with thickness of the nodes. Figure is taken from Kenis et al. (2023).*

The specifications on the capacities of the OWFs and the transmission lines are discussed in the next section, since they are varied across the cases. Regarding the weather data and the hourly nodal load values, the data from Schönheit et al. (2021) was also taken. For the weather data they took hourly capacity factors of France, Belgium and Germany for zones 1-3 respectively for the year 2015 from SETIS (European Commission, 2023). For the offshore bidding zone, the average is taken of the capacity factors of the three other zones. Regarding the load values, node-specific load time series have been generated by Schönheit et al (2021) to fit within the topology of this representative grid. These load values are fixed, assuming perfectly inelastic demand. Both the weather data and the load data will not be varied throughout the cases.

Other data and parameter assumptions consistent across all cases are summarized in Table 6. For instance, the NTC value is always 100% of the transmission capacity of the respective cross-border line, and the MinRAM value is always 70% of the transmission capacity of the AC line. Curtailment costs are set at 0 €/MWh. These assumptions align with regulatory standards and ensure a consistent basis for comparison across cases.

*Table 6: Parameter Assumptions for all Cases.*
**Note that this does not depicts the RAM value put to the market clearing step (See Appendix A, formula A.4)*

| Parameter | Assumption | Implication | Explanation |
|---|---|---|---|
| **NTC** | Value is always 100% of transmission capacity DC line | Limiting equation (4.2f) (Section 4.2.2) | Putting the NTC at 100% means that full transmission capacity of the interconnectors is put to the market clearing. |
| **MinRAM** | Value is always 70% of transmission capacity AC line.* | Limiting part of equation (A.4) (Section 2.3) and thereby limiting equation (4.2e) (Section 4.2.2) | Conform Regulation 2019/943 (Council of the European Union and European Parliament, 2019). |
| **Curtailment Cost** | 0 €/MWh | Curtailment is not monetarily penalized in the objective function (4.2a] | This penalization of curtailment can be considered as renumeration from the TSO to the OWF owner (Schönheit et al, 2021), which is in this thesis considered outside the optimization problem via the TAG. |
| **α (redispatch cost mark-up)** | α is set to 0.10 | Limiting objective function (4.3a) to ensure redispatch actions are taken only for line overloading. | See Section 4.2.2.3. |

## 5.1.2 Defining the Reference Case

Establishing a sound reference case is crucial for analysing the different driving effects of price and volume risk. This allows for the comparison of marginal differences when the cases are varied. The reference case is essential because it provides a baseline against which the impacts of varying input data or parameter differences can be measured.

The first determination for the reference case is the generation mix. Considering that the first hybrid projects in an OBZ are expected to be commissioned around 2030 (ENTSO-E, 2024a) and the typical time between commissioning and operation is approximately five years (RVO, 2023), along with OWFs having a lifespan of at least 15 years (Pakenham et al., 2021), a high penetration of renewable energy sources is appropriate for this thesis. Consequently, the 'very high vRES case' from Schönheit et al. (2021) is used as the input for the generation fleet in the Reference Case. This generation mix will be referred to as the Renewable Mix.

The merit orders of the onshore zones in the Reference Case are illustrated in Figure 17. The minimum and maximum load values are also indicated in the graphs with triangles on the x-axis. Noteworthy is that the installed generation capacity is somewhat over-dimensioned compared to the load data. Since all renewable energy sources are assumed to have marginal costs of 0 €/MWh, their cumulative installed capacity represents the rightward shift of other generators in the merit orders. Additionally, a graph depicting the installed capacities per zone is provided. Moreover, the Fleet Average Marginal Cost (FAMC), representing the weighted average costs of all generators in the bidding zone, is indicated with red dashed lines.

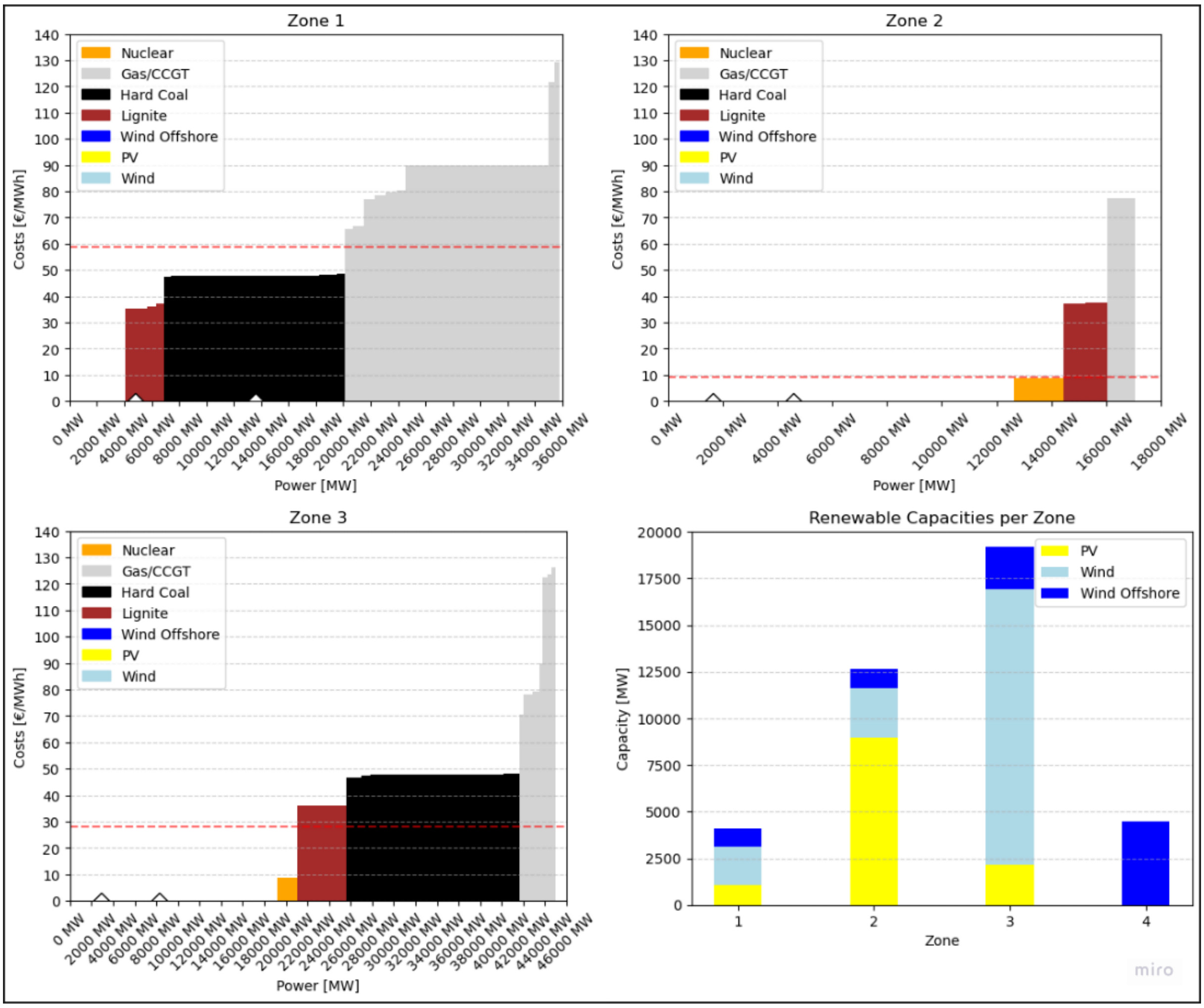


*Figure 17: The Merit Orders and Installed Renewable Capacities per zone for the Reference Case.*

The second determination for the reference case is the offshore system design. A triangular offshore grid topology is chosen for the reference case to ensure all three markets are interconnected via the OBZ. The size of the OWFs is the next important choice within the offshore system design. It is necessary to establish the physical limitations of the AC onshore grid regarding wind injection from the OBZ. As shown in Figure 16, the OBZ has specific landing points at the onshore AC grid, where the generated wind power flows through the DC transmission lines into the entire AC network, following Kirchoff's power laws. Overdesigning the offshore system would mean the generated power of the OWFs cannot be exported to the onshore markets due to physical limitations of the AC grid, which is impractical. Conversely, under-designing the offshore system to always allow the onshore grid to absorb the full wind injection does not reflect the expected reality. For instance, offshore wind power in Germany is often curtailed due to onshore grid congestion (Rajgor, 2024), and the Netherlands urgently needs grid expansion to achieve its offshore wind targets (Tweede Kamer, 2024).

To determine proper OWF capacities with respect the rest of the grid in the model, the maximum net positions of the OBZ is analysed. First, an optimization has been performed for the maximum net position of the OBZ in which only physical grid limitations are considered. The optimization problem formulated in Section 4.3.3 has been used for this. This optimization is carried out for the first day of each quarter, simulating 24 hours with wind farm capacities and transmission cables set to 20 GW each to avoid restrictions of the FB domain by cross-border DC cables. The average maximum net position of the OBZ in this optimization was 5713.18 MWh/h.

Additionally, for the same setup, the FBMC optimization problems (from Section 4.2) have been simulated to assess the average net position of the OBZ when not only physical constraints are considered, but also the market constraints. The average net position of the OBZ in this optimization was 4629.06 MWh/h.

Considering these two numbers, a total installed OWF capacity of 4.5 GW (having 1.5 GW per OWF) seemed a proper assumption since theoretically the maximum possible wind exports from the OBZ in this setup could on average be imported by the adjacent bidding zones, as the total installed capacity is lower than the (maximum) net position of the OBZ. By setting the Export Indicator (EI) to 1.0 and using identical sizes for the internal transmission lines in the OBZ, the Reference Case is established (Table 7).

*Table 7: Offshore Grid Topology Table for the Reference Case.*

| | **Installed OWF capacity ($Q_z^{OWF}$) and transmission capacity ($\bar{F}_{obz\to 1}^{DC}$) in GW** | | | | | | | | | **Export (EI) and Interconnectivity (II) indicators** | | | | | | |
|---|---|---|---|---|---|---|---|---|---|---|---|---|---|---|---|---|
| **Case** | $Q_1^{OWF}$ | $\bar{F}_{obz\to 1}^{DC}$ | $Q_2^{OWF}$ | $\bar{F}_{obz\to 2}^{DC}$ | $Q_3^{OWF}$ | $\bar{F}_{obz\to 3}^{DC}$ | $\bar{F}_{obz,1\to 2}^{DC}$ | $\bar{F}_{obz,1\to 3}^{DC}$ | $\bar{F}_{obz,2\to 3}^{DC}$ | **EI** | $EI_1$ | $EI_2$ | $EI_3$ | $II_1$ | $II_2$ | $II_3$ |
| **Ref** | 1.5 | 1.5 | 1.5 | 1.5 | 1.5 | 1.5 | 1.5 | 1.5 | 1.5 | 1 | 2 | 2 | 2 | 2 | 2 | 2 |

## 5.2 The Case Groups

The cases that have been formulated can be grouped into 5 Case Groups describing the category that will be varied within the group: Generation Mix (Case Group 1), Offshore Grid Topology – Triangular Setup (Case Group 2), Offshore Grid Topology – Dual Setup (Case Group 3), Onshore CNEC (Case Group 4) and Hydrogen Production (Case Group 5). For each case group it is explained why the case group is subject to analysis followed by a hypothesis on the expected outcomes of the case group. Additionally, the most important assumption within the group and how the specific cases in the group are formulated is explained. Table 8 below gives an overview of all cases that have been simulated and analysed in this thesis.

*Table 8: Overview of all Cases included in this thesis. Indicate is the main parameter varied per group and the specifications per case.*

| (No.) Group Name | Parameter Varied | Case Name | Specification |
|---|---|---|---|
| **0. Reference Case** | *n.a.* | **Ref.** | *See Section 5.1* |
| **1. Offshore Grid Topology - Triangular Hybrid** | Transmission capacity of the interconnectors ($\bar{F}^{DC}_{obz \to z}$) | $\mathbf{EI^{+}}$ | Relative direct export capacity from OBZ to shore (i.e. Export Indicator) increased with 33% |
| | | $\mathbf{EI^{-}}$ | Relative direct export capacity from OBZ to shore (i.e. Export Indicator) decreased with 33% |
| | | $\mathbf{II^{+}_{z1}}$ | Relative interconnection capacity of OBZ (i.e. Interconnectivity Indicator) towards Zone 1 doubled |
| | | $\mathbf{II^{+}_{z23}}$ | Relative interconnection capacity of OBZ (i.e. Interconnectivity Indicator) towards Zones 2 and 3 doubled |
| **2. Offshore Grid Topology – Dual Hybrid** | Installed offshore wind capacity ($Q^{OWF}_{z}$) and transmission capacity of the interconnectors ($\bar{F}^{DC}_{obz \to z}$) | **Sym.** | Symmetrical dual hybrid between zones 1 and 3 |
| | | $\mathbf{Asym_{z1}}$ | Asymmetric dual hybrid towards Zone 1 (double $Q^{OWF}_{1}$ and $\bar{F}^{DC}_{obz \to 1}$) |
| | | $\mathbf{Asym_{z3}}$ | Asymmetric dual hybrid towards Zone 3 (double $Q^{OWF}_{3}$ and $\bar{F}^{DC}_{obz \to 3}$) |
| **3. Onshore Grid Attenuation** | Outage of onshore AC transmission lines | $\mathbf{Out^{LP}_{z1}}$ | Outage of AC line at the Landing Point from the OBZ in zone 1 |
| | | $\mathbf{Out^{LP}_{z3}}$ | Outage of AC line at the Landing Point from the OBZ in zone 3 |
| | | $\mathbf{Out^{on}_{z1}}$ | Outage of AC line further Onshore in Zone 1 |
| | | $\mathbf{Out^{on}_{z3}}$ | Outage of AC line further Onshore in Zone 3 |
| **4. Generation Mix** | Installed capacities (and marginal costs) of (dispatchable) generators per bidding zone | **Trans.** | Transition generation mix with less renewables and more fossil generators |
| | | **Fos.** | Fossil dominated generation mix with very low renewable capacity |
| **5. Hydrogen Production** | Inclusion of dispatchable electrolysers with varying willingness-to-pay for electricity. | $\mathbf{H2^{off}_{1}}$ | Three 250 MW electrolysers in the OBZ (WTP = 53.77 €/MWh) |
| | | $\mathbf{H2^{off}_{2}}$ | Three 250 MW electrolysers in the OBZ (WTP = 32.83 €/MWh) |
| | | $\mathbf{H2^{off}_{3}}$ | Three 250 MW electrolysers in the OBZ (WTP = 21.89 €/MWh) |
| | | $\mathbf{H2^{off}_{4}}$ | Three 250 MW electrolysers in the OBZ (WTP = 10.94 €/MWh) |
| | | $\mathbf{H2^{on}_{z1}}$ | One 750 MW electrolyser at the landing point in zone 1 (WTP = 41.70 €/MWh) |
| | | $\mathbf{H2^{on}_{z3}}$ | One 750 MW electrolyser at the landing point in zone 3 (WTP = 41.70 €/MWh) |

## 5.2.1 Case Group 1: Offshore Grid Topology – Triangular Hybrid

In the first Case Group aims to analyse the effect of variations in offshore grid setup with respect to the reference case. Investment decisions in HVDC transmission capacity might follow strategic reasoning of the involved stakeholders in the hybrid project rather than the optimum levels from a social welfare perspective. TSOs and society could potentially benefit from increased interconnectivity as it enables increased cross-border trade, potentially leading to higher congestion rents and lower DA generation costs and redispatch costs. Additionally, increased interconnectivity potentially lowers electricity prices across all zones (including in the OBZ) due to enhanced price convergence, but price collapses are potentially reduced due to the increased transmission capacity, which in return would also mean less curtailment. Reversely, lower transmission capacities with respect to installed wind capacities, reflecting the scenario of overplanting, could potentially be beneficial for OWF developers as the generated wind volumes are relatively increased leading to higher total exports and possibly increased revenues. Therefore, this case group is included to analyse the effects of varying HVDC transmission capacities, based on strategic choices between the involved actors in the triangular hybrid project, on the price and volume risks. The following hypothesis is formulated for this case group:

***H.1**: Increased HVDC transmission capacity from the OBZ to onshore markets leads to higher congestion rents, lower day-ahead generation and redispatch costs, lower electricity prices with fewer price collapses and increased wind exports due to reduced curtailment.*

In the first case of this group, the Export Indicator is increased by 33% symmetrically, meaning that each transmission line from the OBZ to shore is increased from 1.5 GW to 2 GW. This scenario reflects a collective decision by the TSOs of the adjacent countries to enhance the exporting capacity to shore (relative to the installed wind capacity), enabling higher import capacities from the OBZ to each individual country and naturally leading to increased interconnectivity levels. This case is thus referred to as **Case $\mathbf{EI^{+}}$**.

In the second case, the Export Indicator is decreased by 33% symmetrically, resulting in transmission capacities from the OBZ to shore of 1 GW each. This scenario represents a decision by the OWF operators to overplant the farms relative to the transmission capacity to shore, consequently decreasing the interconnectivity level. This case is referred to as **Case $\mathbf{EI^{-}}$**.

The third case explores a scenario where one of the TSOs decides to double its interconnectivity level to facilitate more cross-border trade and additional imports from the OBZ. To identify the country for which this strategy would be most beneficial, the results of the reference case (Section 6.1) were analysed, focusing on the average net positions of the zones and the flow directions and magnitudes on the cross-border DC lines. Zone 1 displayed the most negative average net position throughout the simulated time period (-757.82 MWh), indicating that this zone is importing most power from the other zones. Therefore, zone 1 is expected to benefit from increased interconnectivity whereby the interconnectivity indicator for Zone 1 was doubled, increasing the transmission capacity from 1.5 GW to 3 GW. This case is referred to as **Case $\mathbf{II^{+}_{z1}}$**.

In the fourth case the focus shifts to assessing the effect of increasing the interconnectivity level of the two other zones, Zone 2 and Zone 3. This scenario reflects a decision by two renewable-dominated countries, one with large PV capacities (zone 2) and the other primarily wind-dominated (zone 3), to increase their interconnectivity and use the interconnector to leverage the wind-solar complementarity effect. The interconnectivity indicators for Zones 2 and 3 are doubled, achieved by increasing the transmission capacities to shore to 2.342 GW. This case is referred to as **Case $\mathbf{II^{+}_{z23}}$**.

Table 9 below provides the offshore grid topologies for all cases in this group. The bold indicators represent the parameters that were primarily adjusted to match the desired case descriptions.

*Table 9: Transmission Capacity Variations for Case Group Offshore Grid Topology (Triangular)*

| | **Installed OWF capacity ($Q_z^{OWF}$) and transmission capacity ($\bar{F}^{DC}_{obz\to 1}$) in GW** | | | | | | | | | **Export (EI) and Interconnectivity (II) indicators** | | | | | | |
|---|---|---|---|---|---|---|---|---|---|---|---|---|---|---|---|---|
| **Case** | $Q_1^{OWF}$ | $\bar{F}^{DC}_{obz\to 1}$ | $Q_2^{OWF}$ | $\bar{F}^{DC}_{obz\to 2}$ | $Q_3^{OWF}$ | $\bar{F}^{DC}_{obz\to 3}$ | $\bar{F}^{DC}_{obz,1\to 2}$ | $\bar{F}^{DC}_{obz,1\to 3}$ | $\bar{F}^{DC}_{obz,2\to}$ | **EI** | $EI_1$ | $EI_2$ | $EI_3$ | $II_1$ | $II_2$ | $II_3$ |
| **Ref** | 1.5 | 1.5 | 1.5 | 1.5 | 1.5 | 1.5 | 1.5 | 1.5 | 1.5 | 1 | 2 | 2 | 2 | 2 | 2 | 2 |
| $\mathbf{EI^{+}}$ | 1.5 | **2** | 1.5 | **2** | 1.5 | **2** | 1.5 | 1.5 | 1.5 | **1.33** | 2.67 | 2.67 | 2.67 | 3.56 | 3.56 | 3.56 |
| $\mathbf{EI^{-}}$ | 1.5 | **1** | 1.5 | **1** | 1.5 | **1** | 1.5 | 1.5 | 1.5 | **0.67** | 1.33 | 1.33 | 1.33 | 0.89 | 0.89 | 0.89 |
| $\mathbf{II^{+}_{z1}}$ | 1.5 | **3** | 1.5 | 1.5 | 1.5 | 1.5 | 1.5 | 1.5 | 1.5 | 1.33 | 2 | 3 | 3 | **4** | 3 | 3 |
| $\mathbf{II^{+}_{z23}}$ | 1.5 | 1.5 | 1.5 | **2.34** | 1.5 | **2.34** | 1.5 | 1.5 | 1.5 | 1.37 | 3 | 2.56 | 2.56 | 3 | **4** | **4** |

### 5.2.2 Case Group 2: Offshore Grid Topology – Dual Hybrid

For the second Case Group, the offshore grid setup is simplified to a Dual Hybrid, connecting only two countries to the OBZ instead of three. While the triangular setup in the other case groups resembles the future meshed offshore grid, envisioned by the North Sea Wind Power Hub (NSWHP, 2022a), this case group reflects the initial hybrid projects expected to be primarily in a dual setup (ENTSOE, 2024b).

To determine which zones should be connected in the dual hybrid configuration, the reference case results were analysed (see Section 6.1). The zones showing the highest average price spread throughout the simulated timespan were selected, which were Zone 1 and Zone 3, with average prices of 56.25 €/MWh and 12.98 €/MWh, respectively. This reflects a scenario where a country with higher renewable penetration (and thus a lower average price) is connected to a country with a more fossil-dominated mix. Figure 18 visualises the grid topology for the dual hybrid setup.

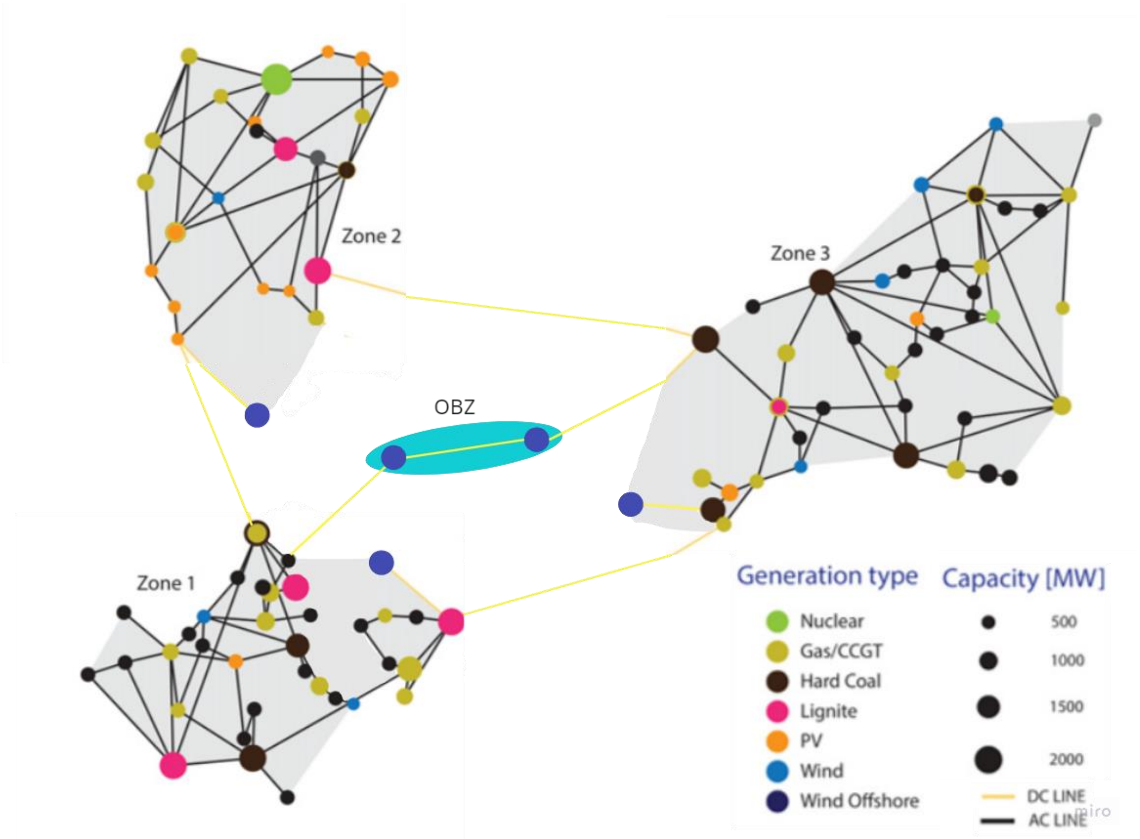


*Figure 18: Grid Topology for the Dual Hybrid setup*

This scenario provides insights into the conflicting benefits for different stakeholders. For example, for OWF developers located in a higher-priced country, being connected via a hybrid interconnector could be undesirable (compared to a radial connection) due to the price convergence effect, which lowers prices in the OBZ. However, from a societal perspective, this connection could be desirable as it would decrease average electricity prices due to increased cross-border trade. Conversely, for developers in the lower-priced zone, a hybrid connection could be advantageous due to the potential to sell wind power at higher average prices compared to a radial setup. However, from a societal perspective, this might be undesirable as it could increase electricity prices by price converging to the higher-priced bidding zone. These strategic choices will be reflected in this case group by asymmetrically changing the transmission and installed wind capacity to either side of the bilateral connected zones. It can be expected that an increased export capacity to the higher priced zone 1 is beneficial for OWFs in the OBZ since this potentially enables additional exports at higher prices, leading to increased revenues. Reversely, having additional export capacity to the lower priced zone 3 opens up additional competition between the OBZ and zone 3 to export to the high-priced zone 1, leading to increased curtailment (primarily by the capacity allocation) and decreased revenues. The following hypothesis can thus be formed.

***H.2:*** *Increased export capacity to the high-priced zone 1 results in higher wind exports at elevated prices, thereby boosting revenues, while increased export capacity to the lower-priced zone 3 leads to higher curtailment due to capacity allocation and reduced revenues.*

For the first case (**Case Sym**) in this case group a symmetrical hybrid setup is chosen with installed wind capacities of 1.5GW and similar interconnector sizes.

For the second case (**Case Asym$_{z1}$**) and the third case (**Case Asym$_{z3}$**) it is chosen to have an asymmetrical setup in terms of installed offshore wind capacity within the OBZ. For Case Asym$_{z1}$ zone 1 has in OWF with 3GW installed capacity (and similar size transmission capacity to shore) while keeping the OWF capacity for zone 3 at 1.5GW, and for Case Asym$_{z3}$ the opposite is done. Table 10 gives the offshore grid topologies of the cases in this group.

*Table 10: Offshore Grid Topology Variations for Case Group 3 with OBZ between zone 1 and zone 3.*

| | Installed OWF capacity ($Q_z^{OWF}$) and transmission capacity ($\bar{F}_{obz\to1}^{DC}$) in GW | | | | | Export (EI) and Interconnectivity (II) indicators | | | | |
|---|---|---|---|---|---|---|---|---|---|---|
| **Case** | $Q_1^{OWF}$ | $\bar{F}_{obz\to1}^{DC}$ | $Q_3^{OWF}$ | $\bar{F}_{obz\to3}^{DC}$ | $\bar{F}_{obz,1\to3}^{DC}$ | **EI** | $EI_1$ | $EI_3$ | $II_1$ | $II_3$ |
| **Sym.** | 1.5 | 1.5 | 1.5 | 1.5 | 1.5 | **1** | 1 | 1 | 1 | 1 |
| **Asym$_{z1}$** | **3** | **3** | 1.5 | 1.5 | 1.5 | 1 | 0.5 | 1 | 0.5 | 1 |
| **Asym$_{z3}$** | 1.5 | 1.5 | **3** | **3** | 1.5 | 1 | 1 | 0.5 | 1 | 0.5 |

## 5.2.3 Case Group 3: Onshore Grid Attenuation

The third case group focusses on the influence of onshore grid attenuations on the price and volume risks in the OBZ. Reflecting on Section 2.4, the Flow-Based (FB) domain is determined by the offshore NTC values of the transmission cables directly adjacent to the Offshore Bidding Zone (OBZ), as well as the RAM values of the onshore CNEs. Where the previous two case groups focused on varying the offshore grid topology, i.e. the HVDC transmission capacities, this case group focusses on the influence of onshore grid attenuations. This is of interest since capacity limitations or outages of onshore transmission lines could shrink the FB domain, whereby exports from the OBZ are limited which lead to an increase in curtailment by the capacity calculation, reducing revenues for the OWFs. Additionally, it is expected that more price collapse hours arise due to the reduced capability of the onshore AC grid to import the generated wind power from the OBZ. Both effects are expected to negatively influence the revenues for the OWFs.

***H.3***: *Onshore grid attenuations lead to a reduced export capability of the OBZ, increasing price collapse hours and curtailment by the capacity calculation, ultimately leading to lower revenues for OWFs.*

Since this thesis does not incorporate LODFs for potential line outages (see Section 2.5), nor does it include any probabilistic mechanism to consider unexpected outages, the only feasible approach within the scope of this thesis is to analyse the effect of outages by manually lowering the transmission capacity of a CNE. Therefore, in this case group, varying transmission capacities of AC lines in the onshore grids are manually set to zero to reflect a scenario of onshore grid attenuations. There are two approaches for choosing a CNE to be structurally weakened throughout the simulation:

1. Selecting an AC line directly connected to the landing point from the OBZ and;
2. choosing an AC line elsewhere in the grid that might also influence the FB domain.

Both options are explored in the following cases and Figure 19 indicates the lines with outages per case.

The first case, **Case** $\mathbf{Out_{z1}^{LP}}$, represents a scenario where the AC line directly connected to the Landing Point of the OBZ within the importing zone (Zone 1) has a structural outage[9] The second case, **Case** $\mathbf{Out_{z3}^{LP}}$, represents a scenario where an AC line directly connected to the landing point of the OBZ within the exporting zone (Zone 3) is out[10].

Additionally, two cases represent a structural CNEC elsewhere in the grid. To ensure that the chosen CNECs would influence the FB domain of the OBZ, the shadow prices of constraint (4.2d) from the reference case were studied, as this constraint considers the impact of the flow on the DC lines on the AC grid (see Section 4.2.2.2). The AC line that showed the most significant non-negative shadow price values for this constraint was set to a capacity of 0 MW to simulate the effect of a structural outage of a restricting CNE. For both Zone 1 (**Case** $\mathbf{Out_{z1}^{On}}$)[11] and Zone 3 (**Case** $\mathbf{Out_{z3}^{On}}$)[12], one case was developed in which an onshore CNE was set to zero to simulate this structural outage scenario.

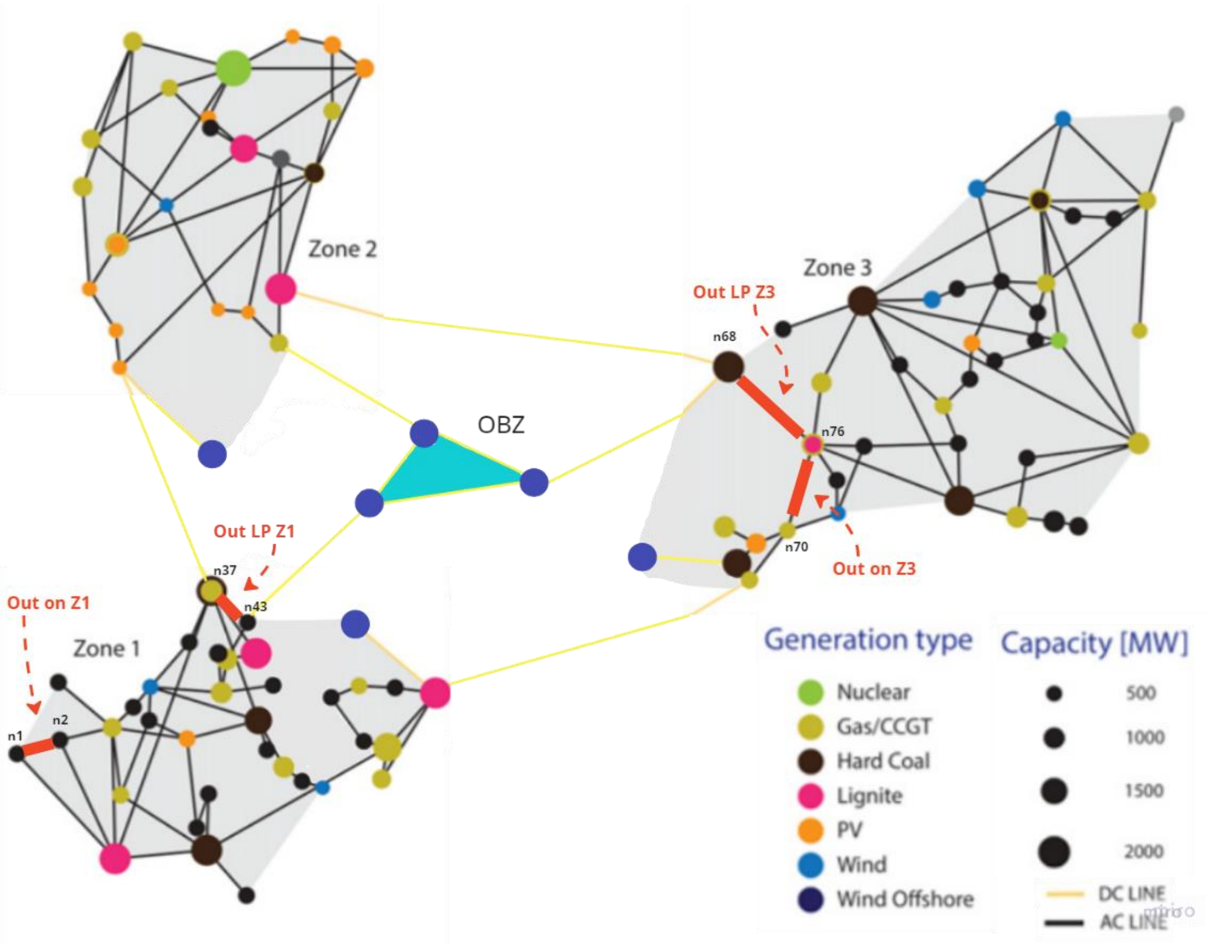


*Figure 19: Grid Topology for the Onshore Grid Attenuation Case Group. Indicated in red are the AC lines with outages per Case.*

### 5.2.4 Case Group 4: Generation Mix

In this Case Group the influence of the renewable energy integration in the generation mixes of the onshore zones is analyses. As mentioned in Section 1.1, the cannibalization effect is expected to be more

[9] The AC line connecting nodes 37 and 43, of which node 43 is the landing point from the OBZ in zone 1.
[10] The three AC lines connecting nodes 68 to 76, of which node 68 is the landing point form the OBZ in zone 3.
[11] The two AC lines connecting nodes 1 and 2 in zone 1.
[12] The two AC lines connecting nodes 70 and 76 in zone 3.

pronounced for hybrid projects (Jansen et al., 2022), whereby it could exacerbate the price and volume risks. The reference case used in this thesis considered a high renewable scenario (Section 5.1.2), whereby the share of renewables will be decreased in this case group to reflect a scenario in which the renewable energy transition does go at the expected pace. Increasing the share of fossil generators could increase and stabilize price levels, potentially leading to increased wind exports due to less curtailment by capacity allocation. As the cannibalisation effect becomes less pronounced, the market coupling will likely favour the cheaper renewable electricity sources in the OBZ over more expensive fossil generators for the scarce transmission capacity on the interconnectors. Thus, the following hypothesis can be formulated for generation mix variations:

***H.4:*** *Decreasing the proportion of renewable energy sources in the generation mix leads to higher and more stable electricity prices, fewer zero-priced hours, decreased curtailment by the capacity allocation, leading to increased exports and higher revenues for OWFs.*

For the two cases that will be simulated in this case group the input generation mixes are the “normal case” and the “high vRES case” from Schönheit et al (2021), hereafter referred to as case Fossil Mix (**Case Fos**) and case Transition Mix (**Case Trans**). The merit orders and installed variable renewable capacities are visualised in Figure 20 and Figure 21 for the Fossil Mix and the Transition Mix, and Table 11 indicates the variation of the total installed capacities of generators in the entire system w.r.t. the reference case.

*Table 11: Total installed capacities variance per generation type for the Generation Mix cases*

| Generation Type | Ref. | Trans. | Fos. |
|---|---|---|---|
| *PV* | 12182 MW | -3% | -61% |
| *Wind* | 19470 MW | -18% | -88% |
| *Wind Offshore* | 8815.6 MW | -7% | -32% |
| *Nuclear* | 3600 MW | +6% | +6% |
| *Lignite* | 9000 MW | +21% | -14% |
| *Hard Coal* | 18400 MW | +73% | -43% |
| *Gas/CCGT* | 20100 MW | +2% | +13% |

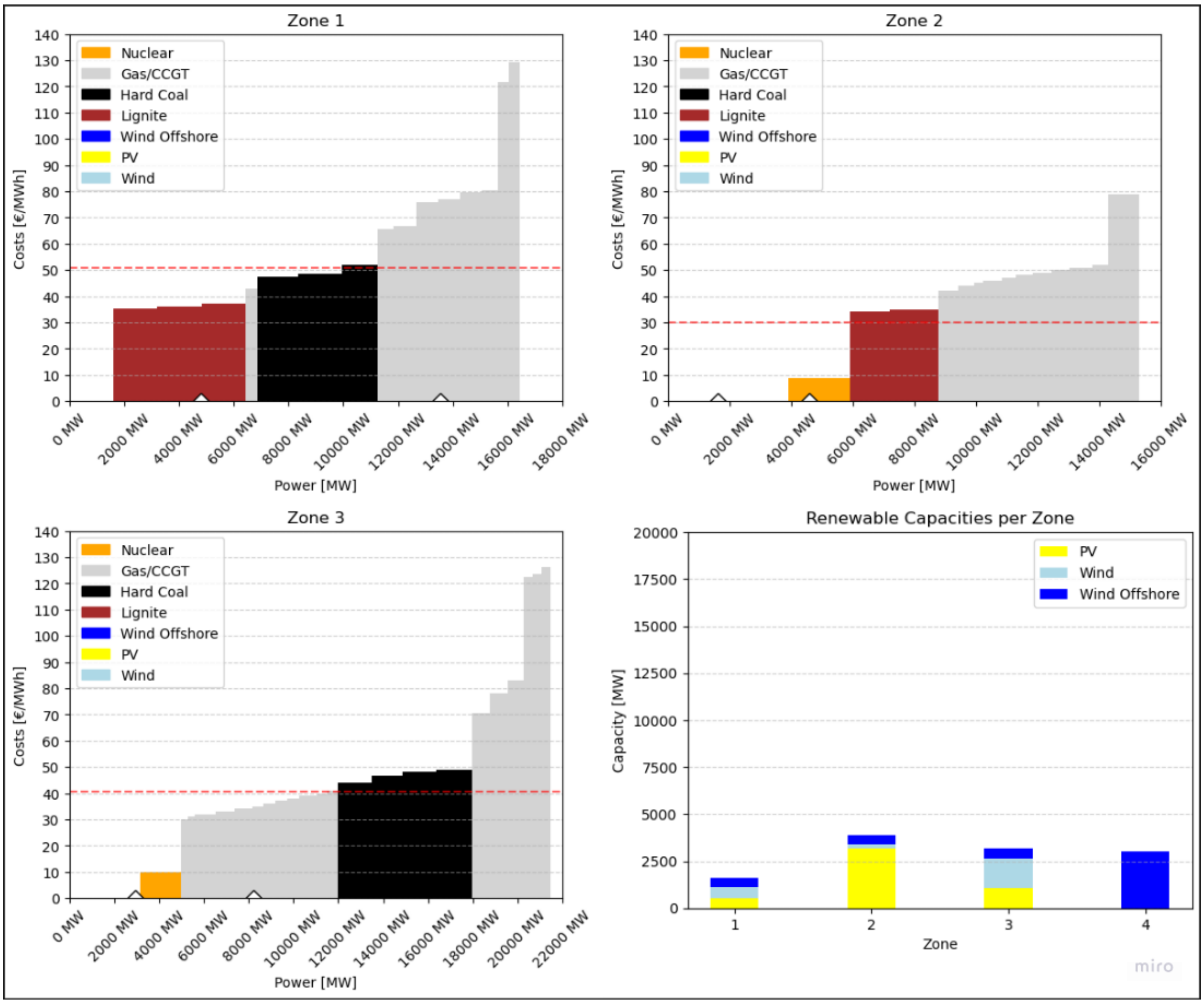


*Figure 20: Merit Orders and Renewable Installed Capacities for the Fossil Mix case.*

In the Fossil Mix, Zone 1 is predominantly fossil-dominated with a substantial lignite, coal, and gas fleet, resulting in a fleet (weighted) average marginal cost (FAMC) just above 50 €/MWh. Zone 2 is primarily gas-dominated, with some lignite and nuclear power, and has the largest installed renewable capacity (mostly photovoltaic), yielding a FAMC of around 30 €/MWh. Zone 3 is mainly gas-dominated with some hard coal and nuclear, slightly fewer renewables than Zone 2, and a FAMC of approximately 40 €/MWh.

In the Transition Mix, Zone 2 has significantly transitioned from fossil to renewable sources, leaving only a few fossil generators and becoming primarily dominated by PV, with a FAMC of about 10 €/MWh. Zone 3 maintains a large coal fleet but also experiences growth in renewable capacity, particularly onshore wind, resulting in a FAMC of around 35 €/MWh. Zone 1 lags behind, with lower increases in renewable capacities compared to the other zones and additional fossil plants compared to the Fossil Mix, leading to a FAMC of approximately 58 €/MWh.

In the Renewable Mix, Zone 1 remains mostly fossil-dominated, with even more fossil generators than in the Fossil Mix, resulting in a FAMC of around 60 €/MWh. Zone 2 is highly renewable-dominated, with a substantial installed capacity of PV and a weighted average marginal cost below 10 €/MWh. Zone

3 has the largest generating fleet, having most renewables (mostly wind) and fossil generators, leading to a FAMC just below 30 €/MWh.

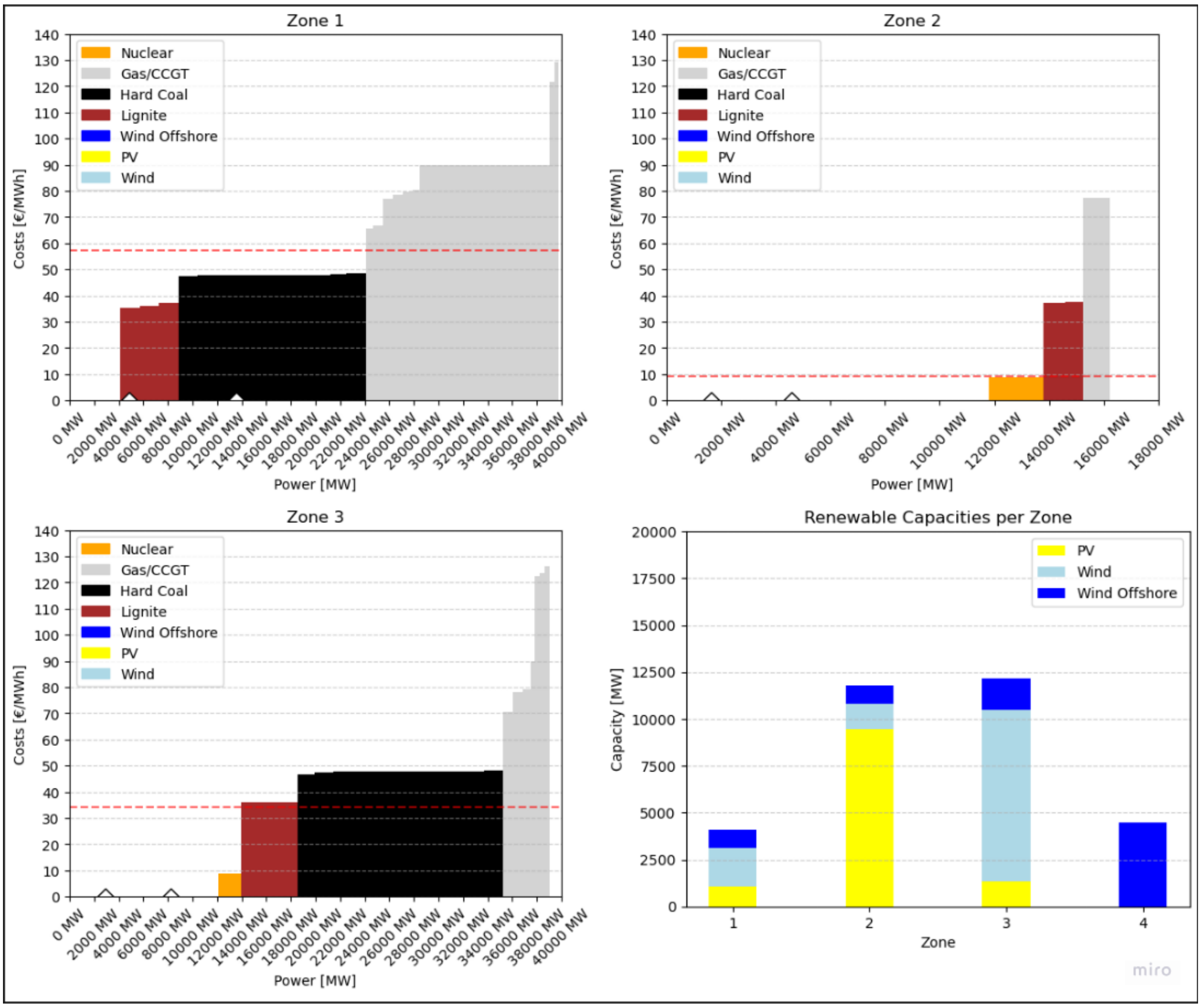


*Figure 21: Merit Orders and Renewable Installed Capacities for the Transition Mix case.*

### 5.2.5 Case Group 5: Hydrogen Production

The last Case Group considered the production of hydrogen. As mentioned in section 3.3.3 and raised by Kenis et al. (2024), offshore hydrogen production can act as a risk mitigating measure. In order to assess the potential role that electrolysers could play in alleviating (part of the) risks, the hydrogen production case group is included. Within the scope of this thesis and the considered grid topology, there exist two possible system designs for hydrogen production, which are to place the electrolyser within the OBZ (and needing pipelines for transportation) or placing the electrolyser directly at the landing point of the HVDC interconnectors from the OBZ (Configurations C and E from Figure 22).

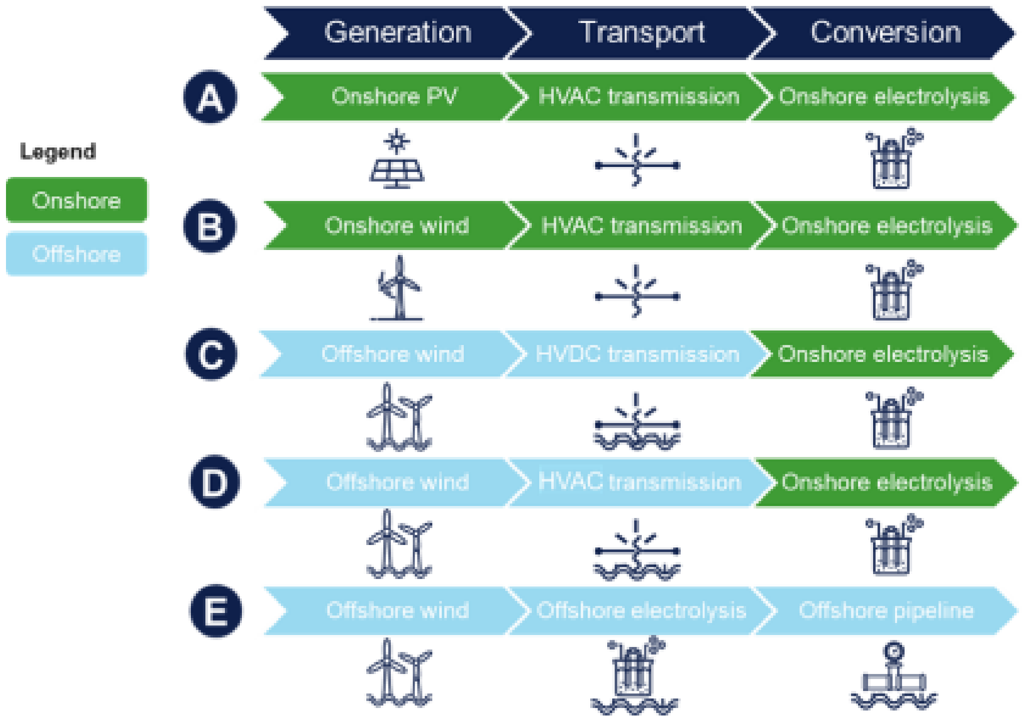


*Figure 22: System configurations for Onshore and Offshore hydrogen values chains in Northern Europe (Source: Van Wingerden et al., 2024).*

Both system configuration options are included because placing the electrolyser offshore could potentially directly influence the price of the OBZ, being the only demand agent in the OBZ, while electrolysers located at the landing point of the OWF could absorb part of the exported power from the OBZ without the power having to flow into the onshore AC grid, potentially avoiding congestion and increasing the overall net position of the OBZ. Specifically, the expected effect of implementing electrolysers is formulated in the following hypotheses:

***H.5***: *Implementing electrolysers increase average electricity prices and reduce the price collapse risk, while wind exports are enhanced and curtailment decreased, ultimately leading to higher revenues for the OWFs.*

It is expected that both offshore and onshore electrolysers show this effect, albeit more pronounced for those electrolysers placed in the OBZ than onshore. This is expected because the presence of local demand agents in the OBZ directly sets the electricity price more often with its WTP and absorbing produced wind power locally, while the presence of an onshore demand agent in one of the three zones is expected to absorb only part of the risks.

In this thesis, the WTP for electricity of electrolysers was based on the Levelised Costs of Hydrogen (LCOH), excluding the electricity cost component, for both onshore and offshore electrolysers. Based on the assumptions and calculations provided in Appendix C, the WTP is set at 43.77 €/MWh for an offshore electrolyser and 41.70 €/MWh for an onshore electrolyser.

For the installed capacity of the electrolyser, it is chosen to take a total installed electrolysis capacity of 750 MW, reflecting a setup with one dedicated offshore wind farm for hydrogen production. This is in line with the ratio of electrolyser capacity to OWF capacity (1:2) from the most recent offshore wind tender in the Netherlands, where a consortium of Vattenfall and Copenhagen Infrastructure Partners have been awarded the permit to install an 1GW electrolyser in the harbour of Rotterdam for the 2GW offshore wind farm IJmuiden Ver Beta (Rijksoverheid, 2024). For model simplicity purposes, there are placed three electrolysers each having 250MW on each of the three wind farms in the OBZ for the offshore cases. For the onshore system setup, there is included one case where one larger 750 MW electrolyser is placed at the landing point in zone 1 (being the highest importing country) and one case where the electrolyser is placed at the landing point iin zone 3 (being the highest exporting country).

Based on the observation in the initial simulation with an offshore electrolyses[13] and on the fact that the lowest LCOH are not per definition achieved by operating at 100% Full-Load Hours (FLH) but rather at an optimum existing between the electricity price and the number of operation hours (Figure 12 in KPMG, 2022), it is decided to scale down the WTP with steps of 25% for the other offshore case. For the onshore case, for the sake of limiting simulations, it is decided to take the 41.70 €/MWh for the WTP for the first case and to add one other case with the WTP scaled down 50% to 20.85 €/MW. Table 12 provides all hydrogen production cases that are simulated.

*Table 12: Hydrogen Cases Descriptions*

| Description | Case Label | WTP | Scale factor WTP |
|---|---|---|---|
| Three 250 MW offshore electrolyser located at the platforms of the three OWFs in the OBZ. | $\mathbf{H2_1^{off}}$ | 43.77 €/MWh | - |
| | $\mathbf{H2_2^{off}}$ | 32.83 €/MWh | -25% |
| | $\mathbf{H2_3^{off}}$ | 21.89 €/MWh | -50% |
| | $\mathbf{H2_4^{off}}$ | 10.94 €/MWh | -75% |
| One 750 MW onshore electrolyser located at the landing point of the OBZ in zone 1 or 3. | $\mathbf{H2_{z1}^{on}}$ | 41.70 €/MWh | - |
| | $\mathbf{H2_{z3}^{on}}$ | 41.70 €/MWh | - |

[13] Out of the 2952 hours simulated the three offshore electrolysers were fully dispatched between 2366 and 2565 hours for a WTP = €43.77, reflecting a maximum Full Load operation of 82%.

# Chapter 6. Results

This chapter presents the Results for all the Simulated Cases. Since the Reference Case serves as a benchmark to which to other cases are compared to, first the results of the Reference Case are extensively presented in Section 6.1. Thereafter, for each case group that has been simulated the results are presented in Sections 6.2 to 6.6. Lastly, Section 6.7 presents the Cross-Case Group results. Each of the sub-sections in this chapter will follow the structure of first presenting the general results, then the price risk results and last the volume risk results.

## 6.1 The Reference Case

First, several snapshots are discussed to explain the price formation in the OBZ under flow-based market coupling (Section 6.1.1). Then, the general results are presented in Section 6.1.2. Thereafter, the price risk results are presented (Section 6.1.3), followed by the volume risk results (6.1.4). This sequence of results presentation is used for further explanations of the case groups

### 6.1.1 Snapshots of Price Formations in the OBZ

**Price convergence to zero:** Figure 23 visualises a snapshot of an hour in which the price of the OBZ converges to 0 €/MWh. During this specific hour, zone 1 is the only bidding zone with a non-zero price and, logically, imports power from zone 2, 3 and the OBZ. The point-to-point interconnectors to zone 1 are fully used up until the maximum transmission capacity of 200 MWh, but the interconnector from the OBZ to zone 1 is not congested. Nevertheless, the OBZ's electricity price is zero, which could be the result of either a price collapse or the convergence to another zone having a price of 0 €/MWh. In this specific hour, the latter is the case. The reason why the interconnector from the OBZ to zone 1 is not fully used is because the onshore grid cannot absorb additional power from the OBZ since the AC line between the landing point of both the point-to-point interconnector between zones 1 and 2 and the interconnector between the OBZ and zone 1 is congested (red line in Figure 23 and Section 4.6.2.2 for explanation). The result is that the price in the OBZ converges to the bidding zone to which an uncongested path exists, which is in this case zone 2 with an electricity price of 0 €/MWh.

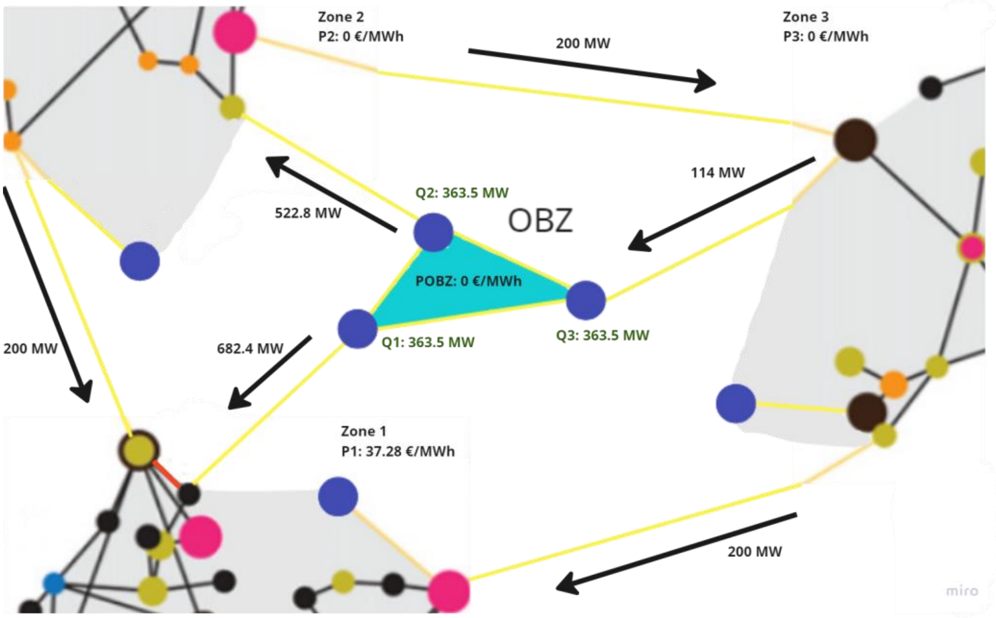


*Figure 23: Snapshot of zero priced hour due to high renewable feed-in (h=121).*

**Price collapse**: Figure 24 visualises a snapshot of an hour in which the price in the OBZ collapses to zero. Since there is no curtailment of wind power nor direct congestion from the OBZ to shore, it is somewhat unexpected that the price in the OBZ collapses to zero. The reason why this happens is the following. There are two AC lines restricting the FB domain of the OBZ. The first is an AC line connecting the landing point of the point-to-point interconnector from zone 2 and the landing point of the OBZ. This AC lines showed a non-zero shadow price of constraint (4.2e) and thus directly constraints the FB domain from the OBZ. The result is that the export from the OBZ to zone 1 is restricted by the onshore AC grid, and not by the congestion of the DC line, whereby the remainder of the power has to be exported to the second highest bidding zone, being zone 2. However, there is another AC line restricting the FB domain of the OBZ in zone 2. The AC line in zone 2 connecting the point-to-point interconnector from zone 3 and the landing point of the OBZ further limits the FB domain of the OBZ. So even though both DC lines are not congested, additional export over these lines is also not possible due to the onshore AC grid directly limiting additional imports. The result is a price collapse in the OBZ.

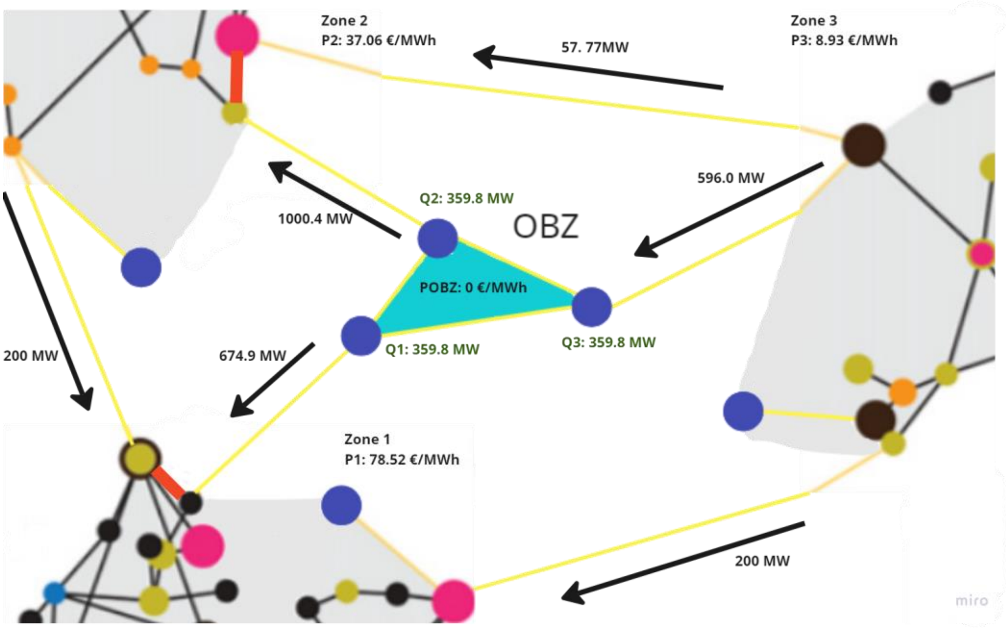


*Figure 24: Snapshot of price collapse hour in OBZ (h=641).*

**'Rule of Thumb' price:** Figure 25 visualises a snapshot of an hour in which the price in the OBZ converges to the lower-priced adjacent bidding zone. An observation here is that the transmission line to the highest priced-zone, being zone 1, is not fully congested, nor is it used upon the maximum injection possible due to onshore grid limitations close to the landing point, which was the case for price collapse snapshot (Figure 24). In this hour, there is an onshore AC line in bidding zone 1 that is further away from the landing point influencing the maximum export capacity from the OBZ to zone 1, being AC line connecting node 1 and 2. The shadow price of constraint 3e for this line showed non-zero values, indicating that in this particular hour the maximum injection from the OBZ to zone 1 is limited due to an onshore CNEC further away from the landing point of the OBZ restricting the FB domain. In this hour, the OBZ can still export its remaining produced wind capacity to zones 2 and 3, whereby the price in the OBZ converges to these zones (being uniform in this hour).

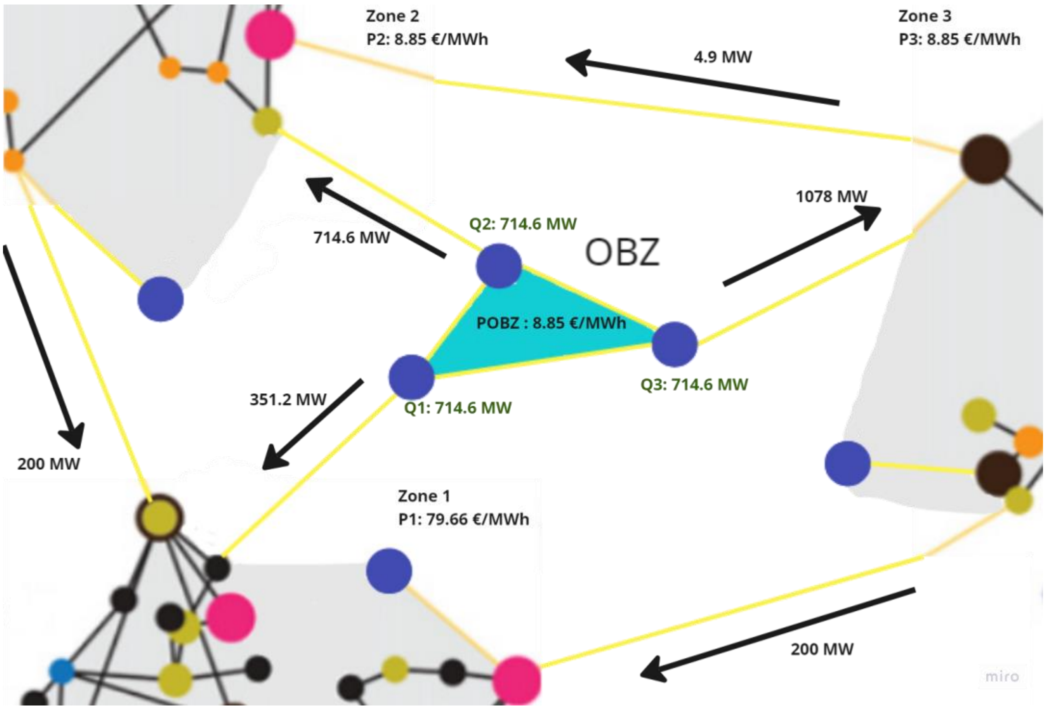


*Figure 25: Snapshot of Price Convergence hour, i.e. following the Rule of Thumb (h=394)*

**Price convergence to middle-priced zone (low-wind hour)**: Figure 26 shows a snapshot of an hour in which the price in the OBZ does not converge to the lowest priced bidding zone, as expected following the rule of thumb explanation, but to the price of the middle-priced bidding zone. This hour shows a very low wind hour with only 28.67 MW of wind production per OWF. The interconnectors cables are primarily used for cross-border trade. As expected, the lowest priced zone 2, exports via the OBZ to the higher priced zone 1. Again, the maximum import capacity to zone 1 is restricted by the AC line between the point-to-point interconnector and the landing point. Further, zone 2 exports power via the OBZ to zone 3 up until the maximum power that does not further increase total social welfare. In addition, a non-intuitive trade is occurring from zone 3 to zone 2 indicating that the highest welfare generating combination of power flows is up until the 365 MW from the OBZ to zone 3. The result is that the OBZ converges to zone 3 and experiences a high electricity price.

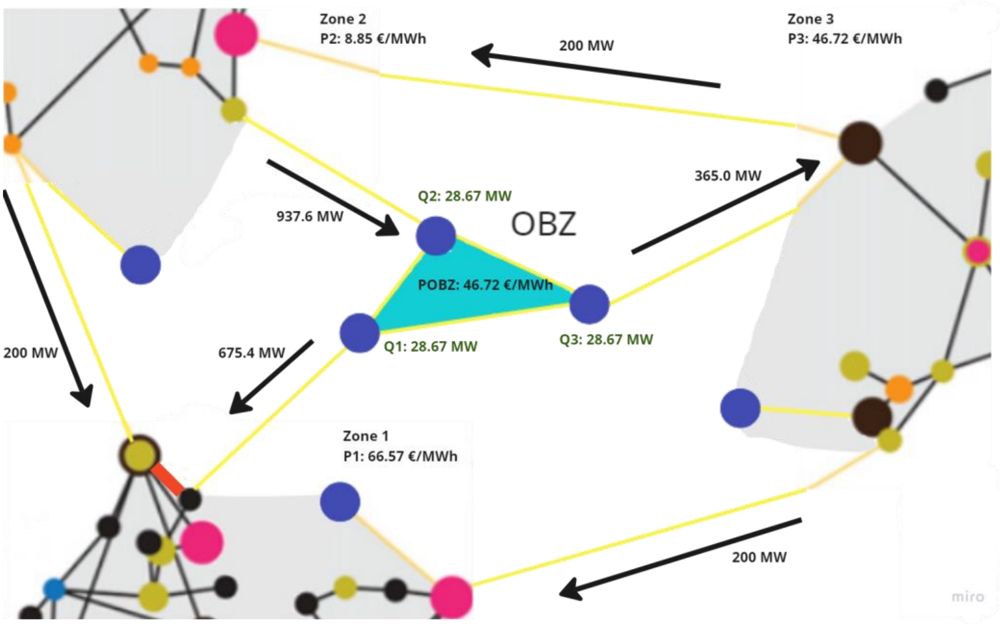


*Figure 26: Snapshot of price convergence to middle-priced zone (h=852).*

**Price convergence to high-priced zone (low-wind, high demand hour):** It can even be the case that the OBZ converge to the higher-priced zone. Figure 27 visualise a snapshot when this happens. This hour represents a winter morning high demand hour with little wind availability, and first light having little PV generation. During this hour, the lower priced zone 3 exports to the higher priced zones 1 and 2 via the OBZ, whereby the price in the OBZ converges to these two higher priced zones, having a uniform price in this hour. This specific set of circumstances – high demand plus low-RES production - could on some occasions lead to higher-then-expected prices in the OBZ.

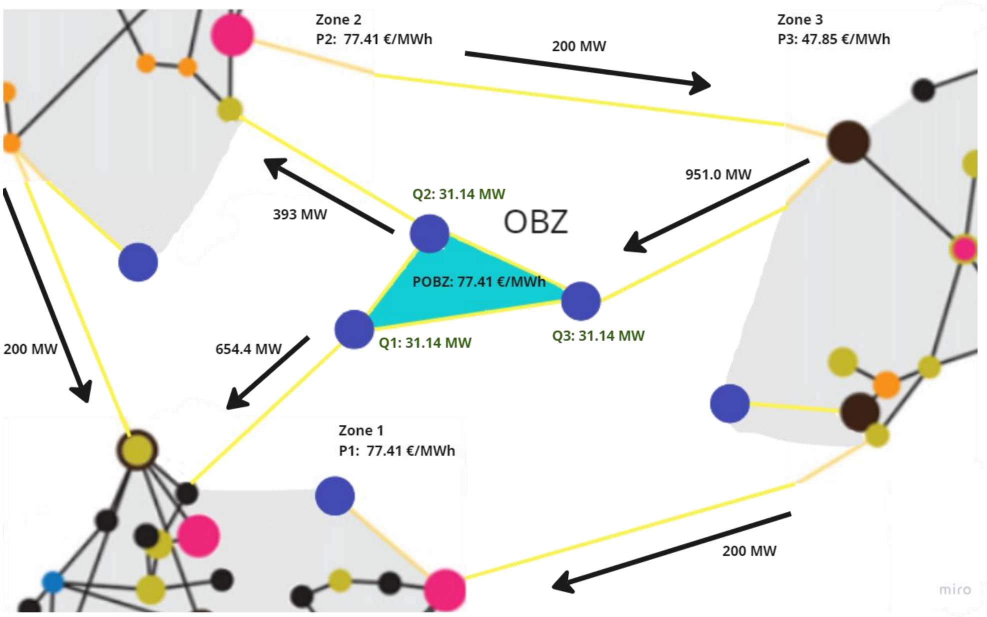


*Figure 27: Snapshot of price convergence to High bidding zone (h=2407).*

**Non-intuitive price:** A last snapshot of a non-intuitive price formation hour is visualised in Figure 28. During this hour, the price in the OBZ is not converging to any adjacent bidding zone. The higher priced bidding zone 1 imports up until the maximum capacity that the onshore AC grid can absorb, restricted by an AC line from node 1 to node 2 in the very left corner of zone 1. Thereafter, zone 3 having a zero priced hour would want to export up until the full capacity to zone 2. However, a non-intuitive flow is occurring again in this hour. Specifically, as one of the two AC lines connected to the landing point of the OBZ in zone 2 is congested, exporting 200 MW via the point-to-point interconnector from zone 2 to 3 makes room for the 1000.4MW of power that is imported via the OBZ to zone 2. A higher welfare generating combination of flows thus exists by non-intuitive exporting from zone to 2 3, whereby additional power can be imported to zone 2 via the OBZ. Therefore, the electricity price in the OBZ is not similar to an adjacent market, but rather reflects the marginal value of alleviating stress on onshore CNECs.

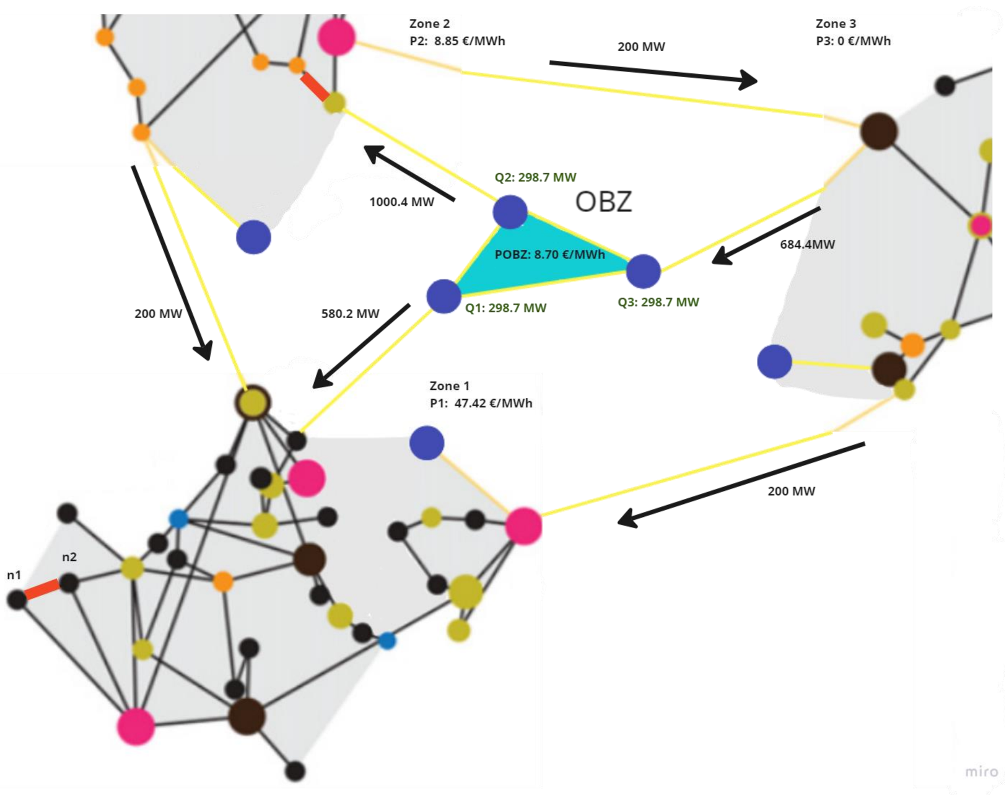


*Figure 28: Snapshot of Non-intuitive price formation (h=2739).*

### 6.1.2 General Results - Reference Case

Table 13 provides an overview of the general results for the Reference Case. In the reference case, the three OWFs of 1.5 GW each in the OBZ together exported around 3 TWh of wind energy, resulting in a revenue of about 15 M€. The total curtailment was about 1.5 TWh, accounting for 33% of the total potential offshore wind energy generation. Section 6.1.4 will further dive into the results on the curtailed volumes. Of the 3 TWh exported wind power, most of the wind energy was exported during zero-priced hours (72.97%), leaving 27.03% of wind energy exported during non-zero-priced hours. What this large share of exported wind without revenues for the OWF operators implies in terms of price

*Table 13: General Results for the Reference Case.*

| | Reference Case |
|---|---|
| **Total Revenue OWFs [M€]** | 15.386 |
| **Total Wind Export [GWh]** | 3085.924 |
| **Total Curtailment [GWh]** | 1520.542 |
| **Total Export at Zero-Price [GWh]** | 2251.727 |
| **Total Export at Positive Price [GWh]** | 834.196 |
| **Total Congestion Rent [M€]** | 141.547 |
| **Total Day-Ahead Cost [M€]** | 715.070 |
| **Total Redispatch Cost [M€]** | 12.748 |

risks is further explained in the next section. With respect to the social welfare distribution, the total Day Ahead costs (i.e. the outcome of the objective function (4.2a) reflecting total cost of generation) for the reference case amounted up to 715 M€ with total redispatch costs of 12.8 M€, while the TSOs amassed 107 M€ of congestion rents[14].

### 6.1.3 Price Risk Results – Reference Case

*Table 14: Price statistics reference case*

| | OBZ | Z1 | Z2 | Z3 |
|---|---|---|---|---|
| **Mean Price** | 7.47 | 56.25 | 15.42 | 12.97 |
| **Std Dev** | 15.009 | 13.010 | 17.570 | 17.716 |
| **CoV** | 2.0100 | 0.2328 | 1.1393 | 1.3654 |

Looking at the results related to the price risk, several observations are made. First, looking at the price statistics of the reference case (Table 14), it can be observed that there is a lot of variability of the price levels in the OBZ. Considering a standard deviation of 15.009 with a mean price of 7.47 €/MWh, and a Coefficient of Variance of 2.0100, these statistics suggest that the prices are not only widely varied but also that this variability is significant when considered in relation to the average price level (CoV).

Figure 30 presents the price duration curves for each bidding zone in the reference case. As to be expected looking at the merit order of zone 1 (see Section 5.1.2, Figure 17), this zone shows the highest price levels throughout the simulated timespan with an average electricity price of 56.25 €/MWh. Zone 2 and zone 3 somewhat converge showing average electricity prices of 15.42 €/MWh and 12.97 €/MWh. Looking at the price duration curve of the OBZ, the electricity price in the OBZ is lowest with an average price of 7.47 €/MWh. The price in the OBZ is for 0.37% of the hours at the price level of the most expensive dispatchable generators in the onshore zone, being to gas powering plants with marginal costs between 76.86 – 77.96 €/MWh. For 6.77% of the time the price clears between 46.72 – 48.53 €/MWh (hard coal), for 7.01% of the time between 35.56 - 37.43 €/MWh (lignite) and for 15.6% pf time at the level of the cheapest dispatchable generators, being the nuclear power plants with MC between 8.85 - 8.93 €/MWh. As mentioned earlier, for the remainder 70.25% the electricity price in the OBZ is at 0 €/MWh. The frequency and severity of the price risk shown in Figure 29 provides more insights into this large share hours without revenues for the OWF operators.

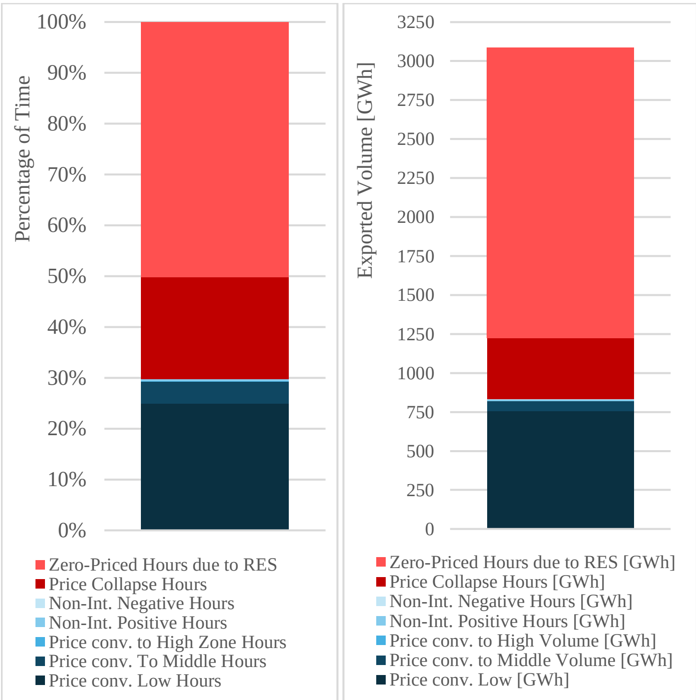


*Figure 29: Frequency (Left) and Magnitude (Right) of the Price Risk categories for the Reference Case.*

The first observation is that the wind export at zero prices is primarily caused by complete saturation of demand by renewable energy sources, accounting for 50.14% of the time and 60.3% of exported wind power. For 20% of the time a price collapse in the OBZ is observed, accounting for

[14] The congestion rents are calculated by the product of the power flow on a cross-border lines and the price difference between the two zones connected by that cross-border line.

12.61% of the total exported wind power. During the hours with positive prices (29.81%), the price in the OBZ converged mostly to the lowest priced adjacent zone (24.86%) accounting for 24.46% of the exported wind power. For 4.4% of the time the OBZ converged to the middle-priced bidding zone and for only 0.17% of the time to the high-priced bidding zone, accounting for 2.11% and 0.02% of the total exported wind power. Non-intuitive prices were mostly negligible, accounting for 0.30% and 0.07% of the time for positive and negative non-intuitive hours, during which 0.27% and 0.17% of wind power was exported.

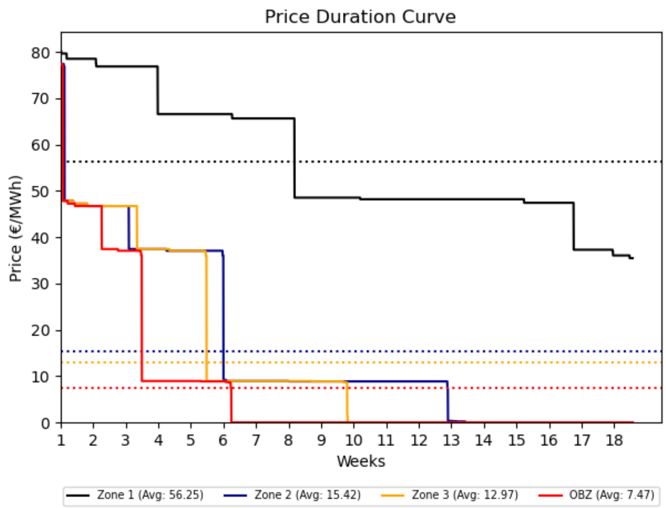


*Figure 30: Price Duration Curves for the Reference Case.*

The large proportion of hours without revenues for the OWFs (70.25%) compared to positive priced hours (27.03%) requires further investigation to understand the implications for the remaining cases. Specifically, the impact of grid topology on competition for scarce transmission capacity needs to be examined. As shown in the extreme values validation (Section 4.6.2.2) and the price collapse snapshot (Section 6.1.1, Figure 24), the onshore CNE at the landing point in Zone 1 structurally limits imports from the OBZ. Appendix D's congestion analysis for the reference case reveals that the onshore grid in Zone 1 primarily limits import capacity due to the AC line at the landing point and further inland AC lines, while the DC line to Zone 1 is never the limiting factor. Given that Zone 1 is the highest priced zone (Table 14) and Zones 2 and 3 have large renewable fleets (Figure 17), competition for scarce transmission capacity on the interconnector from the OBZ to Zone 1 is intensified. This critical result will be further considered in the analysis of other cases.

### 6.1.4 Volume Risk Results – Reference Case

The most notable observation for the volume risk results is that of the 33% of the available wind power that is curtailed, the wind power primarily curtailed by the capacity allocation. Looking at Figure 31, the reference case experiences for 61.42% of the time no volume risks and during 38.58% of the time curtailment is observed. During these volume risk hours, the capacity allocation occurred during all hours, whereas the capacity calculation occurred during 25.45% of these hours. A first observation is thus that the capacity calculation risk is never the sole volume risk occurring: during all hours in which wind power was curtailed by the capacity calculation, there was also wind power curtailed in the capacity allocation. Reversely, it did occur that only the capacity allocation risk causes curtailment. Not surprisingly, the volume curtailed by the capacity allocation is much higher than the volume curtailed by the capacity calculation, accounting for 92.84% of curtailment attributed to the capacity allocation compared to 7.16% to the capacity calculation. The large share of curtailment by the capacity allocation rhymes with the large share of zero-priced hours due to RES (previous section), since the competition between the OWFs in the OBZ and the renewable generators in the zero-priced zone for the allocation of transmission capacity on the interconnectors to the higher priced zone is highest during these hours. This is because during these hours there is no price advantage for cheap wind power from the OBZ in the market clearing, whereby the allocation on the interconnectors is mainly determined by the extent to which power flows potentially relieve the grid and thus enable additional power trading. If the large share of curtailed wind power by the capacity allocation is linked to these zero-priced hours due to renewable energy infeed is further clarified in the next section.

Looking at the duration curve for the two volume risk categories (Figure 32), it confirms that curtailment is mostly attributed to the capacity allocation risk. An interesting observation here is that with lower curtailed volumes, the capacity calculation risk is mostly non-active or accounting for relatively low volumes. Diving into the curtailed volumes per timestep, it was observed that with high total curtailed volumes, the volume curtailed by to the capacity calculation risk significantly increases. Specifically, apart from some outliers, the volume curtailed by the capacity calculation risk notably increases from a total curtailed volume above 2200MW. Furthermore, the volumes curtailed during one hour by the capacity allocation are substantially higher than the volumes curtailed by the capacity calculation. The maximum observed curtailment for one hour was 3818.73 MWh, where 664.84 MWh was caused by the capacity calculation and 3153.89 MWh by the capacity allocation, resulting in 99.55% of the potential wind production in the OBZ being curtailed. During this specific hour[15] only zone 1 experienced a non-zero price of 37.28 €/MWh and the other zones including the OBZ all showed zero-priced hours, indicating the fierce competition between all bidding zones to export power to zone 1.

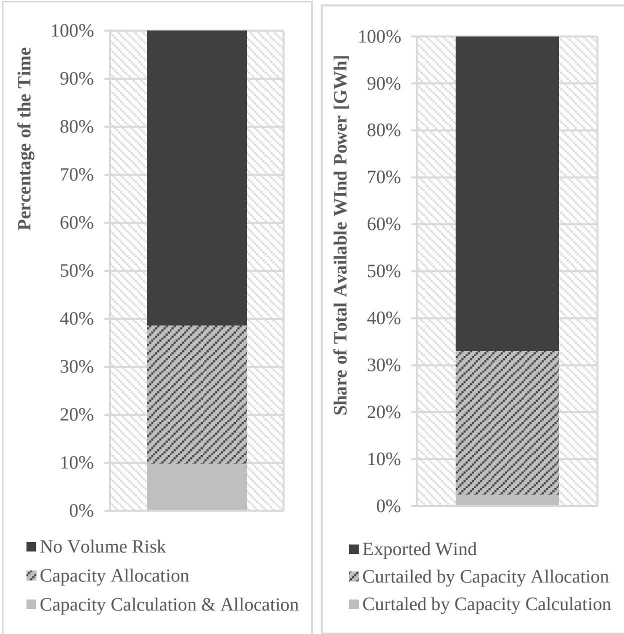


*Figure 31: Volume Risk Frequency (left) and Severity (right) - Reference Case.*

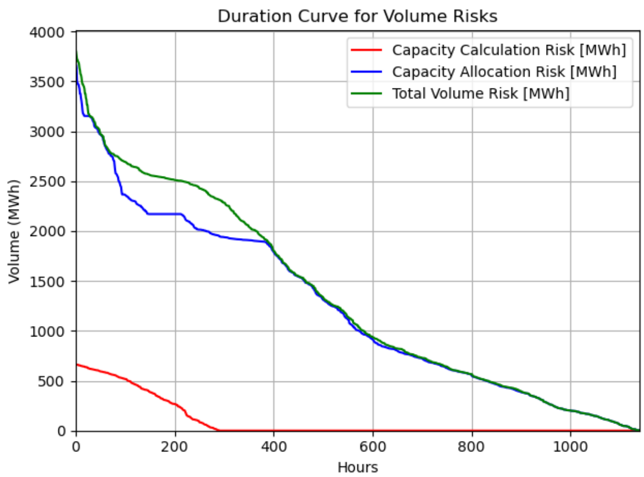


*Figure 32: Duration Curve for Volume Risks - Reference Case*

[15] During hour 343, the load was 18.76% lower than the average, there was no solar irradiation (early morning hour) and strong winds (c.f. between 0.763-0.794 onshore and 0.399-0.981 offshore).

### 6.1.5 Interacting Price and Volume Risk

Table 15 indicates that almost all curtailed volumes occurred during hours in which the OBZ experienced zero-priced hours due to price convergence to a bidding zone with renewables completely supplying demand (99.95%). During 76.89% of the zero-priced hours due to RESs, there was also a volume risk. The distribution of curtailed power by the capacity calculation and allocation during these hours is in line with Figure 31. An almost negligible amount of curtailment by the capacity calculation occurred during price collapse hours (0.05%).

*Table 15: Interacting Price and Volume Risk for the Reference Case. The percentages represent the share of curtailed wind power during each of the price risk categories in which curtailment was observed.*

| Price Risk Hours | Volume Risk | Reference Case |
|---|---|---|
| **Zero-Priced hours due to RES** | *Total Curtailment* | *99.95%* |
| | Curtailed by Cap. Calc. | 7.16% |
| | Curtailed by Cap. All. | 92.79% |
| **Price Collapse hours** | *Total Curtailment* | *0.05%* |
| | Curtailed by Cap. Calc. | 0.00% |
| | Curtailed by Cap. All. | 0.05% |

This observation has two key implications. Firstly, curtailment is primarily driven by competition for scarce transmission capacity between the OBZ and onshore renewables. Since zone 1 never experiences zero prices (Figure 30), zones 2, 3, and the OBZ compete to export to the high-priced zone 1 during zero-priced hours caused by RESs. The onshore grid of zone 1 can import up to 774.5 MWh via the OBZ (Table 5, Section 4.6.2.2), and the interconnectors from the OBZ to zones 2 and 3 have each a capacity of 1500 MW, making the theoretical maximum export from the OBZ 3774.5 MWh. When zones 2 or 3 also have zero prices, competition further intensifies. The competition peaks when all zones, except zone 1, have zero prices, as the transmission capacity to zone 1 will then be allocated based solely on grid alleviation with the absence of price differentiation between the generators in the market clearing algorithm. Table 16 shows that curtailment is highest during these hours, with +22.6% curtailment by capacity calculation and +93.7% curtailment by capacity allocation compared to hours when only the OBZ and one other zone have zero prices. Thus, the volume risk is highest when the competition for transmission capacity to zone 1 is most intense, which is almost entirely during zero-price hours due to RES.

Secondly, the observed interacting price and volume risk does not align with the literature (Section 3.2.4). It was expected that price collapses would be mainly associated with the capacity calculation risk. However, the results show that for the single hour with a price collapse and curtailed volume, curtailment was entirely due to capacity allocation risk. This does not mean that the described interacting price and volume risk is non-existent, but it is not present within the observed results of the reference case in this thesis. Nevertheless, the results do prove that whenever there is a volume risk, the price in the OBZ is zero, since all volume risk hours are associated with zero-priced hours due to RES. This provides quantitative substantiation for the interacting price and volume risk.

*Table 16: Average curtailed volumes during zero-priced hours due to RES.*

| | Share of interacting price and volume risk hours to price risk hour | Average Total Curtailment | Average Curtailment by Capacity Calculation | Average Curtailment by Capacity Allocation |
|---|---|---|---|---|
| **Zero-price RES with volume risk** (with zero-prices in the OBZ and either zone 2 or zone 3) | 46% | 1535.19 MWh | 322.95 MWh | 822.64 MWh |
| **Zero-prices RES with volume risk** (with zero-prices in all zones except zone 1) | 54% | 1880.84 MWh | 395.92 MWh | 1593.34MWh |

## 6.2 Case Group 1: Offshore Grid Topology – Triangular Hybrid

In this case group the offshore grid topology with a triangular hybrid (similar to the reference case) was subject to analysis, where the transmission capacities of the interconnectors was the parameter that has been varied. Two cases have been simulated where the total direct export capacity from the OBZ to shore has been increased (case $\mathrm{EI}^{+}$) and decreased (case $\mathrm{EI}^{-}$) with 33%, and two cases have been simulated where the interconnection capacity from the OBZ towards fossil-dominated, high-priced zone 1 (case $\mathrm{II}_{Z1}^{+}$) and towards renewable-dominated, low-priced zones 2 and 3 (case $\mathrm{II}_{Z23}^{+}$) have been doubled. The box below shows the formulated hypothesis for this case group and the most notable results are briefly discussed hereafter.

***H.1**: Increased HVDC transmission capacity from the OBZ to onshore markets leads to higher congestion rents, lower day-ahead generation and redispatch costs, lower electricity prices with fewer price collapses and increased wind exports due to reduced curtailment.*

The most notable results for the case group reveal that increasing the export capacity symmetrically (Case $\mathrm{EI}^{+}$) led to higher wind exports (+11.43%) and reduced curtailment (-23.20%) but did not significantly increase revenues (+0.10%) because additional wind power was primarily exported during zero-priced hours (+14.93%). Conversely, decreasing the export capacity symmetrically (Case EI-) resulted in lower wind exports (-13.89%) and higher curtailment (+28.18%), but substantially increased revenues (+61%) due to a shift from zero-priced exports (-35.18%) to positive-priced exports (+43.32%). Increasing the interconnectivity to high-priced Zone 1 (Case $\mathrm{II}_{Z1}^{+}$) led to decreased wind exports (-13.89%) and increased curtailment (+27.67%), but still increased revenues (+3.95%), since the reduced exports were mainly during zero-priced hours. Increasing interconnectivity between the two renewable zones 2 and 3 (case $\mathrm{II}_{Z23}^{+}$) demonstrated increased wind exports (+35.28%) and reduced curtailment (-71.61%), leading to higher revenues (+8.43%) and indicating that enhanced transmission capacity to renewable-dominated zones improves export capacity and price convergence.

Overall, these results illustrate that while increased transmission capacity generally boosts wind exports and reduces curtailment, the timing of exports—whether during zero-priced or positive-priced hours—plays a crucial role in determining revenue gains. The underlying factor exacerbating the observed price and volume risks in this case group is the constrained onshore grid of the high-priced Zone 1. Specifically, increased transmission capacity on the interconnectors heightens the competition between the OBZ and other zones for the limited transmission capacity to this restricted, high-priced, importing Zone 1.

### 6.2.1 General Results – Offshore Grid Topology (Triangular)

Table 17 presents the general results of this case group.

*Table 17: Percentual changes of the General Results with respect to the refence case for Case Group Offshore Grid Topology (Triangular).*

| | **Reference Case** | $\mathbf{EI^{+}}$ (2.A) | $\mathbf{EI^{-}}$ (2.B) | $\mathbf{II^{+}_{z1}}$ (2.C) | $\mathbf{II^{+}_{z23}}$ (2.D) |
|---|---|---|---|---|---|
| **Total Revenue OWFs [M€]** | 15.386 | +0.10% | +61.00% | +3.95% | +8.43% |
| **Total Wind Export [GWh]** | 3085.924 | +11.43% | -13.89% | -13.63% | +35.28% |
| **Total Curtailment [GWh]** | 1520.542 | -23.20% | +28.18% | +27.67% | -71.61% |
| **Total Export at Zero-Price [GWh]** | 2251.727 | +14.93% | -35.08% | -19.91% | +43.60% |
| **Total Export at Positive Price [GWh]** | 834.196 | +1.98% | +43.32% | +3.32% | +12.83% |
| **Total Congestion Rent [M€]** | 141.547 | +0.31% | -18.02% | +0.70% | -2.85% |
| **Total Day-Ahead Cost [M€]** | 715.070 | -0.05% | +0.49% | -0.40% | -0.01% |
| **Total Redispatch Cost [M€]** | 12.748 | -1.64% | +29.62% | -26.11% | +1.70% |

As expected, increasing the export capacity symmetrically (cases $\mathrm{EI}^{+}$) leads to increased wind exports (+11.43%) and reduced curtailment (-23.20%). However, no significant increase in revenues is observed (+0.10%), since most additional generated wind power is exported during zero-priced hours (+14.93%) and to a lesser extend during positive priced hours (+1.98%). The price risk results (next section) further explain this observation. The changes in congestion rent (+0.31%), day-ahead generation cost (-0.05%) and redispatch cost (-1.64%) are in line with expectations, albeit with a limited effect.

Decreasing the export capacity symmetrically (cases $\mathrm{EI}^{-}$) leads to decreased wind exports (-13.89%) and increased curtailment (+28.18%), which was to be expected. Surprisingly, the revenues increased substantially for this case (+61%), which is partly due to the shift from power being exported during zero prices (-35.08%) to power being exported during positive prices (+43.32%), as well as due to the substantial increase in average prices in the OBZ (Table 18, next section). The decrease in congestion rent (-18.02%) and increase in day-ahead cost and redispatch cost (+0.49% and +29.62%) are the expected result of decreased interconnection capacity.

Increasing the interconnectivity for the high-priced, fossil dominated zone 1 (case $\mathrm{II}^{+}_{\mathbf{z1}}$) does not lead to increased wind exports. Surprisingly, less wind is exported (-13.89%) and more wind is curtailed (+27.67%). Nonetheless, revenues are increased (+3.95%), which is again due to a shift from wind exports during zero-priced hours (-19.91%) to wind exports during positive priced hours (+3.32%). The price and volume risk results (next sections) further explain the underlying reason for this observed effect. The large decrease in redispatch costs (-29.11%) indicates that the additional transmission capacity to zone 1 especially provides benefits to the TSO in this market, which is the result of the reduced necessity for redispatch actions of expensive dispatchable generators in zone 1. The (small) increase in congestion rent (+0.70%) and decrease in day-ahead cost (-0.40%) are in line with expectation.

Increasing the interconnectivity for the two renewable dominated zones (case $\mathrm{II}^{+}_{\mathbf{z23}}$) leads to increased wind exports from the OBZ (+35.28%) and decreased curtailment (-71.61%). Of these increased wind exports, most additional wind power is exported during zero-priced hours (+43.60%) and to a lesser extend at positive prices (+12.83%). Together with higher mean prices in the OBZ (Table 18, next section), these additional exports during positive prices explain the increased revenue of the OWFs (+8.43%). Congestion rents for this case decreased (-2.85%), where they increased for case $\mathrm{II}^{+}_{\mathbf{z1}}$ (+0.70%), indicating that the increased interconnectivity between zones 1 and 2 led to increased price convergence between the zones

### 6.2.2 Price Risk Results – Offshore Grid Topology (Triangular)

*Table 18: Price Statistics for the OBZ Case Group Triangular Hybrid*

| | Ref | $EI^+$ | $EI^-$ | $II^+_{z1}$ | $II^+_{z23}$ |
|---|---|---|---|---|---|
| **Mean Price** | 7.47 | 7.67 | 13.12 | 7.24 | 8.57 |
| **Std Dev** | 15.009 | 15.020 | 18.128 | 14.576 | 15.855 |
| **CoV** | 2.0100 | 1.9586 | 1.3822 | 2.013 | 1.851 |

The price risk results for case $EI^+$ explain the lag of increased revenue with increased wind exports. The mean price in the OBZ was only slightly higher than in the reference case OBZ (Table 18). Moreover, the additional generated wind was primarily exported during zero priced hours with renewables determining the price (Figure 33, right). An increase in transmission capacity to all three zones thus primarily led to increased exports during hours with high renewable feed in.

For case $EI^-$, the price duration curve (Figure 34 top right) shows much more price convergence to zones 2 and 3, visible in the curves being almost identical for large parts. Regarding the price risk categories (Figure 33, left), a shift is observed in the frequency of price collapse hours (-92.74%) to hours with price convergence to a low- (+67.03%), middle- (+37.69%) and high-priced (+20%) zone, while the frequency of zero-priced hours due to RESs remained relatively stable (-1.55%). This shift from price collapse hours to positive priced hours is also observed in the exported volumes during these hours (Figure 33, right), where the volumes exported during price collapse hours have significantly reduced (-91.49%) and the volumes exported during low price convergence hours increased (+42.23%). Aided with a substantial higher average price and less relative price volatility (Table 18), the increase in revenues for this case is evident.

The shift from price collapse hours to positive-priced hours with reduced transmission capacities to shore can be explained as follows. As defined in Section 3.2.2, price collapses occur when export capabilities are restricted due to reductions in the FB domain. Appendix D identifies the primary factors restricting the FB domain as the inadequate onshore AC transmission grid in Zone 1 and, to a lesser extent, the higher socio-economic welfare generating commercial transactions within Zone 2, while the utilisation of the HVDC interconnectors to both zones is rarely maximised. When transmission capacity is reduced from 1.5GW to 1GW, the degree of limitation due to Zone 1's inadequate grid remains unchanged, as the AC grid can still absorb up to its maximum physical capacity of 774 MWh (see

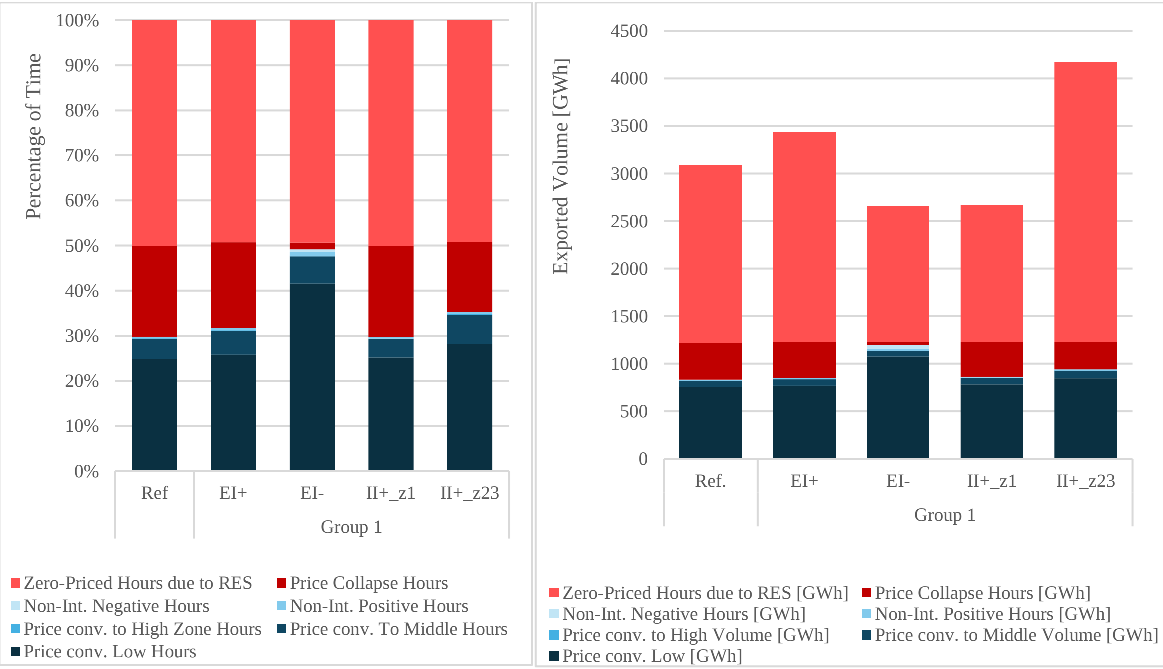


*Figure 33: Frequency (Left) and Magnitude (Right) of the price risk for Case Group Offshore Grid Topology (Triangular)*

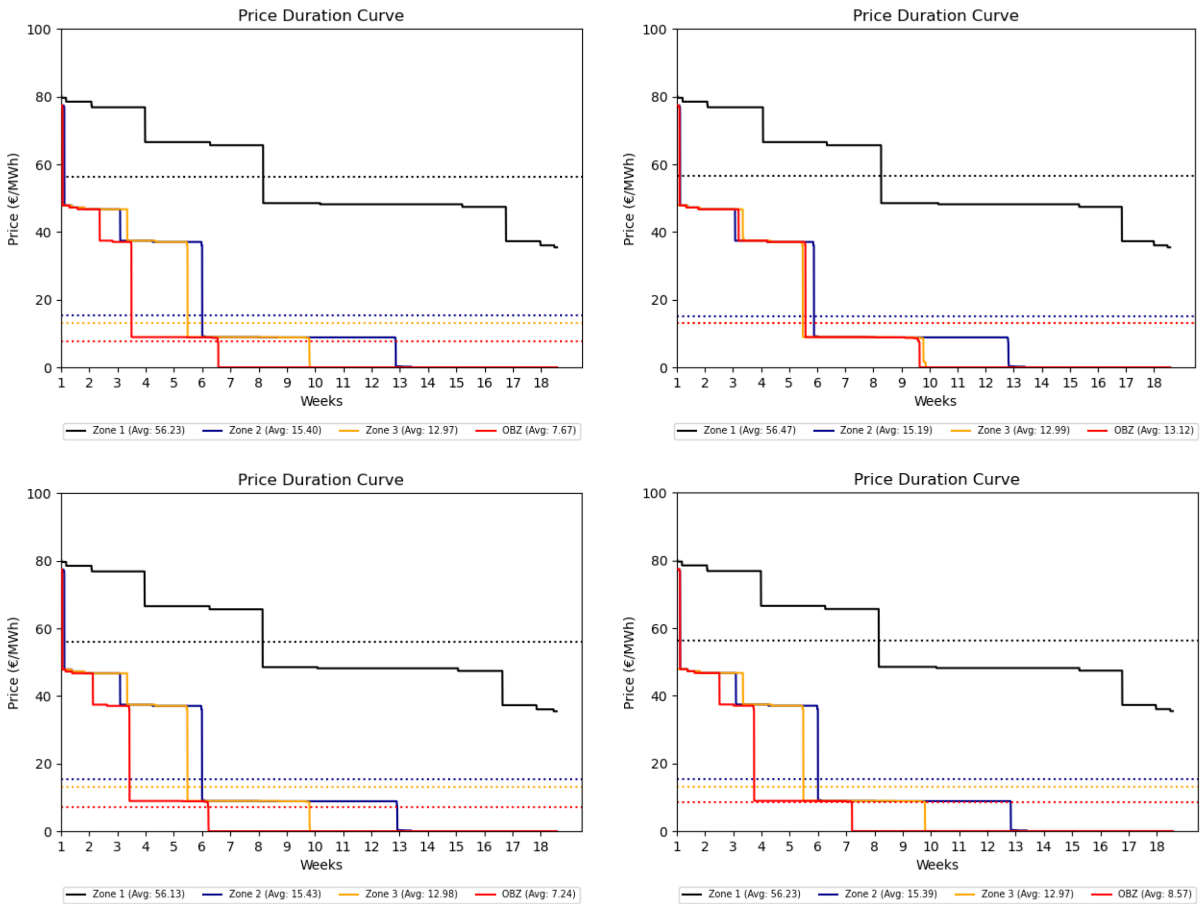


*Figure 34: Price Duration Curves Case Group 2. Top left case $EI^{+}$, top right case $EI^{-}$, bottom left case $II^{+}_{Z1}$ and bottom right case $II^{+}_{Z23}$.*

Section 4.6.2.2). However, reducing the transmission capacity to Zone 2 changes the limiting factor on the FB domain. Previously, the HVDC interconnector to Zone 2 was often utilised up to 1000.37 MWh, beyond which higher imports did not lead to additional DA generation cost reductions. With the capacity now limited to 1000 MW, this threshold is often not reached. Consequently, exports from the OBZ are redirected towards Zone 3 before full exports to Zone 2 are exhausted. This creates an uncongested path to Zone 3, preventing price collapse in the OBZ and instead causing price convergence with this bidding zone.

For case $II^{+}_{Z1}$, the frequency of price risk hours did not change substantially compared to the reference case (see somewhat equal bars in Figure 33 left), while the magnitude of exported power increased during low and middle price convergence hours (+3.59% and +1.49%) and decreased during high price convergence hours (-38.87%). The decrease in curtailment is attributed to the large decrease in exported volumes during RES hours decreased (-23.29%) and to a smaller extend due to the decrease in exports during price collapse hours (-6.68%), while the frequency of and zero-priced hours due to RES and price collapse hours remained relatively stable (-0.14%, +0.68%). The unexpected result of total reduced wind exports (Table 17) thus did not lead to decreased revenues (instead +3.95%), even despite a slightly lower average price in the OBZ (Table 17), since the reduced exports were mainly during zero-priced hours. The price risk result of increasing interconnectivity towards the high-priced zone 1 thus indicate that competition for the scarce transmission capacity towards this zone is further intensified, especially during hours when the OBZ is in direct competition with onshore renewable generators in the other two zones. This volume risk results further confirms this implication for this case.

For case $\mathrm{II}_{z23}^{+}$, the frequency of price convergence hours increased to low (+13.08%), middle (+47.69%) and high (+20%) priced zones, which also translated into the exported volumes during these hours with increases during price convergence hours to low (+12.15%), middle (+24.89%) and high (+10.14%) priced zones. With respect to the hours without revenue for the OWFs, a significant reduction in price collapse hours (-22.64%) is observed associated with reduced exports during these hours (-25.65%). Thus, during the hours where transmission capacity to zones 2 and 3 was previously limited (price collapse hours), the increased capacity on the interconnectors enabled additional price convergence between the OBZ and these zones, which is reflected in the higher mean electricity price (Table 18) , increased revenue and congestion rent (Table 17). Notable is that the frequency of zero-priced hours due to RES slightly decreased (-1.89%) whereas the volumes exported during these hours substantially increased (+58.07%). The implies that the increased interconnectivity between solar zone 2 and wind zone 3 primarily enabled OWFs in OBZ to export additional wind power during hours where the price in at least one of these two zones was already being set by renewable generators.

The non-intuitive price risk did not play a significant role in any of the cases in this Case Group.

### 6.2.3 Volume Risk Results – Offshore Grid Topology (Triangular)

Increasing the export capacity symmetrically (case EI+) led to slightly more hours experiencing no volume risk (+1.99%), where the frequency of hours with both the capacity calculation and allocation risk significantly reduced (-72.07%), but hours with only the capacity allocation increased (+20.38%). Regarding the magnitude of the volume risk for this case (Figure 35), curtailment by the capacity calculation saw a substantial decrease (-93.90%) and curtailment by the capacity allocation also decreased (-17.75%). The decrease in curtailment by the capacity calculation is in line with expectations, since the maximum net position of the OBZ is enlarged with additional transmission capacity in the direction of all zones. The more frequently hours with curtailment by the capacity allocation with lower curtailed volumes during these hours, indicates that the increased transmission capacity opens up more frequently competition between the OBZ and the onshore zones for the allocation of transmission capacity, but due to the increased available transmission capacity more wind volume could still be exported. This is also in line with the increased exports during zero-priced hours due to renewable infeed.

Decreasing the export capacity in case $\mathrm{EI}^{-}$, primarily led to an increase in hours with curtailment by both the capacity calculation and allocation (+92.41%) and a decrease in hours with only curtailment by the capacity allocation (-43.58%). Curtailed volumes by the capacity calculation increased (+21.15%) and curtailed volumes by the capacity allocation saw a substantial increase (+236.0%). The increase in curtailment by the capacity calculation is a logical consequence of the reduction of the maximum possible net position of the OBZ, but the much higher increase in curtailment by the capacity allocation is somewhat surprising. The reason why this happens is that during those hours in which both curtailment by the capacity calculation and allocation takes place, the lower available transmission capacity further drives up competition with the OBZ and wind dominated zone 3 for the allocation of this scarce transmission capacity, resulting in additional curtailment by the capacity allocation.

Case $\mathrm{II}_{z1}^{+}$ saw primarily an increase of capacity allocation hours (+18.26%) and a decrease in hours with both capacity calculation and allocation (-5.86%). The total additional curtailed wind power (+27.67%) is mainly due to the increase in curtailment by the capacity allocation (+29.58%), while curtailment by the capacity calculation remained somewhat stable (-0.83%). This increase in curtailment, primarily due to curtailment by the capacity allocation, is somewhat unexpected with increased interconnection capacity. However, considering again the restricting onshore grid of the high-priced zone 1 (see Section 4.6.2.2), the increase in curtailment can be attributed to the additional competition for the allocation of transmission capacity towards zone 1 between the OBZ and the more renewable-dominated zones 2 and 3. The relative shift from curtailment by the capacity calculation to the capacity allocation further underlines that the grid in zone 1 is already highly constrained in the reference case, which is only further magnified in this case.

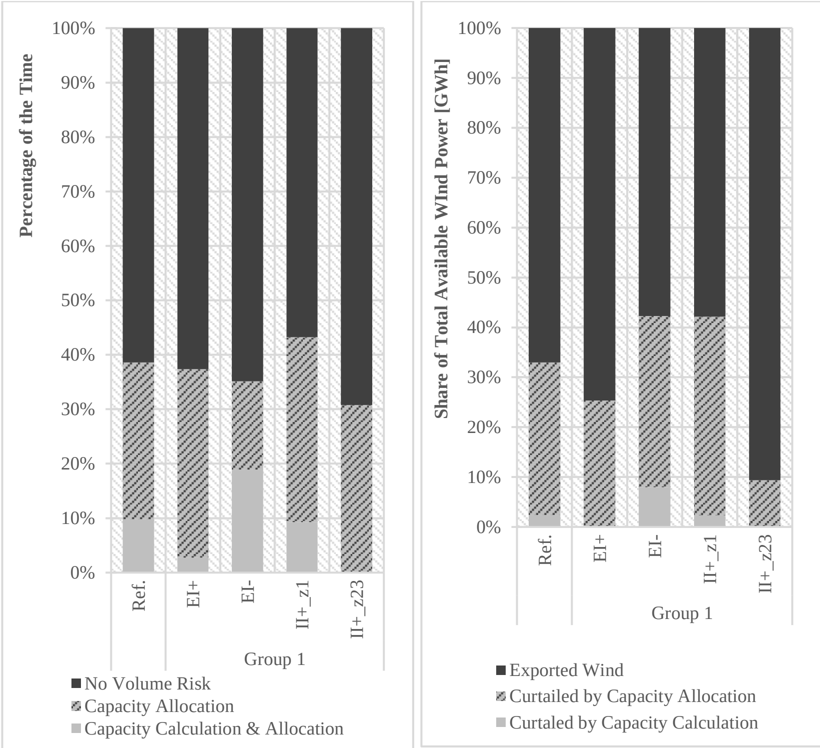


*Figure 35: Frequency (left) and Severity (right) of Volume risk - Case Group 2.*

For Case $\mathrm{II}^{+}_{z23}$, the most notable result is that curtailment by the capacity calculation is no longer existent. The frequency of hours with curtailment by the capacity allocation did increase (+7.07%), but the curtailed volume during these hours also substantially decreased (-69.42%). These observations indicate that the increase in the FB domain due to increased transmission capacity structurally allows for a larger maximum net position for the OBZ, and that onshore grids of zones 2 and 3 physically can absorb this additional potential export from the OBZ. Especially when comparing cases $\mathrm{II}^{+}_{z1}$ and $\mathrm{II}^{+}_{z23}$, it can be concluded that increasing interconnection capacity to zone 1 does not necessarily lead to an increased FB domain, whilst for increasing interconnection capacity to zones 2 and 3 it does increase the FB domain. Lastly, the significant decrease in curtailed power by the capacity allocation risk in case $\mathrm{II}^{+}_{z23}$ shows that with increased interconnection capacity between the renewable dominated markets, the competition between the OBZ and these onshore markets for the capacity of the interconnectors is less fierce, whereby the market coupling more frequently allocates the generated wind capacity in the OBZ.

## 6.2.4 Interacting Price and Volume Risk

*Table 19: Interacting Price and Volume Risk for the Case Group Offshore Grid Topology (Triangular). The percentages represent the share of curtailed wind power during each of the price risk categories in which curtailment was observed..*

| Price Risk Hours | Volume Risk | Ref. | $\mathrm{EI}^{+}$ | $\mathrm{EI}^{-}$ | $\mathrm{II}^{+}_{z1}$ | $\mathrm{II}^{+}_{z23}$ |
|---|---|---|---|---|---|---|
| **Zero-Priced hours due to RES** | *Total Curtailment* | *99.95%* | *100.00%* | *99.49%* | *99.96%* | *100.00%* |
| | Curtailed by Cap. Calc. | 7.16% | 0.57% | 18.61% | 5.56% | 0.00% |
| | Curtailed by Cap. All. | 92.79% | 99.43% | 80.88% | 94.40% | 100.00% |
| **Price Collapse hours** | *Total Curtailment* | *0.05%* | *0.00%* | *0.29%* | *0.04%* | *0.00%* |
| | Curtailed by Cap. Calc. | 0.00% | 0.00% | 0.17% | 0.00% | 0.00% |
| | Curtailed by Cap. All. | 0.05% | 0.00% | 0.12% | 0.04% | 0.00% |

Table 19 indicates, similar to the interacting price and volume risk for the reference case (Section 6.1.5), that (almost) all curtailment took place during hours when prices in the OBZ were zero due to price convergence to an onshore zone where renewables supplied all demand. Only for case $\mathrm{EI}^{-}$ some curtailment took place during price collapse hours, but to a very limited extend. This observation further underlines the relation between the limiting onshore grid in zone 1 and the competition between the OBZ and zones 2 and 3 to export to this zone during hours with high renewable feed-in.

## 6.3 Case Group 2: Offshore Grid Topology – Dual Hybrid

In this case group the offshore grid topology in a dual hybrid form was subject to analysis where both the installed offshore wind capacity and the transmission capacity were the parameters that have been varied. A symmetrical setup (case Sym.) and two asymmetrical setups (cases $Asym_{z1}$ and $Asym_{z3}$) were simulated (see Section 5.2.2). The box below shows the formulated hypothesis for this case group and the most notable results are discussed hereafter.

***H.2:*** *Increased export capacity to the high-priced zone 1 results in higher wind exports at elevated prices, thereby boosting revenues, while increased export capacity to the lower-priced zone 3 leads to higher curtailment due to capacity allocation and reduced revenues.*

The symmetrical case (Sym.), with 3 GW of installed wind capacity, achieved the highest revenues despite having the lowest capacity. This was due to a substantial increase in mean electricity prices and a favourable distribution of price risks. The setup shifted price convergence from the lowest-priced zone to the middle and highest-priced zones, reducing price collapse hours significantly. Consequently, fewer exports occurred during price collapse hours, and more exports happened during higher-priced hours. The reason for this observed effect is less zones and less wind capacity competing for the allocation of transmission capacity towards high-priced zone 1 during hours where renewable energy sources did not set the price.

Case $Asym_{z1}$, which increased wind capacity near the higher-priced Zone 1, led to more curtailment (+52.56%) and fewer wind exports (-25.90%), resulting in a larger revenue decrease (-19.86%), contrary to the hypothesis. This outcome is primarily due to the onshore grid in Zone 1 being unable to import the additional wind power, causing a substantial increase in curtailment by capacity calculation. Conversely, Case $Asym_{z3}$, which increased capacity near Zone 3, showed a smaller increase in curtailment (+19.47%) and a lesser reduction in wind exports (-9.59%), leading to a smaller revenue decrease (-10.88%). The increased transmission capacity towards wind-dominated Zone 3 enabled more exports, as Zone 3 could better absorb the additional wind power, but also additional competition, resulting in increased curtailment by the capacity allocation.

### 6.3.1 General Results – Offshore Grid Topology (Dual)

Table 20 presents the general results of this case group. A first notion is to remember that case Sym. is the only case with a lower total installed wind capacity (3 GW) compared to the reference case and the other cases (4.5GW). The first interesting observation is immediately with this notion, since case Sym. has the highest revenues of all cases, despite having the lowest installed wind capacity and thus. This is primarily due to a substantial

*Table 20: Percentual changes of the General Results with respect to the refence case for case group Offshore Grid Topology (Dual)*

| | Reference Case | Sym. (3.A) | $Asym_{z1}$ (3.B) | $Asym_{z3}$ (3.C) |
|---|---|---|---|---|
| **Total Revenue OWFs [M€]** | 15.386 | -1.79% | -19.86% | -10.88% |
| **Total Wind Export [GWh]** | 3085.924 | -37.36% | -25.90% | -9.59% |
| **Total Curtailment [GWh]** | 1520.542 | -25.16% | +52.56% | +19.47% |
| **Total Export at Zero-Price [GWh]** | 2251.727 | -37.39% | -21.94% | -2.51% |
| **Total Export at Positive Price [GWh]** | 834.196 | -37.28% | -36.58% | -28.71% |
| **Total Congestion Rent [M€]** | 141.547 | -20.73% | -31.94% | -29.92% |
| **Total Day-Ahead Cost [M€]** | 715.070 | +4.51% | -28.16% | -28.71% |
| **Total Redispatch Costs [M€]** | 12.748 | +5660% | +7652% | +12815% |

increase in mean electricity prices (Table 21) and a different distribution of price risks, further elaborated in the next section on price risk.

Case $Asym_{z1}$ shows somewhat unexpected results, since having more installed wind capacity near the higher-priced zone 1 (case $Asym_{z1}$) leads to more curtailment (+52.56%) and less wind exports (-25.90%) while case $Asym_{z3}$ showed a smaller increase in curtailment (+19.47%) and decrease in wind exports (-9.59%). This also led to a larger decrease in revenues for case $Asym_{z1}$ (-19.86%) compared to case $Asym_{z3}$ (-10.88%). The primary reason for this unexpected outcome for case $Asym_{z1}$ is that the onshore grid in zone 1 is physically unable to import the additional wind power available near its shore, which will also be confirmed by a substantial increase in curtailment by the capacity calculation as explained in Section 6.3.3.

With respect to the social welfare changes, all three cases saw a decrease in congestion rents (-20.73%, 31.94%, 29.92%), which is a logical consequence of having only 2 countries connected via the hybrid instead of 3, whereby electricity trading possibilities with price spreads inherently decreases. Case Sym. saw an increase in DA cost (+4.51%), which is explained by the 1.5GW of low-cost offshore wind capacity missing in this case. The decrease in DA costs for cases $Asym_{z1}$ (-28.16%) and $Asym_{z3}$ (-28.71%) indicates that the somewhat focussed interconnectivity between zones 1 and 3 displaces high-cost (fossil) generators in zone 1.

The very extreme increase in redispatch cost (+5560%, +7652% and +12815%) is the consequence of zone 2 being somewhat isolated in the grid topology setup of this case group. Where in the reference case zone 2 had a total of 1900 MW of interconnection capacity, now only 400 GW of interconnection capacity was left, realised by two point-to-point interconnectors. In addition, zone 2 has the lowest installed capacity of dispatchable generators compared to renewable installed capacity (Figure 17, Section 5.1.2), whereby the system balancing at the day of operation is highly dependent on the few available dispatchable generators in this zone. This isolated zone together with limited dispatchable generator availability led to the very substantial increase in the redispatch costs.

### 6.3.2 Price Risk Results – Offshore Grid Topology (Dual)

*Table 21: Price Statistics OBZ Case Group Offshore Grid Topology (Dual)*

| | Ref. | Sym. | $Asym_{z1}$ | $Asym_{z3}$ |
|---|---|---|---|---|
| **Mean Price** | 7.47 | 16.38 | 10.79 | 10.76 |
| **Std Dev** | 15.009 | 24.835 | 18.855 | 18.964 |
| **CoV** | 2.0100 | 1.5166 | 1.7475 | 1.7633 |

Considering the price risk statistics (Table 21), the notion that case Sym. generated most revenues despite having the lowest installed wind capacity can be partially attributed to the substantially higher mean price and lower relative price volatility around that mean price (CoV). Furthermore, looking at the price duration curve of case Sym. (Figure 36, top left), it can be observed that the price duration curve of the OBZ surpasses the price duration curve of zone 3, indicating that the price convergence to this lower priced zone occurs less frequently. Moreover, the price duration curve is somewhat shifted rightwards compared to the other two cases and has more frequently higher price levels (longer horizontal parts at higher prices), indicating structural higher price levels observed in the OBZ.

Considering the frequency and magnitude (Figure 37) of the price risk for case Sym., the relative increased revenues are further substantiated. The symmetrical dual hybrid setup led to a shift from price convergence hours to the lowest priced zone (-46.59%) to price convergence hours to the middle (+44.62%) and, in particular, to the highest-priced zone (+11,880%). This is also visible in the exported volumes during these hours, which decreased for price convergence hours to the lowest priced zone (-62%), but substantially increased for price convergence hours to the middle (+82,44%) and highest priced zone (+18,686%). In addition, significant less price collapse hours were observed (-62.84%), and consequently less exports during these hours (-44.73%). The frequency of zero-priced hours due to RES

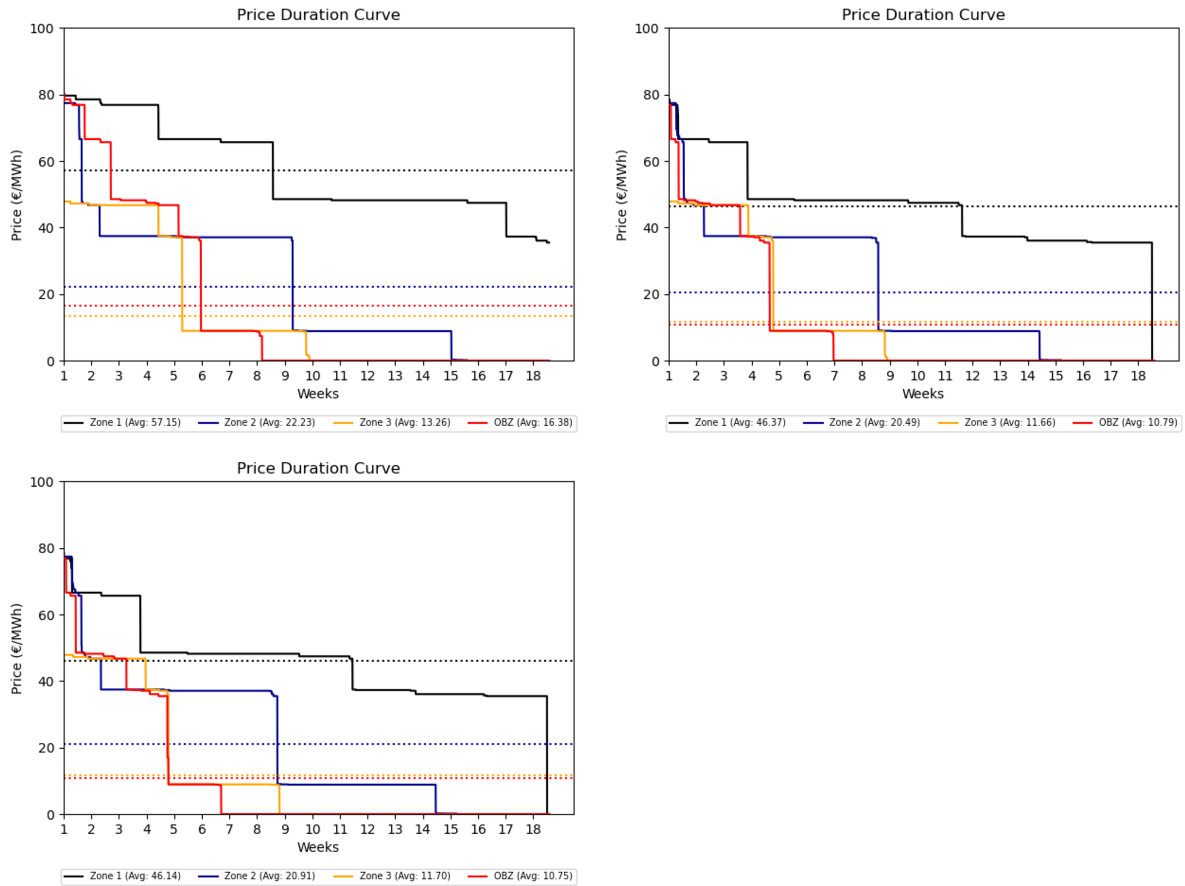


*Figure 36: Price Duration Curves for Case Group Offshore Grid Topology (Dual). Top left case Sym., top right case Asym$_{z1}$ and bottom left case Asym$_{z3}$.*

increase (+3.31%), but less exports took place during these hours (-35.86%).

The underlying causes and implications of these results are as follows. First, zone 1's onshore grid already restricts imports from the OBZ (Section 4.6.2.2). Second, only 3 GW of wind in the OBZ now competes with zone 3 to export to zone 1, instead of 4.5 GW competing with both zones 2 and 3 for this same transmission allocation. Third, zero-price hours due to renewable energy sources remained relatively stable, indicating that the shift from price collapse hours to positive-priced hours occurred primarily during non-renewable hours. These factors led to more frequent price convergence, often to even higher prices, due to fewer zones and less wind capacity competing for the allocation of transmission capacity during non-renewable hours.

These observations underscore the importance of an adequately designed hybrid project suited to the onshore transmission grid to which it is connected. In the grid setup used in this thesis, lower OWF capacities appear more beneficial for developers, as oversupply of wind leads to additional price collapses.

Regarding the two asymmetric cases (case Asym$_{z1}$ and Asym$_{z3}$), the mean price levels are both lower than the mean price in the OBZ of the symmetrical setup, while still being higher than in the reference case (Table 21). Additionally, the relative volatility from the mean price (CoV) is also lower than the symmetric case but higher than the reference case. The price duration curves of the OBZ in these cases show very similar patterns to the price duration curves of zone 3 and do not show any convergence to the price duration curve of zone 2, which logically follows from the dual hybrid setup not connected to zone 2 (See Figure 36 top right and bottom left). Together with the mean price levels in this case of the OBZ and zone 3 being almost similar, these results indicate structural price convergence to zone 3.

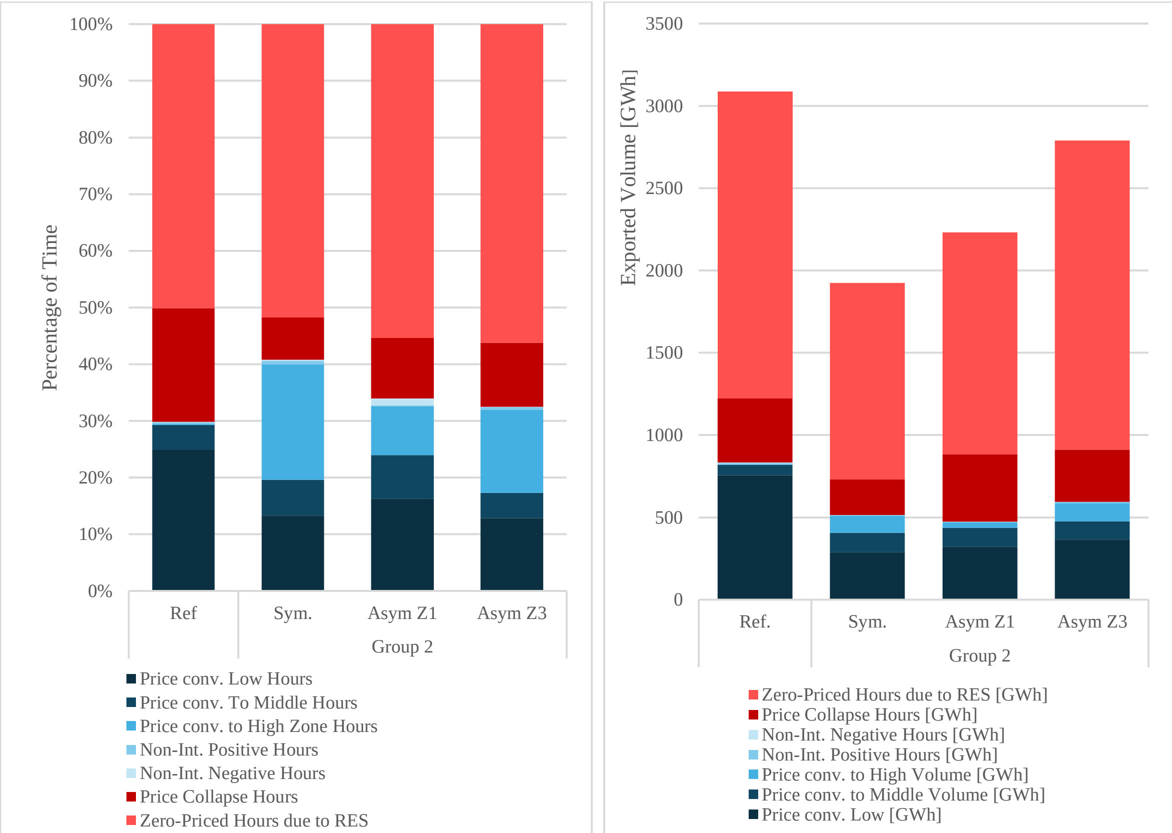


*Figure 37: Frequency (Left) and Magnitude (Right) of the price risk results for Case Group Offshore Grid Topology (Dual)*

The price risk results for these cases (Figure 37) expose an interesting observation. Cases Asym$_{z1}$ and Asym$_{z3}$ showed somewhat similar results in terms of frequencies in total positive priced (33.94% and 32.52% of time), zero-priced hours due to RES (55.38% and 56.30% of time) and price collapse hours (10.67% and 11.28% of time). However, case Asym$_{z3}$ exported more wind power during these hours compared to case Asym$_{z1}$, especially for the total exported power during positive hours (12.89% compared to 10.27% of available wind) and for the exported power during zero-priced hours due to RES (40.77% compared to 29.29% of available wind). These similar frequency of hours with increased magnitudes of exported volumes for case Asym$_{z3}$ compared to case Asym$_{z1}$ indicate that the increased transmission capacity from the OBZ towards zone 3 enables additional exports from the OBZ than increased transmission capacity towards zone 1. This is again in line with the limiting capability of the onshore zone 1 to absorb increased power injections form the OBZ. The volume risk results further substantiate this implication.

### 6.3.3 Volume Risk Results – Offshore Grid Topology (Dual)

Regarding the volume risk results, the frequency of hours experiencing a volume risk for case Sym. remains relative equal to the reference case (-0.35%), with a shift from hours with only the capacity allocation risk (-2.00%) to hours with both the capacity calculation and allocation volume risk (+4.48%). Following logically from the decreased installed capacity from 4.5GW to 3GW, the total curtailed volume decreased (-25.15%), with both a decrease in curtailment by the capacity calculation (-35.0%) and allocation (-24.41%). These results were line with expectations.

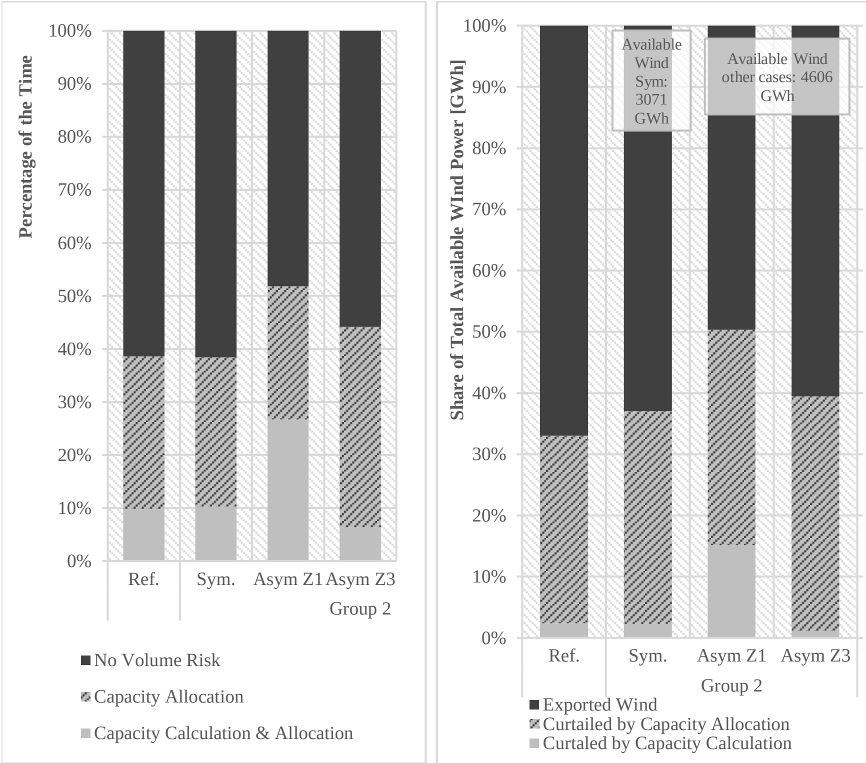


*Figure 38: Frequency (left) and Severity (right) of Volume Risk for Case Group Offshore Grid Topology (Dual).*

The results for cases Asym$_{z1}$ and Asym$_{z3}$ show more interesting results. Starting with case Asym$_{z1}$, a very substantial increase in hours with both the capacity calculation and allocation risk is observed (+171.72%), which translates also in the substantial increase in curtailment by the capacity calculation (+540.3%) and allocation (+14.39%). The reason for this very substantial increase in curtailment by the capacity calculation is the following. First, it must be remembered that the maximum net position in the OBZ, which determines the curtailment by the capacity calculation, is inherently lower in this dual setup than in a triangle setup, since 1 out of 3 export directions in no longer available. However, doubling the transmission capacity towards zone 1 in case Asym$_{z1}$ does not significantly enlarge the FB domain. As shown in the extreme values validation (Section 4.6.2.2), in zone 1 there is an onshore CNE limiting the trade via the OBZ. This is observed in this case too, as the maximum flow on the DC line internal to the OBZ is 491.56 MWh. This resulted in the fact the maximum net position possible for the OBZ was 2186.596 MWh, primarily restricted by the onshore CNE in zone 1. Whenever wind production exceeds this maximum net position, corresponding to a capacity factor of roughly 0.73, curtailment by the capacity calculation occurred. Hence the substantial increase in curtailment by the capacity calculation (+540.3%).

The increase in curtailed power due to the capacity allocation volume risk is directly linked to the higher frequency of zero-price hours caused by renewable energy supply. This occurs because the hybrid is only connected to zones 1 and 3, with zone 3 experiencing more zero-priced hours due to its high renewable feed-in. This is evident from the price duration curve, which shows a substantial flat part at 0 €/MWh for zone 3, and the similarity between the price duration curves of the OBZ and zone 3. Additionally, zone 3's generation fleet consists largely of wind power (see Figure 17, Section 5.1.2), leading to a generation pattern similar to that of the OBZ. These factors result in fierce competition during high wind injection hours, causing the OWFs in the OBZ to be curtailed more frequently, thereby increasing the capacity allocation risk and the frequency of zero-price hours due to renewable energy supply.

Moving to case Asym$_{z3}$, where zone 3's OWF capacity and transmission capacity is doubled, something different happens. This case shows a decrease in hours with a volume risk (-9.05%), where hours with both curtailment by the capacity calculation and allocation decreased (-35.17%) and hours with only curtailment by the capacity allocation increased (+31.33%). This translates also in the reduced curtailment by the capacity calculation (-51.37%) but increased curtailment by the capacity allocation (+24.93%). The decrease in curtailment by the capacity calculation is caused since the additional transmission capacity to zone 3 now leads to a substantial increase of the maximum net position of the OBZ (3679.808 MWh), indicating that zone 3 can physically absorb additional generated wind power from the increased installed wind capacity. The downside, however, is that the increased transmission capacity to zone 3 also led to additional direct competition between the OBZ and zone 3. As mentioned, the large wind capacity in zone 3 and the focussed competition by definition of the dual hybrid led to the increase in the curtailment by the capacity allocation (+24.93%) for this case.

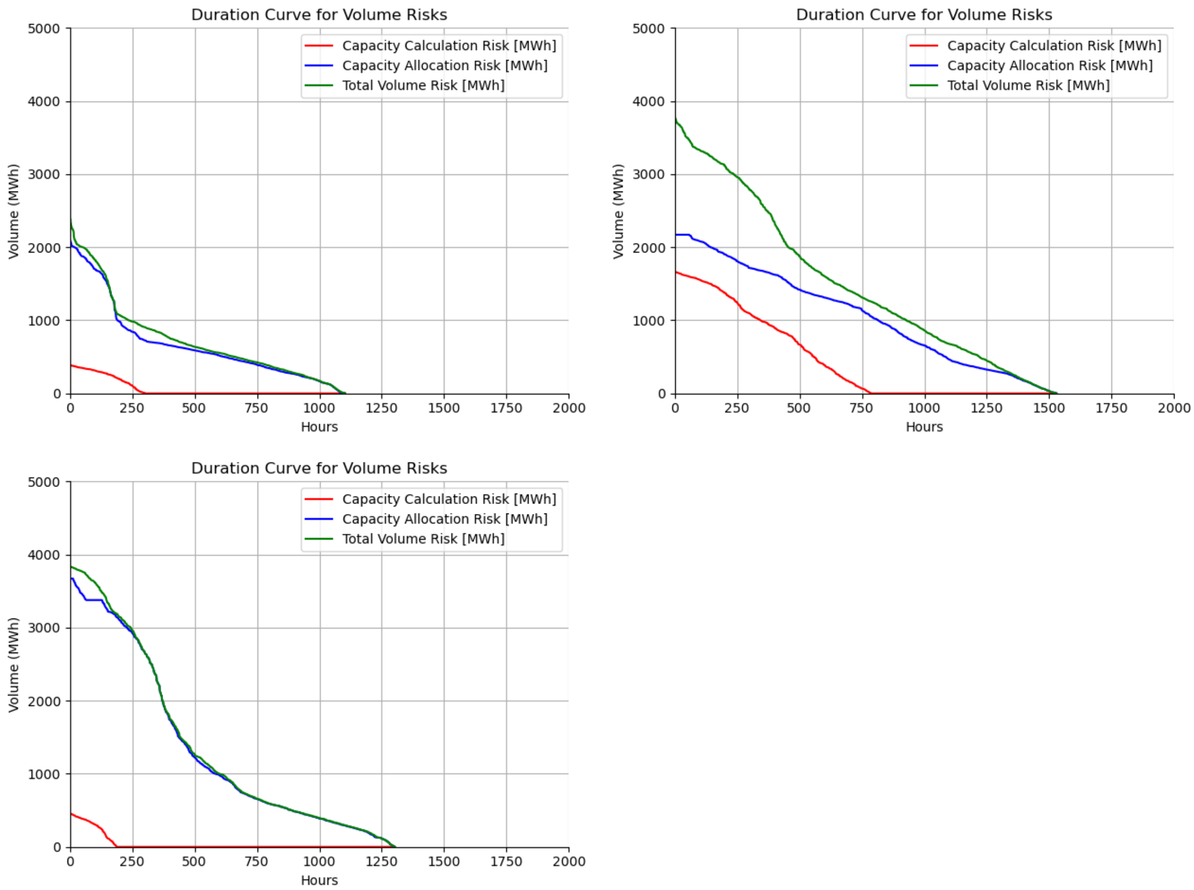


*Figure 39: Volume Risk Duration Curves for Case Group Offshore Grid Topology (Dual). Top left case Sym., top right case Asymz1 and bottom left case Asymz3.*

### 6.3.4 Interacting Price and Volume Risk

The results of the interacting price and volume risk (Table 22) confirm again that curtailment is primarily induced during zero-priced hours due to RES, reflecting the fierce competition for the scarce transmission capacity. While case Asym$_{z1}$ shows some correlation for volume risks occurring during price collapse hours, the magnitude of these volumes is negligible compared to the volumes curtailed during renewable priced hours.

*Table 22: Interacting Price and Volume Risk for the Case Group Offshore Grid Topology (Dual). The percentages represent the share of curtailed wind power during each of the price risk categories in which curtailment was observed.*

| Price Risk Hours | Volume Risk | Ref. | Sym | $\mathrm{Asym}_{z1}$ | $\mathrm{Asym}_{z3}$ |
|---|---|---|---|---|---|
| **Zero-Priced hours due to RES** | *Total Curtailment* | *99.95%* | *99.94%* | *99.14%* | *100.00%* |
| | Curtailed by Cap. Calc. | 7.16% | 6.22% | 29.72% | 2.92% |
| | Curtailed by Cap. All. | 92.79% | 93.72% | 69.43% | 97.08% |
| **Price Collapse hours** | *Total Curtailment* | *0.05%* | *0.06%* | *0.86%* | *0.00%* |
| | Curtailed by Cap. Calc. | 0.00% | 0.00% | 0.34% | 0.00% |
| | Curtailed by Cap. All. | 0.05% | 0.06% | 0.52% | 0.00% |

## 6.4 Case Group 3: Onshore Grid Attenuation

In this case group the onshore grid attenuation was subject to analysis where both outages the transmission lines directly at the landing point (LP) of the OBZ and outages of CNEs further onshore (on) were the parameters that have been varied. These parameters have been varied for the high-priced fossil dominated zone 1 (cases $\mathrm{Out}_{z1}^{LP}$ and $\mathrm{Out}_{z1}^{on}$) and for the low-priced wind dominated zone 3 (cases $\mathrm{Out}_{z3}^{LP}$ and $\mathrm{Out}_{z3}^{on}$). The box below shows the formulated hypothesis for this case group and the most notable results are discussed hereafter.

> ***H.3****: Onshore grid attenuations lead to a reduced export capability of the OBZ, increasing price collapse hours and curtailment by the capacity calculation, ultimately leading to lower revenues for OWFs.*

$\mathbf{Out}_{\mathbf{z1}}^{\mathbf{LP}}$: Revenues for the OBZ decreased (-20.25%) with a reduction in positive-priced wind exports (-16.55%). The outage of a line at the landing point of the OBZ directly reduced import capacity to this zone, whereby the OBZ was forced into increased competition with renewable-rich Zones 2 and 3. This led to reduced price collapse hours (-6.08%), increased zero-priced hours due to RES (+10.61%) and increased hours with curtailment by both the capacity calculation and allocation (+159.04%). Redispatch costs increased significantly (+468.2%) due to Zone 1's reliance on costly fossil generators and reduced import capability.

$\mathbf{Out}_{\mathbf{z3}}^{\mathbf{LP}}$: Revenues for the OBZ increased (+109.92%) due to a shift from zero-priced hours (-45.88%) o positive-priced wind exports (+67.44%). The significant reduction in physical import capacity to Zone 3, combined with zone 1's grid already limiting the OBZ's export capacity, reduced competition between the OBZ and this wind-dominated zone 3 and somewhat forced wind exports to Zone 2, resulting in higher electricity prices and increased revenues. Non-intuitive prices reflected the positive (or negative) value of alleviating (or stressing) Zone 3's grid. Increased curtailment by the capacity calculation (+262.26%) resulted from reduced physical import capacity to Zone 3, while reduced curtailment by the capacity allocation (-45.63%) was due to decreased competition between the OWFs in the OBZ and Zone 3's onshore wind generators.

$\mathbf{Out}_{\mathbf{z1}}^{\mathbf{on}}$: Revenues for the OBZ decreased (-41.21%) and positive-priced wind exports decreased (-30.96%) due to less price convergence hours and lower mean prices. A substantial increase in positive non-intuitive priced hours is observed due to power trades via the OBZ alleviating the stressed grid in zone 1. Negative (non-intuitive) electricity prices are observed due to the stress on Zone 1's restricted grid from the cheap wind imports via the OBZ, combined with high competition with zone 2 and 3 for transmission capacity during high renewable supply hours. Increased curtailment by the capacity allocation (+48.72%) and a reduction in total curtailment by the capacity calculation (-6.48%) were observed, as a results of intensified competition with zones 2 and 3. Notably, 36.78% of total curtailment took place during the negative-priced hours.

$\mathbf{Out_{z3}^{on}}$: Revenues increased (+79.27%) and positive-priced wind exports rose (+37.61%) with reduced zero-priced wind exports (-26.59%). The reduced import capacity to Zone 3 led to more stable prices and fewer zero-priced hours for the same reason as case $\mathrm{Out_{z3}^{LP}}$, albeit to a lesser extent. Comparing case $\mathrm{Out_{z3}^{on}}$ to case $\mathrm{Out_{z3}^{LP}}$, increased curtailment by the capacity calculation was unexpectedly higher (+687.49% vs. +262.26), while curtailment by the capacity allocation decreased to a smaller extent (-32.91% vs. -45.63%), due to increased competition with onshore wind generators in Zone 3, frequently pushing total curtailment beyond the OBZ's maximum net position.

## 6.4.1 General Results – Onshore Grid Attenuation

Since the main parameter varied in this case group, the outages of onshore AC lines, directly influences the maximum import capacity from the OBZ to the respective zones, it is first important to consider the changes in physical import capabilities of the onshore grids as this influences the commercial flows in the entire system, and thus the price and volume risks.

*Table 23: Maximum observed and average physical import capacity per zone. Results are from the net position maximization optimization problem (section 4.2.4.1).*

| | **Ref.** | | $\mathbf{Out_{z1}^{LP}}$ | | $\mathbf{Out_{z3}^{LP}}$ | | $\mathbf{Out_{z1}^{on}}$ | | $\mathbf{Out_{z3}^{on}}$ | |
|---|---|---|---|---|---|---|---|---|---|---|
| | *Max.* | *Avg.* | *Max.* | *Avg.* | *Max.* | *Avg.* | *Max.* | *Avg.* | *Max.* | *Avg.* |
| **Zone 1** | -686.6 | -676.2 | **-40%** | **-79%** | 0% | 0% | **+118%** | **-5%** | 0% | 0% |
| **Zone 2** | -1500 | -1106 | 0% | -1% | 0% | 3% | **+27%** | 0% | 0% | 3% |
| **Zone 3** | -1900 | -1554 | 0% | -2% | **-88%** | **-86%** | 0% | 1% | **-21%** | **-80%** |

From Table 23 it is evident that with AC line outages directly at the landing point from the OBZ, the import capacity of that zone decreases. Note that onshore grid in zone 1 is already restricted (see Section 4.6.2.2. and results reference case in Section 6.1), whereby the decrease in maximum import capacity for case $\mathrm{Out_{z3}^{LP}}$ is in absolute terms more significant than for case $\mathrm{Out_{z1}^{LP}}$. Put differently, an onshore grid attenuation at the landing point in a market zone already experiencing grid constraints has a lower effect on the total exporting capacity of the OBZ than an onshore grid attenuation at the landing point in a market zone without previous existing grid constraints.

The outage of an AC lines further onshore in zone 1 ($\mathrm{Out_{z1}^{on}}$) surprisingly could lead to additional imports (max net position observed +118%), but on average still leads to reduced importing capacity (-5%). Surprisingly, where previously zone 2 showed a maximum import capacity of 1500 MW, corresponding to full import from the OBZ and balanced import/export over the point-to-point interconnectors, the outage of the onshore AC line in zone 1 leads to additional import capacity over the point-to-point interconnectors from zone 1 to zone 2. The outage of an AC line further onshore in zone 3 ($\mathrm{Out_{z1}^{on}}$) leads to a substantial decrease in average maximum import capabilities to zone 3 (-80%).

The influence of these changed physical import capabilities per case on the price and volume risks is explained hereafter.

*Table 24: Percentual changes of the General Results with respect to the refence case for case Group Onshore Grid Attenuation.*

| | Ref. | $\mathrm{Out}_{z1}^{LP}$ | $\mathrm{Out}_{z3}^{LP}$ | $\mathrm{Out}_{z1}^{on}$ | $\mathrm{Out}_{z3}^{on}$ |
|---|---|---|---|---|---|
| **Total Revenue OWFs [M€]** | 15.386 | -20.25% | +125.23% | -42.24% | +79.27% |
| **Total Wind Export [GWh]** | 3085.924 | -24.01% | -15.25% | -22.06% | -9.23% |
| **Total Curtailment [GWh]** | 1520.542 | +48.72% | -23.57% | +44.76% | +18.74% |
| **Total Export at Zero-Price [GWh]** | 2251.727 | -26.77% | -45.88% | -28.67% | -26.59% |
| **Total Export at Positive Price [GWh]** | 834.196 | -16.55% | +67.44% | -30.96% | +37.61% |
| **Total Congestion Rent [M€]** | 141.547 | -30.74% | -20.91% | +17.36% | -13.30% |
| **Total Day-Ahead Cost [M€]** | 715.070 | +4.85% | -4.46% | +19.81% | +0.91% |
| **Total Redispatch Cost [M€]** | 12.748 | +468.2% | -35.72% | +248.7% | +0.91% |

A first observation for this case group, consistent with the **H.3**, is the change in total wind exports and curtailed wind power from the OBZ. Wind exports increased with 24.01%, 4.48%, 22.01% and 9.23% for cases $\mathrm{Out}_{z1}^{LP}$, $\mathrm{Out}_{z3}^{LP}$, $\mathrm{Out}_{z1}^{on}$ and $\mathrm{Out}_{z3}^{on}$, while total curtailed wind power decreased with -24.01%, -4.48%, -22.06% and -9.23%.

A second observation is that the outages in the higher priced, fossil-dominated importing zone 1 (cases $\mathrm{Out}_{z1}^{LP}$ and $\mathrm{Out}_{z1}^{on}$) led to reductions in revenues for the OBZ (-20.25% and -41.21%), whereas outages in the lower priced, renewable-dominated exporting zone 3 (cases $\mathrm{Out}_{z3}^{LP}$ and $\mathrm{Out}_{z3}^{on}$) led to increased revenues for the OBZ (+109.92% and +79.27%). This substantial increase in revenues is an unexpected result and urges deeper analysis.

A first aspect why these revenues substantially vary over these cases is that where outages in zone 1 (cases $\mathrm{Out}_{z1}^{LP}$ and $\mathrm{Out}_{z1}^{on}$) led to a decrease in exported wind power during positive-priced hours (-16.55% and -30.96%), outages in zone 3 (cases $\mathrm{Out}_{z3}^{LP}$ and $\mathrm{Out}_{z3}^{on}$) led to an increase in exported wind power during positive-priced hours (+67.44% and +37.61%). Additionally, all cases saw a substantial decrease in exported wind power during zero-priced hours, with the largest decrease observed for case $\mathrm{Out}_{z3}^{LP}$ (-45.88%). The changed price formation dynamics (further elaborate in next section), with a shift from exports during zero-priced hours to exports during positive priced hours, contributed to the increased revenues for the cases with an AC line outage in zone 1, aided with the more than doubled mean electricity price in the OBZ for the cases with outages in zone 3 (Table 25). The underlying cause for this shift from zero-priced hours to positive priced hours is the substantial reduction in the physical import capability of the grid in zone 3 (Table 23), aided with the onshore grid in zone 1 already being restricted, whereby the wind production in the OBZ was somewhat forced to be exported to zone 2. With zone 2 having primarily a large installed PV capacity (see Section 5.1.2), the OBZ could benefit from the reduced competition with wind dominated zone 3 to export to zone 2 during windy hours.

With respect to social welfare changes, the substantial increase in redispatch costs for cases $\mathrm{Out}_{z1}^{LP}$ (+468.2%) and $\mathrm{Out}_{z1}^{on}$ (+248.7%) stand out. Zone 1's reliance on costly fossil generators, combined with reduced import capability due to onshore CNE outages, significantly diminishes the ability to import cheap power from the OBZ or other zones via the OBZ. This increased reliance on expensive domestic generators for redispatch actions led to significantly higher redispatch costs.

## 6.4.2 Price Risk Results – Onshore Grid Attenuation

*Table 25: Price Statistics OBZ Case Group Onshore Grid Attenuation*

| | Ref. | $\mathrm{Out}_{z1}^{LP}$ | $\mathrm{Out}_{z3}^{LP}$ | $\mathrm{Out}_{z1}^{on}$ | $\mathrm{Out}_{z3}^{on}$ |
|---|---|---|---|---|---|
| **Mean Price** | 7.47 | 5.99 | 18.30 | 4.60 | 15.36 |
| **Std Dev** | 15.009 | 13.252 | 21.873 | 11.273 | 21.690 |
| **CoV** | 2.0100 | 2.2125 | 1.1955 | 2.4478 | 1.4117 |

Starting with the cases with outages in zone 1 ($\mathrm{Out}_{z1}^{LP}$ and $\mathrm{Out}_{z1}^{on}$), Table 25 shows a substantial decrease in the mean electricity price in the OBZ. Considering the frequency of price convergence hours (Figure 40, left), the lower mean prices for cases $\mathrm{Out}_{z1}^{LP}$ and $\mathrm{Out}_{z1}^{on}$ is explained as they see a decrease in price convergence to low (-2.32% and -16.89%) middle (-68.46% and -82.31%) priced hours, and no longer is the price in the OBZ converging to the higher priced zone (both -100%). Since the magnitudes of exported power during these price convergence hours shows similar reductions as the frequency of hours (Figure 40, right), the decreased revenue for these cases is the consequence, which was expected.

An unexpected result with regard to the price risks for the cases with outages in zone 1 is a decrease in frequency of price collapse hours (-6.08% and -7.77%), associated with reduced exports during these hours (-14.09 and 13.94%). For case $\mathrm{Out}_{z1}^{LP}$, the reduction in the frequency of price collapse hours was associated with an increase in zero-priced hours due to RES (+10.61%). This is the consequence of the direct reduction of the export capability form to OBZ towards zone 1 by outage of the AC line at the landing point, further forcing the OBZ in competition with onshore renewables from zone 2 and 3 (further substantiated in volume risk results). For case $\mathrm{Out}_{z1}^{on}$, the reduced frequency of price collapse hours (and reduced zero-priced hours due to RES (-3.58%)) is associated with a substantial increase in non-intuitive priced hours, further substantiated hereafter in subsection 6.4.2.1.

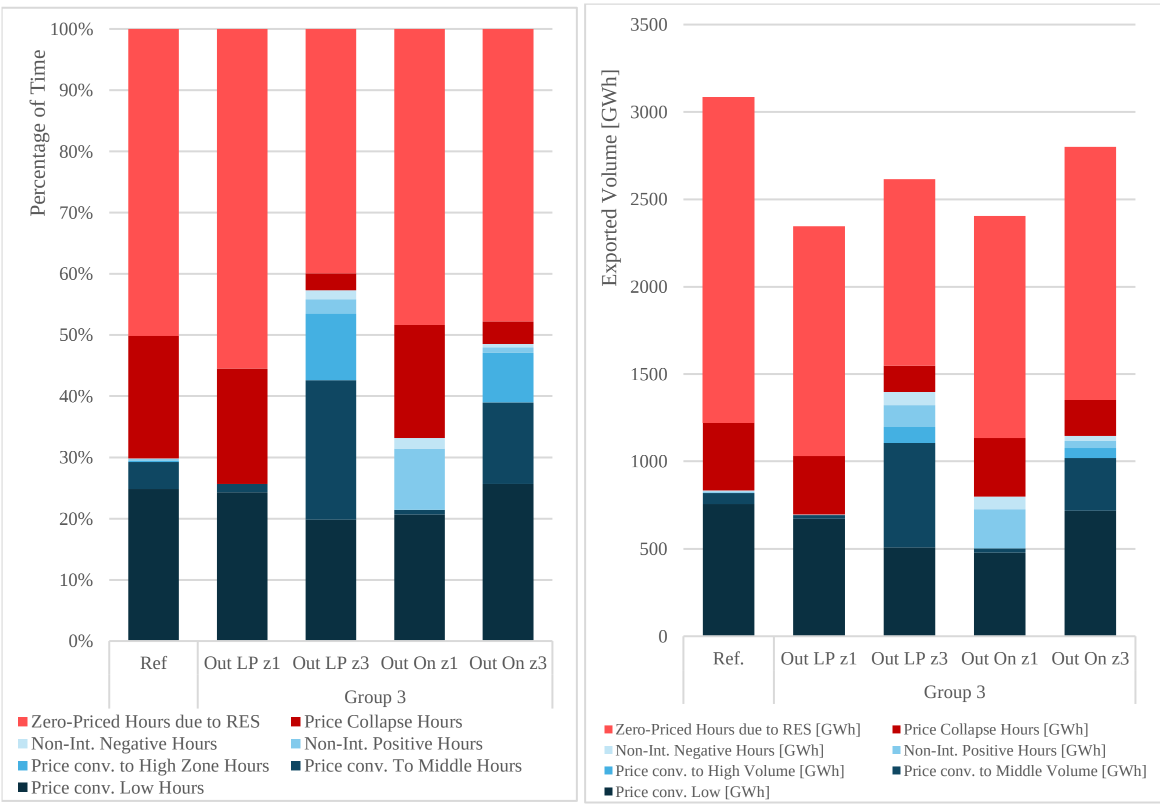


*Figure 40: Frequency (Left) and Magnitude (Right) of the Price Risks for Case Group Onshore Grid Attenuation*

Moving to the cases with outages in zone 3 ($\mathrm{Out}_{z3}^{LP}$ and $\mathrm{Out}_{z3}^{on}$), where the substantial increased revenues are observed, the mean electricity prices have more than doubled (Table 25) and the relative variance around that higher mean price (the CoV) is substantially lower, especially for case $\mathrm{Out}_{z3}^{LP}$, indicating more stable prices. The price duration curves of cases $\mathrm{Out}_{z3}^{LP}$ and $\mathrm{Out}_{z3}^{on}$ (Figure 41, graphs right-hand side) indicate less frequent zero-priced hours for the OBZ, evidenced by the first positive-priced hours in the red lines occurring further from the origin. Moreover, the price duration curves of the OBZ and zone 2 are almost identical in these two cases, indicating frequent convergence of OBZ prices to zone 2's price level. The substantial increase in hours with price convergence to middle (+413.1% and +202.3%) and high (+6260% and +4700%) priced zones, associated with extreme increases in exports during these hours (+819.0% and 361.1% for middle, +16769% and 10693% for high) further explain the increased revenues for cases $\mathrm{Out}_{z3}^{LP}$ and $\mathrm{Out}_{z3}^{on}$. The underlying reason for these observed effects is that outages in Zone 3 significantly reduced the export capacity to this zone by shrinking the FB domain, thereby lessening competition for the allocation of transmission capacity to Zones 1 and 2. This reduction in competition with wind-dominated Zone 3 allowed the OBZ to secure a more favourable position for exporting to Zone 2, leading to more price convergence hours and higher electricity prices and this increased revenues. Since the outage at the landing point in zone 3 reduced the physical import capacity more than an outage further onshore in zone 3 (Table 23), this effect is more pronounced for case $\mathrm{Out}_{z3}^{LP}$ than case $\mathrm{Out}_{z3}^{on}$, explaining the substantial increase in revenues (+125.23%).

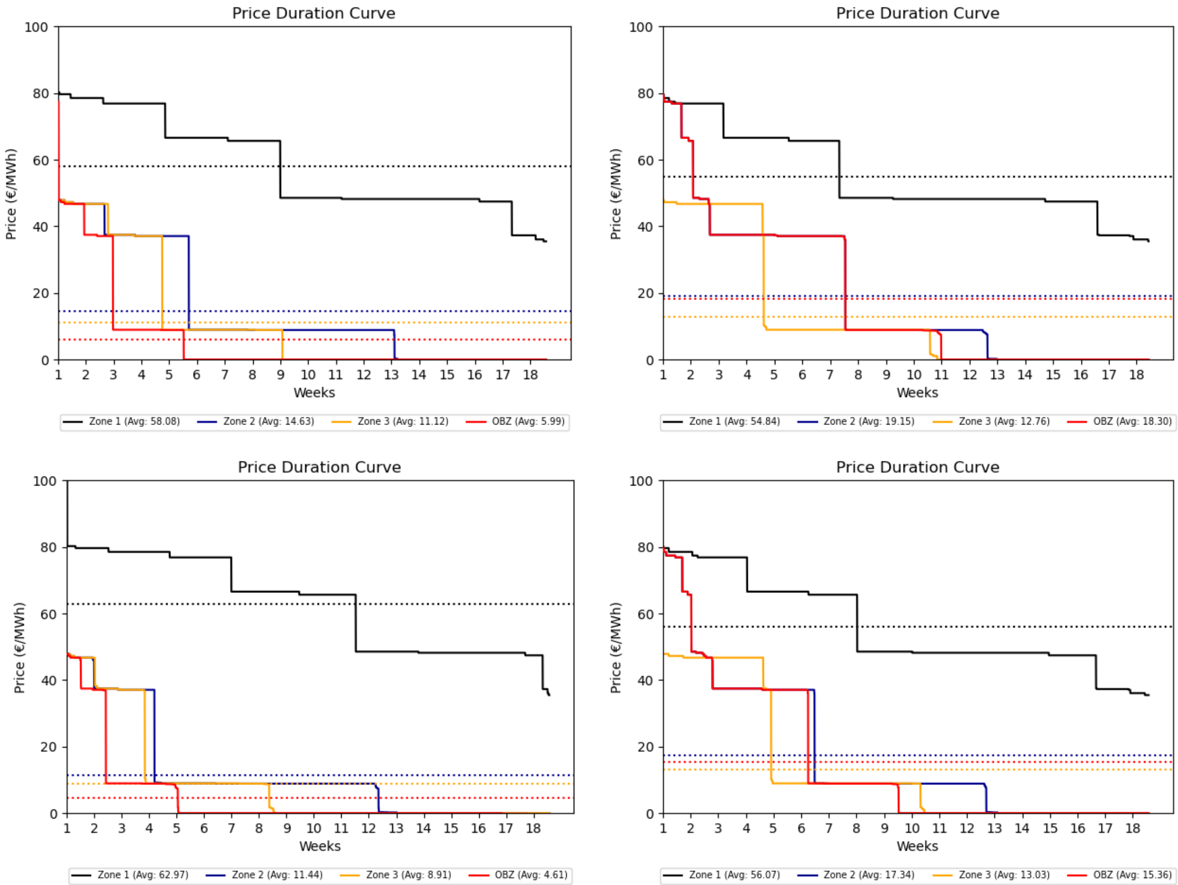


*Figure 41: Price Duration Curves for Case Group Onshore Grid Attenuation. Top left is case $Out_{z1}^{LP}$, top right case $Out_{z3}^{LP}$, bottom left case $Out_{z1}^{on}$ and bottom right case $Out_{z3}^{on}$.*

### 6.4.2.1 The role of non-intuitive price formation

The most outstanding price risk result for this case group is the role of the non-intuitive price formation (see Section 3.2.2 for definition). All cases, except case $\mathrm{Out}_{z1}^{LP}$, saw substantial increases in non-intuitive price formation. The reason why the outage at the landing point in zone 1 did not lead to increased non-intuitive price formation is because the onshore grid in zone 1 was already restricting the FB domain, whereby the only effect of the outage of this specific line is a direct reduction of the FB domain of the OBZ. For the other cases, different, more indirect mechanisms are taking place.

Among the three other cases, case $\text{Out}_{z1}^{on}$ experienced the largest increase in non-intuitive priced hours, with 12.33% of total wind exports occurring during these hours—9.29% during positive and 3.05% during negative non-intuitive priced hours. Given that Zone 1 has the costliest generators and its intra-zonal power exchanges are limited by the onshore CNE outage, reducing line loadings in Zone 1 by exporting power to the OBZ can achieve day-ahead generation cost reductions. This is evident from the large share of wind exports during positive-priced non-intuitive hours, indicating that power trades via the OBZ alleviate the stressed grid in Zone 1.

Additionally, this case is the only one where negative electricity prices in the OBZ have been observed, caused by the following combination of effects. First, the cheap wind imports from the OBZ to Zone 1 significantly reduce total generation costs in that zone, which are highly valued in the market clearing algorithm. Second, these imports simultaneously put additional stress on Zone 1's restricted grid. Third, during high renewable supply hours, when Zones 2 and 3 experience zero-prices, competition is at its highest for the allocation of transmission capacity to Zone 3. As a result, the market clearing allocates the cheap power from Zones 2 and 3 while partially curtailing the OWFs, further substantiated in Section 6.4.2.1. Meanwhile, the exports via the OBZ to Zone 1 continue to stress its grid. The consequence is that the OBZ sees negative electricity prices, reflecting the stress that the exports via the OBZ put on Zone 1's grid.

For case $\text{Out}_{z3}^{LP}$ 7.54% of total wind exports took place during non-intuitive priced hours, with 4.68% during positive and 2,89% during negative priced hours. The effect for case $\text{Out}_{z3}^{on}$ was less pronounced, with 2.5% of total exports taking placing during non-intuitive priced hours, 1.52% during positive and 0.98% during negative. The exports during positive non-intuitive priced hours for these cases reflect the value of unloading of the restricted onshore grid in zone 3 by the exports via the OBZ to zone 2 (see previous section). The negative non-intuitive prices for this case were never negative electricity prices, but merely lower (positive) observed electricity prices in the OBZ than any of the other bidding zones. This indicates that whenever zone 3, with its restricted onshore grid, saw positive prices, the wind exports from the OBZ contributed to the generation cost-reduction in this zone, while also stressing the grid, as reflected in the negative-non intuitive prices.

### 6.4.3 Volume Risk Results – Onshore Grid Attenuation

For the volume risk, all cases saw an increase in hours with curtailment (Figure 42, left).

Case $\text{Out}_{z1}^{LP}$ primarily saw an increase in hours with both curtailment by the capacity calculation and allocation (+50.76%), where the largest increase in curtailed volume was by the capacity calculation (+260.18%) and to a lesser extent by the capacity allocation (+32.41%). This was expected, as the outage on a CNE at the landing point directly reduced Zone 1's import capacity, leading to increased curtailment by the capacity calculation. The available wind power in the OBZ also faced increased competition with Zones 2 and 3 during high renewable hours, due to the reduced import capacity to zone 1, resulting in higher curtailment by the capacity allocation.

The onshore outage in zone 1 ($\text{Out}_{z1}^{on}$) saw a small increase in hours with curtailment by both the capacity calculation and allocation (+1.69%) and a larger increase in hours with only curtailment buy the capacity allocation (+44.88%), associated with reduced total curtailment by the capacity calculation (-6.48%) but increased curtailment by the capacity allocation (+48.72%). As shown in Table 23, the outage onshore in zone 1 on average leads to lower import capacity but could occasionally lead to additional maximum import capacity in specific hours. This reflects the increase in hours with curtailment by both the capacity calculation and allocation, while the total curtailment by the capacity calculation reduced: on average zone 1 could import less from the OBZ, but occasionally large imports are physically possible, whereby curtailment taking place during these hours is not attributed to the capacity calculation but rather to the capacity allocation. The increased curtailment by the capacity allocation reflects the intensified competition between the OWFs in the OBZ and zones 2 and 3 for the allocation of transmission capacity to the weaker grid in zone 1.

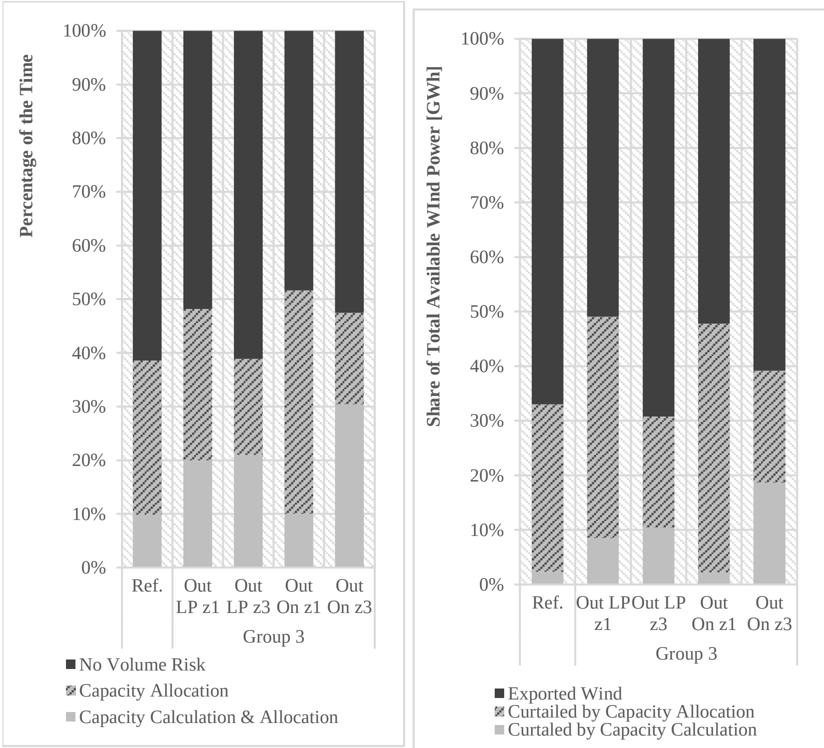

*Figure 42: Frequency (left) and Severity (right) of the Volume risk for Case Group 4*

Having an outage at the landing point of zone 3 ($\mathrm{Out}_{z3}^{LP}$) also led to a substantial increase in hours with both curtailment by the capacity calculation and allocation (+53.15%), while hours with only curtailment by the capacity allocation reduced (-37.81%). This is also reflected in the increased curtailment by the capacity calculation (+262.26%) and decreased curtailment by the capacity allocation (-45.63%). The increased curtailment by the capacity calculation is the result of the reduced physical import capacity to zone 3. The decreased curtailment by the capacity allocation underlines again the reduced competition with wind-dominated zone 3.

Comparing case $\mathrm{Out}_{z3}^{LP}$ with case $\mathrm{Out}_{z3}^{on}$ gives yields somewhat surprising results. The case with an onshore outage in Zone 3 ($\mathrm{Out}_{z3}^{on}$) saw a significant increase in hours with curtailment by both the capacity calculation and allocation (+67.63%), along with a substantial rise in curtailment by the capacity calculation (+687.49%) and a decrease in curtailment by the capacity allocation (-32.91%). Given that the physical import capacity to Zone 1 is more restricted for $\mathrm{Out}_{z3}^{LP}$ than for $\mathrm{Out}_{z3}^{on}$ (Table 23), it was expected that the former would experience higher curtailed volumes by the capacity calculation. However, the competition between the OBZ and Zone 3 for the allocation of scarce transmission capacity to Zones 1 and 2 is less reduced in $\mathrm{Out}_{z3}^{on}$ than in $\mathrm{Out}_{z3}^{LP}$, leading to higher total curtailed volumes within individual hours. During hours where $\mathrm{Out}_{z3}^{LP}$ experienced only curtailment by the capacity allocation, the additional competition with wind generators in Zone 3 resulted in more curtailment for $\mathrm{Out}_{z3}^{on}$. This increased competition frequently pushed total curtailment beyond the maximum net position of the OBZ, resulting in more curtailment attributed to the capacity calculation.

Thus, even though the FB domain in the OBZ is on average larger for $\mathrm{Out}_{z3}^{on}$ than for $\mathrm{Out}_{z3}^{LP}$ (yet still smaller than in the reference case), the added competition with onshore generators in Zone 3 for $\mathrm{Out}_{z3}^{on}$ led to more frequent and higher magnitude curtailment, often exceeding the maximum net position of the OBZ, resulting in increased curtailment by the capacity calculation.

### 6.4.4 Interacting Price and Volume Risk

The most notable results of the interacting price and volume risk for this case group is that for case $\mathrm{Out}_{z1}^{on}$ 36.78% of total curtailment took place during non-intuitive priced hours, with most volume curtailed by the capacity allocation. Additionally, a reduction in curtailment during zero-priced hours due to RES is observed (62.96% instead of 99.95%), indicating that the curtailment during non-intuitive priced hours would otherwise have taken place during hours with high renewable competition. These curtailments thus took place during the unique observed negative priced hours (see Section 6.4.2.1.).

*Table 26: Interacting Price and Volume Risk for the Case Group Offshore Grid Topology (Triangular). The percentages represent the share of curtailed wind power during each of the price risk categories in which curtailment was observed.*

| Price Risk Hours | Volume Risk | Ref. | $\mathbf{Out}_{z1}^{\mathbf{LP}}$ | $\mathbf{Out}_{z3}^{\mathbf{LP}}$ | $\mathbf{Out}_{z1}^{on}$ | $\mathbf{Out}_{z3}^{on}$ |
|---|---|---|---|---|---|---|
| **Zero-Priced hours due to RES** | *Total Curtailment* | *99.95%* | *99.92%* | *97.60%* | *62.96%* | *97.18%* |
| | Curtailed by Cap. Calc. | 7.16% | 17.30% | 31.80% | 0.94% | 44.83% |
| | Curtailed by Cap. All. | 92.79% | 82.62% | 65.80% | 62.02% | 52.36% |
| **Price Collapse hours** | *Total Curtailment* | *0.05%* | *0.05%* | *2.36%* | *0.20%* | *2.78%* |
| | Curtailed by Cap. Calc. | 0.00% | 0.04% | 2.13% | 0.00% | 2.68% |
| | Curtailed by Cap. All. | 0.05% | 0.00% | 0.22% | 0.20% | 0.10% |
| **Non-intuitive Priced hours** | *Total Curtailment* | *0.00%* | *0.00%* | *0.00%* | *36.78%* | *0.00%* |
| | Curtailed by Cap. Calc. | 0.00% | 0.00% | 0.00% | 3.69% | 0.00% |
| | Curtailed by Cap. All. | 0.00% | 0.00% | 0.00% | 33.10% | 0.00% |

## 6.5 Case Group 4: Generation Mix

In this case group the generation mix of the onshore zones was subject to analysis where the share of renewable generators in the generation mix was the parameter that has been varied. Where the reference case included a high share of renewables in the generation mix, the proportion of renewable energy sources in the generation mix were reduced for case Transition Mix (Trans) and substantially reduced for case Fossil Mix (Fos) (see Section 5.2.4). The box below shows the formulated hypothesis for this case group and the most notable results are discussed hereafter.

***H.4:*** *Decreasing the proportion of renewable energy sources in the generation mix leads to higher and more stable electricity prices, fewer zero-priced hours, decreased curtailment by the capacity allocation, leading to increased exports and higher revenues for OWFs.*

The results show that, in line with the hypothesis, cases Trans and Fos experienced increased total wind exports (+13.29% and +44.44%) and decreased total curtailment (-26.98% and -90.18%), primarily due to the substantial decrease in curtailment by the capacity allocation (-30.17% and -98.88%). The increased total exports during positive prices (+52.03% and +228.8%) due to increased price convergence hours, along with higher and less volatile electricity prices in the OBZ, led to substantial revenue increases (+56.17% and +431.1%). A shift from zero prices due to RES to price collapses occurred because the reduced renewable capacity caused the market clearing to favour OWFs in the OBZ, leading to wind exports up to the maximum export capacity, resulting in price collapses during high wind hours. These price collapse hours were always associated with curtailment, mostly by the capacity calculation, substantiating the described interacting price and volume risk in the literature.

### 6.5.1 General Results – Generation Mix

The first observation for this case group, which is in line with hypothesis **H.4**, is the increased revenues with decreased installed RES capacity for cases Trans and Fos (+56.17% and +431.1%), while wind total wind exports increased (+13.29% and +44.44%) and total curtailment decreased (-26.98% and -90.18%). Comparing the curtailed power to total potential wind generation, the decrease in curtailment is more evident with decreasing shares of renewable generation. In the reference case, 33% of total potential wind generation was curtailed, reducing to 24.10% for case Trans and to 3.24% for case Fos.

Moreover, the generated wind power in the OBZ was to a larger extend exported at positive prices (+52.03% and +228.75%) and to a smaller extend exported at zero prices (-1.06% and -23.85%), further contributing to the increased profitability for the OWF operators.

With respect to changes in social welfare, what stands out is that case Trans sees a reduction in DA generation cost (-8.99%) while for case Fos the DA cost more than double (+108%). The substantial increase in DA generator cost in a system dominated by fossil generators (case Fos), is an expected result. The decrease in DA generation cost for case Trans, while having less cheap renewables compared to the reference case, is because during non-renewable hours case Trans had additional cheaper coal and lignite generators at its disposal (Table 11, Section 5.2.4). The decrease in redispatch costs with reduced renewable capacity (-21.55% and -92.20% for cases Trans and Fos) indicates that the inherent intermittency of renewables necessitates more redispatch actions, primarily due to the different geographical locations and distances to demand centres of renewables compared to fossil generators.

*Table 27: Percentual changes of the General Results with respect to the refence case for Case Group Generation Mix.*

| | **Renewable Mix** (Reference Case) | **Transition Mix** | **Fossil Mix** |
|---|---|---|---|
| **Total Revenue OWFs [M€]** | 15.386 | +56.17% | +431.1% |
| **Total Wind Export [GWh]** | 3085.924 | +13.29% | +44.44% |
| **Total Curtailment [GWh]** | 1520.542 | -26.98% | -90.18% |
| **Export at Zero-Price [GWh]** | 2251.727 | -1.06% | -23.85% |
| **Export at Positive Price [GWh]** | 834.196 | +52.03% | +228.8% |
| **Total Congestion Rent [M€]** | 141.547 | -28.85% | -4.13% |
| **Total Day-Ahead Cost [M€]** | 715.070 | -8.99% | +103% |
| **Total Redispatch Cost [M€]** | 12.748 | -21.55% | -92.20% |

## 6.5.2 Price Risk Results – Generation Mix

Price statistics in Table 28 confirm the expectations that decreased proportions of renewable energy sources lead to higher and more stable prices, visible in the increased mean price for cases Trans and Fos and the lower relative variability around this mean price (CoV).

*Table 28: Price Statistics OBZ Case Group Generation Mix.*

| | **Ref.** | **Trans.** | **Fos.** |
|---|---|---|---|
| **Mean Price** | 7.47 | 9.18 | 19.02 |
| **Std Dev** | 15.009 | 18.806 | 16.503 |
| **CoV** | 2.0100 | 1.7221 | 0.8678 |

Comparing the price duration curves of the Transition Mix and the Fossil Mix (Figure 43) shows that as renewable energy sources decrease in the generation mix, the price levels in zone 2, zone 3, and the OBZ are zero for a larger portion of time, as evidenced by the rightward shift of the curves. In the Transition Mix, the OBZ and zones 2 and 3 frequently experiences zero-priced hours, suggesting the possibility of both zero-priced hours due to renewable energy saturation and price-collapses in the OBZ. What stands out for the Fossil Mix is that the OBZ, zone 2 and zone 3 show very similar price duration curves with higher average mean prices, indicating high price convergence of the OBZ to these two zones. The increase for case Trans and Fos in price convergence hours (Figure 43 left) and wind exports during price convergence hours (Figure 44 right) substantiate this observation.

Regarding the price risk results (Figure 44), the frequency of zero-priced hours due to RES decreased for cases Trans (-17.84%) and Fos (-99.80%), aligning with the substantial reduction in renewables in the generation mix. However, an increase in price collapse hours for cases Trans (+5.91%) and Fos (+98.65%) is observed, along with higher exported magnitudes during these hours (+11.87% and +338.31%). This significant increase in price collapse hours, particularly for the Fossil Mix, indicates that the market clearing allocates cheap wind power from the OBZ up to its maximum export capacity. Previously, the OBZ competed with onshore generators, resulting in higher zero-priced hours due to RES. Now, the OWFs in the OBZ are structurally favoured, leading to a substantial increase in total

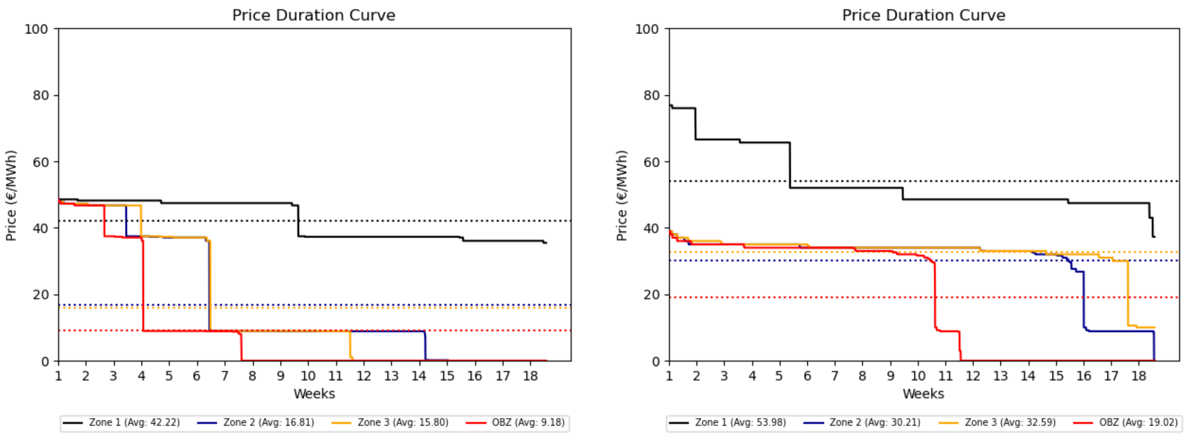


*Figure 43: Price Duration Curve of Transition Mix (Left) and Fossil Mix (Right).*

wind exports (Table 28). Nevertheless, during high wind hours (exceeding a capacity factor of 0.839, see Section 4.6.2.2), the export capacity (i.e. FB domain) of the OBZ remains restricted, resulting in price collapses. These price collapses are associated with curtailment by the capacity calculation (see Section 6.5.4).

Another notable result is the substantial increase in the frequency of non-intuitive priced hours, particularly negative non-intuitive priced hours, for cases Trans (+900%) and Fos (+3350%), along with a significant rise in exported power during these hours (+997% and +3802%). This indicates that the market clearing continues to allocate transmission capacity to the OWFs in the OBZ due to the availability of cheap wind power. However, this allocation adds stress to the onshore grids, resulting in negative non-intuitive prices.

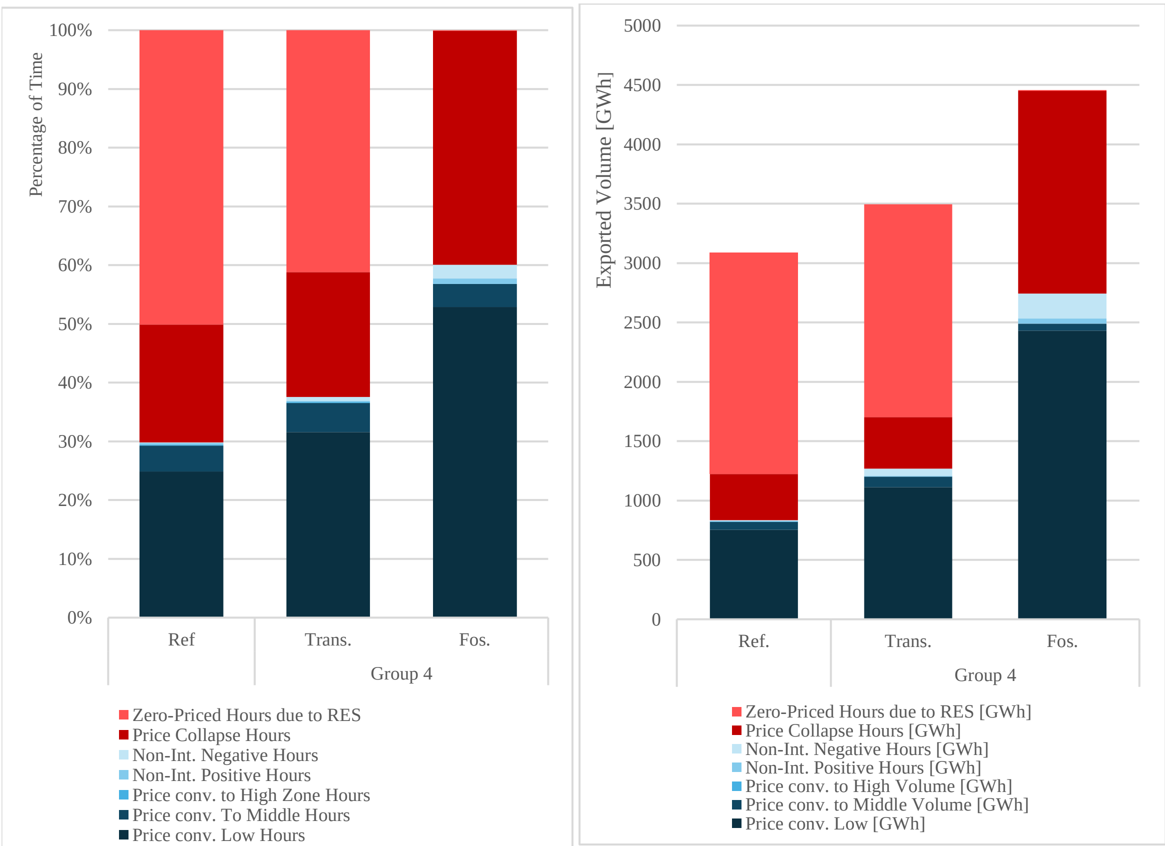


*Figure 44: Frequency (Left) and Magnitude (Right) of the Price Risks for Case Group Generation Mix.*

### 6.5.3 Volume Risk Results - Generation Mix

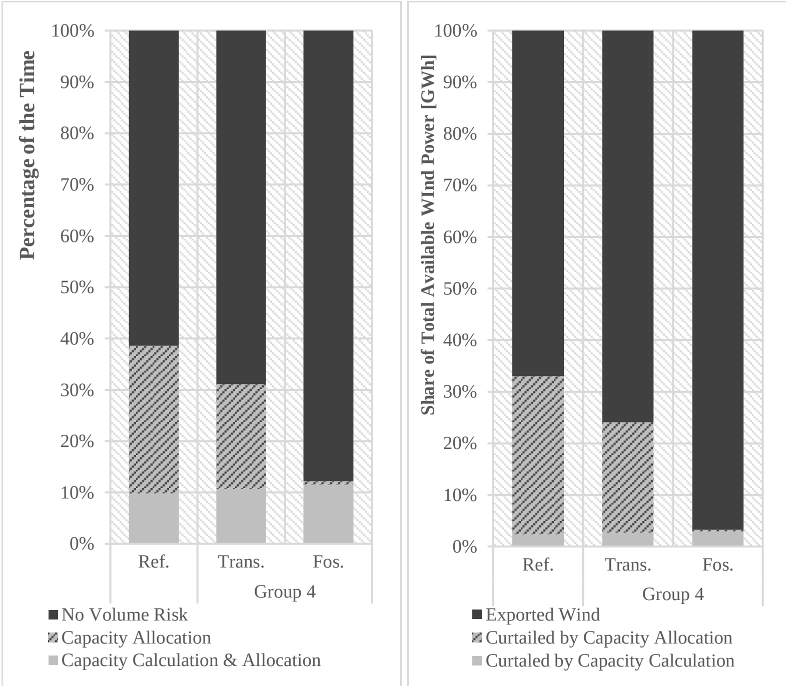


*Figure 45: Frequency (left) and Severity (right) of Volume Risk Case Group Generation Mix.*

As expected, the decreasing proportion of renewable energy sources in the generation mix leads to less volume risk hours, where case Trans saw an increase of 12.19% and case Fos of 42.91% in frequency of hours without a volume risk. Of the hours with a volume risk, as expected, the hours with only curtailment by the capacity allocation decreased for case Trans (-29.09%) and substantially for case Fos (-97.64%), also visible in the decrease in the volumes curtailed by the capacity allocation (-30.17% and -98.88%). This clearly indicates that with the absence of redundant renewables in the entire system, the market clearing favours the cheap wind power in the OBZ whereby the OWFs are able to export more wind power (at positive prices), increasing revenues substantially.

Notably, the quantity of wind power curtailed by the capacity calculation remains relatively consistent across varying generation mixes. This consistency is expected, as curtailment by the capacity calculation occurs when available wind generation exceeds the grid's maximum commercial export capacity, determined by the grid's physical characteristics rather than the generation mix. Changes in curtailment observed are due to varying reference flows calculated during the D-2 base case nodal clearing, which influence the RAM values in the optimisation determining the maximum net position of the OBZ, as generators are located on different nodes with different capacities. The volume duration curves confirm the substantial reduction curtailment the capacity allocation. In a more fossil-dominated system, wind

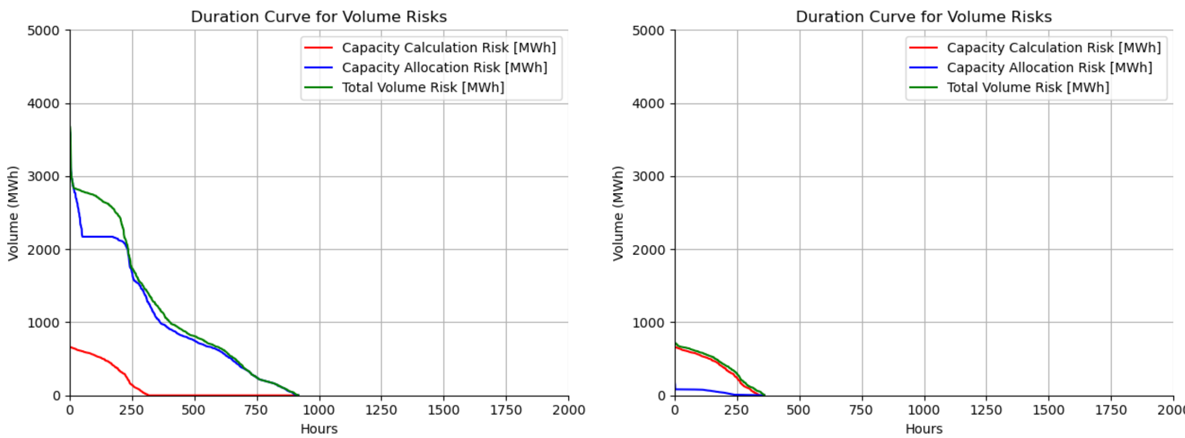


*Figure 46: Volume Risk Duration Curve of cases Transition Mix (left) and Fossil Mix (right).*

power is primarily curtailed due to the onshore grid's inability to absorb all wind power from the OBZ. In a more renewable-dominated system, wind power is curtailed primarily due to a higher welfare-generating market clearing combination, which partially reduces the available transmission capacity for the OBZ's generated wind power.

### 6.5.4 Interacting Price and Volume Risk

Table 29 confirms that for case Fos, nearly all curtailment occurred during price collapse hours and was primarily due to the capacity calculation. This suggests that the interacting price and volume risk for case Fos aligns more closely with the risks described in the literature than it does for the reference case (see Section 6.1.5).

*Table 29: Interacting Price and Volume Risk for the Case Group Generation Mix. The percentages represent the share of curtailed wind power during each of the price risk categories in which curtailment was observed.*

| Price Risk Hours | Volume Risk | Ref. | Trans | Fos |
|---|---|---|---|---|
| **Zero-Priced hours due to RES** | *Total Curtailment* | *99.95%* | *99.85%* | *0.80%* |
| | Curtailed by Cap. Calc. | 7.16% | 11.17% | 0.46% |
| | Curtailed by Cap. All. | 92.79% | 88.68% | 0.33% |
| **Price Collapse hours** | *Total Curtailment* | *0.05%* | *0.09%* | *99.20%* |
| | Curtailed by Cap. Calc. | 0.00% | 0.04% | 88.92% |
| | Curtailed by Cap. All. | 0.05% | 0.05% | 10.28% |

## 6.6 Case Group 5: Hydrogen Production

In this case group the flexible demand agents in the form of electrolysers as technological risk mitigation measure were subject to analysis where location of the electrolysers and their Willingness-to-Pay for electricity were the parameters caried. Four cases have been simulated with decreasing WTPs where electrolysers were placed offshore in the OBZ (cases $\mathrm{H2}_1^{\mathrm{off}}$, $\mathrm{H2}_2^{\mathrm{off}}$, $\mathrm{H2}_3^{\mathrm{off}}$ and $\mathrm{H2}_4^{\mathrm{off}}$) and two cases have been simulated with electrolysers placed at the landing point of the OBZ in zone 1 (case $\mathrm{H2}_{\mathrm{z1}}^{\mathrm{on}}$) and zone 3 (case $\mathrm{H2}_{\mathrm{z3}}^{\mathrm{on}}$) (see Section 5.2.5). The box below shows the formulated hypothesis for this case group and the most notable results are discussed hereafter.

> ***H.5****: Implementing electrolysers increase average electricity prices and reduce the price collapse risk, while wind exports are enhanced and curtailment decreased, ultimately leading to higher revenues for the OWFs.*

Overall, the results of this case group analysis confirm the hypotheses. For the offshore electrolyser cases OBZ ($\mathrm{H2}_1^{\mathrm{off}}$, $\mathrm{H2}_2^{\mathrm{off}}$, $\mathrm{H2}_3^{\mathrm{off}}$ and $\mathrm{H2}_4^{\mathrm{off}}$), wind exports increased by 4.88% to 4.99% while curtailment decreased by 9.90% to 10.13%. These changes, coupled with a substantial increase in wind power exports during positive-priced hours (+66.76% to +66.89%) and a decrease in zero-priced hours (-17.89% to -18.08%), led to significant revenue increases for OWFs, ranging from +71.26% to +108.11%. The offshore electrolysers also drove up the average electricity prices and reduced price volatility in the OBZ, with price convergence to the lowest-priced zone occurring 46.58% to 47.36% of the time. Price collapse risk was almost entirely mitigated, with frequency reductions of 98.28% to 98.31% and magnitude reductions of 97.13% to 97.47%. Additionally, the frequency of zero-priced hours due to RES decreased by 6.96% to 7.09%.

For the onshore electrolyser cases, there was a notable difference in outcomes between cases $\mathrm{H2}_{\mathrm{z1}}^{\mathrm{on}}$ and $\mathrm{H2}_{\mathrm{z3}}^{\mathrm{on}}$. Despite the limited electrolyser dispatch in case $\mathrm{H2}_{\mathrm{z1}}^{\mathrm{on}}$ (2% of time at FLH), decrease in volume risk hours (-6.58%) and less curtailment by both capacity calculation (-23.40%) and allocation (-

10.30%) were observed due to the 750 MW electrolyser increasing direct import capacity and reducing competition with onshore renewables. Nevertheless, revenues decreased (-13.83%) due to a shift from exports at positive prices (-3.96%) to exports at zero-prices (+9.05%), together with a lower mean price.

Conversely, the $H2_{z3}^{on}$ case saw a significant revenue increase (+61.70%), with the highest wind exports (+37.37%) and the least curtailment (-75.84%) of all cases. This case also completely mitigated the capacity calculation risk, attributing all remaining curtailment to the capacity allocation. Moreover, this case completely mitigated price collapse hours because the additional demand from the electrolyser in Zone 3 absorbed excess wind power, shifting the competition with Zone 3 from exporting via the OBZ to importing from the OBZ. This substantially reduced curtailment and kept the remaining curtailed volumes below the OBZ's maximum net position, thus avoiding curtailment by the capacity calculation and reducing curtailment by the capacity allocation. Additionally, increased price convergence to low (+26.98%), middle (+1001.54%), and high-priced zones (+20%), together with higher mean prices further increased revenue.

## 6.6.1 General Results – Hydrogen Production

Table 31 presents the general results for this case group. Firs the general results for the offshore electrolyser cases are discussed, thereafter for the onshore electrolyser cases.

*Table 31: Percentual changes of the General Results with respect to the refence case for Case Group Hydrogen Production.*

| | Ref. | $H2_1^{off}$ | $H2_2^{off}$ | $H2_3^{off}$ | $H2_4^{off}$ | $H2_{z1}^{on}$ | $H2z_3^{on}$ |
|---|---|---|---|---|---|---|---|
| **Total Revenue OWFs [M€]** | 15.386 | +108.1% | +97.24% | +84.29% | +71.26% | -13.83% | +61.70% |
| **Total Wind Export [GWh]** | 3085.924 | +4.99% | +4.91% | +4.89% | +4.88% | +5.54% | +37.37% |
| **Total Curtailment [GWh]** | 1520.542 | -10.13% | -9.96% | -9.93% | -9.90% | -11.24% | -75.84% |
| **Total Export at Zero-Price [GWh]** | 2251.727 | -17.89% | -18.04% | -18.08% | -18.08% | +9.05% | +35.69% |
| **Total Export at Positive Price [GWh]** | 834.196 | +66.76% | +66.85% | +66.89% | +66.85% | -3.96% | +41.91% |
| **Total Congestion Rent [M€]** | 141.547 | -23.30% | -21.27% | -20.16% | -18.99% | -8.18% | -7.54% |
| **Total Day-Ahead Cost [M€]** | 715.070 | -9.19% | -6.56% | -4.21% | -1.87% | -0.29% | -8.79% |
| **Total Redispatch Cost [M€]** | 12.748 | +51.09% | +41.99% | +42.58% | +42.26% | +55.27% | +46.77% |

The first observation that stands out is that for all 4 cases with offshore hydrogen production, cases $H2_1^{off}$, $H2_2^{off}$, $H2_3^{off}$ and $H2_4^{off}$, the total wind exports increased (+4,99%, +4.91%, +4.89% and +4.88%) and the total curtailment decreased (-10.13%, -9.96%, -9.93% and -9.90%). Additionally, less wind power was exported during zero-priced hours (-17.89%, -18.04%, -18.08% and -18.08%) and more wind was exported during positive-priced hours (+66.76%, +66.85%, +66.89% and +66.85%), which together resulted in substantial increases in revenues for the OWFs (+108.11%, +97.24%, +84.29% and +71.26%) for cases $H2_1^{off}$, $H2_2^{off}$, $H2_3^{off}$ and $H2_4^{off}$.

*Table 30: Percentage of Full Load Hours in simulated time.*

| Case | $El.^{z1}$ | $El.^{z2}$ | $El.^{z3}$ |
|---|---|---|---|
| $H2_1^{off}$ | 83.50% | 80.15% | 82.35% |
| $H2_2^{off}$ | 67.07% | 68.70% | 65.51% |
| $H2_3^{off}$ | 67.07% | 68.56% | 65.68% |
| $H2_4^{off}$ | 67.04% | 68.60% | 65.58% |
| $H2_{z1}^{on}$ | 2.03% | n.a. | n.a. |
| $H2_{z3}^{on}$ | n.a. | n.a. | 78.79% |

Looking at the number of Full Load Hours to assess whether the operation of the electrolysers makes sense, the results are also positive as even for the case with the lowest WTP for electricity (case $H2_4^{off}$ with WTP = 10.94 €/MWh), the lowest observed operation is for the electrolyser located closest to zone 3 with 65.58% of the time operating at full load.

Regarding the onshore electrolysers, there is a substantial difference in the results observable between the two cases $H2_{z1}^{on}$ and $H2_{z3}^{on}$. For both cases $H2_{z1}^{on}$ and $H2_{z3}^{on}$ the total exported wind power increased (+5.54% and +37.37%) and total curtailment decreased (-11.24% and 75.84%). However, in case $H2_{z1}^{on}$ the exported wind at positive prices decreased (-3.96%) while for case $H2_{z3}^{on}$ it increased substantially

(+41.91%), resulting in a revenue decrease for the former (-13.83%) and a revenue increase for the latter (+61.70%). Looking at the Full Load Hours of these cases, it becomes clear that the electrolyser in zone 1 (El.$^{z1}$) in case $\mathrm{H2}_{z1}^{on}$ only operated at full load for 2.0% of the time. The reason why is due to its WTP being too low with respect to the electricity prices in zone 1 (see next section). On the other hand, the electrolyser in zone 3 (El.$^{z3}$) in case $\mathrm{H2}_{z3}^{on}$ operated for 78.79% of the time at full load, explaining the substantial difference between the two onshore cases.

Moreover, case $\mathrm{H2}_{z3}^{on}$ sees by far the most exported wind power of all cases in this case group and the least curtailment. Considering also the lower DA generation costs while OWF operators see increased revenue, this case seems to be beneficial for both a society's perspective (most emission-free wind injection and low DA generation cost) and for the wind farm owners. It does come at a small decrease in congestion rents for the TSOs, however (-7.54%).

Interesting to see is that with the placement of the electrolyser in zone 1 (case $\mathrm{H2}_{z1}^{on}$) wind exports did increase compared to the reference case, but a shift is observed from power being exported during positive hours to power being exported during zero-priced hours, resulting in the lower revenues in this case. Thus, despite the electrolyser being operational during small parts of the time (2.03%), it reduced revenues for the OWFs substantially (-13.83%).

While all cases led to decreased DA generation costs, the congestion rents decreased and the redispatch costs increased, indicating that implementing electrolysers in the system might lead to a shift in social-welfare distribution.

## 6.6.2 Price Risk Results – Hydrogen Production

*Table 32: Price Statistics OBZ Case Group Hydrogen Production.*

| | Ref. | $\mathrm{H2}_1^{off}$ | $\mathrm{H2}_1^{off}$ | $\mathrm{H2}_3^{off}$ | $\mathrm{H2}_4^{off}$ | $\mathrm{H2}_1^{on}$ | $\mathrm{H2}_2^{on}$ |
|---|---|---|---|---|---|---|---|
| **Mean Price** | 7.47 | 15.57 | 14.84 | 14.09 | 13.34 | 6.10 | 11.36 |
| **Std Dev** | 15.009 | 19.172 | 18.224 | 17.680 | 17.570 | 13.272 | 17.762 |
| **CoV** | 2.0100 | 1.2316 | 1.2282 | 1.2553 | 1.3170 | 2.1756 | 1.5640 |

Looking at the price statistics of the offshore electrolyser cases (Table 32), it is clear that the offshore electrolysers both drive up the price and aid in reducing the price volatility in the OBZ, since the CoVs for all these cases is substantially lower than in the reference case. From the price duration curves (Figure 48) it can be observed that the average price in the OBZ is almost identical to the average price in zone 3. Additionally, the price duration curves of the OBZ and zone 3 show similar patterns as their curves are almost identical. This points to the fact that the OBZ's prices are primarily converging to zone 3.

The price risk results (Figure 47) confirm this price convergence pattern. Of the simulated hours, cases $\mathrm{H2}_1^{off}$, $\mathrm{H2}_2^{off}$, $\mathrm{H2}_3^{off}$ and $\mathrm{H2}_4^{off}$ showed 46.58%, 47.29%, 47.36% and 47.36% of the time price convergence to the lowest priced zone. Subsequently, the volumes of wind power exported during these hours also increased compared to the reference case (+70.31%, +71.65%, +72.06% and +72.06%). Moreover, the price collapse risk is almost completely mitigated for these cases, with frequency reductions of -98.28%, -98.22%, -98.32% and -98.31% and magnitude reductions of -97.13%, -97.13%, -97.47% and -97.30% for cases $\mathrm{H2}_1^{off}$, $\mathrm{H2}_2^{off}$, $\mathrm{H2}_3^{off}$ and $\mathrm{H2}_4^{off}$ compared to the reference case. There remain zero-priced hours due to high renewable supply, but the frequency these hours occur are reduced ( -6.96%, -7.64%, -7.16% and -7.09%), as are the quantities exported during these hours (-1.09%, -1.29%, -1.31% and -1.31%) compared to the reference case.

The shift from price collapse hours to price convergence hours (particularly to Zone 3) is due to increased local consumption in the OBZ, which prevents total exports from reaching the point where export capacity is restricted by the onshore grids, thus avoiding price collapses. This leaves more room

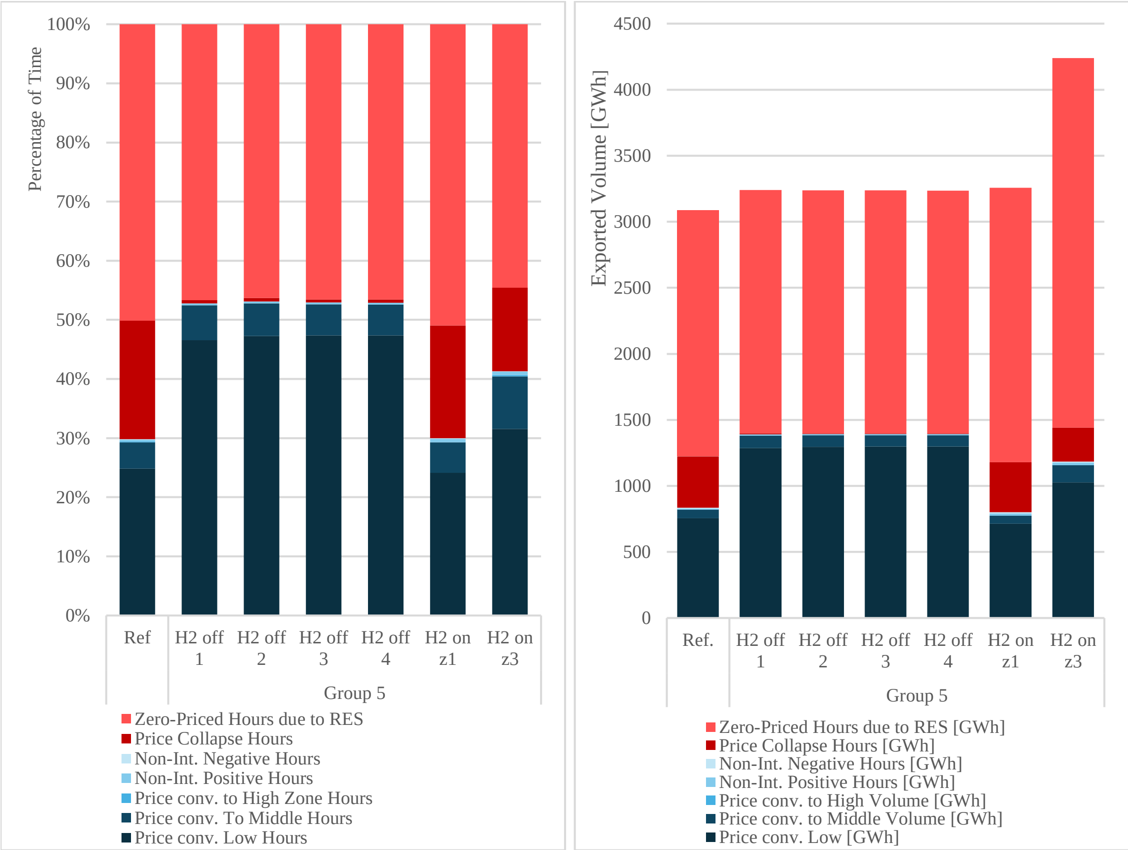


*Figure 47: Frequency (Left) and Magnitude (Right) of the Price risk categories for Case Group Hydrogen Production*

on the interconnectors for additional power trade, allowing the price to be set more frequently by the adjacent zones, primarily Zone 3.

For case $H2_{z1}^{on}$ the prices in the OBZ dropped compared to the reference case and was more volatile (higher CoV). These lower mean prices combined with the lower wind exports during hours with price convergence to low (-5.35%), middle (-5.81%) and high (-51.26%) priced zones further explains the lower revenues for the OWFs in this case. Despite the small shift in frequency from zero priced hours due to price collapses (-5.07%) to zero-priced hours due to RES competition (+1.62%), the total number of hours with zero prices remains relatively the same (+0.29%) case for this case. Additionally, comparing the WTP of 40.70 €/MWh with the price duration curve of zone 1 for case $H2_{z1}^{on}$, only for the very right end of the price duration curve the price in zone 1 is below the WTP of the electrolyser, explaining the low FLHs in this case. The electrolyser in this case simply does not dispatch due to the electricity prices in zone 1 being higher than its WTP. During most of those hours in which the electrolyser did dispatch, the price in the OBZ was zero due to RES supply, thus increasing wind exports during these hours (+11.52%).

For the $H2_{z3}^{on}$ case, both the frequencies and quantities exported during hours with price convergence to low (freq. +26.98%, magn. +36.08%), middle (freq. +1001.54%, magn. +99.53%), and high (freq. +20%, magn. +10.14%) priced zones increased compared to the reference case. These increases in exports during price convergence hours result from the local electricity consumption of the electrolyser in Zone 3, reducing direct competition with the onshore wind generators in this zone, thereby allowing the generated wind in the OBZ to be more frequently allocated for export by the market clearing. These higher price convergence exports, along with the higher mean price in the OBZ (Table 32), contributed to increased revenue for the OWFs. Additionally, wind exports during price collapses decreased (-34.12%) while exports during zero-priced hours due to RES increased (+50.27%). The reduction in price collapses was expected. The substantial increase in exports during renewable hours is a serendipity caused by the same reason as the increased price convergence hours: reduced competition with wind-dominated Zone 3 allowing for additional exports from the OBZ.

Non-intuitive price formation did not play a significant role for this case group.

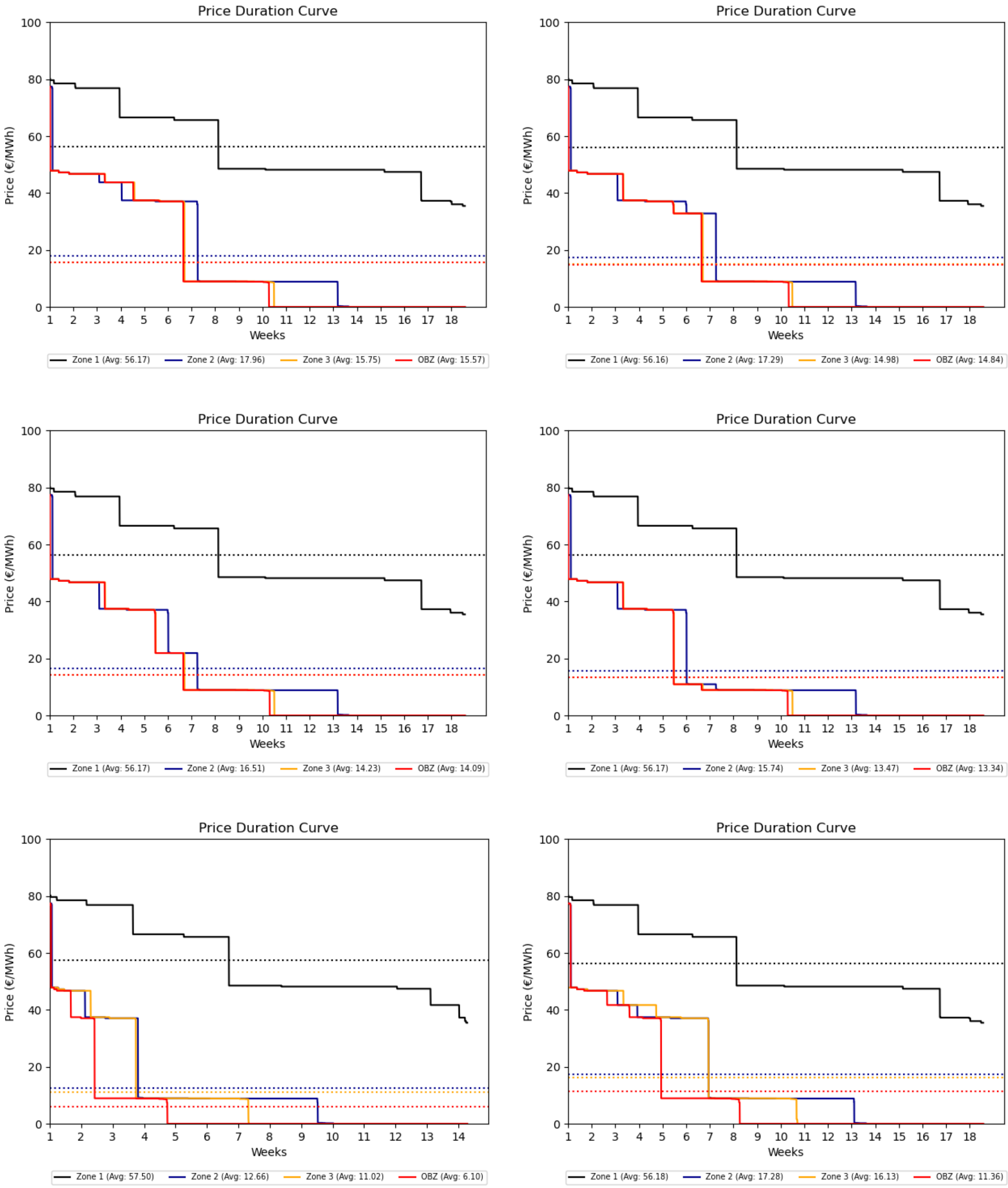


*Figure 48: Price duration curves Case Group Hydrogen Production. Top left is case $H2_1^{off}$, top right case $H2_2^{off}$, middle left case $H2_3^{off}$, middle right case $H2_4^{off}$, bottom left case $H2_{z1}^{on}$ and bottom right case $H2_{z3}^{on}$.*

### 6.6.3 Volume Risk Results – Hydrogen Production

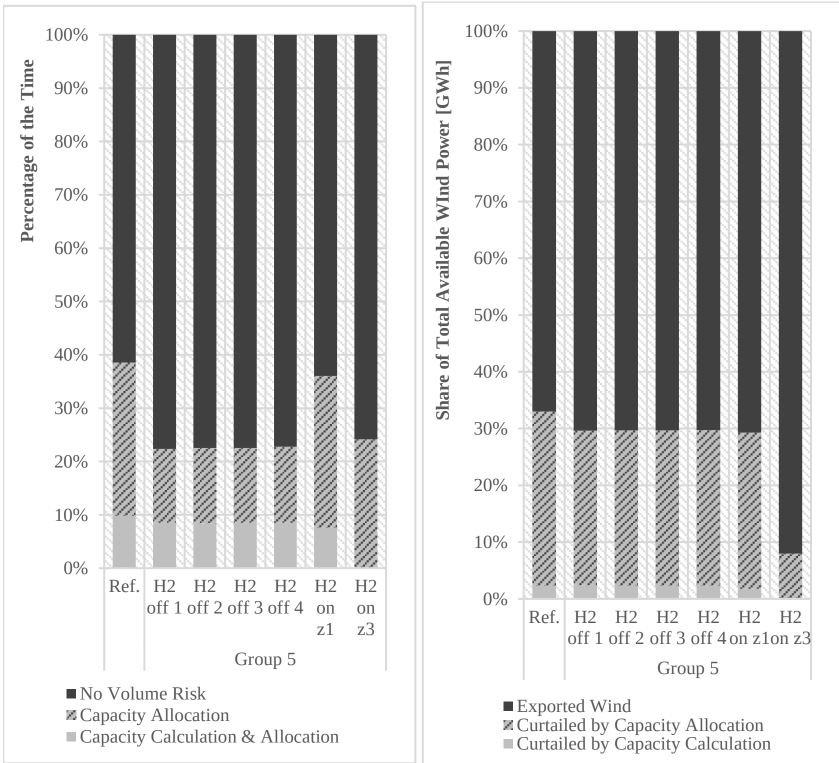


*Figure 49: Frequency (left) and Severity (right) of Volume Risk for Case Group Hydrogen Production.*

For the volume risk, it can be observed that the offshore hydrogen production cases see a substantial decrease in both frequency and severity of the volume risk (See Figure 49). For cases $H2_1^{off}$, $H2_2^{off}$, $H2_3^{off}$ and $H2_4^{off}$ the frequency of hours with no volume risks increased with +26.42%, +26.14%, +26.14% and +25.76% and the magnitude of the total volume risk decreased with -10.24%, -10.07%, -10.03% and -10.01% compared to the reference case. These changes are mainly due to the decrease in curtailed volumes by the capacity allocation (-11.08%, -10.86%, -10.84%, and -10.81%) while the curtailed volumes by the capacity calculation remained relatively stable (+0.64%, +0.17%, +0.43%, and +0.39%). The limited variation in curtailment by the capacity calculation is expected as local electrolysers in the OBZ do not alter the FB domain, keeping the maximum theoretical export capacity of the OBZ unchanged. Curtailment by the capacity allocation decreased because offshore electrolysers in the OBZ absorb part of the locally generated wind power, reducing the total wind volume competing with onshore renewables for the allocation of scarce transmission capacity. Thus, the competition between the OBZ and the onshore zones itself is not altered, but the volume of wind power with which the OBZ competes with these onshore renewable generators is reduced.

For the onshore case $H2_{z1}^{on}$, a decrease in frequency of volume risk hours is observed (-6.58%) with also less curtailed volumes by the capacity calculation (-23.40%) and capacity allocation (-10.30%). These reductions occurred primarily during hours with both curtailment by capacity calculation and allocation, as the frequency of these hours decreased by 20.89%, while hours with only curtailment by capacity allocation decreased by 1.06%. Previously, the maximum import capacity of Zone 1 was 774 MWh (see Section 4.6.2.2). The 750 MW of installed electrolyser capacity allows the OBZ to export additional wind power when the electrolyser is in operation. This increased export capacity primarily reduced curtailment by the capacity calculation and partly reduced curtailment by the capacity allocation. The additional power sink increased the direct import capacity from the OBZ, reducing capacity calculation curtailment, and lessened competition with onshore renewables in other zones to export to Zone 1, reducing capacity allocation curtailment as the increased electricity demand made it less competitive to supply power. Despite the limited dispatch of this electrolyser (2% of the time at FLH), the reductions in curtailment by both the capacity calculation and allocation demonstrate the substantial impact of placing an electrolyser at the congested landing point of the OBZ in Zone 1 on mitigating volume risks.

The onshore case $H2_{z3}^{on}$ completely mitigated the capacity calculation risk, as no curtailment by the capacity calculation is observed, with all curtailment attributed to the capacity allocation. This mitigation can be explained as follows. The primary factor restricting the FB domain of the OBZ is the onshore grid in Zone 1, and to a lesser extent, the commercial transactions in Zone 2 (Appendix D). In the reference case, this led to substantial curtailment by both capacity calculation and allocation. The added demand by the electrolyser in Zone 3 does not increase the FB domain as the 1.5GW interconnector remains the limiting factor. However, it adds 750 MWh of additional demand at the OBZ's landing point, which can be supplied by onshore renewables or OWFs in the OBZ. The substantial increase in wind exports from the OBZ indicates the latter. With these increased exports to zone 3, the export pattern from the OBZ changes. Previously, the OBZ competed with Zone 3 for the scarce transmission capacity primarily to high-priced zone 1, and to a lesser extend to zone 2. However, the additional demand agent in Zone 3 changes this competition to export via the OBZ into the necessity to import from the OBZ to supply the electrolyser, drastically reducing curtailed wind power. With the FB domain unchanged, the remaining curtailments during high renewable competition hours were never large enough per hour to exceed the maximum net position of the OBZ, thus avoiding curtailment by the capacity calculation and resulting only in (to a lesser extent) curtailment by the capacity allocation.

### 6.6.4 Interacting Price and Volume Risk

The interacting price and volume risk for this case group (Table 33) show similar patterns to the reference case, with almost all wind power being curtailed during the high renewable dominated hours.

*Table 33: Interacting Price and Volume Risk for the Case Group Offshore Grid Topology (Dual). The percentages represent the share of curtailed wind power during each of the price risk categories in which curtailment was observed.*

| Price Risk Hours | Volume Risk | Ref. | $H2_1^{off}$ | $H2_2^{off}$ | $H2_3^{off}$ | $H2_4^{off}$ | $H2_{z1}^{on}$ | $H2z_3^{on}$ |
|---|---|---|---|---|---|---|---|---|
| **Zero-Priced hours due to RES** | *Total Curtailment* | *99.95%* | *99.53%* | *99.53%* | *99.53%* | *99.53%* | *99.94%* | *100%* |
| | Curtailed by Cap. Calc. | 7.16% | 8.02% | 7.97% | 7.99% | 7.98% | 6.18% | 0.00% |
| | Curtailed by Cap. All. | 92.79% | 91.51% | 91.56% | 91.54% | 91.55% | 93.76% | 100% |
| **Price collapse hours** | *Total Curtailment* | *0.05%* | *0.00%* | *0.00%* | *0.00%* | *0.00%* | *0.06%* | *0.00%* |
| | Curtailed by Cap. Calc. | 0.00% | 0.00% | 0.00% | 0.00% | 0.00% | 0.00% | 0.00% |
| | Curtailed by Cap. All. | 0.05% | 0.00% | 0.00% | 0.00% | 0.00% | 0.06% | 0.00% |
| **Other price hours** | *Total Curtailment* | *0.00%* | *0.36%* | *0.36%* | *0.36%* | *0.36%* | *0.00%* | *0.00%* |
| | Curtailed by Cap. Calc. | 0.00% | 0.00% | 0.00% | 0.00% | 0.00% | 0.00% | 0.00% |
| | Curtailed by Cap. All. | 0.00% | 0.36% | 0.36% | 0.36% | 0.36% | 0.00% | 0.00% |

## 6.7 Regulatory Mitigation Measures Analysis

As described in Section 4.2.3, the FTR and TAG are considered in this analysis as the regulatory mitigation measures. First the results of the TAG analysis are presented (Section 6.7.1), followed by the results of the FTR (Section 6.7.2). This section concludes with an assessment on the impact on the revenues by the implementation of these two mitigation measures combined (Section 6.7.3). In this analysis, Case Group 5 is not considered, since these cases are already a mitigation measure in itself and because the exemptions of the TAG might include the presence of demand agents that absorb part of the risk (Section 3.3.3).

### 6.7.1 TAG Results

Figure 50 presents the results of the TAG payments. Since the TAG only compensates for the curtailed volume by the capacity calculation (see Section 4.3.2), the total curtailed volumes by the capacity calculation for all cases are also presented in Figure 51.

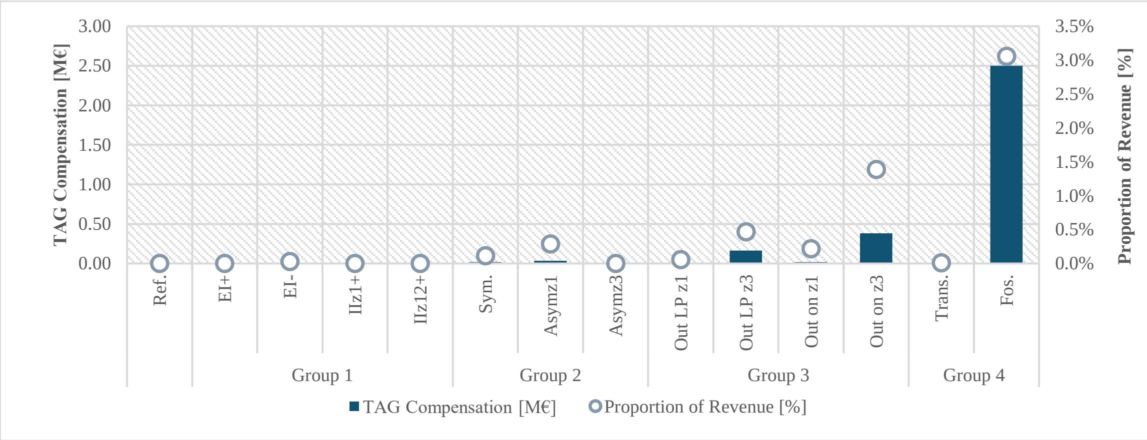


*Figure 50: TAG Compensations for all cases. Visualised are total TAG compensation payments and the TAG compensation as a proportion of the revenue of the considered case.*

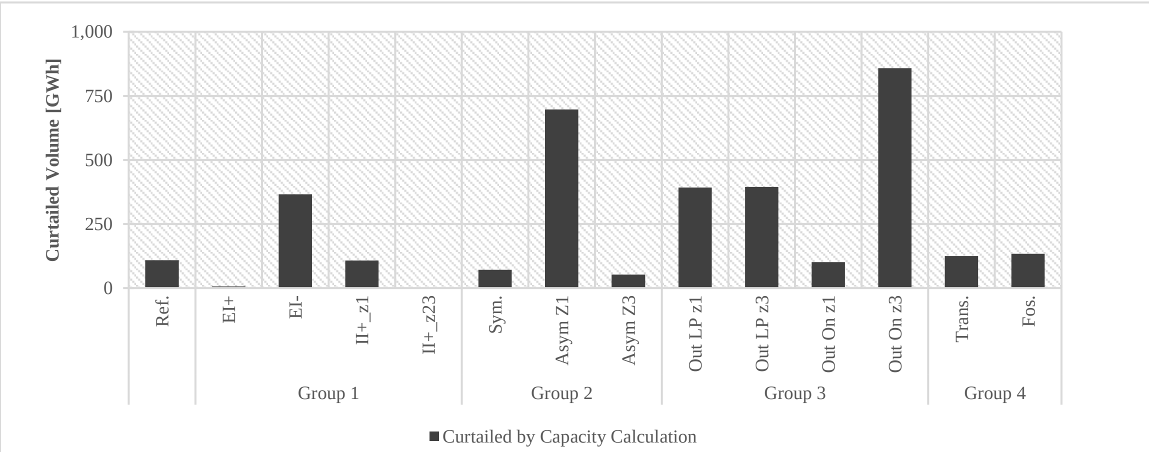


*Figure 51: Curtailed Volumes by the Capacity Calculation for all cases.*

The first observation that stand out is the discrepancy between the TAG compensations and the curtailed volumes by the capacity calculation over all cases. That is, considering that the TAG payment is calculated by the product of the curtailed volume by the capacity calculation and the difference between the reference price and the OBZ's price, it is expected that the TAG compensation is somewhat proportional to the curtailed volume by the capacity calculation. The cases with the largest curtailed volume by the capacity calculation were cases $\mathrm{EI}^{-}$, Asym$_{z1}$, and $\mathtt{Out}_{z1}^{LP}$, $\mathtt{Out}_{z3}^{LP}$ and $\mathtt{Out}_{z3}^{on}$ (Figure 51). Whilst cases $\mathtt{Out}_{z3}^{LP}$ and $\mathtt{Out}_{z3}^{on}$ did receive some TAG compensation payments, the case with the Fossil Mix received by far the largest TAG compensation, despite not having the largest curtailed volumes by the capacity calculation.

The reason for this discrepancy lies in how the TAG compensation is calculated. Equations (4.8) (see Section 4.2.3) determine the compensation price as the difference between the reference bidding zone price and the OBZ's price. If this difference is negative, the compensation price is zero. In this analysis, the reference price is the lowest price of the bidding zones connected to the hybrid. Therefore, when the OBZ's price is zero due to renewable energy sources supplying all demand (i.e. at least one other zone also shows a price of 0 €/MWh) the compensation price becomes 0 €/MWh. Evidenced from the results on the interacting price and volume risk, it is observed that for most cases almost all curtailment by the capacity calculation took place during zero-priced hours due to RES, resulting in no or little TAG compensation.

Specifically, in case group 1 (Table 19, Section 6.2.4) for cases $\mathrm{EI}^{+}$, $\mathrm{II}_{z1}^{+}$ and $\mathrm{II}_{z23}^{+}$, all curtailment by the capacity calculation took place during these zero-priced hours due to RES, resulting in no TAG compensation. For case $\mathrm{EI}^{+}$, only 0.17% of total curtailment was attributed to curtailment by the capacity calculation during price collapse hours, which led to TAG compensations during these hours totalling a mere 0.03% of total revenue. In case group 2 (Table 22, Section 6.3.4) only case $\mathrm{Asym}_{z1}$ showed curtailment by the capacity calculation not taking place during zero-priced hours due to RES (but during price collapse hours), leading to a total TAG compensation of 0.29% of total revenue.

In case group 3, case $\mathrm{Out}_{z3}^{on}$ received the highest TAG compensation (1.39% of revenue), resulting from 2.68% of total curtailment being attributed to the capacity calculation during price collapse hours (Table 26, Section 6.4.4). In case $\mathrm{Out}_{z3}^{LP}$ 2.13% of total curtailment was attributed to the capacity calculation during price collapse hours, but with lower curtailed volumes by the capacity calculation, this case obtained TAG compensation of 0.47% of revenue.

The TAG compensation for Case $\mathrm{Out}_{z1}^{on}$ is rather interesting as for this case all curtailment by the capacity calculation occurred during non-intuitive prices, which were primarily negative electricity prices during hours where other zones showed zero-prices due to RES (see Section 6.4.2.1). Because of these negative electricity prices in the OBZ while other zones experience zero-prices, the TAG compensation price becomes positive instead of zero[16] whereby TAG compensation is received during these negative priced hours. Since the observed negative electricity prices were never extreme (minimum observed price of -0.30 €/MWh), it resulted only in TAG compensation of 0.22% of total revenue. Nevertheless, this indicates the potential effectiveness of the TAG in mitigating the volume risk during negative priced hours.

The Fossil Mix case was the only case that received substantial TAG compensation, both in absolute terms (2.5 €M) as in proportion to its revenue (3.06%). This was the result of almost all curtailment (88.92% of total) in this case being curtailed by the capacity calculation during price collapse hours (see table 29, Section 6.5.4). Considering that the curtailment by the capacity calculation accounted for 2.90% of the total available wind power (Figure 45 right, Section 6.5.3), this TAG compensation of 3.06% of total revenue seems to be a reasonable amount. Noteworthy is that the total curtailed volume by the capacity calculation for this case was almost the same as in the Transition Mix case and the high renewable mix used in the reference case, while these two cases obtained negligible TAG compensation.

## 6.7.2 FTR Results

Figure 52 presents the results of the FTR analysis. The FTR payments per OWF correspond to the payments as contracted with the bidding zone closest to the OWF. The TAG compensations are added in the figure too. The (old) revenue without the FTR and TAG payments and the (new) revenue with the FTR and TAG payments per case also indicated.

[16] With the TAG price being $\max(\mathrm{p}_{\mathrm{TAG}}^{\mathrm{ref}} - \mathrm{P}_{\mathrm{market}}^{\mathrm{OBZ}}, 0)$, $\mathrm{p}_{\mathrm{TAG}}^{\mathrm{ref}} = 0$ €/MWh and $\mathrm{P}_{\mathrm{market}}^{\mathrm{OBZ}} = -\mathrm{x}$ €/MWh, the compensation prices becomes: $\max(0 - (-\mathrm{x}), 0) = +\mathrm{x}$ €/MWh (See equation 4.8, section 4.3.2).

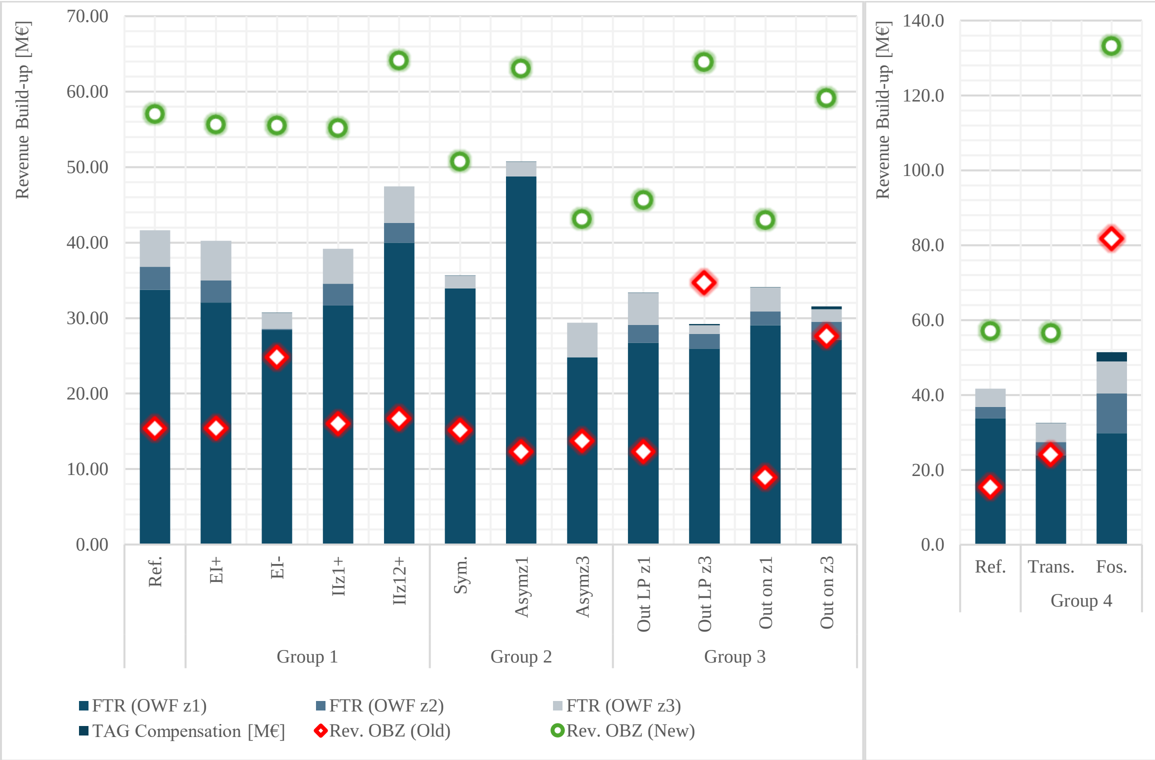


*Figure 52: Results of FTR and TAG analysis for case groups 1-3 (left) and case group 4 (right).*

The first notable observation is that FTRs from Zone 1 primarily contribute to the total FTR compensations for all cases. Given that Zone 1 is the high-priced zone, the significant portion of FTR payments from this zone is expected, as the price spread across the OBZ and Zone 1 was generally the largest. Additionally, the price risk results indicate that hours with price convergence to the highest-priced market (Zone 1) were the fewest across all cases, showing that the frequency of hours with a price spread between the OBZ and Zone 1 is also highest. Thus, both the magnitude of the price spread and the frequency of these hours with a price spread between the OBZ and Zone 1 contributed most to the FTR compensation payments.

Regarding FTR payments from Zones 2 and 3, the overarching observation is that for cases with high price convergence to a specific zone, there were correspondingly lower FTR payments from that zone. For example, case EI$^-$ showed high price convergence to Zone 3 (see Section 6.1.3), resulting in little FTR payments from this zone. In the dual hybrid cases (group 2), no OWF was connected to Zone 2, so logically, these cases did not have FTR compensations from this zone. The much higher FTR compensation from Zone 1 in case Asymz1 compared to case Asymz3 is due to the double installed OWF capacity near Zone 1 for the former case.

The case with the Fossil Mix showed the highest FTR payments, primarily due to substantially higher FTR payments from Zones 2 and 3. Previously, the OBZ frequently showed zero-prices due to RES, resulting in no FTR compensation from zones with high renewable supply. In the Fossil Mix, these hours became price collapse hours (see Section 6.5.2), leading to non-zero FTR compensations during these hours.

### 6.7.3 Impact of FTR and TAG on Revenue

Comparing the revenues before the FTR and TAG compensation payments (red diamonds, Figure 52) with the revenues after both instruments are in place (green circles, Figure 52), it is evident that the revenues substantially increased over all cases. Table 34 shows that the FTR compensation primarily contributes to the revenue increase compared to the TAG compensation, except in the Fossil Mix case.

Cases Asym$_{z1}$, Asym$_{z3}$, $\mathrm{Out}_{z1}^{LP}$ and $\mathrm{Out}_{z1}^{on}$ which experienced the largest decreases in revenues compared to the reference case (-19.86%, -10.88%, -20.25% and -42.24%), saw substantial revenue increases with the implementation of both instruments (+412%, +214%, +272%, and +384%), indicating that these regulatory instruments, particularly the FTR, provide effective hedging mechanisms for economic viability in this system setup.

Lastly, it is important to note that the combined payments from the FTR and TAG never exceeded the congestion rents amassed by the TSOs. Specifically, the TAG payments ranged from 0% to 1.84% and the FTR payments ranged from 20.5% to 52.6% of congestion rents amassed by the TSOs (Table 34).

*Table 34: TAG and FTR payments relative to revenues and congestion rents.*

| (No.) Case Group | Case | Revenue increase by TAG payments | Revenue increase by FTR payments | Total Revue increase | Share of TAG payments to Congestion Rent | Share of FTR payments to Congestion Rent |
|---|---|---|---|---|---|---|
| (0) Reference | Ref. | 0.00% | 271% | 271% | 0.00% | 29.4% |
| (1) Offshore Grid Topology - Triangular Hybrid | $\mathbf{EI^+}$ | 0.00% | 261% | 261% | 0.00% | 28.3% |
| | $\mathbf{EI^-}$ | 0.03% | 124% | 124% | 0.01% | 26.5% |
| | $\mathbf{II_{Z1}^+}$ | 0.00% | 245% | 245% | 0.00% | 27.5% |
| | $\mathbf{II_{Z23}^+}$ | 0.00% | 284% | 284% | 0.00% | 34.5% |
| (2) Offshore Grid Topology – Dual Hybrid | Sym. | 0.12% | 236% | 236% | 0.02% | 31.7% |
| | Asym$_{z1}$ | 0.29% | 411% | 412% | 0.04% | 52.6% |
| | Asym$_{z3}$ | 0.00% | 214% | 214% | 0.00% | 29.6% |
| (3) Onshore Grid Attenuation | $\mathbf{Out_{z1}^{LP}}$ | 0.06% | 272% | 272% | 0.01% | 34.0% |
| | $\mathbf{Out_{z3}^{LP}}$ | 0.47% | 84% | 84% | 0.14% | 26.0% |
| | $\mathbf{Out_{z1}^{on}}$ | 0.22% | 383% | 384% | 0.01% | 20.5% |
| | $\mathbf{Out_{z3}^{on}}$ | 1.39% | 113% | 114% | 0.31% | 25.4% |
| (4) Generation Mix | Trans. | 0.01% | 135% | 135% | 0.00% | 32.2% |
| | Fos. | 3.06% | 60% | 63% | 1.84% | 36.0% |

## 6.8 Cross – Case Group Results

This section presents the Cross-Case Group Results, with risk matrices summarized in Table 35 (Price Risk Metrics), Table 36 (Volume Risk Metrics) and Table 37 (General Metrics). The discussion focuses on the most frequent and severe price and volume risks.

In the risk matrices presented in the tables hereafter, the price and volume risk results for all simulated cases are presented in a standardised manner (See Appendix E for all results), based on metrics being a benefit (B) or costs (C) from the perspective of OWF developers (see Section 4.4.1). The green cells represent 'less risky' metrics, and the red cells represent 'riskier' metrics. The dark red to dark green colour scheme is applied for the standardised results between -0.50 and +0.50. Additionally, for extra emphasis on the visualisation, standardised values between (-)0.50 and (-)0.75 have given a white fond and values between (-)0.75 and (-)1 have given a white bold and italic fond.

*Table 35: Risk Matrix for the Price Risk Results*

| | Risk Category | Price Risk Metric | C/B | Ref. Case | Group 1 | | | | Group 2 | | | Group 3 | | | | Group 4 | | Group 5 | | | | | |
|---|---|---|---|---|---|---|---|---|---|---|---|---|---|---|---|---|---|---|---|---|---|---|---|
| | | | | | $EI^+$ | $EI^-$ | $II^+_{z1}$ | $II^+_{z23}$ | Sym. | $Asym_{z1}$ | $Asym_{z3}$ | $Out^{LP}_{z1}$ | $Out^{LP}_{z3}$ | $Out^{on}_{z1}$ | $Out^{on}_{z3}$ | Trans. | Fos. | $H2^{off}_1$ | $H2^{off}_2$ | $H2^{off}_3$ | $H2^{off}_4$ | $H2^{on}_{z1}$ | $H2^{on}_{z3}$ |
| | *Flat Price Risk* | Mean Price | B | 0.00 | 0.01 | 0.39 | -0.02 | 0.08 | 0.63 | 0.23 | 0.23 | -0.10 | ***0.75*** | -0.20 | 0.55 | 0.12 | ***0.80*** | 0.56 | 0.51 | 0.46 | 0.41 | -0.06 | 0.27 |
| | | CoV OBZ | C | 0.00 | 0.03 | 0.40 | 0.00 | 0.10 | 0.32 | 0.17 | 0.16 | -0.13 | 0.52 | -0.28 | 0.38 | 0.18 | 0.72 | 0.49 | 0.49 | 0.48 | 0.44 | -0.04 | 0.28 |
| Frequency | *Struct Price Conv. Eff.* | Price conv. Low Hours | B | 0.00 | 0.02 | 0.42 | 0.01 | 0.08 | -0.29 | -0.21 | -0.30 | -0.01 | -0.13 | -0.10 | 0.02 | 0.17 | 0.70 | 0.54 | 0.56 | 0.56 | 0.56 | -0.02 | 0.17 |
| | | Price conv. To Middle Hours | B | 0.00 | 0.04 | 0.08 | -0.01 | 0.10 | 0.09 | 0.15 | 0.00 | -0.14 | ***0.83*** | -0.17 | 0.41 | 0.03 | -0.02 | 0.07 | 0.05 | 0.04 | 0.04 | 0.03 | 0.20 |
| | | Price conv. to High Zone Hours | B | 0.00 | 0.00 | 0.00 | -0.01 | 0.00 | ***0.99*** | 0.42 | 0.71 | -0.01 | 0.52 | -0.01 | 0.39 | 0.00 | -0.01 | -0.01 | -0.01 | -0.01 | -0.01 | -0.01 | 0.00 |
| | *Non-Int. Price Risk* | Non-Int. Positive Hours | C | 0.00 | -0.02 | -0.04 | 0.00 | -0.02 | -0.03 | 0.02 | -0.02 | 0.03 | -0.21 | ***-0.97*** | -0.06 | 0.01 | -0.06 | 0.00 | 0.00 | 0.00 | 0.00 | -0.02 | -0.03 |
| | | Non-Int. Negative Hours | C | 0.00 | 0.03 | -0.25 | 0.00 | 0.03 | -0.06 | -0.49 | 0.01 | 0.01 | -0.58 | -0.71 | -0.19 | -0.26 | ***-0.97*** | 0.03 | 0.03 | 0.03 | 0.03 | -0.03 | 0.00 |
| | *Price Coll. Risk* | Number of Price Collapse Hours | C | 0.00 | 0.03 | 0.47 | 0.00 | 0.12 | 0.32 | 0.24 | 0.22 | 0.03 | 0.44 | 0.04 | 0.42 | -0.03 | -0.50 | 0.50 | 0.50 | 0.50 | 0.50 | 0.03 | 0.15 |
| | | Number of Zero-Priced Hours RES | C | 0.00 | 0.02 | 0.01 | 0.00 | 0.02 | -0.03 | -0.09 | -0.11 | -0.09 | 0.19 | 0.03 | 0.04 | 0.16 | ***0.89*** | 0.06 | 0.07 | 0.06 | 0.06 | -0.01 | 0.10 |
| Magnitude | *Struct. Price Conv. Eff.* | Price conv. Low Volume [MWh] | B | 0.00 | 0.01 | 0.16 | 0.01 | 0.05 | -0.14 | -0.14 | -0.11 | -0.06 | 0.25 | -0.12 | 0.14 | 0.20 | ***0.86*** | 0.25 | 0.25 | 0.25 | 0.25 | -0.01 | 0.16 |
| | | Price conv. to Middle Volume [MWh] | B | 0.00 | 0.01 | 0.15 | 0.01 | 0.04 | -0.22 | -0.20 | -0.18 | -0.04 | -0.11 | -0.13 | -0.02 | 0.17 | ***0.78*** | 0.25 | 0.25 | 0.25 | 0.25 | -0.02 | 0.13 |
| | | Price conv. to High Volume [MWh] | B | 0.00 | 0.00 | -0.01 | 0.00 | 0.03 | 0.09 | 0.08 | 0.08 | -0.08 | ***0.92*** | -0.07 | 0.41 | 0.04 | -0.01 | 0.05 | 0.04 | 0.03 | 0.03 | -0.01 | 0.11 |
| | *Non-Int. Price Risk* | Positive Hours [MWh] | C | 0.00 | -0.03 | -0.04 | 0.00 | -0.02 | 0.01 | 0.02 | 0.00 | 0.04 | -0.51 | ***-0.96*** | -0.15 | 0.01 | -0.16 | -0.01 | -0.01 | -0.01 | -0.01 | -0.03 | -0.05 |
| | | Negative Hours [MWh] | C | 0.00 | 0.03 | -0.18 | 0.00 | 0.03 | 0.03 | 0.03 | 0.03 | 0.01 | -0.33 | -0.33 | -0.11 | -0.26 | ***-0.97*** | 0.03 | 0.03 | 0.03 | 0.03 | -0.02 | 0.00 |
| | *Price Coll. Risk* | Price Collapse Hours [MWh] | C | 0.00 | 0.01 | 0.21 | 0.02 | 0.06 | 0.10 | -0.01 | 0.04 | 0.03 | 0.14 | 0.03 | 0.11 | -0.03 | ***-0.77*** | 0.23 | 0.22 | 0.23 | 0.23 | 0.01 | 0.08 |
| | | Zero-Priced Hours due to RES [MWh] | C | 0.00 | -0.12 | 0.15 | 0.14 | -0.37 | 0.23 | 0.18 | -0.01 | 0.19 | 0.27 | 0.20 | 0.14 | 0.02 | 0.63 | 0.01 | 0.01 | 0.01 | 0.01 | -0.07 | -0.32 |

*Table 36: Risk Matrix for the Volume Risk Results*

| | Volume Risk Metric | C/B | Ref. Case | Group 1 | | | | Group 2 | | | Group 3 | | | | Group 4 | | Group 5 | | | | | |
|---|---|---|---|---|---|---|---|---|---|---|---|---|---|---|---|---|---|---|---|---|---|---|
| | | | | $EI^+$ | $EI^-$ | $II^+_{z1}$ | $II^+_{z23}$ | Sym. | $Asym_{z1}$ | $Asym_{z3}$ | $Out^{LP}_{z1}$ | $Out^{LP}_{z3}$ | $Out^{on}_{z1}$ | $Out^{on}_{z3}$ | Trans. | Fos. | $H2^{off}_1$ | $H2^{off}_2$ | $H2^{off}_3$ | $H2^{off}_4$ | $H2^{on}_{z1}$ | $H2^{on}_{z3}$ |
| Frequency | No Volume Risk | B | 0.00 | 0.03 | 0.09 | -0.12 | 0.20 | 0.00 | -0.33 | -0.14 | -0.24 | -0.01 | -0.33 | -0.23 | 0.19 | 0.67 | 0.41 | 0.41 | 0.41 | 0.40 | 0.06 | 0.36 |
| | Capacity Calculation & Allocation | C | 0.00 | 0.23 | -0.30 | 0.02 | 0.32 | -0.01 | -0.56 | 0.11 | -0.33 | -0.37 | -0.01 | -0.68 | -0.03 | -0.06 | 0.04 | 0.05 | 0.04 | 0.04 | 0.07 | 0.32 |
| | Capacity Allocation | C | 0.00 | 0.03 | 0.09 | -0.12 | 0.20 | 0.00 | -0.33 | -0.14 | -0.24 | -0.01 | -0.33 | -0.22 | 0.19 | 0.67 | 0.41 | 0.41 | 0.41 | 0.40 | 0.06 | 0.36 |
| Magnitude | Total Wind Export [GWh] | B | 0.00 | 0.14 | -0.17 | -0.17 | 0.43 | -0.46 | -0.32 | -0.12 | -0.29 | -0.19 | -0.27 | -0.11 | 0.16 | 0.54 | 0.06 | 0.06 | 0.06 | 0.06 | 0.07 | 0.46 |
| | Total Volume Risk [MWh] | C | 0.00 | 0.16 | -0.20 | -0.19 | 0.50 | 0.18 | -0.37 | -0.14 | -0.34 | 0.17 | -0.31 | -0.13 | 0.19 | 0.63 | 0.07 | 0.07 | 0.07 | 0.07 | 0.08 | 0.53 |
| | Capacity Calculation [MWh] | C | 0.00 | 0.12 | -0.30 | 0.00 | 0.13 | 0.04 | -0.69 | 0.07 | -0.33 | -0.33 | 0.01 | ***-0.87*** | -0.02 | -0.03 | 0.00 | 0.00 | 0.00 | 0.00 | 0.03 | 0.13 |
| | Capacity Allocation [MWh] | C | 0.00 | 0.12 | -0.08 | -0.20 | 0.47 | 0.17 | -0.10 | -0.17 | -0.22 | 0.31 | -0.33 | 0.22 | 0.20 | 0.67 | 0.08 | 0.07 | 0.07 | 0.07 | 0.07 | 0.50 |

*Table 37: Risk Matrix for the General Results*

| General Metric | C/B | Ref. Case | Group 1 | | | | Group 2 | | | Group 3 | | | | Group 4 | | Group 5 | | | | | |
|---|---|---|---|---|---|---|---|---|---|---|---|---|---|---|---|---|---|---|---|---|---|
| | | | $EI^+$ | $EI^-$ | $II^+_{z1}$ | $II^+_{z23}$ | Sym. | $Asym_{z1}$ | $Asym_{z3}$ | $Out^{LP}_{z1}$ | $Out^{LP}_{z3}$ | $Out^{on}_{z1}$ | $Out^{on}_{z3}$ | Trans. | Fos. | $H2^{off}_1$ | $H2^{off}_2$ | $H2^{off}_3$ | $H2^{off}_4$ | $H2^{on}_{z1}$ | $H2^{on}_{z3}$ |
| Total Revenue OWFs [M€] | B | 0.00 | 0.00 | 0.13 | 0.01 | 0.02 | 0.00 | -0.04 | -0.02 | -0.04 | 0.26 | -0.09 | 0.17 | 0.12 | ***0.91*** | 0.23 | 0.21 | 0.18 | 0.15 | -0.03 | 0.13 |
| Total Wind Export [GWh] | B | 0.00 | 0.14 | -0.17 | -0.17 | 0.43 | -0.46 | -0.32 | -0.12 | -0.29 | -0.19 | -0.27 | -0.11 | 0.16 | 0.54 | 0.06 | 0.06 | 0.06 | 0.06 | 0.07 | 0.46 |
| Total Curtailment [GWh] | C | 0.00 | 0.16 | -0.20 | -0.19 | 0.50 | 0.18 | -0.37 | -0.14 | -0.34 | 0.17 | -0.31 | -0.13 | 0.19 | 0.63 | 0.07 | 0.07 | 0.07 | 0.07 | 0.08 | 0.53 |
| Total Export at Zero-Price [GWh | C | 0.00 | -0.17 | 0.39 | 0.22 | -0.49 | 0.42 | 0.25 | 0.03 | 0.30 | 0.51 | 0.32 | 0.30 | 0.01 | 0.27 | 0.20 | 0.20 | 0.20 | 0.20 | -0.10 | -0.40 |
| Total Export at Positive Price [G | B | 0.00 | 0.01 | 0.16 | 0.01 | 0.05 | -0.14 | -0.14 | -0.11 | -0.06 | 0.25 | -0.12 | 0.14 | 0.20 | ***0.86*** | 0.25 | 0.25 | 0.25 | 0.25 | -0.01 | 0.16 |
| Total Congestion Rent [M€] | B | 0.00 | 0.01 | -0.37 | 0.01 | -0.06 | -0.42 | -0.65 | -0.61 | -0.62 | -0.42 | 0.35 | -0.27 | -0.59 | -0.08 | -0.47 | -0.43 | -0.41 | -0.39 | -0.17 | -0.15 |
| Total Day-Ahead Cost [M€] | C | 0.00 | 0.00 | 0.00 | 0.00 | 0.00 | -0.03 | 0.21 | 0.22 | -0.04 | 0.03 | -0.15 | -0.01 | 0.07 | ***-0.78*** | 0.07 | 0.05 | 0.03 | 0.01 | 0.00 | 0.07 |
| Total Redispatch Cost [M€] | C | 0.00 | 0.00 | 0.00 | 0.00 | 0.00 | -0.44 | -0.59 | ***-0.99*** | -0.04 | 0.00 | -0.02 | 0.00 | 0.00 | 0.01 | 0.00 | 0.00 | 0.00 | 0.00 | 0.00 | 0.00 |

To start, the risk matrices show that hydrogen production effectively mitigates price and volume risks when electrolysers are placed offshore or onshore with a willingness to pay for electricity not consistently higher than the onshore market price (case $\mathrm{H2}_{z1}^{on}$). Offshore electrolysers create local demand, increasing prices and reducing volatility, while onshore electrolysers in wind-dominated zones enhance price convergence and reduce curtailment, though their effectiveness in high-priced zones is limited by low dispatch frequency (See Discussion for further elaboration).

The price collapse risk was most frequent and severe for the Fossil Mix case, while the frequency and magnitude of zero-priced hours due to RES substantially reduced. In the Reference Case, 50.14% of the time and 60.3% of exported wind power occurred during zero-priced hours due to RES (Section 6.1.3). This shift with a lower proportion of renewable energy sources shows that the underlying factors for zero-priced hours are both market dynamics (generation mix) and the physical grid's characteristics. If only the installed renewable capacity influenced zero-priced hours, the substantial increase in price collapse hours for the Fossil Mix would not be observed. During high wind hours, the restricted export capacity of the OBZ leads to price collapses associated with curtailment by the capacity calculation (Section 6.4.4).

The role of the grid's topology in risk formation becomes clearer in cases where the offshore and onshore grid topology parameters were varied. Cases $\mathrm{EI}^{-}$, $\mathrm{Out}_{z3}^{\mathrm{LP}}$ and $\mathrm{Out}_{z3}^{\mathrm{on}}$ show the largest reduction (excluding the hydrogen cases) in the frequency and magnitude of price collapse risk (Table 35), associated with increases in exports during positive-priced hours. The decrease in price collapse hours for these cases is due to reduced export capacity (shrunken FB domain) to wind-dominated Zone 3, which lessened competition for transmission capacity allocation to Zones 1 and 2 from the OBZ. This allowed the OBZ to export to Zone 3 instead of competing with it, creating an uncongested path that prevents price collapses and causes price convergence with Zone 3. This is evidenced by the substantial increase in price convergence hours (particularly to Zone 3), exports at positive prices, and increased exports at zero prices, reflecting the reversed power flow over the interconnector between the OBZ and Zone 3 during high renewable hours. Thus, reduced import capacity to Zone 3 avoids price collapses as the market clearing favours the OBZ exporting to Zone 3 instead of competing with Zone 3 to export to other zones.

Furthermore, the volume risk results also underline this interplay between the grid's physical characteristics and the commercial dynamics resulting from different market structures in the onshore zones. Regarding the capacity calculation volume risk, the most frequent occurrence of hours with curtailment by both the capacity calculation and allocation and curtailed volumes by the capacity calculation have been observed for cases $\mathrm{EI}^{-}$, $\mathrm{Asym}_{z1}$, $\mathrm{Out}_{z1}^{\mathrm{LP}}$, $\mathrm{Out}_{z3}^{\mathrm{LP}}$ and $\mathrm{Out}_{z3}^{on}$ (Table 36). The common denominator among all these cases is the reduction in the export capacity of the OBZ (i.e., the FB domain), albeit for different reasons:

- Case $\mathrm{EI}^{-}$ reduces the FB domain by lowering interconnection capacity to all zones.
- Case $\mathrm{Asym}_{z1}$ reduces the FB domain by disconnecting from Zone 2 and doubling installed wind and transmission capacity near Zone 1 (having no effect on FB domain as onshore grid zone 1 restricts the FB domain, Appendix D), while maintaining only 1.5 GW transmission capacity to Zone 3.
- Case $\mathrm{Out}_{z1}^{\mathrm{LP}}$ reduces import capacity towards Zone 1 due to the outage of the AC line at the landing point. Case $\mathrm{Out}_{z1}^{on}$ shows only a small reduction in import capacity to Zone 1 (Table 23, Section 6.4.1), resulting in a less pronounced capacity calculation volume risk for this case (See Section 6.4.3).
- Cases $\mathrm{Out}_{z3}^{\mathrm{LP}}$ and $\mathrm{Out}_{z3}^{on}$ reduce the FB domain towards zone 3 due to outages in this zone. Despite the lower reduction in import capacity for case $\mathrm{Out}_{z3}^{on}$ compared to case $\mathrm{Out}_{z3}^{\mathrm{LP}}$ (Table 23, Section 6.4.1), increased competition with renewables led to higher curtailments per hour,

pushing total curtailment beyond the OBZ's maximum net position and resulting in highest observed curtailment by the capacity calculation for case $\mathrm{Out}_{z3}^{on}$.

Regarding the capacity allocation volume risk, the market dynamics primarily influence the frequency and severity of this risk. The cases with the most frequent and severe curtailment by the capacity allocation were cases $\mathrm{II}_{z1}^{+}$, Asym$_{z1}$, $\mathrm{Out}_{z1}^{\mathrm{LP}}$ and $\mathrm{Out}_{z1}^{\mathrm{on}}$ (Table 36). The common denominator across these cases is the altered competition between the OBZ and onshore (renewable) generators for the allocation of scarce transmission capacity:

- In Case $\mathrm{II}_{z1}^{+}$ the already restricting onshore grid in zone 1 together with increased interconnection capacity to zone 1 further opens up competition during high wind hours. Case $\mathrm{II}_{z23}^{+}$ further substantiates this as the increased interconnectivity to the renewable dominated zones 2 and 3 reduced direct competition with the OBZ, resulting in significantly less curtailment by the capacity allocation.
- In Case Asym$_{z1}$ the competition with wind generators in zone 3 is intensified due to the disconnection from zone 2. Additionally, the FB domain for this case was also reduced, further intensifying competition to be allocated to export to zone 1.
- In Cases $\mathrm{Out}_{z1}^{\mathrm{LP}}$ and $\mathrm{Out}_{z1}^{\mathrm{on}}$ the reduced import capacity to zone 1 intensified competition between the OWFs in the OBZ and renewable generators in zone 2 and 3.

In conclusion, the key factor leading to the most frequent and severe capacity calculation volume risk is the direct reduction of the FB domain and the key factor leading to the most frequent and sever capacity allocation volume risk is the increased competition between the OWFs in the OBZ and onshore renewable generators. Moreover, the combination of these effects exacerbates curtailment by the capacity calculation (e.g. for case $\mathrm{Out}_{z3}^{on}$) and curtailment by the capacity allocation (e.g. for cases Asym$_{z1}$, $\mathrm{Out}_{z1}^{\mathrm{LP}}$ and $\mathrm{Out}_{z1}^{\mathrm{LP}}$).

Lastly, the impact on economic viability differs across cases with high frequencies and magnitudes of price and volume risks. Notably, cases $\mathrm{EI}^{-}$, $\mathrm{Out}_{z3}^{\mathrm{LP}}$ and $\mathrm{Out}_{z3}^{on}$, which had the highest wind exports during positive-priced hours and higher mean prices in the OBZ, showed the largest revenue increases despite also experiencing volume risks. This is due to the shift from price collapse hours to price convergence hours; reduced import capacity to Zone 3 prevented price collapses as the market clearing favours OBZ exports to Zone 3 instead of competing with it to export to other zones.

# Chapter 7. Discussion

In this chapter, the results from Chapter 6 are discussed, focusing on key factors leading to risks (Section 7.1.1), the impact on the economic viability of OWFs (Section 7.1.2), and the effectiveness of mitigation measures (Section 7.1.3). Additionally, the findings are examined in light of contextual considerations (Section 7.1.4) and conflicting observations from the literature (Section 7.1.5). The chapter concludes by addressing the research limitations (Section 7.2).

## 7.1 Discussion of results

### 7.1.1 Key Factors Leading to Price and Volume Risks

The results of this research underscore the complexities of the interactions and forces at play leading to price and volume risks for hybrid projects located in an OBZ under FBMC and AHC. Nevertheless, the results uncovered two key factors and their interactions leading to the most frequent and severe price and volume, being the transmission *grid's physical characteristic* and the *market characterises* of the bidding zones connected via the hybrid interconnector. More specifically, with the grid's physical characteristics it is meant the export capacity of the OBZ, or in FB terminology the size of the FB domain, which is influenced by the offshore gid topology and onshore attenuations as further discussed in short notice. With the market characteristics it is meant the extent to which the OBZ is in competition with the adjacent bidding zones for the allocation of scarce transmission capacity, which is primarily influenced by the proportion of cheap renewable generators in the onshore markets, further discussed hereafter. Since the Flow Based approach couples the markets by allocating cross-border transmission capacities while accounting for the actual physical power flows and grid constraints and the AHC method ensures consideration of the impact of these allocated cross-zonal power exchanges over the HVDC interconnectors on the physical margins of the CNEs in the FB region (see Section 2.1), the interplay between the grid's physical characteristics and the market characteristics leads to different patterns in the frequency and severity. The specific combination of these factors and the risk patterns they induce are discussed hereafter for each of the risk categories considered in this thesis.

First, the factors leading to *non-intuitive price risk* are the combination of onshore grid attenuations restricting import capacity and the trade-off between enhancing social welfare and grid loading due to power exchanges between the OBZ and the restricted onshore zone (see Section 6.4.2.1). Specifically, non-intuitive price risk emerges from CNE outages in adjacent zones. The nature of non-intuitive price formation—positive or negative—depends on the market conditions where the outage occurs. Outages in high-priced importing markets typically lead to negative non-intuitive price formation, as market clearing favours cheap wind imports via the OBZ for social welfare enhancement over the additional stress on the grid resulting from these imports. Conversely, outages in low-priced exporting markets generally result in positive non-intuitive price formation, as alleviating the low-priced exporting zone's grid through exports via the OBZ is positively valued in market clearing.

The primary factor leading to the *price collapse risk* is related to the export capacity of the OBZ as determined by the transmission grid's physical characteristics. Direct reductions of the OBZ's export capacity, albeit due to reductions in transmission capacity of the interconnectors (case $\mathtt{EI}^{-}$) or due to outages of onshore CNEs (cases $\mathtt{Out}_{\mathtt{z1}}^{\mathtt{LP}}$, $\mathtt{Out}_{\mathtt{z1}}^{\mathtt{on}}$ and $\mathtt{Out}_{\mathtt{z3}}^{\mathtt{on}}$) are the cause for the price collapse risk to occur. The frequency and severity of this risk depend on the extent to which the physical grid limit the OBZ's export capacity and the altered market characteristics because of reductions in the OBZ's export capacity. Specifically, in the system setup of this thesis the high-priced importing zone primarily restricted the export capacity of the OBZ (see Section 4.6.2.2), whereby during high-wind hours the generated wind power in the OBZ could not fully be exported, leading to price collapses. Conversely, reducing the import capacity of a low-priced renewable dominated zone that leads to reduced competition between the OBZ and this renewable dominated zone, can reduce price collapses since that competition to export via the OBZ is changed into the need to import wind power from the OBZ (as observed for cases $\mathrm{EI}^{-}$, $\mathrm{Out}_{z3}^{\mathrm{LP}}$, and $\mathrm{Out}_{z3}^{\mathrm{on}}$, Section 6.2.2).

The key factor leading to the *capacity calculation volume risk* is the restricted export capacity of the OBZ or the limited FB domain. Like the price collapse risk, all alternations in the transmission grid causing direct reductions of this export capacity (cases, $\mathrm{Out}_{z1}^{\mathrm{LP}}$, $\mathrm{Out}_{z3}^{\mathrm{LP}}$, $\mathrm{Out}_{z1}^{\mathrm{on}}$ and $\mathrm{Out}_{z3}^{\mathrm{on}}$) cause curtailment by the capacity calculation. The frequency and severity of this risk is influenced by various additional factors. First, the extent to which alternations in the transmission grid reduce direct import capacity of a specific zone is of influence (see Section 6.8), with larger reductions of the import capacity generally leading to more frequent and severe curtailment by the capacity calculation. Second, if outages of CNEs in onshore zones with a transmission grid already restricting the OBZ’s export capacity occur, the effect on the capacity calculation risk is less pronounced then for outages in zones without a previously limiting onshore grid (see Section 6.4.3). Lastly, the changed competition between the OBZ and onshore renewable generators for the allocation of scarce transmission capacity due to reductions of the OBZ’s export capacity caused by alterations in the transmission grid is of influence. Specifically, increased competition with onshore renewables by outages in a low-priced renewable dominated zone can lead to elevated curtailed volumes for the OWFs in the OBZ, pushing the total curtailment beyond the OBZ's maximum net position and resulting in increases curtailment by the capacity calculation (see Section 6.8).

The key factor leading to the *capacity allocation volume risk* is the level of competition for the scarce transmission capacity on the interconnection of the hybrid project between the OBZ and cheap (renewable) generators in the adjacent bidding zones. The frequency and severity of this risk depends on several factors. First, the dependency of the connected market on the interconnection via the hybrid project for cross-zonal power trade is a key determinant for the perception of this risk. Specifically, higher dependency of coupled markets on the hybrid interconnectors for cross-border trade intensifies competition for the transmission capacity on that interconnector, thereby pushing the available wind capacity in the OBZ more often out of the market-clearing and leading to more frequent and severe curtailment by the capacity allocation. Second, the proportion of cheap renewable generators in onshore markets is a key determinant for the frequency and severity of this risk. Generally, higher proportions of cheap renewable generators in onshore markets make the economic value of allocating transmission capacity between the generated wind power in the OBZ and the onshore renewable zone equivalent (assuming zero marginal costs for all renewable generators). This increased competition pushes the OWFs out of the market clearing, leading to curtailment by capacity allocation. The underlying mechanism is that transmission capacity allocation prioritizes the highest welfare-generating combination of bids. This often favours exports from cheap renewable zones over wind exports from the OBZ, as the former frees up physical capacity on the onshore CNEs, enabling additional internal power trade in the exporting bidding zone. Consequently, curtailment by the capacity allocation is exacerbated whenever transmission grid alterations increase competition between the OBZ and onshore generators (cases $\mathrm{II}_{z1}^{+}$, $\mathrm{II}_{z23}^{+}$, $\mathrm{Asym}_{z1}$ and $\mathrm{Asym}_{z3}$).

Lastly, the key factor leading to *interacting price and volume risk* is the restriction of the OBZ’s export capacity, as this is the primary cause for both the price collapse risk and the capacity calculation volume risk to occur. The frequency and severity of the interacting price and volume risk depends on the same individual reasons as discussed for the price collapse risk and the capacity calculation risk.

### 7.1.2 Impact on Economic Viability of OWFs

The results of the cases simulated show varying results in terms of their impact on economic viability of the OWFs in the OBZ, discussed hereafter per case group.

In Case Group 1, the transmission capacities of the interconnectors were studied (Section 6.2), with the hypothesis that increased HVDC transmission capacity would lead to higher congestion rents, lower generation and redispatch costs, lower electricity prices with fewer price collapses, and increased wind exports due to reduced curtailment. The results confirmed this partially. Increased export capacity (Case $\mathrm{EI}^{+}$) led to higher wind exports and reduced curtailment, primarily by the capacity calculation, but did not significantly increase revenues because the additional wind power was primarily exported during zero-priced hours (expected). Conversely, decreasing export capacity (Case $\mathrm{EI}^{-}$), equivalent to overplanting of wind capacity, substantially increased revenues (unexpected) due to a shift from zero-priced to positive-priced exports, as reduced export capacity decreased competition with onshore renewables (price collapse risk, observed in Section 7.1.1). Increasing interconnectivity to high-priced Zone 1 (Case $\mathrm{II}^{+}_{\mathrm{z1}}$) led to decreased wind exports and increased curtailment by capacity allocation (unexpected) due to increased competition between the OBZ and onshore renewables in zone 2 and 3. Nevertheless, revenues were still increased (expected) as the remaining wind exports were mainly during zero-priced hours. Increasing interconnectivity between two renewable zones (Case $\mathrm{II}^{+}_{\mathrm{z23}}$) improved export capacity and eliminated curtailment by the capacity calculation and reduced curtailment by the capacity allocation leading to higher revenues (expected). These findings indicate that while increased transmission capacity generally increases wind exports and reduces curtailment, it does not necessarily lead to increased revenues due to the changed competition dynamics resulting from the transmission grid alternations (observed in Section 7.1.1).

In Case Group 2, the offshore grid topology in a dual hybrid form was analysed (Section 6.3), varying both installed offshore wind capacity and transmission capacity. The hypothesis was that increased export capacity to high-priced Zone 1 would result in higher wind exports at elevated prices, increasing revenues, while increased export capacity to lower-priced Zone 3 would lead to higher curtailment due to capacity allocation and reduced revenues. The results showed that the symmetrical case (Sym.) achieved the highest revenues (unexpected) due to increased mean electricity prices, a shift in price convergence from the lowest-priced zone to middle and highest-priced zones, thereby reducing price collapse hours and resulting in higher-priced exports. The factors that led to this were less zones and less wind capacity competing for the allocation of transmission capacity towards the high-priced zone during hours where renewable energy sources did not set the price. Doubling wind and transmission capacity near high-priced Zone 1 (Case $\mathrm{Asym}_{z1}$) led to more curtailment and fewer wind exports resulting in lower revenues (unexpected) due to the onshore grid in Zone 1 being unable to import the additional wind power (capacity calculation risk, observed in Section 7.1.1). Conversely, doubling wind and transmission capacity near low-priced Zone 3 (Case $\mathrm{Asym}_{z3}$) showed a decrease in curtailment by the capacity calculation and an increase in curtailment by the capacity allocation with a lesser reduction in wind exports (compared to Case $\mathrm{Asym}_{z1}$), leading to a smaller revenue decrease (expected). The factors leading to this were that wind-dominated zone 3's grid could better absorb addition wind power generation from the OBZ (lower capacity calculation) while increasing competition between the OBZ and wind generation in zone 3 (higher capacity allocation). These findings indicate that increasing transmission capacity towards renewable-dominated zones improves export capacity and price convergence, but the inability of the onshore grid to absorb additional wind power can lead to increased curtailment and reduced revenues

In Case Group 3, onshore grid attenuation was analysed by varying the outages of transmission lines directly at the landing point of the OBZ and further onshore CNEs (Section 6.4). The hypothesis was that onshore grid attenuations would lead to reduced export capability of the OBZ, increasing price collapse hours and curtailment by the capacity calculation, ultimately leading to lower revenues for OWFs. The results confirmed this hypothesis for most cases. An outage at the landing point of the hybrid project in the high-priced zone 1 (case $\mathrm{Out}^{\mathrm{LP}}_{\mathrm{z1}}$) decreased revenues (expected) due to reduced positive-priced wind exports and increased curtailment. The outage of a line at the landing point directly reduced import capacity of zone 1, forcing the OBZ into increased competition with renewable-rich Zones 2 and

3. Conversely, an outage at the landing point of the hybrid project in low-priced Zone 3 (case $\mathrm{Out}_{z3}^{LP}$) increased revenues (unexpected) due to a shift from zero-priced to positive-priced wind exports. The factors leading to this were the reduction in physical import capacity to Zone 3, combined with high-priced zone 1's grid already restricting the OBZ's export capacity, reduced competition between the OBZ and zone 3 and forced wind exports to Zone 2, resulting in higher prices and revenue. An outage further onshore in high-priced zone 1 (case $\mathrm{Out}_{z1}^{on}$), decreased revenues (expected) due to less price convergence and lower mean prices, with substantial increases in non-intuitive priced hours. For an outage further onshore in low-priced Zone 3 (case $\mathrm{Out}_{z3}^{on}$), reduced import capacity to Zone 3 led to more stable prices and fewer zero-priced hours leading to increased revenues (unexpected), for the same reason as case $\mathrm{Out}_{z3}^{LP}$, albeit to a lesser extent. These findings highlight that onshore grid attenuations can significantly impact economic viability, primarily through changes in competition dynamics and the ability of onshore grids to absorb wind power.

In Case Group 4, the generation mix of the onshore zones was analysed by varying the share of renewable generators. The hypothesis was that decreasing the proportion of renewable energy sources would lead to higher and more stable electricity prices, fewer zero-priced hours, decreased curtailment by the capacity allocation, increased exports, and higher revenues for OWFs. The results confirmed this hypothesis. Cases Trans and Fos experienced increased total wind exports and decreased total curtailment, primarily due to the substantial decrease in curtailment by the capacity allocation. The increased total exports during positive prices, along with higher and less volatile electricity prices in the OBZ, led to substantial revenue increases (expected). These findings underline the influence of the presence of cheap renewable generator in the adjacent markets on the level of competition between the OBZ and those onshore markets for the allocation of scarce transmission capacity, highly influencing the price and volume risks' frequency and severity (Section 7.1.1) and the economic viability of the OWFs.

## 7.1.3 Discussion on Effectiveness of Mitigation Measures

### 7.1.2.1 Technological Mitigation Measures

The results of case group 5 (see Section 6.6), where flexible demand agents in the form of electrolysers are incorporated the market clearing, show that this technological measure effectively mitigates both price and volume risk when placed offshore or onshore with a willingness to pay for electricity not consistently higher than the onshore market price.

Specifically, implementing *offshore electrolysers* (cases $\mathrm{H2}_1^{off}$, $\mathrm{H2}_2^{off}$, $\mathrm{H2}_3^{off}$ and $\mathrm{H2}_4^{off}$) creates local demand in the OBZ, leading to increased average electricity prices and reduced price volatility. This mitigation measure almost entirely prevented price collapses by setting a floor price in the OBZ determined by the WTP for electricity. Additionally, the need for wind exports is reduced due to local consumption of electricity, leaving more room for power trade on the interconnectors by adjacent bidding zones, allowing the price to be set more frequently by the adjacent zones. Moreover, this reduced need for the generated wind to be exported out of the OBZ led to reduced competition between the generated wind in the OBZ and onshore renewables for the allocation transmission capacity, thereby reducing curtailment by the capacity allocation. This combination of effects resulted in revenue increases ranging from +71.26% to +108.11%, with the highest WTP for electricity leading to the highest revenue gains. An important observation is that even with a low WTP (case $\mathrm{H2}_4^{off}$, WTP = 10.94 €/MWh), the lowest observed electrolyser dispatch was 65.58% of the time at Full Load, indicating the

Implementing an *onshore electrolyser in low-priced, renewable-dominated* Zone 3 (Case $\mathrm{H2}_{z3}^{on}$, Section 6.6) led to the highest wind exports (92.03% of available wind) and lowest curtailment, associated with increased price convergence and mean prices leading to higher revenues (+61.70%). Moreover, the price collapse risk and the capacity calculation risk were completely mitigated because the additional demand from the electrolyser in Zone 3 absorbed excess wind power, reduced curtailment, and shifted competition from exporting via the OBZ to importing wind power from the OBZ, keeping curtailed volumes below the OBZ's maximum net position. Curtailment by the capacity allocation remained, but also with substantial decreases (-73.98%).

The effectiveness of implementing an *onshore electrolyser in high-priced, fossil-dominated* Zone 1 (Case $H2_{z1}^{on}$, Section 6.6) was limited because the WTP was consistently lower than the electricity price, resulting in only 2% Full Load operation. Despite this, curtailment by both capacity calculation and allocation decreased due to the 750 MW additional load at the landing point, which increased the OBZ's export capacity and reduced competition with onshore renewables. This suggests that placing an electrolyser at the landing point of a congested zone can directly reduce volume risk by increasing the OBZ's export capacity and lessening competition with onshore renewables, provided its WTP algins better with the onshore electricity prices.

Based on these findings, it can be concluded that the implementation of flexible demand agents, considered here in the form of electrolysers, can effectively mitigate price and volume risk for hybrid projects located in an OBZ. While offshore demand agents are most favourable from the perspective of OWF developers due to the elevated revenues, onshore demand agents at the landing point of the hybrid interconnector also prove highly effective in mitigating price and volume risk. While only electrolysers are considered in this analysis, any type of flexible demand agent, and in particular Power-to-Gas solution (see Section 3.2.2.2), could prove effective in mitigation risks for hybrid project. It should be noted that their implementation potentially leads to a shift in social-welfare distribution, with decreased congestion rents and increased redispatch costs observed by their implementation.

#### 7.1.2.2 Regulatory Mitigation Measures

The findings of the TAG analysis (Section 6.7.1) have the following implications. The effectiveness of the TAG is determined by two interacting dimensions: the technical dimension (the grid's ability to absorb wind injection, reflected in curtailment by the capacity calculation) and the market dimension (price dynamics in adjacent bidding zones, reflected in the reference price). While the technical need for the TAG is evident due to observed curtailments by the capacity calculation, market dynamics often set the reference price to zero because of the high supply of renewables in the system, diminishing the TAG's effectiveness. This cannibalisation effect pushes the TAG reference price to zero. However, the Fossil Case results indicate that in a less renewable-dominated system, the TAG can effectively compensate for curtailment by the capacity calculation. Additionally, the TAG compensates for curtailed wind power during negative-priced hours in the OBZ**.**

While the TAG compensations mitigated the capacity calculation risk to a limited extend, leading also to small increases in revenues, the specific TAG design used, and certain modelling assumptions have led to this effectiveness being relatively conservative.

First, the TAG design used in this thesis is based on the current interpretation of the proposal for the amendment of the EC's EMD Regulation See Section 4.3.2), in the absence of the publication of the final EMD reform package. Based on this interpretation, the TAG reference price was determined by the lowest price of the adjacent markets and the compensation volume was set only for the curtailed volume by the capacity calculation. Alternative TAG reference prices, for example based on the electricity price in the Home Market or on the electricity price of the zone where congestion occurs, and inclusion of curtailment by the capacity allocation would lead to increased TAG compensation outcomes (see for example Magid and Winge (2024) for TAG design variations).

Second, the system setup used in the model limited the TAG's effectiveness. Specifically, the over-dimensioning of generation compared to load (see Section 5.1.2) in combination with high installed renewable capacity, led to elevated zero-priced hours due to renewables. Evidenced from the fossil case results, these hours changed in price collapse hours and during those hours the TAG did prove effective.

Nevertheless, this over-dimensioning of cheap renewable generation compared to demand is currently in reality not seen, although this problem could form by the time the first hybrid projects come online (see next section).

The findings of the FTR analysis (Section 6.7.2) indicate that the FTR is effective in covering the price spread between the OBZ and the onshore zone where the FTR contract is in place, particularly if the price spreads are large and occur frequently, as observed for Zone 1. Furthermore, during all price collapse hours in all cases, FTR compensation payments occurred, providing an effective hedging instrument for lost revenues up to the contracted volume of the FTR, thus mitigating the price collapse risk for the contracted part. Additionally, FTR compensations occurred during all non-intuitive priced hours, mitigating this risk. Similar to the TAG compensation, the FTR compensation price during negative-priced hours was positive, partially offsetting the negative revenues for OWF operators during these times. Overall. the implementation of the FTR effectively mitigated all price risks for that part being contracted in the FTR and increased revenues across all cases.

Noteworthy is that for the contracted volume for the FTR used in this analysis assumes an equal distribution with a 1:4 ratio to installed OWF capacity. If this ratio of contracted volume to OWF capacity is increased (e.g. being 1:2 as used in the example provided in Section 4.3.3 in PROMOTioN (2020)) the effectiveness of the FTR in mitigating the price risk and providing increased revenues also increases. Where Laur et al. (2022) propose that (part of) the FTRs should be allocated for free to the OWFs in the hybrid project, simply allowing for increased rights to be contracted over the interconnectors could also be a strategy.

Finally, the combined payments from the FTR and TAG never exceeded total congestion rents amassed by the TSOs (Table 34, Section 6.7.3). This indicates that the FTR payout does not reach its cap of the total received congestion rents by the TSO as indicated by PROMOTioN (2020). Additionally, the concern raised by TenneT (2024) on the availability of TAG compensation for generators (see Section 3.3.1.4) is unlikely to take form considering that the highest observed TAG payment was 1.84% of total congestion rent. Nevertheless, the priority objectives for the use congestion rent remain relevant, as discussed in Section 7.1.4.2. Lastly, the issue raised by ENTSO-E (2023b) that TAG's implementation shields developers for volume risks from competitive market forces is partially refutable based on the results of this analysis, as the high level of competition led to the TAG not sufficiently compensating for the volume risk.

In conclusion, the implementation of FTR and TAG together could be a good combination of regulatory instruments that together address all price risks and the capacity calculation risk. Nevertheless, these instruments are not the only pathway and should be considered in the wider context in which the hybrid project operates, as discussed in the next section.

### 7.1.4 Contextual Considerations on Findings

Hybrid projects involve numerous uncertainties and risks, and their effective deployment is not solely determined by the market risks and potential mitigation measures primarily considered in this thesis. Successful implementation of new technologies also depends on the socio-technical regime in which they are embedded and the exogenous context factors influencing that regime (Geels & Schot, 2007). Additionally, market conditions are part of the socio-technical system, and all influencing factors also affect these conditions, impacting price and volume risk. The contextual considerations on the findings are discussed hereafter: first, their influence on the key factors leading to risk (Section 7.1.4.1), then on the mitigation measures (Section 7.1.4.2), and lastly, multi-actor considerations (Section 7.1.4.3).

#### 7.1.4.1 Contextual Considerations for the Key Factors Leading to Risk

The results of this research underscore the complexities of the interactions and forces at play that lead to price and volume risks for hybrid projects located in an OBZ under FBMC and AHC. Two primary factors and their interactions lead to the most frequent and severe price and volume risks: the physical characteristics of the transmission grid and the market characteristics of the bidding zones connected via the hybrid interconnector. These factors are influenced by contextual considerations.

First, the design choices of the hybrid project should be correctly aligned with the physical characteristics of the transmission grid to which the hybrid is connected since this directly influences the export capacity (or FB domain) of the OBZ. For example, the choice of the landing point of the hybrid interconnector is crucial; selecting a landing point in an already congested onshore grid could restrict the export capacity, leading to price collapses and capacity calculation risks. Additionally, developments in the transmission grids in the coupled markets can influence the export capacity of the OBZ. For instance, a 4GW HVDC transmission cable in Germany, connecting the northern windy states with industrial centres in the south, is expected to be completed in 2028 (Wehrmann, 2023). If this construction is delayed while a hybrid project comes online expecting this interconnector to be in place, the unresolved congestion in Germany's market could restrict the OBZ's export capacity, leading to increased price collapses and curtailment by the capacity calculation, as observed in cases with onshore outages. Furthermore, developments in interconnection transmission capacity between coupled markets in the FB region could influence the capacity allocation risk if these developments alter the dependency of the connected markets on the hybrid project's interconnector for cross-zonal trade. For example, if the Netherlands and the UK are connected with a hybrid interconnector (e.g. via the LionLink (TenneT, n.d.)) and the PtP interconnector between Belgium and the UK is out of operation (e.g. due to technical limitations), the UK's dependency for cross-border trade on the hybrid interconnector to the Netherlands increases, thereby increasing the competition for scarce transmission capacity on this interconnector leading to increased curtailment by the capacity allocation for the OWF.

Secondly, all market developments that alter the competition between the OBZ and onshore markets can further influence price and volume risks. A key consideration here is the speed of development of renewable generation capacity in relation to the formation of demand for electricity. Wind and solar power generation in the EU grew fivefold from 2009 to 2023, significantly increasing their share in the power mix from 5% to 27% (Brown & Jones, 2024). Moreover, the European Commission has set a binding target to achieve at least 42.5% of renewable energy in its overall energy mix by 2030 (European Parliament and European Commission, 2023), further accelerating the integration of renewable energy sources in Europe's electricity markets. On the other hand, while electricity demand in Europe is expected to rise between 2021 and 2030 with roughly 27.5% (McKinsey & Company, 2022), this growth of demand is not at the same pace of the growth of installed renewable capacity. Specifically, the slower pace of electrification in the industrial sector has been a major contributing factor to the lagging demand for electricity, with full-scale industrial electrification anticipated post-2035 (Brown & Jones, 2024). However, until electrification of the industry increases electricity demand, a mismatch between renewable energy supply and electricity demand can formulate around the time the first hybrid projects come only (post 2030). As the results have shown, a system with somewhat over-dimensioned renewable generation capacity compared to the demand for electricity leads to substantial zero-priced hours in the OBZ and more severe curtailment by capacity allocation. The first hybrid projects are thus especially vulnerable to this expected mismatch between supply and demand. This contextual development is crucial to consider, particularly when selecting risk mitigation strategies, as discussed in the subsequent section.

#### 7.1.4.2 Contextual Considerations for the Mitigation Measures

In addition to the potential direct mitigation of price and volume risks by flexible demand agents, their deployment could also address the anticipated mismatch between supply and demand. Dedicated support for renewable flexible demand technologies, such as electrolysers, could concurrently resolve the issue of lagging demand while mitigating some price and volume risks associated with the OWFs in the hybrid project. One viable approach could involve specifically promoting the rollout of electrolysers.

Furthermore, several trade-offs exist when choosing between offshore and onshore deployment for hybrid projects. Offshore deployment lacks local hydrogen demand, necessitating hydrogen transport and storage, which is associated with significant energy losses (Burke et al., 2024). Conversely, onshore deployment near industrial clusters avoids additional transport and storage, thus favouring energy conservation. Additionally, cost trade-offs between HVDC transmission and hydrogen pipelines—whether constructing new pipelines or retrofitting existing gas pipelines—must be considered. Typically, HVDC is more cost-effective near the shore, whereas hydrogen pipelines become more economical over longer distances (Taieb & Shaaban, 2019). All these factors must be meticulously evaluated to optimize the system configuration.

Another pathway, not reliant on demand agents, involves regulatory mitigation instruments. The analysis suggests that a combination of FTRs and TAG could be effective. However, other instruments such as Contracts for Difference (CfDs), particularly capability-based two-sided CfDs as envisioned for the PEZ hybrid project (Elia Group, 2024), also show potential in mitigating price and volume risks. Considering the issue of lagging demand, a strategy implementing CfDs for the initial hybrid projects, anticipated to be operational by 2030, could address the demand-supply mismatch. Once this imbalance is rectified, the strategy could transition from CfDs to a more merchant-based approach with the combination of FTRs and TAG.

The rationale behind this strategy is the following. The oversupply of inexpensive renewable generators relative to demand leads to the cannibalization effect, which depresses prices in the bidding zones and results in increased instances of zero-prices in the OBZ, as well as heightened capacity allocation risks due to intense competition. This scenario is not adequately addressed by FTR and TAG alone but can be mitigated by CfDs. This is because, while the effectiveness of FTRs and TAG depends on the day-ahead prices of the involved bidding zones, the strike price of CfDs is independent of day-ahead market prices and remains unaffected by the cannibalization effect. Additionally, the TAG (in its considered form) only covers the capacity calculation risk, where the CfDs (if 2-sided capability-based) also cover curtailment by the capacity allocation.

Finally, the social welfare redistribution as effectuated by the implementation of the mitigation measures must be considered. For the technological mitigation measures, congestion rents decreased and redispatch costs increased, while DA generation costs somewhat decreased (see Section 6.6.1), indicating some changes in social welfare distribution. As discussed in Section 7.1.2.2, the regulatory instruments necessitated between 20.5% and 52.6% of congestion income, indicating a more pronounced change in social welfare distribution. However, considering that the OBZ setup initially redistributes social-welfare with decreased income for OWFs and increased congestion rents (Kenis et al., 2023), these findings address this issue, which was also the rationale for their implementation. Nevertheless, it is crucial for TSOs to recover the investment costs of the interconnectors, ideally through congestion rents. If these costs are not covered by congestion rents, they would likely need to be recouped through increased grid tariffs on consumers, thereby shifting the financial burden on society. While this thesis primarily considered the perspective of OWF developers in ensuring a favourable investment climate for these hybrid projects to be realised, the design of the risk mitigation measures must still be considered in this broader context to avoid putting the final burden on the consumer.

#### 7.1.4.3 Multi-Actor Considerations

Hybrid projects inherently require international and multi-actor collaboration, including Transmission System Operators (TSOs), governmental entities, wind developers, and industrial partners. Before the market risks considered in this thesis can become a reality, the multi-actor decision process could form a barrier to implementation. For instance, if a hybrid project connects the Netherlands to the UK (such as LionLink) and the UK wind farm receives a Contract for Difference (CfD) while the Dutch side does not, a skewed risk pattern arises between the OWFs participating in the hybrid project.

Additionally, the responsibility for the construction of the transmission cables connecting the Offshore Wind Farms (OWFs), and thereby the influence on determining the transmission capacity, can vary across countries. Consider a hybrid project between the UK and the Netherlands, with OWFs on both sides being hybrid interconnected. In the Netherlands and Germany, TenneT is the designated operator of the offshore grid and responsible for all offshore transmission infrastructure, including the offshore transmission platforms (Rijkswaterstaat, n.d.). In contrast, in the UK, wind farm developers initially build these transmission assets. Once the wind farm becomes operational, these assets must be transferred to an Offshore Transmission Owner (OFTO). Wind farm developers generally decide on the transmission capacity during the design and construction phase (Ofgem, n.d.). However, these decisions are subject to regulatory approval to ensure they meet the necessary standards and are compatible with the overall grid infrastructure.

If the UK wind developer decides to either over-dimension the transmission cable to enable more cross-border trade, or under-dimension the cable (e.g., for cost-saving reasons), both the export capacity and the level of competition for that export capacity are altered, thereby changing the risk dynamics (see Section 7.1.1).

### 7.1.5 Conflicts with Literature

A key implication of the findings in this thesis that conflicts with literature regards the price collapse risk. Within the scope of the considered system in this thesis, price collapses were observed to occur 20% of the time for the reference case (see Section 6.1.3). Although the grid topology used in this thesis has its limitations and is no proximate of reality (see Ssection 7.2.2), the notion made by TenneT (2024) that "*price collapses are presumably not likely to occur"* is questioned by these quantitative findings. Only improved FBMC modelling on hybrid projects under FBMC with transmission grids better approximating reality can determine the exact magnitude of the price collapse risk, but presuming a high likelihood for the price collapse risk not to occur is strongly advised against based on the findings of this thesis.

Furthermore, it is noteworthy that the interacting price and volume risk observed in this study is broader than defined in the literature, which expected only the coexistence of price collapse risk and capacity calculation risk (see Section 3.2.4). Specifically, curtailment, both by capacity calculation and capacity allocation, is observed during zero-priced hours not solely linked to price collapse hours but as a result of price convergence to zero-priced bidding zones due to high renewable supply. Nevertheless, this study provides quantitative evidence that curtailment consistently occurs during zero (or negative) priced hours, even if not exclusively linked to price collapse hours.

## 7.2 Research Limitations

### 7.2.1 Modelling Limitations

A first limitation is that the model does not consider unit commitment constraints, ramping times, or the specific operational constraints of thermal power plants. This simplification overestimates the flexibility of these generators. In reality, some power plants, particularly nuclear power plants, are designed to run continuously and are not able to ramp up or down based on hourly demand variations. This lack of flexibility of conventional generation causes negative electricity prices during hours of increase wind and solar energy production (Götz et al., 2014). By not considering these ramping constraints in this model, negative price formation is excluded in the model[17]. Including unit commitment and ramping constraints in future modelling exercises would provide a more realistic representation of the power system's operational dynamics.

Second, the model assumes perfectly inelastic demand for the nodal load values. In reality, demand for electricity does vary with price to some extent, even if the elasticity is low. Disregarding demand elasticity in the model thus somewhat ignores price responsiveness. The flexible demand agents in the form of electrolysers included in this thesis can be somewhat seen as demand with price elasticity. However, since these hydrogen production units operate purely based on its Willingness-to-Pay for electricity they exhibit a more binary response to price thresholds rather than the continuous and proportionate adjustments typical of truly elastic demand. This binary operation of the electrolysers is also a limitation. Therefore, incorporating elastic demand would more accurately reflect real-world conditions.

Third, forecast errors in wind production are not accounted for in this model. In reality, discrepancies between forecasted and actual wind production can impact the capacity calculation and allocation processes. The model assumes perfect foresight in wind production forecasts, which simplifies the simulation but does not capture the uncertainty faced by system operators. A practical improvement would be to use separate datasets for forecasted and actual wind production capacities based on random probability of a certain range of forecast errors, simulating the discrepancies that occur between the day-ahead (D-1) and two-day-ahead (D-2) forecasts. Related to this is the limitation of the model in assuming no uncertainty of information as input in the FBMC process. In reality, the FBMC process evolves with more accurate information becoming available closer to the delivery time (Schönheit et al., 2021). This more accurate information influences the FB parameters that serve as input in the D-1 market clearing. This model assumes that information is passed stepwise from D-2 to D-1 without any uncertainty, which does not reflect reality.

Fourth, the model does not incorporate the N-1 planning criterion (see Section 2.5). The N-1 planning criterion can be modelled using Load Outage Distribution Factors (See Schönheit et al., 2021). By only considering the N-0 (normal) state without contingencies, the model neglects crucial aspects of network reliability and the potential impact of single line outages as per the N-1 criterion. An enhancement of this model would be to include the N-1 criterion to refine the accuracy of the flow-based market coupling simulation.

Lastly, the model does not include intraday markets, which play a crucial role in balancing supply and demand closer to real-time. Intraday trading allows for adjustments based on more accurate forecasts and could potentially absorb some of the price and volume risks in the OBZ.

### 7.2.2 Grid Topology Limitations

The use of a representative grid model introduces inherent limitations. While it effectively highlights key risks, its direct applicability to actual power systems is constrained. The simplified grid structure facilitates understanding of the effects of flow-based market coupling (FBMC) but fails to capture the full complexity of larger, real-world grids. With three bidding zones adjacent to the offshore bidding zone (OBZ), the results were dependent on these markets. In reality, multiple bidding zones behind the directly connected zones would distribute the effects more broadly.

A more specific implication on the results from the grid topology used in this research was already pointed out in the extreme values validation (Section 4.6.2.2). The CNE in zone 1 connecting the Point-

[17] Noteworthy is that negative electricity prices have been observed, albeit as the consequence of negative non-intuitive price formation in the OBZ (see Section 6.4.2.1) rather than as the consequence of inflexible thermal generation.

to-Point interconnector from zone 2 and the landing point of the hybrid interconnector from the OBZ structurally limited the maximum export capacity of the OBZ, i.e. reducing the FB domain. Because of this, potentially higher curtailment by the capacity calculation is observed. Additionally, this setup potentially led to increased curtailments by the capacity allocation, as the limited import capacity to zone 1 structurally forced the OBZ into additional competition with the renewable dominated zones 2 and 3.

Furthermore, the maximum transmission capacity of the PtP interconnectors between the onshore bidding zones were limited to 200 MW, while the transmission cables of the hybrid interconnectors had transmission capacities of 1500 MW in the reference case. This setup, where 4500 MW out of the total 5100 MW of cross-border interconnection capacity passed through the OBZ, led to a very high dependency of the connected markets on the hybrid for cross-zonal power trade. As discussed in Section 7.1.1, this dependency is a key factor leading to the capacity allocation risk, whereby this grid topology setup artificially increased the level of competition on the hybrid interconnectors leading to elevated results in terms of the frequency and severity of the capacity allocation risk. In reality, this high dependency of coupled markets on the hybrid interconnectors is less likely, as markets are generally better interconnected due to more bidding zones and higher capacity interconnectors between zones compared to those connecting the hybrid project.

Despite these limitations in the grid topology used in this thesis, the smaller grid model proved advantageous for analytical purposes. It allowed for a clearer observation of key risk factors across various cases without the increased FB complexities present in larger grids. Moreover, it effectively demonstrated the OBZ's vulnerability to onshore grid constraints and competition with coupled renewable-dominated markets.

### 7.2.3 Data Input Limitations

Regarding implications of the results in relation to data inputs, the first important notion is that the generation capacities in the onshore markets were somewhat over-dimensioned compared to the load data used in the model (see Section 5.1.2). Additionally, it was chosen to include a high share of renewable capacity in the generation mix for the reference case. The implication if this combination of over-dimensioned generation compared to load in a high-renewable system specifically resulted in increased competition between the OBZ and these renewable energy sources which is, as discussed in Section 7.1.1, a key factor leading to both price and volume risks. This specific setup thus led to somewhat elevated results in terms of the frequency and magnitude of the price and volume risks. Nevertheless, it aided in highlighting the risk patterns and underlying mechanisms that come with this elevated level of competition, which is considerably of higher scientific relevance than the specific frequencies and magnitudes of the price and volume risks associated with this specific system setup.

A second data related implication on the results regards the assumption on the 70% rule for the onshore CNECs. The calculation used for the RAM values for the onshore CNECs assumed that the largest value of either the estimated RAM by the D-2 base case computation, or the 70% of the thermal capacity of the AC lines was used in the D-1 market clearing optimization (Equation A.4). Because of this assumption, there is relatively more transmission capacity in the AC lines put available to the market then would be the case in reality. That is, in reality TSO's often donnot respect the 70% rule and put even lower capacities available to the market. While this data assumption is relatively low to the results outcomes, it might have slightly increased the maximum export capacity from the OBZ to the onshore zones.

A last data related assumption regards the NTC value assumption for the cross-border DC lines. The NTC values were assumed to be 100% of the thermal capacity to avoid trade restrictions on the interconnectors. This assumption was intended to mimic the more integrated nature of bidding zones within the CORE CCR. However, in scenarios involving multiple CCRs, e.g. when connecting and the Netherlands to the UK or to Norway via a hybrid interconnector, this NTC assumption would have to be adjusted since assuming 100% would in these cases not be an adequate assumption. Future modelling considering hybrid projects across different CCRs should consider more conservative assumptions on NTC values to better simulate real-world conditions.

# Chapter 8. Conclusion & Recommendations

In this chapter, the conclusions to the research' subquestions and main research question are provided (Section 8.1). Thereafter, recommendations for policy makers and stakeholders are provided (Section 8.2), as well as future modelling and research recommendations (Section 8.3)

## 8.1 Conclusions

The main objective of this thesis was to identify the key factors leading to price and volume risks for hybrid projects and to assess the effectiveness of their mitigation measures. In order to achieve this objective, four subquestions have been answered, to ultimately answer the main research question.

> **SQ.1**: *What are the specific Price and Volume risks emerging for hybrid OWFs in an OBZ under flow-based market coupling?*

The specific price risks are the *flat price risk*, the increased risk of uncertain and fluctuating electricity prices in the OBZ, the *non-intuitive price risk*, the risk that the capture price in the OBZ could be 'out of bounds' compared to adjacent bidding zones due to the influence of CNECs on price formation, and the *price collapse risk*, the risk that restricted export capacity from the OBZ lead to the electricity price to collapse to zero. The specific volume risks are the *technical unavailability volume risk*, the risk of curtailment by the interconnectors' technical, the *capacity calculation volume risk*, the risk of curtailment by restricted export capacity from the OBZ to the surrounding AC onshore grid as determined by the flow-based capacity calculation, and the *capacity allocation volume risk,* the risk of curtailment by transmission capacity not being allocated to the OWFs in the OBZ as determined by the flow-based capacity allocation. The *interacting price and volume risk* is the coexistence of the price collapse risk and the capacity calculation volume risk.

> **SQ.2**: *What are Regulatory and Technological Mitigation Measures for Price and Volume risks and how could they alleviate the risks?*

Regulatory mitigation measures include CfDs, FTRs and the TAG, with the PPAs being an additional hedging instrument without direct governmental intervention. CfDs stabilise revenue by compensating for price differences with respect to a set strike price, mitigating all price risks and, if 2-sided and capability-based, both the capacity calculation and allocation volume risk. FTRs stabilise revenues by bridging price differences across bidding zones, mitigating all price risks for the contracted volume. The TAG protects against the capacity calculation volume risks by ensuring compensation if export capacities are curtailed due to transmission constraints. PPAs secure long-term sales at predetermined prices, mitigating all price risks and, depending on the specific PPA design, both the capacity calculation and allocation volume risk. The combination of the FTRs and the TAG were selected for further analysis.

Technological mitigation measures include all flexible demand technologies deployable either offshore, within the OBZ, or onshore, directly at the landing point of the hybrid interconnector. Power-to-Gas technologies, i.e. hydrogen or ammonia production, potentially mitigate all price and volume risks. Energy storage solutions, i.e. BESS, CAES, PHS and underground hydrogen storage, could mitigate all price and volume risks, except the technical unavailability volume risk, but to a limited extent as they primarily shift the exported power instead of consuming it. Hydrogen production has been selected for further analysis, both in the form of offshore and onshore electrolysers.

> **SQ.3**: *What are the key factors leading to the most frequent and severe price and volume risks and what is their impact on the economic viability of OWFs?*

Two key factors leading to the most frequent and severe price and volume risk are observed: the transmission *grid's physical characteristic*, i.e. the OBZ's export capacity or FB domain as influenced by the offshore grid topology and onshore outages, and the *market characterises* of the bidding zones connected via the hybrid interconnector, i.e. the level of competition between the OBZ and onshore (renewable) generators for the allocation of scarce transmission capacity.

The interplay between the grid's physical characteristics and market characteristics, driven by the FBMC approach and AHC method, results in varying patterns of frequency and severity across each of the price and volume risk categories, as discussed in Section 7.1.1. Additionally, all variables that directly or indirectly alter the export capacity of the OBZ and/or the level of competition between the OBZ and onshore (renewable) generators lead to different distributions, frequencies, and severities of price and volume risks, subsequently impacting the economic viability of OWFs, as discussed in Section 7.1.2.

> **SQ.4**: *To what extent can Regulatory and Technological measures potentially mitigate price and volume risk?*

Offshore flexible demand agents, such as offshore electrolysers, effectively mitigate price and volume risks by increasing local demand in the OBZ. This raises average electricity prices, reduces price volatility, and decreases the need for wind exports, resulting in revenue increases between 71.26% and 108.11%. Onshore electrolysers are also effective in reducing curtailment and increasing price convergence in low-priced, renewable-dominated zones, leading to a 61.70% revenue increase. However, their effectiveness in high-priced, fossil-dominated zones is limited due to their dependency on the alignment of their WTP with onshore electricity prices and restricted operation at full load. The effectiveness of the TAG is influenced by the magnitude of curtailment by the capacity calculation and the price dynamics in adjacent bidding zones, resulting in limited effectiveness in this thesis (revenue increases between 0% and 3.06%) due to minimal price differences between zones caused by the cannibalization effect and high curtailments by the capacity calculation. FTRs are highly effective in mitigating price risks by covering the price spread between OBZ and onshore zones, ensuring compensation during price collapse, non-intuitive, and negative-priced hours. With only a 1:4 ratio in OWF capacity to contracted FTRs, revenues were enhanced between 60% and 411%.

> **RQ:** *How do the offshore grid topology, onshore grid attenuations and the integration of renewable energy sources influence price and volume risk and to what extend do regulatory and technological measures mitigate these risks?*

Offshore grid topology changes influence price and volume risks primarily through alterations in export capacity from the OBZ and the resulting market dynamics. Increased transmission capacity generally reduces curtailment by the capacity calculation, but its influence on price collapses and curtailment by the capacity allocation depends on pre-existing onshore grid restrictions limiting import capacity, the level of increased competition between the OBZ and low-priced zones to export to high-priced zones as a consequence of this grid enhancement, and the shifted market dynamic from competition to export to the necessity to import from the OBZ. Connecting with two markets instead of three in a hybrid project concentrates competition, leading to increased price convergence between these markets and increased total curtailment. However, depending on asymmetry in installed wind and transmission capacity close to either the high-priced or low-priced market, there are varying impacts on price collapses and the distribution of curtailment by the capacity calculation and allocation risk.

Similar to offshore grid topology changes, onshore grid attenuations influence price and volume risks primarily through changes in export capacity from the OBZ and the resulting market dynamics. Outages in high-priced (fossil) zones with a pre-existing weak grid typically reduce that zone's import capacity, intensifying competition to export to this zone. This results in increased curtailment by the capacity allocation, price collapses, reduced price convergence, and thus increased revenues. Outages at the landing point lead to increased curtailment by the capacity calculation, while outages further onshore decrease curtailment by the capacity calculation and substantially increase negative non-intuitive price formation. Outages in low-priced (renewable) zones reduce that zone's import capacity, resulting in increased curtailment by the capacity calculation and increased positive non-intuitive price formation, but decreased curtailment by the capacity allocation and price collapses due to the shift from competing to export to necessitating import from the OBZ. This effect is more pronounced for onshore outages than for outages at the landing point.

The integration of renewable energy sources in onshore markets increases the competition for scarce transmission capacity, leading to more frequent and severe curtailment by capacity allocation and price collapses during high-wind hours. Depending on pre-existing grid restrictions, this also exacerbates curtailment by the capacity calculation.

## 8.2. Policy and Stakeholder Recommendations

This thesis has developed a profound understanding of the factors leading to price and volume risks associated with hybrid projects and assessed the effectiveness of various mitigation measures. Based on these findings, recommendations can be formulated for policy makers, TSOs and industry actors to proactively address these risk-driving factors during the design and implementation process of the first hybrid projects to contribute to their timely development.

### 8.2.1 Recommendations for Policy Makers

The first recommendation for policy makers is to actively stimulate the deployment of flexible demand technologies, such as electrolysers, as no-regret option. These technologies help balance the supply-demand mismatch, benefiting not only hybrid projects but all renewable energy generation. Furthermore, TSOs should decide on a specific support strategy for hybrid projects, with two main flavours emerging: a merchant-based (technological) approach or a regulatory-only approach.

For the merchant-based approach, it is recommended to specifically stimulate the deployment of flexible demand, e.g. electrolysers, in combination with the development of the hybrid project, with a choice between offshore and onshore deployment. For offshore applications, implementing a separate tender process to auction the electrolyser could be a strategy to ensure fair competition and prevent gaming in the OBZ. For onshore installations, the current Dutch offshore wind tender strategy, as evidenced by the most recent tender (Rijksoverheid, 2024), is adequate since its system integration component leaves room for deploying a dedicated flexible demand sink at the landing point. Energy conservation, proximity to demand and infrastructure cost must be carefully considered when choosing between offshore and onshore applications. The optimisation model by Kenis et al. (2024) can aid in optimising these endogenous infrastructure investments. The merchant-based strategy leaves room for PPAs.

For the regulatory-only approach, implementing the combination of FTRs and the TAG is recommended, with the optional inclusion of 2-sided capability-based CfDs to be implemented for the first hybrid projects until the supply/demand mismatch is resolved. Here, ensuring a sufficiently high ratio of contracted volume to OWF capacity for the FTRs potentially leaves the recommendation of Laur et al. (2022) for (partial) free allocation of rights to developers unnecessary. The TAG design considered in this thesis is a minimal compensation structure, with potential for alternative reference price determination and optional inclusion of curtailment by the capacity allocation.

Choosing between these two strategies necessitates careful consideration regarding the fair redistribution of costs and benefits between developers and TSOs, while avoiding shifting financial burdens to consumers.

### 8.2.1 Recommendations for TSOs

For TSOs it is highly recommended to carefully consider the selection of landing points for these hybrid projects to avoid structural congestion since this highly impacts the hybrid project's vulnerability to price and volume risks. Locating landing points further inland can reduce dependency on limited onshore CNECs, reducing this vulnerability. Prioritising grid enhancements near landing points to address potential structural congestion is also essential. Moreover, the delay of crucial intra-zonal transmission cables or cross-border transmission developments, both in bidding zones directly adjacent the hybrid as further away, must be identified and communicated to developers in timely manner since they can alter the OBZ's export capacity and/or the dependency on the hybrid interconnectors for cross-border trade, thereby impacting risks.

### 8.2.3 Recommendations for Developers

For developers, it is recommended to explore investments in flexible demand assets. Offshore demand technologies, such as electrolysis, even in small scales, can help mitigate price collapse risks and increase OWF revenues by setting a floor price in the OBZ, making them a worthwhile investment. Additionally, strategically investing in onshore flexible demand assets near expected landing points before the tender process for hybrid projects is advisable. If the developer of these flexible demand assets also participates in the OWF tender, the pre-existing reduced risk profile allows for more competitive bids, enhancing the likelihood of winning the tender. If developers do not participate in the OWF tender, they can still establish a favourable position for corporate PPAs with the developer who does.

Moreover, it is highly recommended for developers to include FBMC modelling exercises, preferably with the inclusion of AHC, in determining risk profiles and market expectations for future offshore wind investments. This is especially crucial when participating in the tendering process of these first hybrid projects.

### 8.2.4 International Multi-Actor Recommendations

Uniform decision-making across all actors and North Sea countries is crucial, in particular with respect to alignment in design choices for the hybrid project and symmetry in deployment of support instruments to reallocate costs and benefits. Strategies to facilitate this could include the establishment of an independent Offshore Transmission System Operator (OTSO) in the North Sea, which would be the responsible party and owner of all transmission assets involved in hybrid projects, thereby facilitating decision-making in the technical design between the involved countries. Additionally, the proposal of an Offshore Investment Bank (OIB) by Elia Group and Orsted (2024) could act as an independent entity responsible for the reallocation of costs and benefits among the stakeholders involved, while facilitating and de-risking investments in hybrid projects.

## 8.3 Model Development and Future Research

Future research should utilize comprehensive grid models, such as PyPSA (Brown et al., 2018) or POMATO (Weinhold & Mieth, 2021), incorporating numerous bidding zones and realistic generation mixes to provide a more accurate representation of market dynamics and interdependencies. Additionally, future models should consider stricter Net Transfer Capacity (NTC) values to better simulate real-world conditions and the impact of cross-border transmission constraints on the Flow-Based (FB) domain for different Capacity Calculation Regions (CCRs), especially for projects like LionLink (TenneT, n.d.) that connect the UK with the Netherlands via a hybrid interconnector, thereby linking different CCRs. Incorporating these elements will enhance the robustness and applicability of the models, providing more accurate insights for decision-making.

Furthermore, when multiple hybrid projects are modelled simultaneously in the North Sea, such as for ENTSO-E's entire offshore network development plan (ENTSO-E, 2024a), considering offshore nodal pricing (ONP) per hybrid project rather than one central offshore bidding zone for all projects is recommended. ONP better represents congestion between OWFs, as multiple disconnected hybrid projects are not expected to be located together in one OBZ. However, the introduced modelling step in this thesis—operationalizing the difference between curtailment by the capacity calculation and allocation in FBMC modelling—becomes more complex under ONP. This complexity arises because flows between OWFs now also flow between bidding zones, influencing each other's net positions. Optimizing the individual net positions of the nodal zones per OWF based on the capacity calculation outcomes, as introduced in this thesis, may not accurately reflect the physical export capacity per OWF due to these flows. Future research should focus on finding a solution for this if modelling ONP while distinguishing between capacity calculation and allocation risk is desired.

Finally, a significant area for improvement lies in developing a replicable electricity market model that captures the complexities of Euphemia and FBMC while closely mirroring the real-world procedures of TSOs. The simplified FBMC process used in this thesis, which is a common practice in FBMC modelling, does not precisely replicate the detailed steps taken by TSOs. One of the major challenges in achieving a more accurate model is the limited access to critical data and procedural insights from TSOs available to the scientific community and industry.

# Chapter 9. Reflection

Embarking on my thesis project marked the culmination of my academic journey and the beginning of my professional career. Initially sparked by a genuine interest in energy islands and power hubs during a previous internship at Eneco, the focus of this project shifted to the complex topic of flow-based market coupling. My fascination with electricity market design, innovative multi-actor renewable infrastructure projects, and complex modelling deepened through this challenging project. The complexities of the modelling exercise required for this thesis far exceeded my initial expectations, teaching me valuable lessons for future projects and better preparation for such significant undertakings.

Throughout my life, I have consistently challenged myself, often finding these challenges manageable. However, this project required complete dedication from start to finish, a commitment that my friends and family likely noticed through my frequent absences at social gatherings. Pushing myself to the limits taught me a lot, but I realised the importance of understanding the scope of a project before diving in. While academic research inherently involves unknowns, this project felt somewhat like opening Pandora's box without knowing it. Nevertheless, I am proud of my successful completion of this ambitious project.

One significant challenge was fully understanding the model I was working with. I initially created a demo model but quickly moved to the more complex one by Kenis et al. (2023) before thoroughly understanding the simpler version. This premature shift led to delays in implementing additional modelling steps and postponed result creation and analysis to the project's final stages. In hindsight, this approach could have been improved by better structurally demarcating modelling functionalities and understanding before moving to the bigger model. Additionally, generating results and analysing them earlier is something I should have done since this would have highlighted errors or inadequate functionalities of the model sooner.

My programming skills saw a steep learning curve, particularly with the Julia language. I had limited programming experience, primarily with basic Python scripts and Agent Based Modelling in NetLogo. With the aid of AI tools like ChatGPT, I rapidly learned to write, use, and implement different coding techniques in Julia. This support was crucial, and I acknowledge that without it, learning Julia would have taken at least twice as long, making the project's scope unachievable for me.

Additionally, the internship at RWE and attending the 2024 WindEurope Conference in Bilbao allowed me to engage with and learn from various industry experts, including offshore wind developers, TSO representatives, and energy ministers. These interactions elevated my interest and engagement in the project to a higher level and a broader perspective. It made me realise that my research is only a very narrow yet crucial aspect of the complex socio-technical system surrounding hybrid projects. This realisation motivated me even more to work towards a successful completion while keeping in mind the bigger context I was operating in. On the other hand, engaging with these various stakeholders and working from within one of the world’s leading offshore wind developers made me aware of the significant lack of knowledge transfer from the academic world to the right industry and governmental actors working on the implementation of hybrid projects. A lack of knowledge diffusion across the actors in the emerging socio-technical system surrounding hybrid projects can form a key barrier hampering the technology to move from the current pre-development stage to the development stage (Hekkert et al., 2007; Hekkert et al., 2011). With this thesis, in this collaborative form between TU Delft and RWE, I hope to partially contribute to this highly necessary knowledge diffusion.

Overall, this project has been a lesson in time management, problem-solving, and maintaining a broad perspective amidst intricate challenges. The structured environment of the internship and practical experience have significantly complemented my academic pursuits, underscoring the importance of balancing theoretical knowledge with real-world application. I look back on a very interesting and challenging graduation project that far exceeded my expectations. I consider it a successful culmination of my academic journey and the beginning of a professional career in which I aim to seek the most impactful journey in tackling one of the greatest societal challenges: mitigating human-induced global warming.

# Bibliography


ACER & CEER. (2022). *ACER and CEER REFLECTION ON THE EU STRATEGY TO HARNESS THE POTENTIAL OF OFFSHORE RENEWABLE ENERGY FOR A CLIMATE NEUTRAL FUTURE*. https://eur-lex.europa.eu/legal-content/EN/TXT/PDF/?uri=CELEX:52020DC0741&from=EN

ACER (2015). *Congestion Income Distribution methodology: in accordance with Article 73 of the Commission Regulation (EU) 2015/1222 of 24 July 2015 establishing a guideline on Capacity Allocation and Congestion Management.* .https://www.acer.europa.eu/sites/default/files/documents/Individual%20Decisions_annex/ACER_Decision_16-2023_on_CIDM-Annex_I.pdf

Alfa Laval, Hafnia, Haldor Topsoe, Vestas & Siemens Gamesa (2020). Ammonfuel – An industrial view of ammonia as a marine fuel (Version 09.9). https://www.topsoe.com/hubfs/DOWNLOADS/DOWNLOADS%20-%20White%20papers/Ammonfuel%20Report%20Version%2009.9%20August%203_update.pdf

Amprion (2018). FLOW BASED MARKET COUPLING: DEVELOPMENT OF THE MARKET AND GRID SITUATION 2015 – 2017. https://www.amprion.net/Dokumente/Dialog/Downloads/Studien/CWE/CWE-Studie_englisch.pdf

Antonopoulos, G., Vitiello, S., Fulli, G., & Masera, M. (2020). Nodal pricing in the European Internal Electricity Market. *European Commission. JRC Technical Reports.* https://doi.org/10.2760/41018

Arellano-Prieto, Y., Chavez-Panduro, E., Salvo Rossi, P., & Finotti, F. (2022). Energy storage solutions for offshore applications. *Energies*, *15*(17), 6153.

Benford, D. (2008). Risk—What is it?. *Toxicology letters*, 180(2), 68-71.

Bonamente, M. (2017). Statistics and Analysis of Scientific Data (3rd ed.). *Springer.*

Brown, T., Hörsch, J., & Schlachtberger, D. (2017). PyPSA: Python for power system analysis. a*rXiv preprint arXiv:1707.09913*.

Brown, S. & Jones, D. (2024). European Electricity Review 2024: Europe's electricity transition takes crucial strides forward. *Ember*.

Bruninx, K. (2022). *To derive the KKT conditions of an optimization problem, always follow these steps*. [Lecture notes]. SEN1511 Engineering Optimisation, TU Delft. Available from Brightspace [Restricted access].

Burke, A., Ogden, J., Fulton, L., & Cerniauskas, S. (2024). Hydrogen Storage and Transport: Technologies and Costs. *Institute of Transportation Studies, UCD-ITS-RR-24-17*.

CEER (2004). *Security of Electricity Supply*. https://www.ceer.eu/documents/104400/-/-/1b77d632-1ea6-72e7-0c44-dd9282118cec

Core TSOs (2023). the Second amendment of the Day-Ahead Capacity Calculation Methodology of Core Capacity Calculation Region. https://www.acm.nl/system/files/documents/bijlage-2-voorstel-tweede-wijziging-day-ahead-capaciteitsberekening-core.pdf.

Council of the European Union and European Parliament (2019). *Regulation (EU) No 2019/943 of the European Parliament and of the Council of 5 June 2019 on the internal market for electricity*. https://eur-lex.europa.eu/eli/reg/2019/943/oj

Dedecca, J. G., Hakvoort, R. A., & Herder, P. M. (2017). Transmission expansion simulation for the European Northern Seas offshore grid. Energy, 125, 805–824. https://doi.org/10.1016/j.energy.2017.02.111

Dedecca, J. G., Lumbreras, S., Ramos, A., Hakvoort, R. A., & Herder, P. M. (2018). Expansion planning of the North Sea offshore grid: Simulation of integrated governance constraints. Energy Economics, 72, 376–392. https://doi.org/10.1016/j.eneco.2018.04.037

De Vries, L. J., Correljé, A. F., Knops, P. A., & Van der Veen, R. (2020). Electricity: Market design and policy choices.

Dinh, Q. V., Mosadeghi, H., Pereira, P. H. T., & Leahy, P. G. (2023). A geospatial method for estimating the levelised cost of hydrogen production from offshore wind. *International Journal of Hydrogen Energy, 48*(40), 15000-15013.

Directive 2019:944. on common rules for the internal market for electricity and amending Directive 2012/27/EU. https://eur-lex.europa.eu/legal-content/EN/TXT/?uri=uriserv:OJ.L_.2019.158.01.0125.01.ENG&toc=OJ:L:2019:158:TOC

Tweede Kamer (2024). Electricity cost assessment for large industry in the Netherlands, Belgium, Germany and France – Management Summary Report. *E-Bridge*. Retrieved on 16-06-2024, from: https://www.tweedekamer.nl/downloads/document?id=2024D13165

Elia Group (2024). Public consultation Task Force Princess Elisabeth Zone. *Consultation Report*.

Elia Group & Orsted (2024). Making Hybrids Happen: Enabling offshore hybrid projects to en hance Europe's energy transition. https://orstedcdn.azureedge.net/-/media/www/docs/corp/com/about-us/whitepaper/elia-group-x-orsted-making-hybrids-happen.pdf?rev=e405a760ebc040d6bfea7879fa82c3b3&hash=FAB14D870BB4AC1B2ABA6CB3B215EF7C

Elia Group (n.d.). TritonLink. Retrieved on 30-07-2024 from: https://www.tennet.eu/lionlink

ENTSO-E (n.d.). Day-ahead capacity calculation. Retrieved on 05-08-2024 from: https://www.entsoe.eu/bites/ccr-core/day-ahead/

ENTSO-E. (2020a). *European Network of Transmission System Operators for Electricity ENTSO-E Position on Offshore Development Market and Regulatory Issues*. https://eepublicdownloads.azureedge.net/clean-documents/Publications/Position%20papers%20and%20reports/entso-e_pp_Offshore_Development_Market_Reg_Issues_201014.pdf

ENTSO-E (2020b). *Capacity Calculation Regions Assessment Report.* European Network of Transmission System Operators for Electricity. Retrieved on 20-06-2024 from: https://eepublicdownloads.entsoe.eu/clean-documents/Network%20codes%20documents/Implementation/ccr/200930_ALL_TSOs_CCR_Assessment_report.pdf

ENTSO-E (2023a). *CACM Congestion Income Distribution methodology*. All TSOs' proposal for amendment of Congestion Income Distribution methodology in accordance with Article 73 of the Commission Regulation (EU) 2015/1222 of 24 July 2015 establishing a guideline on Capacity Allocation and Congestion Management .

ENTSO-E (2023b). *ENTSO-E Position on the EC proposals on Market Design*. https://eepublicdownloads.blob.core.windows.net/public-cdn-container/clean-documents/Publications/Position%20papers%20and%20reports/2023/entso-e_EMDR_One-pagers_230331.pdf

ENTSO-E. (2024a). *Offshore Network Development Plans: European offshore network transmission infrastructure needs*. https://eepublicdownloads.blob.core.windows.net/public-cdn-container/tyndp-documents/ONDP2024/ONDP2024-pan-EU-summary.pdf

ENTSO-E (2024b). *Day Ahead Capacity Calculation*. Retrieved on 05-06-2024, from: https://www.entsoe.eu/bites/ccr-core/day-ahead/#fc11

Epexspot (2024). *Market Data*. Retrieved on 05-06-2024, from: https://www.epexspot.com/en/market-data

European Commission (2015). Establishing a guideline on capacity allocation and congestion management. *COMMISSION REGULATION (EU) 2015/1222.*

European Commission (2016). Commission Staff Working Document: Impact Assessment. *SWD(2016) 410 final. Brussel.*

European Commission. (2020a). *COMMUNICATION FROM THE COMMISSION TO THE EUROPEAN PARLIAMENT, THE COUNCIL, THE EUROPEAN ECONOMIC AND SOCIAL COMMITTEE AND THE COMMITTEE OF THE REGIONS: An EU Strategy to harness the potential of offshore renewable energy for a climate neutral future*. COM(2020) 741. https://eur-lex.europa.eu/legal-content/EN/TXT/PDF/?uri=CELEX:52020DC0741

European Commission (2020b). *COMMISSION STAFF WORKING DOCUMENT, Accompanying the document COMMUNICATION FROM THE COMMISSION TO THE EUROPEAN PARLIAMENT, THE COUNCIL, THE EUROPEAN ECONOMIC AND SOCIAL COMMITTEE AND THE COMMIITTEE OF THE REGIONS: An EU strategy to harness the potential of offshore renewable energy for a climate neutral future.* SWD(2020) 273. https://eur-lex.europa.eu/legal-content/EN/TXT/PDF/?from=EN&uri=CELEX%3A52020SC0273

European Commission (2020c). *Proposal for a regulation of the European Parliament and of the Council on guidelines for trans-European energy infrastructure and repealing Regulation (EU) No 347/2013*. https://energy.ec.europa.eu/system/files/2020-12/revised_ten-e_regulation__0.pdf

European Commission (2023). *European Meteorological derived High Resolution RES generation time series for present and future scenarios* – EMHIRES. https://data.jrc.ec.europa.eu/collection/id-0055

European Parliament and European Council (2023). *Directive (EU) 2023/2413 of the European Parliament and of the Council of 20 November 2023 on the promotion of the use of energy from renewable sources*. Official Journal of the European Union. https://eur-lex.europa.eu/legal-content/EN/TXT/?uri=OJ:L_202302413

European Parliament and European Council (2024). *REGULATION OF THE EUROPEAN PARLIAMENT AND OF THE COUNCIL amending Regulations (EU) 2019/942 and (EU) 2019/943 as regards improving the Union's electricity market design*. Official Journal of the European Union. https://eur-lex.europa.eu/eli/reg/2024/1747/oj

Geels, F. W., & Schot, J. (2007). Typology of sociotechnical transition pathways. *Research policy*, *36*(3), 399-417.

Gouda, E. M., Fan, Y., Benaouicha, M., Neu, T., & Luo, L. (2021). Review on Liquid Piston technology for compressed air energy storage. *Journal of Energy Storage*, *43*, 103111.

Götz, P., Henkel, J., Lenck, T., & Lenz, K. (2014). Negative Electricity Prices: Causes and Effects: An analysis of recent developments and a proposal for a flexibility law. *Agora Energiewende.* https://www.agora-energiewende.de/fileadmin/Projekte/2013/Agora_Negative_Electricity_Prices_Web.pdf

Green, R., Hu, H., & Vasilakos, N. (2011). Turning the wind into hydrogen: The long-run impact on electricity prices and generating capacity. *Energy Policy, 39*(7), 3992-3998.

Gurobi (n.d.). Gurobi Optimizer: The World's Fastest Solver. Accessed on 9-6-2024 Retreived from: https://www.gurobi.com/solutions/gurobi-optimizer/

Hekkert, M. P., Suurs, R. A. A., Negro, S. O., Kuhlmann, S., & Smits, R. E. H. M. (2007). Functions of innovation systems: A new approach for analysing technological change. *Technological Forecasting and Social Change*, 74(4), 413–432.

Hekkert, M. P., Negro, S., Heimeriks, G., Harmsen, R. (2011). Technological Innovation System Analysis: A manual for analysts. *Utrecht University: Utrecht*.

Hillier, F. S., & Lieberman, G. J. (2015). Duality Theory. In *Introduction to Operations Research* (10th ed., pp. 197-221). McGraw-Hill Education.

Huang, D. (2011). Dynamic PTDF Implementation in the Market Model (Master Thesis). *TU Delft, Delft University of Technology*.

Jansen, M., Duffy, C., Green, T. C., & Staffell, I. (2022). Island in the Sea: The prospects and impacts of an offshore wind power hub in the North Sea. *Advances in Applied Energy*, *6*. https://doi.org/10.1016/j.adapen.2022.100090

JAO (2020). Documentation of the CWE FB MC solution. *Version 5.0*. https://www.jao.eu/sites/default/files/2021-05/CWE%20FBMC%20AP%20Main%20Document%20v20200710%20.pdf

JAO (2022). *Core Flow-Based Markte Coupling.* https://www.jao.eu/core-fb-da-mc

Jetten, R. A. A. (2024). Kamerbrief over vergunningverlening windenergie op zee (4 GW): IJmuiden Ver Gamma en Nederwiek I. Retrieved on 28-07-2024, from: https://open.overheid.nl/documenten/35f2feba-72cc-4c62-8731-c34261f0aee1/file

JuMP (2024). What is JuMP? Retrieved on 26-06-2024, from: https://jump.dev/

Kenis, M., Delarue, E., Bruninx, K., & Dominguez, F. (2023). Off-shore Bidding Zones Under Flow-Based Market Coupling. In *2023 IEEE Belgrade PowerTech* (pp. 1-6). IEEE.

Kenis, M., Dvorkin, V., Schittekatte, T., Bruninx, K., Delarue, E., & Botterud, A. (2024). Evaluating Offshore Electricity Market Design Considering Endogenous Infrastructure Investments: Zonal or Nodal?. *IEEE Transactions on Energy Markets, Policy and Regulation.*

KPMG (2022). *How to evaluate the cost of green hydrogen business case? – Assessing green hydrogen production costs.* Retrieved on 17-06-2024, from: https://assets.kpmg.com/content/dam/kpmg/be/pdf/2022/hydrogen-industry-1.pdf

KU Leuven. (2015). Cross-border electricity trading: towards flow-based market coupling. *Eifact Sheet,* 2.

Laur, A., Küpper, G., & Henneaux, P. (2022). *Support on the use of congestion revenues for Offshore Renewable Energy Projects connected to more than one market*. European Commission. https://energy.ec.europa.eu/system/files/2022-09/Congestion%20offshore%20BZ.ENGIE%20Impact.FinalReport_topublish.pdf

Li, M. & Seguinot, B. (2017). Modelling of Flow-Based Domains in Antares for Adequacy Studies. *RTE*. https://antares-simulator.org/media/files/page/ZHX0N-171024-Rte-Modelling-of-Flow-Based-Domains-in-Antares-for-Adequacy-Studies.pdf

Magid, S. H. C. & Winge, S. (2024). Use of congestion revenues to manage the volume and price risks related to offshore bidding zones in combination with hybrid projects (Master Thesis). *Technical University of Denmark.*

McKinsey & Company (2022). Global Energy Perspective 2022. Executive Summary. https://www.mckinsey.com/~/media/McKinsey/Industries/Oil%20and%20Gas/Our%20Insights/Global%20Energy%20Perspective%202022/Global-Energy-Perspective-2022-Executive-Summary.pdf

Miglietta, M. M., Huld, T., & Monforti-Ferrario, F. (2017). Local complementarity of wind and solar energy resources over Europe: an assessment study from a meteorological perspective. *Journal of Applied Meteorology and Climatology, 56*(1), 217-234.

Muhammed, N. S., Haq, M. B., Al Shehri, D. A., Al-Ahmed, A., Rahman, M. M., Zaman, E., & Iglauer, S. (2023). Hydrogen storage in depleted gas reservoirs: A comprehensive review. *Fuel*, *337*, 127032.

Müller, C., Hoffrichter, A., Büchel, H. B., Schwarz, A., & Schnettler, A. (2017). Integration of hvdc-links into flow-based market coupling: Standard hybrid market coupling versus advanced hybrid market coupling. *In CIGRE Symposium.*

Netbeheer Nederland (2024). *Capaciteitskaart invoeding elektriciteitsnet.* Accessed on 8-5-2024 from: https://capaciteitskaart.netbeheernederland.nl/?_gl=1*ozc8iq*_up*MQ..*_ga*ODk2OTI5OTkzLjE3MTU3OTczNzk.*_ga_C4KC7RL1SC*MTcxNTc5NzM3OS4xLjAuMTcxNTc5NzM3OS4wLjAuMA..

NEMO Committee (2019). Euphemia Public Description : Single Price Coupling Algoritm. https://www.epexspot.com/sites/default/files/2020-02/Euphemia_Public%20Description_Single%20Price%20Coupling%20Algorithm_190410.pdf

Nordic CCM Project (2023). News Update: Nordic Flow-based Market Coupling Go-live expected October 2024. https://nordic-rcc.net/wp-content/uploads/2023/11/News-update-7-November-2023.pdf

NSEC (2022). Joint Statement on the North Seas Energy Cooperation. *North Seas Energy Cooperation*. https://www.benelux.int/wp-content/uploads/2023/02/dublin-statement.pdf

NSWPH (2021). Market setup options for hybrid projects. *North Sea Wind Power Hub*. NSWPH_Market-setup-options-for-hybrid-projects_Discussion-paper-2_final.v2.pdf (northseawindpowerhub.eu)

NSWPH (2022a). Hubs and spokes - viable beyond theory, Sharing of Feasibility Results. *Concept Paper. North Sea Wind Power Hub Programme.*

NSWPH (2022b). Pathway Study: Key messages from the study. *North Sea Wind Power Hub Programme.*

NSWPH (2023). Commercial framework offshore bidding zone. *Discussion paper #4*. https://northseawindpowerhub.eu/files/media/document/NSWPH_Commercial%20framework%20offshore%20bidding%20zones_Discussion%20paper%20%234_0.pdf

Ocean Grazer (n.d.). Ocean Battery: Utility scale offshore energy storage. Retrieved on 10-6-2024, from: https://oceangrazer.com/

Ofgem (n.d.). Offshore Electricity Transmission (OFTO). Retrieved on 05-8-2024, from: https://www.ofgem.gov.uk/energy-policy-and-regulation/policy-and-regulatory-programmes/offshore-electricity-transmission-ofto

OTC (2024). Unlocking the potential of the North Seas. *Offshore TSO Collaboration*. Working Paper II.

Ovaere, M., Kenis, M., Van den Bergh, K., Bruninx, K., & Delarue, E. (2023). The effect of flow-based market coupling on cross-border exchange volumes and price convergence in Central Western European electricity markets. *Energy Economics*, *118*, 106519.

Poplavskaya, K., Totschnig, G., Leimgruber, F., Doorman, G., Etienne, G., & De Vries, L. (2020). Integration of day-ahead market and redispatch to increase cross-border exchanges in the European electricity market. *Applied Energy*, *278*, 115669.

Poplavskaya, K. (2021). *Balancing and redispatch: the next stepping stones in European electricity market integration: Improving the market design and the efficiency of the procurement of balancing and redispatch services.* [Dissertation (TU Delft), Delft University of Technology]. https://doi.org/10.4233/uuid:fb8c99cc24d6-4718-8986-95833ffc1f49

PROMOTioN (2020). Final Deployment Plan. *TenneT TSO B.V.* https://www.promotion-offshore.net/fileadmin/PDFs/D12.4_-_Final_Deployment_Plan.pdf

Rajgor, G. (2024). Grid congestion reducing Germany North Sea wind production – TenneT. *Windpower monthly*. Retrieved on 14-07-2024, from: https://www.windpowermonthly.com/article/1860641/grid-congestion-reducing-german-north-sea-wind-production-%E2%80%93-tennet

Rezaei, M., Akimov, A., & Gray, E. M. A. (2024). Levelised cost of dynamic green hydrogen production: A case study for Australia's hydrogen hubs. *Applied Energy, 370*, 123645.

Rijksoverheid (2024). Noordzeker en Zeevonk II winnen tenders windparken op zee IJmuiden Ver Alpha en Beta. Accessed on 13-06-2024, from: https://www.rijksoverheid.nl/actueel/nieuws/2024/06/11/noordzeker-en-zeevonk-ii-winnen-tenders-windparken-op-zee-ijmuiden-ver-alpha-en-beta

Rijkswaterstaat. (n.d.). Offshore grid. *In North Sea Loket*. Retrieved on 06-08-2024, from: https://www.noordzeeloket.nl/en/functions-and-use/offshore-wind-energy/offshore-grid/

RVO (2023). Concept voorschriften vergunning IJmuiden Ver, kavel Beta. Retrieved on 18-06-2024 from: https://www.rvo.nl/sites/default/files/2024-02/Concept-voorschriften-vergunning-IJver-Beta-24-11-2023.pdf

Schönheit, D., Kenis, M., Lorenz, L., Möst, D., Delarue, E., & Bruninx, K. (2021). Toward a fundamental understanding of flow-based market coupling for cross-border electricity trading. *Advances in Applied Energy*, 2, 100027.

Schönheit, D., & Marjanović, I. (2024). Introducing advanced hybrid coupling: Non-discriminatory coalescence of flow-based and net transfer capacity calculation regions. *arXiv preprint arXiv:2405.10010*.

Singh, S. (2023). Shades Of Gray, Blue And Green: Future Of (Sustainable) Hydrogen Economy. *Forbes*. Retrieved on 12-6-2024, from: https://www.forbes.com/sites/sarwantsingh/2023/06/01/shades-of-gray-blue-and-green-future-of-sustainable-hydrogen-economy/

Statnett (n.d.). *Capacity calculation methodologies explained: Flow Based market coupling (FB) & Coordinated Net Transfer Capacity coupling (CNTC).* https://www.statnett.no/globalassets/for-aktorer-i-kraftsystemet/utvikling-av-kraftsystemet/flow_based_capacity_calculation_methodology.pdf

Swiegers, G. (2023). A High-performance Capillary-fed Electrolysis Cell Promises More Cost-competitive Renewable Hydrogen. *SSRN 4493420.*

TenneT (n.d.). Electricity Markets. Retrieved on 15-06-2024, from: https://netztransparenz.tennet.eu/electricity-market/about-the-electricity-market/what-kind-of-markets-are-there-and-how-do-they-work/

TenneT (n.d.) LionLink. Retrieved on 30-06-2024, from: https://www.tennet.eu/lionlink

TenneT Holding B.V. (2023). *Integrated Annual Report 2023*. https://tennet-drupal.s3.eu-central-1.amazonaws.com/default/2024-03/TenneT%20Integrated%20Annual%20Report%202023.pdf

TenneT (2024). The offshore bidding zone - a blueprint by TenneT. https://tennet-drupal.s3.eu-central-1.amazonaws.com/default/2024-04/The%20offshore%20bidding%20zone%20-%20a%20blueprint%20by%20TenneT.pdf

THEMA Consulting Group. (2020). *Market arrangements for offshore hybrid projects in the North Sea.* European Commission. Directorate-General for Energy. https://op.europa.eu/en/publication-detail/-/publication/28ff740c-25aa-11eb-9d7e-01aa75ed71a1/language-en

Van Delzen, T. (2023). CfD designs for offshore wind farms in the offshore bidding zone approach: What are the advantages and disadvantages of different CfD designs for offshore wind farms in the North Sea? (Master Thesis). *Delft University of Technology.* https://repository.tudelft.nl/file/File_f903d793-4358-437b-8f07-6f8a3489b670?preview=1

Van den Bergh, K., Delarue, E., & D'haeseleer, W. (2014). DC power flow in unit commitment models. *KU Leuven Energy Institute*

Van den Bergh, K., Boury, J., & Delarue, E. (2016). The flow-based market coupling in central western europe: Concepts and definitions. *The Electricity Journal*, 29(1), 24-29.

Van Wingerden, T., Geerdink, D., Taylor, C., Hülsen, C., F. (2023). Specification of a European Offshore Hydrogen Backbone. *DNV.*

Wehrmann, B. (2023). Germany starts construction of North-South power line pivotal for energy transition. Retrieved on 05-08-2024, from: https://www.cleanenergywire.org/news/germany-starts-construction-north-south-power-line-pivotal-energy-transition

Weibelzahl, M. (2017). Nodal, zonal, or uniform electricity pricing: how to deal with network congestion. Frontiers in Energy, 11, 210-232.

Weinhold, R. (2021). Evaluating policy implications on the restrictiveness of flow-based market coupling with high shares of intermittent generation: A case study for central western europe. *arXiv preprint arXiv:2109.04940*.

Weinhold, R., & Mieth, R. (2021). Power Market Tool (POMATO) for the analysis of zonal electricity markets. *SoftwareX, 16,* 100870.

# Appendices

## Appendix A: Substantiation for the Flow-Based Parameters

The $PTDF_l^n$ matrix is based on the physical characteristics of the transmission network and the electrical properties of the power system (Van den Bergh et al., 2014). Specifically, the $PTDF_l^n$ is based on the incidence matrix $\boldsymbol{A}$, which is a line-to-node matrix describing which lines are connected to which nodes depicting the grid topology, and the line susceptance matrix $\boldsymbol{B_d}$ describing the reactive power flow characteristics through the transmission lines and measured in Siemens (S). Equation (A.1) gives the $PTDF_l^n$:

$$PTDF_l^n = (\boldsymbol{B_d} \cdot \boldsymbol{A}) \cdot \left(\boldsymbol{A^T} \cdot \boldsymbol{B_d} \cdot \boldsymbol{A}\right)^{-1} \quad (A.1)$$

The $PTDF_l^z$ matrix is based on the nodal PTDF values and the GSKs, obtained via equation (A.1)

$$zPTDF_l^z = \sum_{n \in \mathcal{N}} nPTDF_l^n \cdot GSK_{n,z} \quad (A.2)$$

The Zonal PTDF is thus obtained by summing the product of each node's PTDF and its respective GSK for a given zone, effectively aggregating the line's sensitivity to power injections across all nodes within that zone.

PTDFs are calculated with the slack node serving as the reference point. This configuration means that all PTDFs reflect the changes in line flows resulting from power transfers from the slack node to other nodes. The selection of the slack, or reference, node does not influence the actual line flow values calculated using the PTDFs; it merely simplifies calculations and reduces the complexity of matrix dimensions. In the PTDF matrix, the row corresponding to the slack node contains all zero values, effectively acting as a virtual sink by absorbing discrepancies between generation and load across the network (Huang, 2011).

To calculate the zonal PTDF matrix, the GSKs are thus needed (See equation (A.2)). There are different strategies to calculate GSK values, grouped under the 'flat' strategy and the capacity-weighted' strategy (Schönheit, et al. 2021). In the flat GSK strategy, all generation units at a node are assumed to participate equally in market changes. This approach assigns equal weights to all generators at a node when calculating the GSK values. The capacity-weighted GSK strategy considers the capacity of each generator at a node when determining their contribution to zonal changes. Generators with higher capacities have a greater impact on the net position of zones. This thesis assumes a pro rata capacity-weighted GSK strategy, using equations (A.3)

$$GSK_{n,z} = \frac{\sum_{g \in \mathcal{G}(n)} Q_g^s}{\sum_{n \in \mathcal{N}} \sum_{g \in \mathcal{G}} Q_g^s} \quad (A.3)$$

**Box A: The PTDF and GSKs in a simple case**

When taking the 5-nodal, 3-zonal working example, the PTDF matrices (nodal and zonal) and the GSKs can be exemplified. Assuming that node 1 is the slack node, the node-to-line PTDF becomes:

| | *l1-2* | *l1-3* | *l2-4* | *l3-4* |
|---|---|---|---|---|
| *n1* | 0 | 0 | 0 | 0 |
| *n2* | -0.75 | -0.25 | 0.25 | -0.25 |
| *n3* | -0.25 | -0.75 | -0.25 | 0.25 |
| *n4* | -0.5 | -0.5 | -0.5 | -0.5 |
| *n5* | 0 | 0 | 0 | 0 |

Assuming that node 1 contains a nuclear generator, node 4 a lignite generator and node 5 the OWF, the GSK matrix becomes:

| | *n1* | *n2* | *n3* | *n4* | *n5* |
|---|---|---|---|---|---|
| *z1* | 1.0 | 0 | 0 | 0 | 0 |
| *z2* | 0 | 0 | 0 | 1 | 0 |
| *z3* | 0 | 0 | 0 | 0 | 1 |

And finally, the zone-to-line PTDF becomes:

| | *l1-2* | *l1-3* | *l2-4* | *l3-4* |
|---|---|---|---|---|
| *z1* | 0 | 0 | 0 | 0 |
| *z2* | -0.65625 | -0.34375 | -0.03125 | -0.34275 |
| *z3* | 0 | 0 | 0 | 0 |

Equation (A.3) calculates the GSK value as the ratio of the total generating capacity at a specific node $n$ to the total generating capacity of all nodes within the same zone $z$, effectively distributing generation responsibilities proportionally based on installed capacity. The GSK matrix is then formed by these individual GSK values for each node and zone, where each row represents a node and each column a zone. The sum of each column for a specific zone should sum to 1, indicating that 100% of the generating capacity for that zone is accounted for across the various nodes. Having computed the GSKs, the zonal PTDF can then be obtained with equation (A.2). For further substantiation of these FB parameters, see Box A where the parameters are applied to the 5-nodal, 3-zonal Working Example.

In this thesis, the RAM values for each line $l$ are considered as follows:

$$RAM_l = max\left(\bar{F}_l \pm \left[F_l^{ref} - \sum_{z \in Z} zPTDF_l^z \cdot p_z^{ref}\right], [MinRAM \cdot \bar{F}_l]\right) \quad (A.4)$$

As depicted in Equation (A.4), for each line l, two RAM values are computed —positive and negative - by taking the maximum value of two sub-equations that each determine the RAM slightly different. The first is the RAM value as determined by the maximum allowed flow (e.g. thermal capacity) on line $l$ ($\bar{F}_l$) plus the expected flow as determine in the two days ahead base case calculation, subtracted by the flow that is expected to be flowing over that line due to exports (or imports) determined by the reference zonal position ($p_z^{ref}$), and distributed over the lines with the $zPTDF_l^z$. Alternatively, the RAM value is determined by taking a fraction of the thermal capacity based on a default safety margin (MinRAM). For this second approach the MinRAM is in this thesis set to 0.7, to leave sufficient remaining available margin for power flows that reflects the EC's 70% rule. The maximum of the two is taken to ensure that as much transmission capacity is being left available for the day ahead market clearing algorithm to make use of, such that the highest welfare generating combination of power flows can be allowed in the grid. After all, if the RAM as calculated via the reference flows and zonal PTDFs leaves less space on the AC lines for trade (e.g. having a lower value) than is depicted in the minRAM criterium (right hand side of equation IV), the minimum required safety margin can be taken as input for to the DA market clearing algorithm. Alternatively, if the RAM values calculated via the reference flows and zonal PTDFs leave more space on the AC lines than is required by the minRAM criterium, this higher RAM value can be used as input parameter the market clearing algorithm since it safely accounts for the impact on the AC lines due to the expected flows and cross-border trades, whereby it allows for a higher social welfare generating market clearing to be obtained.

This approach thus differs from the approach depicted by JAO (2020) explained in Section 2.3. This is for model simplicity purposes, since the FAV is a parameter in which TSOs incorporate expert knowledge, which is impossible to incorporate in modelling efforts without having this knowledge. Additionally, the AMR parameter, which adds a virtual RAM value of the minRAM target is not achieved, is somewhat incorporated by taking the maximum value of the left- and right-hand sides of equation (A.4). Noteworthy is that it could be argued that having this approach overestimates the remaining available capacity, but in the context of this thesis it is a practical workaround to incorporate the AMR parameter that is normally used (equation (2.3)).

# Appendix B: Karush-Kuhn-Tucker Conditions

AHC Optimization Problem

[1a] $\min DAC = \sum_{g \in G} MC_g \cdot Q_g^s \cdot v_g + c_n \cdot CC$

s.t.

[1d] $\sum_{g \in G} (Q_g^s \cdot v_g) + \sum_{n \in N} R_n - c_n - Q_n^d = p_z \quad \forall z \in Z$

[1e] $\cancel{\sum_{g \in G} Q} \sum_{l \in L} f_l^{AC} \cdot I_{l,z}^{AC} + \sum_{h \in H} f_h^{DC} \cdot I_{h,z}^{DC} = p_z \quad \forall z \in Z$

[4a] $p_z^{FB} = p_z - \sum_{h \in H} f_h^{DC} \cdot I_{h,z} \quad \forall z \in Z$

[4b] $-RAM_l^- \leq \sum_{z \in Z} zPTDF_l^z \cdot p_z^{FB} + \sum_{h \in H'} f_h^{DC} \cdot \left[ nPTDF_l^{n(h+)} \cdot I_{n(h+),h}^{ACDC} + nPTDF_l^{n(h-)} \cdot I_{n(h-),h}^{ACDC} \right] \leq RAM_l^+ \quad \forall l \in L$

[4c] $-NTC_{z,z'} \leq \sum_{h \in H} f_h^{DC} \cdot I_{h,z,z'} \leq NTC_{z,z'}^+ \quad \forall z,z'$

[1k] $0 \leq v_g \leq 1 \quad \forall g \in G$

[1C] $0 \leq c_n \leq R_n \quad \forall n \in N$

Decision Variables:

In Julia

(v) $v_g$ [dispatch] (F_FBMC) $f_l^{AC}$ [commercial AC-flow]

(c) $c_n$ [curtailment] (F_DC) $f_h^{DC}$ [commercial DC-flow]

(p) $p_z$ [total zonal position]

(p_FB) $p_z^{FB}$ [flow-based position]

Equality Constraints

$$\sum_{g \in G} (Q_g^s \cdot v_g) + \sum_{n \in N} R_n - C_n - Q_n^d - P_z = 0 \quad [\lambda_1]$$

$$\sum_{\ell \in L} f_\ell \cdot I_{\ell,z} + \sum_{h \in H} f_h^{DC} \cdot I_{h,z} - P_z = 0 \quad [\lambda_2]$$

$$P_z^{FB} - P_z + \sum_{h \in H} f_h^{DC} \cdot I_{h,z} = 0 \quad [\lambda_3]$$

Inequality Constraints

$$-\underline{RAM_\ell} - \sum_{z \in Z} {}_zPTDF_\ell^z \cdot P_z^{FB} * - \quad [\underline{\mu_1}]$$

$$\sum_{h \in H'} f_h^{DC} \cdot [{}_nPTDF_\ell^{n(h-)} \cdot I_{n(h-),h}^{ACDC} + {}_nPTDF_\ell^{n(-h)} \cdot I_{n(-h),h}^{ACDC}] \leq 0$$

$$\sum_{z \in Z} {}_zPTDF_\ell^z \cdot P_z^{FB} + \sum_{h \in H'} f_h^{DC} \cdot [{}_nPTDF_\ell^{n(h-)} \cdot I_{n(h-),h}^{ACDC} + {}_nPTDF_\ell^{n(-h)} \cdot I_{n(-h),h}^{ACDC} \leq 0$$

$$-\overline{RAM_\ell} \quad [\overline{\mu_1}]$$

$$-\underline{NTC_{z,z'}} - \sum_{h \in H} f_h^{DC} \cdot I_{h,z,z'} \leq 0 \quad [\underline{\mu_2}]$$

$$-\overline{NTC_{z,z'}} + \sum_{h \in H} f_h^{DC} \cdot I_{h,z,z'} \leq 0 \quad [\overline{\mu_2}]$$

$$0 - v_g \leq 0 \quad [\underline{\mu_3}] \quad v_g - 1 \leq 0 \quad [\overline{\mu_3}]$$

$$0 - C_n \leq 0 \quad [\underline{\mu_4}] \quad C_n - R_n \leq 0 \quad [\overline{\mu_4}]$$

~~Primal feasibility~~ Lagrangian (1)

$$\mathcal{L} = \sum_{g\in G} MC \cdot Q_g^s \cdot v_g + c_n \cdot CC \; +$$

$$\Big[\Big(\sum_{g\in G}(Q_g^s \cdot v_g) + \sum_{n\in N} R_n \cdot c_n - Q_n^d - P_2\Big)\cdot\lambda_1$$

$$+ \Big(\sum_{l\in L} f_l^{AC}\cdot I_{l,2} + \sum_{h\in H} f_h^{DC}\cdot I_{h,2}^{DC} - P_2\Big)\cdot\lambda_2$$

$$+\Big(P_2^{FB} - P_2 + \sum_{h\in H} f_h^{DC}\cdot I_{h,2}^{DC}\Big)\cdot\lambda_3\Big]$$

$$+\Big[\Big(-RAM_l^- - \sum_{z\in Z} zPTDF_l^z \cdot P_z^{FB}$$

$$- \sum_{h\in H} f_h^{DC}\cdot\big[nPTDF_l^{n(h-)}\cdot I_{n(h-)}^{ACDC} + nPTDF_l^{n(-h)}\cdot I_{n(-h),h}^{ACDC}\big]\Big)\Big]\cdot\underline{\mu_1}$$

$$+\Big(-RAM_l^+ + \sum_{z\in Z} zPTDF_l^z\cdot P_z^{FB}$$

$$+ \sum_{h\in H} f_h^{DC}\cdot\big[nPTDF_l^{n(h-)}\cdot I_{n(h-)}^{ACDC} + nPTDF_l^{n(-h)}\cdot I_{n(-h),h}^{ACDC}\big]\Big)\cdot\overline{\mu_1}$$

$$+\Big(-NTC_{z,z'}^- - \sum_{h\in H} f_h^{DC}\cdot I_{h,z,z'}\Big)\underline{\mu_2}$$

$$+\Big(-NTC_{z,z'}^+ + \sum_{h\in H} f_h^{DC}\cdot I_{h,z,z'}\Big)\overline{\mu_2}$$

$$+(0 - v_g)\cdot\underline{\mu_3} \quad + (v_g - 1)\overline{\mu_3}$$

$$+(0 - c_n)\cdot\underline{\mu_4} \quad + (c_n - R_n)\overline{\mu_4}$$

# Optimality Conditions !!!

$$\frac{\partial L}{\partial v_g} = \sum_{g \in G} MC_g \cdot Q_g^s + \sum_{g \in G} Q_g^s \cdot \lambda_1 - \underline{\mu}_3 + \overline{\mu}_3 = 0$$

$$\frac{\partial L}{\partial c_n} = CC - \lambda_1 - \underline{\mu}_4 + \overline{\mu}_4 = 0$$

$$\frac{\partial L}{\partial p_z} = -\lambda_1 - \lambda_2 - \lambda_3 = 0$$

$$\frac{\partial L}{\partial p_z^{FB}} = -\sum_{z \in Z} zPTDF_\ell^z \cdot \underline{\mu}_1 + \sum_{z \in Z} zPTDF_\ell^z \cdot \overline{\mu}_1 = 0$$

$$\frac{\partial L}{\partial f_\ell^{AC}} = \sum_{\ell \in L} I_{\ell,z} \cdot \lambda_2 = 0$$

$$\frac{\partial L}{\partial f_h^{DC}} = \sum_{h \in H} I_{h,z}^{DC} \cdot \lambda_2 + \sum_{h \in H} I_{h,z}^{DC} \cdot \lambda_3$$

$$- \left[ nPTDF_\ell^{n(h-)} \cdot I_{n(h-)}^{ACDC} + nPTDF_\ell^{n(-h)} \cdot I_{n(-h),h}^{ACDC} \right] \cdot \underline{\mu}_1$$

$$+ \left[ nPTDF_\ell^{n(h-)} \cdot I_{n(h-)}^{ACDC} + nPTDF_\ell^{n(-h)} \cdot I_{n(-h),h}^{ACDC} \right] \cdot \overline{\mu}_2$$

$$- \sum_{h \in H} I_{h,z,z'} \cdot \underline{\mu}_2 + \sum_{h \in H} I_{h,z,z'} \cdot \overline{\mu}_2 = 0$$

## Primal feasibility

$$\frac{\partial L}{\partial \lambda_1} = \sum_{g \in G} (Q_g^s v_g) + \sum_{n \in N} R_n - c_n - Q_n^d - P_z = 0$$

$$\frac{\partial L}{\partial \lambda_2} = \sum_{l \in L} f_l^{AC} \cdot I_{l,z} + \sum_{h \in H} f_h^{DC} \cdot I_{h,z} - P_z = 0$$

$$\frac{\partial L}{\partial \lambda_3} = P_z^{FB} - P_z + \sum_{h \in H} f_h^{DC} \cdot I_{h,z} = 0$$

$$-RAM_l^- - \sum_{z \in Z} zPTDF_l^z \cdot P_z^{FB} - \sum_{h \in H'} f_h^{DC} \cdot \left[ nPTDF_l^{n(h-)} \cdot I_{n(h-)}^{ACDC} + nPTDF_l^{n(-h)} \cdot I_{n(-h),h}^{ACDC} \right] \leq 0$$

$$-RAM_l^+ + \sum_{z \in Z} zPTDF_l^z \cdot P_z^{FB} + \sum_{h \in H'} f_h^{DC} \cdot \left[ nPTDF_l^{n(h-)} \cdot I_{n(h-)}^{ACDC} + nPTDF_l^{n(-h)} \cdot I_{n(-h),h}^{ACDC} \right] \leq 0$$

$$-NTC_{z,z'}^- - \sum_{h \in H} f_h^{DC} \cdot I_{h,z,z'} \leq 0$$

$$-NTC_{z,z'}^+ + \sum_{h \in H} f_h^{DC} \cdot I_{h,z,z'} \leq 0$$

$$0 - v_g \leq 0$$

$$v_g - 1 \leq 0$$

$$0 - c_n \leq 0$$

$$c_n - R_n \leq 0$$

## Complementary Slackness Conditions

$$\left[ \xi - RAM_l^- - \sum_{z \in Z} {}_zPTDF_l^z \cdot p_z^{FB} - \sum_{h \in H} f_h^{DC} \cdot \left[ {}_nPTDF_l^{n(h-)} \cdot I_{n(h-)}^{ACDC} + {}_nPTDF_l^{n(-h)} \cdot I_{n(-h),h}^{ACDC} \right] \right] \cdot \underline{\mu_1} = 0$$

$$\left[ -RAM_l^+ + \sum_{z \in Z} {}_zPTDF_l^z \cdot p_z^{FB} - \sum_{h \in H} f_h^{DC} \cdot \left[ {}_nPTDF_l^{n(h-)} \cdot I_{n(h-)}^{ACDC} + {}_nPTDF_l^{n(-h)} \cdot I_{n(-h),h}^{ACDC} \right] \right] \cdot \overline{\mu_1} = 0$$

$$\left( -NTC_{z,z'}^- - \sum_{h \in H} f_h^{DC} \cdot I_{h,z,z'}^{DC} \right) \cdot \underline{\mu_2} = 0$$

$$\left( -NTC_{z,z'}^+ + \sum_{h \in H} f_h^{DC} \cdot I_{h,z,z'}^{DC} \right) \cdot \overline{\mu_2} = 0$$

$$(0 - v_g) \cdot \underline{\mu_3} = 0$$

$$(v_g - 1) \cdot \overline{\mu_3} = 0$$

$$(0 - c_n) \cdot \underline{\mu_4} = 0$$

$$(c_n - R_n) \cdot \overline{\mu_4} > 0$$

## Dual feasibility

$$\underline{\mu_1}, \overline{\mu_1}, \underline{\mu_2}, \overline{\mu_2}, \underline{\mu_3}, \overline{\mu_3}, \underline{\mu_4}, \overline{\mu_4} \geq 0$$

# Appendix C: Substantiation on WTP for electricity of electrolysers

As explained in Section 4.2.3, the mathematical model was extended to include flexible demand agents, considered here in the form of hydrogen production units. Having this new variable in the optimization problem means that the WTP for electricity of the electrolysers now influence the outcome of the market clearing, whereby choosing a correct WTP is an important assumption that must be made.

To determine the WTP for electricity by an electrolyser, the key factor is the marginal cost of producing hydrogen. The WTP should be set at a level where the marginal cost equals the expected revenue from selling the hydrogen produced. Given that the electrolyser operator aims to sell the produced hydrogen at a minimum price that covers the total cost over the lifetime of the electrolyser plant, the Levelized Cost of Hydrogen (LCOH), excluding the electricity cost component, serves as an appropriate benchmark value. This benchmark ensures that the operator can at least sell the hydrogen at a price that makes the investment viable.

The Levelized Cost of Hydrogen (LCOH) varies depending on several factors, such as assumed operating hours, discount rate, operational lifespan, capital expenditures, and annual production (Razaei et al., 2024). Additionally, for dedicated offshore electrolysis at an OWF, variables like natural conditions (e.g., wind speed and water depth) and infrastructure availability (e.g., ports and hydrogen injection points) further influence the LCOH (Dinh et al., 2023).

Due to the variations in cost components based on specific cases and underlying assumptions, it is crucial to assume an LCOH calculated with assumptions fitting the offshore system design considered in this thesis. Van Wingerden et al. (2023) provide tailored LCOH levels for different onshore and offshore electrolysers in combination with offshore wind (See Figure 22). Within their scenarios, scenarios C and E in 2040 best reflect the system design of this thesis—dedicated offshore wind production far from shore (+150 km) with either HVDC transmission and onshore electrolysis at the landing point or offshore electrolysis with hydrogen pipeline transportation. The LCOH (excluding the cost of energy) for these scenarios will serve as inputs for further calculations: 2.21 €/kg for onshore electrolysis and 2.32 €/kg for offshore electrolysis.

To determine the WTP for electricity, the total efficiency of the electrolyser must be considered, in which the energy efficiency (HHV) of the electrolyser stack conversing water to hydrogen with electricity is considered, and the balance of plant energy consumption to account for operational losses. According to Swiegers (2023) the state-of-the-art commercial water electrolysers typically require ~53 kWh of electricity to produce 1 kg of hydrogen. Following the equation: $WTP_e = LCOH \cdot \eta_{total}$, the WTP becomes 43.77 €/MWh for an offshore electrolyser and 41.70 €/MWh for an onshore electrolyser

# Appendix D: Congestion Analysis for the Reference Case

This Appendix provides a congestion analysis for the Reference Case, focussing on the zero-priced hours. The results in Table 38 provide key insights into congestion patterns and their impact on price collapse hours and zero-priced hours due to renewable energy sources (RES). Figure 53 shows the grid topology with the transmission lines indicated with red that are show congested values throughout the simulated hours of the reference case.

*Table 38: Results Congestion Analysis Reference Case.*

| | **Zero-Priced Hours** (70.19% of time) | |
|---|---|---|
| **Congestion on Lines** | **Price Collapse Hours** (20.05% of time) | **Zero-Priced Hours due to RES** (50.14% of time) |
| *AC line onshore Z1* | 28.38% | 99.39% |
| *AC line Landing Point Z1* | 72.47% | 0% |
| *AC line Landing Point Z2* | 1.01% | 24.66% |
| *DC Line to Z1* | 0% | 0% |
| *DC Line to Z2* | 0.51% | 12.64% |
| *DC Line to Z3* | 14.02% | 63.58% |
| *Both AC and DC lines* | 14.53% | 68.24% |

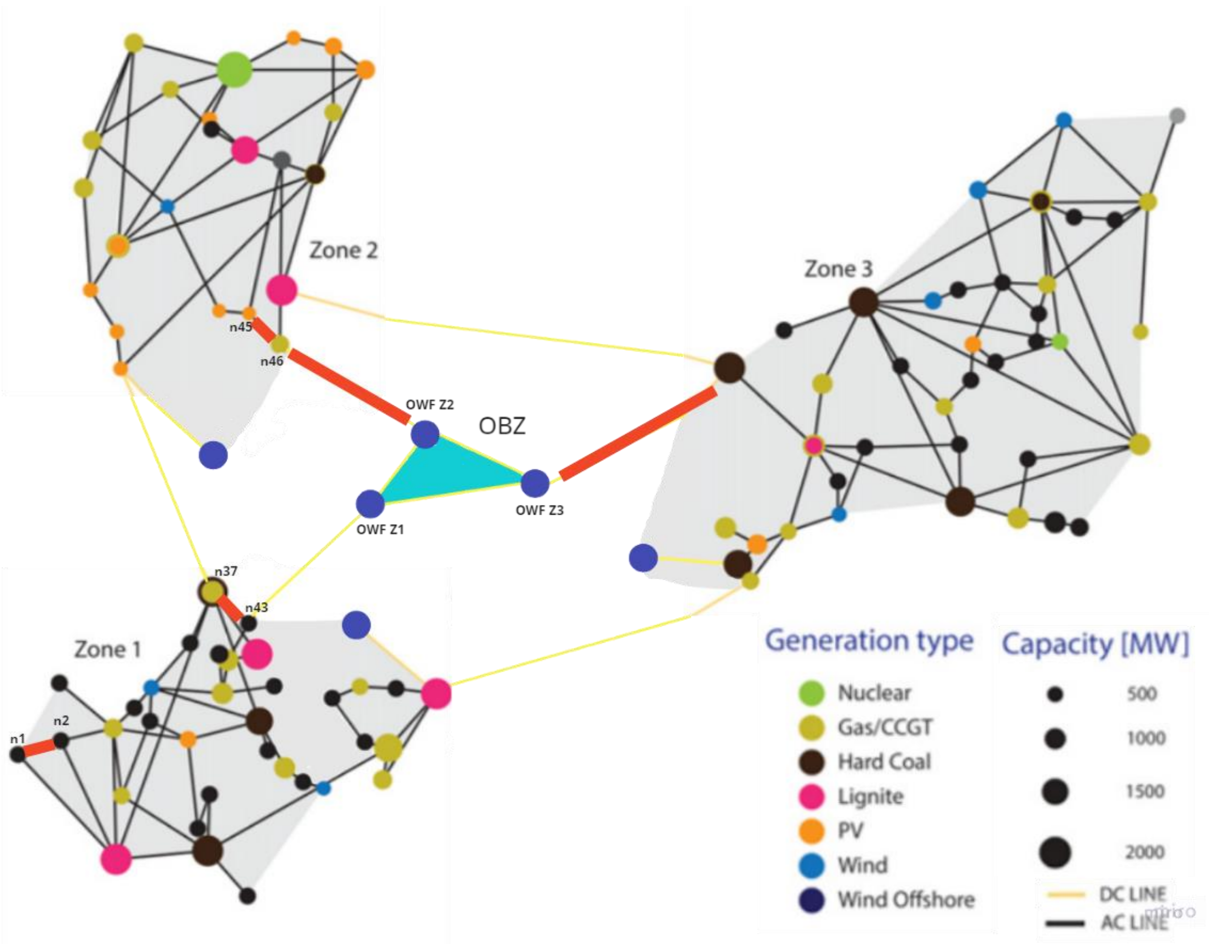


*Figure 53: Grid Topology with Congested Transmission lines indicated in red.*

Since price collapse hours occur whenever the export capabilities from the OBZ to the adjacent bidding zones is limited, i.e. the OBZ's FB domain is restricted, it proves useful to investigate what exactly is the limiting factor of the restricted FB domain. During price collapse hours, the AC line at the landing point of zone 1 emerges as the primary restricting factor, being congested 72.47% of the time. This indicates that the transmission capacity at this point significantly limits the flow-based domain, leading to price collapses. Additionally, the AC line further onshore in Zone 1 is congested 28.38% of the time during these hours, demonstrating its significant impact despite being located far from the OBZ. Notably, the DC line to Zone 1 is never congested, which means that it is the onshore AC grid that limit imports from the OBZ rather than the DC line itself (also confirmed in extreme values validation Section 4.6.2.2).

Furthermore, congestion on the DC lines to Zone 3 (14.02%) and Zone 2 (0.51%) occurs occasionally but always in conjunction with onshore AC line congestion, indicating that the DC interconnectors are never the sole limiting factor. Additionally, the minimal congestion on the DC line to Zone 2 during price collapse hours (0.51%) further indicates that the onshore grid in Zone 2 also limits the flow-based domain of the OBZ. Analysis of the power flows on the DC line from the OBZ to Zone 2 revealed that 1000.37 MWh was exported during 27.8% of the simulated time, with congestion occurring only 2.44% of the time. Although Zone 2's transmission grid could physically absorb more power from the OBZ (max 1500 MWh), the utilisation of this interconnector is rarely being maximised. In addition, the CNE at the landing point of zone 2 only restricted the FB domain for 1.01% of the price collapse hours, indicating its limited role. Since the D-1 market clearing allocates transmission capacity to achieve the highest socio-economic welfare generating set of commercial exchanges, it can be concluded that the HVDC interconnector form the OBZ to zone 2 is underutilised because maximisation of its utility does not lead to the highest welfare generating set of commercial transactions.

In terms of zero-priced hours due to RES, the AC line onshore in Zone 1 is almost always congested, accounting for 99.39% of these hours. This highlights the significant impact of this line on the transmission capacity. Additionally, congestion on the DC lines from Zone 3 (63.58%) and Zone 2 (12.64%) suggests that renewable energy zones often export up to their full transmission capacity via the OBZ. It is also noteworthy that in most cases where DC lines are congested, AC lines are also congested (68.24%), which shows combined transmission capacity constraints.

In conclusion, the onshore grid in Zone 1 structurally limits the import capacity from the OBZ. This is primarily due to the AC line at the landing point from the offshore wind farms, as anticipated by extreme values analysis in Section 4.6.2.2. Additionally, the AC line further onshore in zone 1 also plays a significant role. Moreover, despite zone 2 being physically able to import power up until the maximum transmission capacity of the interconnector to the OBZ (1500 MWh), the results show that the commercial transactions limit the import capability to this zone. In the grid topology setup used for the reference case, the DC interconnectors are never the sole limiting factor during price collapse hours, as they always coincide with AC onshore congestion. The key takeaway from this analysis is that the onshore grid in Zone 1 is inadequately designed to import power via the OBZ, primarily due to the AC line at the landing point and also due to further inland AC lines. In addition, the commercial transactions inside zone 2 further restricts the FB domain rather than the inability of the AC grid in this zone, while the DC line to Zones 1 and 2 are (almost) never the limiting factor restricting the FB domain.

The key takeaway from this analysis is that the FB domain of the OBZ is restricted due to different factors for Zones 1 and 2. For Zone 1, the inadequacy of the onshore AC transmission grid, both at the landing point and further inland, is the primary limitation, not the HVDC interconnector's capacity. For Zone 2, it is the commercial transactions rather than the onshore AC grid or the HVDC interconnector that restricts the FB domain. Thus, the DC lines to both zones are almost never the limiting factors.

# Appendix E: Price and Volume Risk Results for All Cases

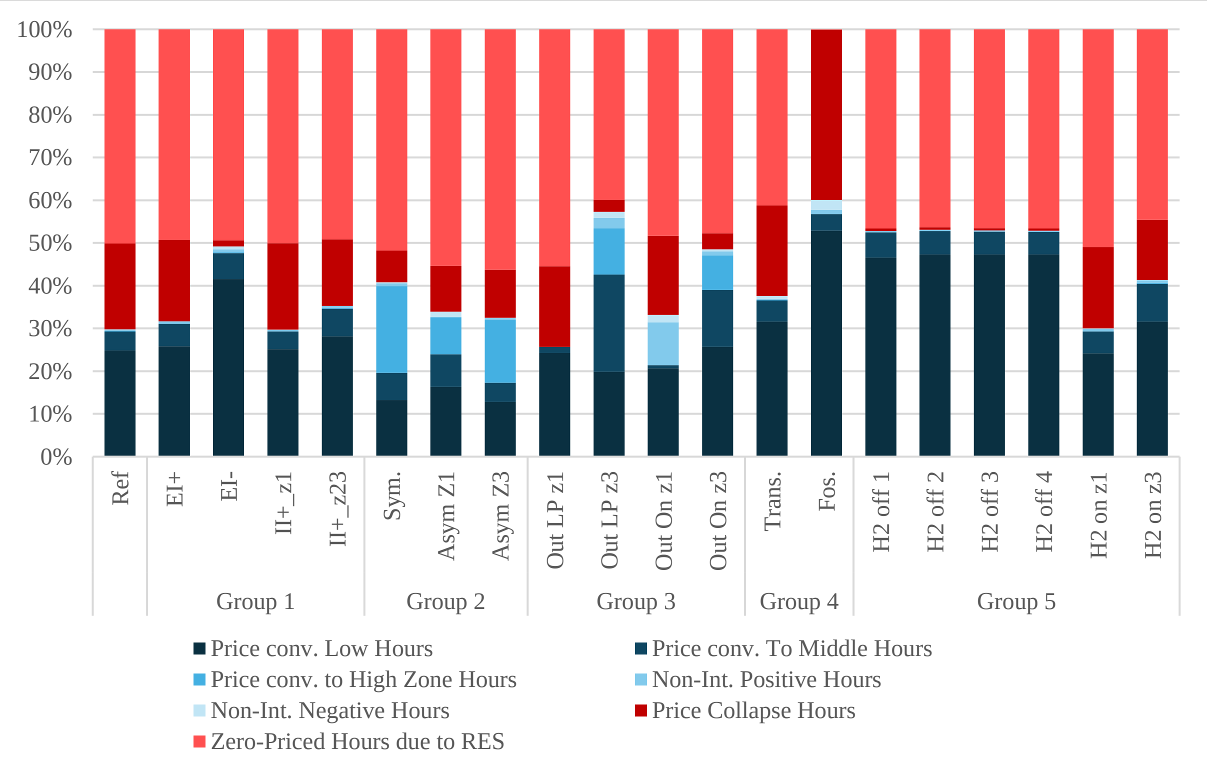


*Figure 54: Frequency of the price risk for all cases.*

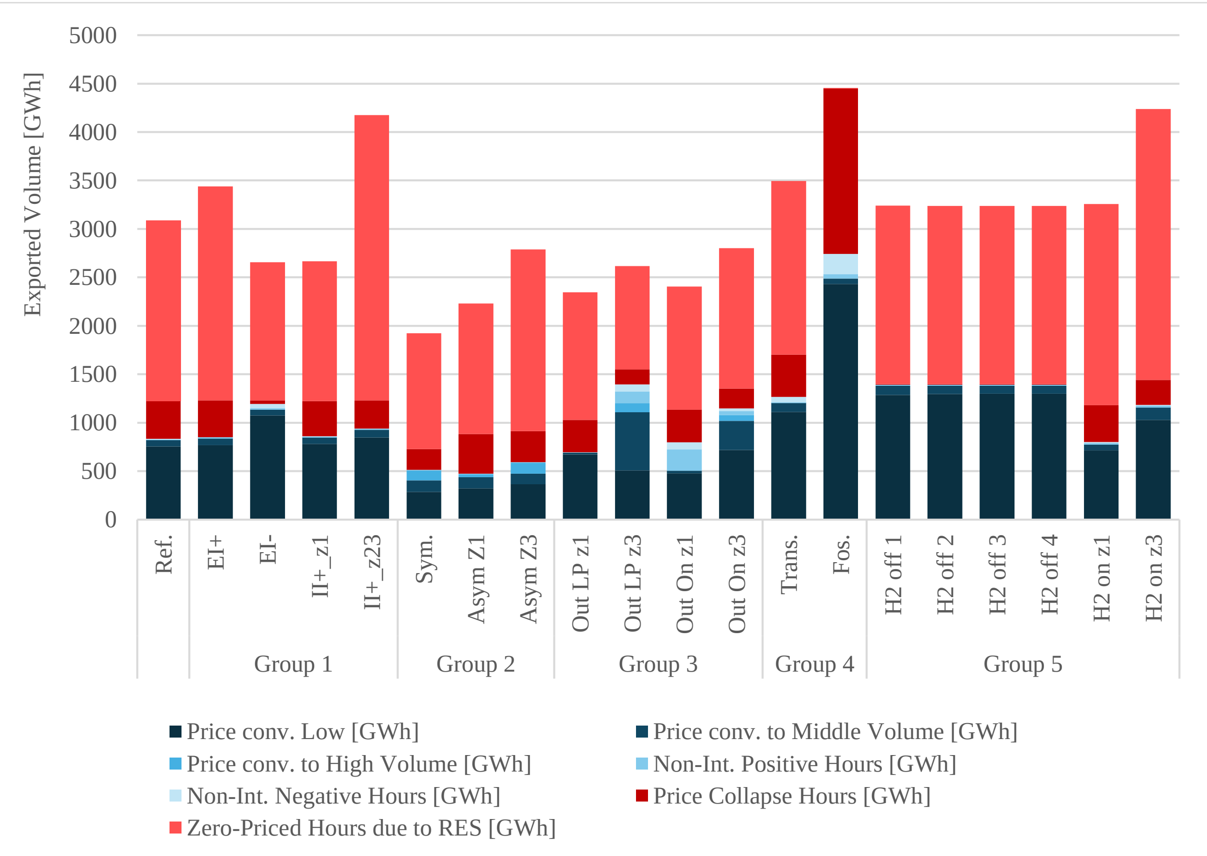


*Figure 55: Magnitude of the price risks for all cases.*

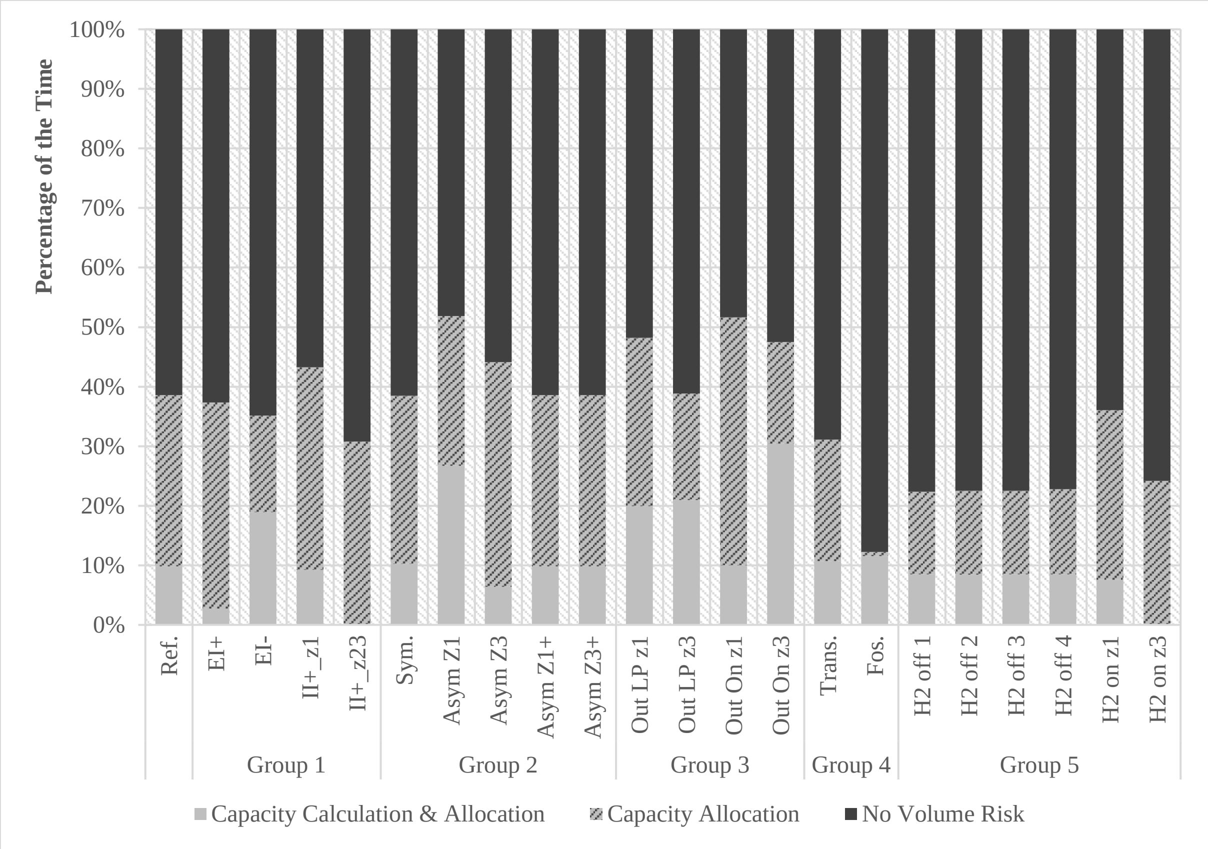


*Figure 56: Frequency of the volume risk for all cases.*

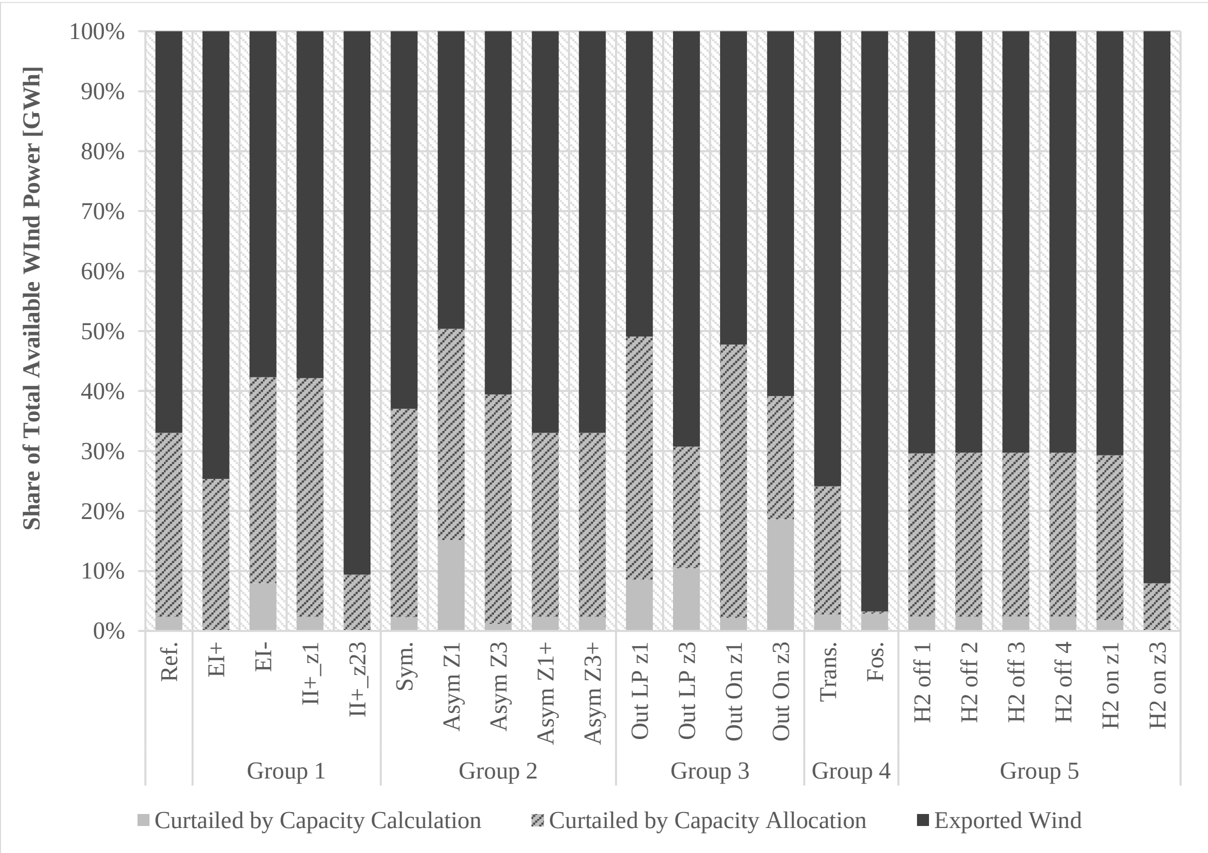


*Figure 57: Magnitude of the volume risk for all cases.*